A Sheffield Hallam University thesis

101 227 601 5

TELEPEN

2/4 16:55

ProQuest Number: 10701122

ProQuest 10701122

TRANSFORMATION AND PRECIPITATION

IN VANADIUM TREATED STEELS

BY

ANDREAS DEMETRIOU VASSILIOU M. Sc.

A THESIS SUBMITTED TO THE COUNCIL FOR NATIONAL ACADEMIC AWARDS
IN PARTIAL FULFILMENT FOR THE DEGREE OF

DOCTOR OF PHILOSOPHY

SPONSORING ESTABLISHMENT:

DEPARTMENT OF METALS
AND MATERIALS ENGINEERING
SHEFFIELD CITY POLYTECHNIC
POND STREET
SHEFFIELD S1 1WB

COLLABORATING ESTABLISHMENT:

UNION CARBIDE CORPORATION
PITTSBURGH
U.S.A.

MAY 1987
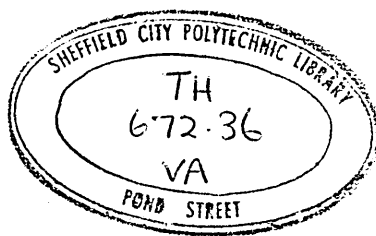
TRANSFORMATION AND PRECIPITATION IN VANADIUM TREATED STEELS

The work reported in this thesis is based on an investigation
carried out at the Sheffield City Polytechnic during the period of
October 1978 to July 1982, under the supervision of Dr.
F.B. Pickering and Mr. G. Butterworth. The following courses of
the M. Sc. at Sheffield City Polytechnic were attended :-

1. Heat Treatnent and Transformation
2. High Strength Steels
3. Numerical Analysis and Computer Programming

In addition the following conference were attended :-

1. "Hot Working and Forming Processes" Held at The
   University of Sheffield, 17-20 July 1979.
2. "Design as Related to Properties of Materials" One day
   conference held at British Steel Corporation, Sheffield
   Laboratories, Hoyle street, 6 March 1979.
3. "Steels for Line Pipe and Pipeline Fittings"
   International Conference, Metals Society, London 21-23
   October 1981.

The results presented in this thesis are to the best of my
knowledge, original except where reference is made to other
authors, and no part of it has been submitted for a degree any
other University or College.

A. D. Vassiliou

ACKNOWLEDGEMENTS

<u>ABSTRACT</u>

A D Vassiliou

Transformation and precipitation in Vanadium Treated Steels.

A series of carbon manganese steels containing varying amounts of
carbon, vanadium and nitrogen was investigated in relation to the
solubility of VC and VN in austenite, the grain coarsening
characteristics of austenite, the tempering of martensite and other
structures, the transformation during continuous cooling, the
effect of vanadium addition and increasing nitrogen content on
the thermo-mechanical processing of austenite, and the
transformation of various morphologies of austenite to ferrite.
The sites for preferential nucleation and growth of ferrite were
identified and the effect of ferrite grain size inhomogeneity
was investigated with a view to minimising it.

The C/N ratio in the V(CN) precipitates was largely controlled by
C/N ratio in the steel and it was also influenced by the
austenitising treatment. As expected, the solubility of VN was
less than that of VC.

A systematic investigation of austenitising time and temperature
on the grain coarsening characteristics was carried out showing
the effects of vanadium, carbon and nitrogen. It was tentatively
suggested that C-C and N-N clustering in the vanadium free steels
controlled the grain growth whereas in the presence of vanadium,
it was shown that VN and VC pinned the austenite grain boundaries
and restricted grain growth. However coarsening or solution of VC
and VN allowed the grain bondaries to migrate and grain
coarsening occurred. The grain coarsening temperature was
controlled predominantly by VN, whilst the VC dissolved
frequently below the grain coarsening temperature.

In the as quenched martensite, increasing nitrogen progressively
increased the as quenched hardness, and the hardness also
greatly increased with increasing carbon and vanadium added
together. Examining the precipitation strengthening in tempered
martensite showed that in the absence of vanadium, martensite
softened progressively with increasing temperature and time.
Vanadium additions increased the hardness level during low
temperature tempering and at higher tempering temperature
introduced secondary hardening. The intensity of secondary
hardening increased with increasing vanadium, whereas
austenitising temperature had little or no effect. The softening
after the secondary hardening was faster after austenitising at
the higher temperature and when recrystallisation occurred at
the highest tempering temperatures, the hardness was lower due to
coarse recrystallised ferrite.

Isothermal transformation studies showed that vanadium additions raised the Ar_3 temperature and accelerated ferrite nucleation, whilst the growth of ferrite was delayed due to the formation of V(CN) interphase and general precipitation pinning, of the transformation front. Increasing nitrogen content in the V-steel increased the incubation period for ferrite nucleation and increasingly reduced the ferrite growth by increasing V(CN) precipitation pinning of the transformation front.

Transformation during continuous cooling was examined in relation to the effect of vanadium, carbon and nitrogen together with the effect of austenitising temperature. Increasing austenitising temperature increased the austenite grain size, and it then became apparent that increasing vanadium, carbon and nitrogen increased the hardenability and raised the hardness level of the jominy curve for the non-martensitic products. This was particularly the case for the higher austenitising temperature, but at lower austenitising temperatures the effects were much less. A small increase in hardness was observed at some distance from the quenched end of the jominy specimen, which distance increased with increasing austenitising temperature. Tempering at 550°C caused small increases in hardness which developed into maxima, and occurred at shorter distances from the quenched end. Increasing tempering temperature and time caused the peak to be overaged and the general hardness level was increased. This increase in general hardness was attributed to the dislocation density and supersaturation of the transformation products, which caused hardening during tempering by precipitation of V(CN) particles.

The effects of vanadium addition and increasing nitrogen, together with the deformation temperature and amount of deformation, were examined in relation to the austenite morphologies and subsequent ferrite nucleation and growth. Vanadium additions, increased ferrite nucleation by refining the austenite grain size and increased the volume fraction of ferrite at a given transformation time by providing additional nucleation sites both at the V(CN) precipitates, and at the austenite/ferrite interfaces. In the absence of apparent retained deformation, and at low nitrogen contents, nucleation of ferrite was delayed but the ferrite grew rapidly due to insufficient V(CN) to pin the ferrite/austenite interface. Increasing nitrogen however retarded both ferrite nucleation and growth, and reasons for this have been discussed. The growth of ferrite during isothermal holding was dictated by the nucleation sites such as grain boundaries, deformation bands and intra-granular nucleation sites. Both grain boundary and deformation band nucleated ferrite formed small ferrite grain sizes

due to the numerous nuclei and their early impigement, whereas intragranularly nucleated ferrite grew rapidly and formed large ferrite grains due to insufficient precipitation to pin the transformation front. This type of structure led to duplex ferrite grain sizes and inhomogeneous type structures. Continuously cooled specimems verified these effects.

Method

CHAPTER 1 __INTRODUCTION__

It has long been known, that small additions of precipitate forming
elements can refine the austenite grain size which on subsequent
transformation refines the ferrite. The beneficial effects of
such refinement, especially of ferrite grain size, is a major
contributor to improving the yield strength and yet at the same time
causes an increase in toughness by lowering the ductile to brittle
transition temperature. The mechanisms by which these elements exercise
their influence on the mechanical properties, are generally understood
and in an attempt to utilise them to their fullest potential, micro-
alloying additions of Nb, V, Ti and Al are commonly employed in High
Strength Low Alloy (H.S.L.A.) steels. These alloying additions combine
with the interstitial elements such as carbon and nitrogen in the steel
to form precipitates. Such precipitation can pin the austenite grain
boundaries, thereby retaining the fine austenite grain size which on
transformation results in the requisite fine ferrite grain size.

The micro-addition of vanadium combines with carbon and nitrogen to
form V(CN) precipitates in austenite causing austenite grain refinement
and hence considerable ferrite grain refinement during and after
transformation. However, if the precipitates are formed during
transformation they can pin only the ferrite grain boundaries and
contribute only partially to ferrite refinement, whereas if
precipitation takes place after transformation it contributes only to
ferrite strengthening and not to ferrite refinement. Vanadium addition
in steels, under appropriate processing conditions, apart from ferrite
refinement gives further strengthening effects by precipitation
hardening. The use of thermo-mechanical treatment involving controlled
amounts of deformation in specific temperature ranges, coupled with
cooling at controlled rates, can materially enhance the properties of
high strength low alloy steels by causing further ferrite refinement
and optimising precipitation strengthening effects.

The strengthening effect due to precipitation hardening is attributed
to the difference in solubility of micro-alloying additions in ferrite
and austenite, the former being much less than the latter. Thermo-
mechanical processing of micro-alloyed austenite in conjunction with

1

controlled cooling activates precipitation to take place and cause retardation of recrystallisation of austenite. The synergistic effects of micro-alloying additions with carbon and nitrogen in H.S.L.A. steels in thermo-mechanically processed and controlled cooled materials are well known. These arise because vanadium can combine with carbon and nitrogen to form carbides and nitrides of different stabilities, vanadium carbide (VC) being much more soluble than vanadium nitride (VN). It is well known that precipitation of VC takes place during transformation of thermo-mechanically processed austenite, causing age hardening of ferrite by interphase precipitates. On the other hand VN may precipitate in austenite during or after the thermo-mechanical treatment above the transformation temperature and thereby retard recrystallisation. It is also known that the VC and VN are isomorphous and that the precipitating phase may be a complex V(CN) containing different carbon to nitrogen ratios. It is not entirely clear if the carbon and nitrogen content in the steel dictates the carbon and nitrogen in the precipitates or the temperature of deformation and the thermo-mechanical processing conditions under which precipitation takes place.

The synergistic effect of V, C and N during thermo-mechanical processing of austenite and during the austenite/ferrite transformation are incompletly understood, which in turn limits the most effective use of V as a micro-alloying addition. Nitrogen is always present in steels as an interstitial element with certain harmful effects on toughness. Removal of nitrogen by vanadium can render these harmful effects less marked. To retard austenite recrystallisation and consequently influence the transformation of austenite to ferrite so as to refine the ferrite grain size, precipitation of V(CN) should precede recrystallisation. Such precipitation of V(CN) can occur above A_3 but critical supersaturation is a pre-requisite to nucleate the V(CN), which will depend on the precipitation temperature and on the nitrogen content of the steel.

The nucleation sites for V(CN) precipitation, which are so important, i.e. prior austenite grain boundaries, sub-boundaries, dislocations and deformation bands, will depend on the amount of deformation and temperature of deformation. The growth of V(CN) to a critical size is

also important, depending on the factors already mentioned together with the deformation enhanced diffusion. In fact these nucleation and growth effects which govern the recrystallisation of austenite critically depend on the nitrogen content of the steel which in turn controls the optimum thermo-mechanical processing conditions.

The formation of a fine uniform ferrite grain size, which is so important for optimum properties, is controlled by the nucleation and growth of ferrite from thermo-mechanically treated austenite. It is qualitatively known that ferrite can nucleate at the prior austenite grain boundaries, on deformation bands, on undissolved carbonitrides, and also recent work has shown that ferrite can nucleate on the recovered substructure decorated by strain induced precipitates. In fact whilst there is qualitative information on the formation of ferrite formed from thermo-mechanically worked austenite, no quantitative nucleation and growth data are available. How these effects depend on the C, N and even V contents is not properly understood.

H.S.L.A. steels after thermo-mechanical treatment are continuously cooled and it is necessary to know how cooling rate influences the nucleation and growth of ferrite. Cooling rates can also greatly influence the growth of V(CN), which is precipitating during the austenite to ferrite transformation or from ferrite itself. These precipitates of V(CN) will not only control the subsequent grain growth of ferrite i.e. during cooling coiled strip, but also control the strength by an overaging effect. The effect of overaging, as well as the initial mechanisms by which the V(CN) is formed, on the toughness are also important.

The present work considers the effects of thermo-mechanical processing of vanadium steels containing enhanced nitrogen, to investigate the parameters which influence:-

> a. austenite grain growth,
> b. recrystallisation and transformation of thermo-
>   mechanically worked austenite,
> c. nucleation and growth of ferrite,

3

d. precipitation of V(CN) from austenite and ferrite.

Due to the uncertainties regarding the formation of V(CN) and its
dependancy on V:C and V:N ratio in the steel, and the effects of
thermo-mechanical processing in austenite, investigations have also
being pursued as follows:-

      a. to determine the solubility of VC, VN and V(CN) in
         austenite as a function of temperature and the C:N
         ratio in steel.

      b. to investigate precipitation :-
         i. from martensite during tempering,
        ii. from polygonal ferrite during tempering or
         aging.

In addition a small investigation has been made of the effects of
V, N and C on the hardenability.

4

During the hot working of metals, recrystallisation occurs and is
preceded by the recovery of the structure produced by the hot
deformation, to produced recovered subgrains in which the dislocations
of opposite sign are annihilated and the excess dislocations align
themselves into the recovered (or polygonised) sub-boundaries. This
process of recovery will not be discussed in detail, but the
involvement of the recovered subgrains will be considered with respect
to the subsequent process of recrystallisation.

Recrystallisation is a nucleation and growth process to develop small
regions of nearly perfect crystal which are capable of sustained
growth, in unstable deformed and recovered material. The transient
recovered structure which exists in a high energy state by virtue of
its dislocation density, reverts during recrystallisation towards the
equilibrium state. The low energy recrystallised grains can be formed
by homogeneous or heterogeneous nucleation. Homogeneous nucleation for
a transformation is difficult, particularly in industrial practices,
and heterogeneous nucleation is more predominant. Nucleation therefore
normally takes place at the high energy sites such as grain boundaries,
deformation bands, inclusions or at large second phase particles. As
will be discussed later, fine precipitates often retard or inhibit
recrystallisation.

2.1   Homogeneous Nucleation

The concept of classical nucleation theory was first formulated by
Volmer and was then applied to recrystallisation by Becker[1] and
reconsidered critically by Burke and Turnbull[2]. Volmer's model of
homogeneous nucleation for a phase transformation is based on the
concept of the random condensation of a group of atoms which come
together to form an embryo. If the embryo is too small it will not grow
but will shrink and disappear, but if it is sufficiently large it will
become a viable nucleus, capable of sustained growth. In thermodynamic
terms the stability of the embryo depends on the balance between the
surface energy which has to be provided to create a stable nucleus, and
the volume free energy change due to the transformation, which provides

5

the energy available to create the nucleus. Consequently, at a critical size the embryo will become a viable nucleus. The model, initially applied to the condensation of a vapour, was later adapted to liquid-solid and solid-solid transformations without changing the essential concept, and when applied to recrystallisation assumes the recrystallised material to have the same composition as the deformed and recovered material.

The energy required in the formation of a nucleus consists of (a) the energy of the interface, (b) elastic strain energy arising from any change in volume accompanying the structural change and (c) strain energy associated with the lattice distortion produced by partial or complete coherency between the two lattices. Conventional homogeneous nucleation theory has been applied by Byrne[3] to recrystallisation processes.

The critical embryo size for sustained growth into a viable nucleus is determined from the thermodynamic condition of stability. The change in free energy of formation of a spherical embryo of radius r for a recrystallised region within a deformed and recovered matrix is:-

$$\Delta G_T = \frac{4}{3}\pi r^3 \Delta G_u + 4\pi r^2 \gamma \qquad\qquad 1$$

where ΔG_T is the total energy change per unit volume,

  ΔG_u is the difference between the energy of recrystallised and the deformed and recovered states,

  r is the radius of the embryo,

and γ is the interfacial energy per unit area of the recrystallised-unrecrystallised interface.

Thermodynamically the free energy of formation of a stable nucleus is that for which,

$$\frac{\partial \Delta G_T}{\partial r}_{r=r_c} = 0 \qquad\qquad 2$$

Differentiation of Eq. 1 with respect to r and the application of

6

Eq. 2 gives,

$$r_c = -\frac{2\gamma}{\Delta G_u} \qquad 3$$

The change in total free energy required to form the critical
nucleus size $\Delta G_{T(c)}$ is given by :-

$$\Delta G_{T(c)} = \frac{16\pi\gamma^3}{3\,\Delta G_u^2} \qquad 4$$

This model assumes that subcritically sized embryos are constantly
being created and destroyed, and that occasionally an embryo will by
chance exceed the critical nucleus size and then be capable of
sustained growth.

This model can account for an incubation period, predicts that high
energy sites will be preferred nucleation sites as is observed, and
predicts feasible values of the nucleation frequency and critical
nucleus size. But it has limitations because the interfacial energy
values of recrystallised grains with the unrecrystallised matrix should
result in slow growth whereas growth is rapid, and no effect of the
paramount influence of purity is allowed for. Also, it has been shown
that the activation energies predicted were far greater than observed,
as also to some extent are the critical nucleus sizes.

2.2 Heterogeneous Nucleation

In many cases nucleation in the deformed materials takes place at sites
not distributed randomly, but occurring at particular sites in the
matrix, most frequently at some crystal defects. These nucleation sites
are mainly, grain boundaries, grain edges, grain corners, dislocations
stacking faults, deformation bands and inclusions. The formation of a
recrystallised nucleus on a pre-existing defect is such that the energy
of formation of the nucleus is reduced by that proportion of the defect
energy that is consumed by the nucleus as it forms. For nucleation on
the boundary of matrix grains, Fig. 1, the grain boundary that has been

7

destroyed is shown by a dashed line within the new grain. In considering the creation of a viable nucleus it is necessary to take to account :-

a. the energies of the recrystallised/unrecrystallised interface $\gamma_{U/R}$ and the grain boundary interfacial energies between the contiguous unrecrystallised grain γ_U. If θ is the angle of contact, balance of the horizontally resolved interfacial forces requires that :-

$$\gamma_U = 2\gamma_{U/R} \cos\theta \qquad\qquad 5$$

when $2\theta = 180°$, nucleation is of the homogeneous type.

b. The volume free energy change which is represented by the difference between deformed and recrystallised states.

The incubation time can be considered as the initial period of isothermal annealing during which a sequence of thermal fluctuations and dislocation re-arrangements occur, giving rise to the creation of strain-free regions equal to, or greater than the critical size for stability.

Following Burke and Turnbull[2] the critical size nucleus is given by:-

$$r_c = -\frac{2\gamma_{U/R}}{E} \qquad\qquad 6$$

where E is the strain energy of the deformed metal. Similarly, the energy formation of a viable nucleus is given by :-

$$\Delta G_{T(c)} = \frac{16\pi\gamma_{U/R}^3}{3E^2} \qquad\qquad 6a$$

and the nucleation rate in a region after the incubation period is given by :-

$$\overset{\bullet}{N\epsilon} = n \ \frac{kT}{h} \ \exp \left[- \ \frac{(\Delta Fa)g}{kT} \ \right] \ \exp \left[- \ \frac{16\pi\gamma^3}{3kTE^2} \right] \quad 6b$$

where $\overset{\bullet}{N\epsilon}$ is the nucleation rate in a region of strain,

$(\Delta Fa)g$ is the free energy of activation for grain
boundary self diffusion,

n is the number of atoms per unit volume,

k and h are Boltzman's and Planck's constant
respectively.

2.2.1 Subgrain-Growth

Preformed nuclei exist at some stage during or after deformation of a
metal but are not immediately thermodynamically capable of growth. The
important point to note is that there is no collective and simultaneous
reorganisation of atoms into a newly oriented lattice but a gradual
decrease of the energy of a region of a badly distorted matrix lattice,
until it becomes perfect enough to acquire the thermodynamic ability to
grow. Orowan[4] intuitively suggested such a process without proposing
a detailed model. In a highly distorted region the lattice is highly
curved. This enables the region that becomes a nucleus to grow into
neighbouring higher energy material. The mechanisms of formation of a
preformed nucleus have been the source of much investigation. Cahn[5]
and Beck[6], independently proposed the process of polygonisation. Cahn
proposed the formation of walls of similar sign dislocations during
annealing after bending. Such walls would form a boundary having a
lower overall strain energy than the more random dislocation
arrangement existing prior to annealing. It is well recognised in the
work of Gay et. al.[7] that the distribution of dislocations in a
plastically deformed metal is not uniform, and that the structure
consists of subgrains or cells, the interiors of which have a
comparatively low dislocation concentration while the small angle cell
boundaries are packed with dislocations.

During a subsequent recovery treatment, both climb and short range
glide of dislocations is required to form the new walls. This leads to
the formation of boundaries. Production of boundary segments takes

place, which causes the isolated dislocations at some distance away to glide into the vicinity of the boundary and then climb sufficiently to find a place in the boundary. Polygonisation then progresses by the merging of adjacent short-range boundaries, thus giving a somewhat longer boundary which is still of the low-angle type Fig. 2. The driving force for polygonisation is derived from the progressive reduction of the boundary energy per dislocation as the misorientation increases, which lead to the formation of a viable dislocation free nucleus as predicted by Eq. 3. Thus, as the misorientation of the growing sub-grain increases, it will grow at the expense of neighbouring sub-grains to form a recrystallisation nucleus, and this will be more effective if the growing sub-grain has a marked size advantage.

2.2.2 Subgrain Coalescence

The subgrain coalescence theory was formulated by Hu[8,9] as a result of an extensive study of recrystallisation in 3% Si-Fe single crystals. The results showed the gradual disappearance of the boundaries between neighbouring subgrains. During this process the relevant regions showed decreasing contrast, thus indicating that they were merging into a common orientation. As a result such a coalesced group became a sub-grain of substantially greater size than its neighbours, and the mechanism implies sub-grain rotation.

This process is explained by Hu[8,9] as a gradual movement of dislocations from the disappearing subgrain boundary into other boundaries around subgrains. This probably requires some dislocation climb along the disappearing boundary, and a rotation of the subgrain itself, with movement of some of the atoms situated immediately around the relevant boundaries.

An analysis of subgrain rotation during recrystallisation has been made by Li[10]. Figure 3 shows a schematic representation of Li's model for the process. Misorientation between the two central subgrains is shown in Fig. 3(a). The common boundary (CH) can be eliminated by rotation of the right hand subgrain. This is achieved by the diffusion of the atoms along the boundaries from the shaded regions to the unshaded region in

Fig. 3(b). Figure 3(c) depicts the coalesced subgrain at this stage in the process. Finally the coalesced subgrain will take up the form shown in Fig. 3(d) as result of rearrangement of the boundaries to achieve low energy configurations, and remove the unstable re-entrant boundary angles.

Li[10] used a thermodynamic analysis of the process in terms of the misorientation angles and energies of the subgrain boundaries. He proposed that a subgrain can rotate in such a way either to increase or decrease the angle of misfit. The rate controlling process can be either the co-operative diffusion of vacancies in the lattice or the co-operative movement of dislocations in the boundaries.

Hu[8,9] has extended this model qualitatively, to apply to the formation of recrystallised grains in the manner shown in Fig. 4. Figure 4(a) is a subgrain stucture in which increasing misorientation across a boundary is indicated by increasing thickness of the line. In Fig. 4(b) the subgrains AB and CD are coalescing to eliminate their common boundaries (shown as dotted lines). After boundary adjustment Fig. 4(c), the process continues with the coalescence of the two enlarged subgrains, until a region is produced which has the characteristic of a viable recrystallisation nucleus. Finally since a high angle boundary segment will have high mobility, futher growth will take place by the migration of the high angle boundaries into the surrounding uncoalesced subgrain regions. This part of the specimen will therefore have passed from the nucleation stage into the growth stage of primary recrystallisation.

2.2.3   Strain Induced Boundary Migration (SIBM)

Beck and Sperry[11] described in detail the formation of recrystallisation nuclei by strain induced boundary migration. They showed that the formation of new nuclei was less frequently observed than the formation of regions relatively free from substructure by strain-induced migration of already existing boundaries. The process is depicted in Fig. 5 in which 1 and 2 show two positions of a migrating boundary which originally separated two deformed grains, A and B. A distinctive feature of this type of migration is that the boundaries

11

move in the direction away from their centres of curvature.

The mechanism suggested for these observation[11] is depicted in Fig. 6. It is assumed that there is a strain energy difference between grains A and B for high boundary mobility to occur. The boundary migration was said to be initiated by that part of its length which formed a boundary with one of the larger subgrains in the lesser strained grain A. The direction of migration is away from this grain into the more heavily strained grain. This leads to a reduction in the internal energy which is equivalent to the difference between the stored energy released in the consumed region and the energy required to extend the length of the migrating boundary. Therefore the material in the bulge will be similar orientation to that of the region of the lesser strained grain from which it originated.

Bailey[12] developed a detailed analysis of this so-called bulge nucleation, in which the process was envisaged to occur by segments of the boundary of length 2L bulging out to form spherical caps of radius R, which then continue to migrate. This process is depicted in Fig. 7 in which successive stages of migration are marked 1, 2 and 3.

The necessary condition required for the bulge to grow is given by :-

$$L \rangle \frac{2\gamma}{\Delta E} \qquad\qquad 7$$

where γ is the surface energy of the migrating boundary,

ΔE is the difference in stored energy per unit volume across the migrating boundary.

Bailey and Hirsch[13] examined a large number of annealed foils and found that recrystallisation occurred by the formation of bulges of local regions of the grain boundaries. The regions inside the bulges, through which the boundaries had migrated were virtually dislocation free. This suggests that the segments of the boundaries capable of migrating had only a few dislocations terminating on their concave side. Another important feature was that the overall recrystallisation process was found to be inhomogeneous. In regions of the foil which had not been involved in the bulging process there were no obvious changes

12

of structure compared with the deformed and recovered state, thus providing further verification of the Beck and Sperry suggestion.

2.2.4 General Comparison of Nucleation Mechanisms

In comparing the occurrence of the various nucleation mechanisms it is necessary to consider the sites at which nucleation can occur and the appropriateness of the various models for those sites.

For a successful nucleation model, it is necessary that nuclei form preferentially in regions where there is a high degree of deformation[14] and/or local lattice curvature or misorientation. At low deformations there is usually more deformation at grain edges and/or grain corners than is the case for the grain interiors. However, as the amount of deformation increases, the stored energy distribution becomes homogeneous. Consequently the grain boundaries do not necessarily have the same significance, and recrystallisation nuclei can be found in the interior of the original grains, as well as at the grain boundaries. In addition any dispersed particle-matrix interfaces provide sites for nucleation.

Whatever the location of the nucleus within the general microstucture the proposed mechanism must lead to the production of a strain free region of supercritical size, which is surrounded by a potentially mobile high angle grain boundary. Therefore a viable nucleus must be a relatively large region having an orientation similar to the same region in the deformed state but being surrounded at least partially by a high misorientation interface.

This general requirement is described by the models which have been considered, i.e. the sub-grain growth, subgrain coalescence, strain-i uced boundary migration or grain boundary bulging models. The distinction between them lies in the specific way in which this selective development occurs.

A basic requirement of the strain-induced boundary migration mechanism is the presence of a significant stored energy difference between the grains on either side of the relevant boundary. This deformation

13

distribution is particularly prevalent at low deformations which are associated with relatively few unevenly deformed regions within the interior of the grain. Strain-induced boundary migration will thus be the dominant mechanism for the formation of recrystallised nuclei at low deformations. Recrystallisation kinetics will be particularly sensitive to the changes in the original grain size since this will determine the grain boundary area per unit volume (Sv) which is available to act as nucleation sites.

However as the amount of deformation increases there will be a tendency to produce more unevenly deformed grain interiors. Thus the possibility of formation of recrystallised nuclei within the interior of the original grains will increase. Consequently nucleation will become increasingly prevalent at sites within the grain interiors, in conjuction with those at grain boundaries.

Using normal deformation, nucleation takes place in the interior of the grains at some selected subgrains in order to acquire the appropriate misorientation to become a viable nucleus. Such a development is likely to occur either by polygonisation or by sub-grain coalescence.

In each of these mechanisms a well developed subgrain structure is required as a starting point for nucleation. In the case of grain boundary nucleation, the subgrain structure provides a low dislocation density region from which the strain-induced grain boundary migration can form a bulge, whilst in the case of grain-interior nucleation sharply defined subgrains are clearly required before they can coalesce to form a large nucleus. Since the predicted critical nucleus size is far to small to be observed by available experimental techniques no method of nucleation can be solely supported or rejected, but there is experimental evidence for nucleation in iron by S.I.B.M.[14], in Fe-Si alloys by subgrain coalescence[15] and S.I.B.M.[16], and in aluminium-killed steel by S.I.B.M.[17].

2.3 Grain Boundary Structure and Grain Boundary Migration

During recrystallisation, after the formation of a viable recrystallisation nucleus, the nucleus grows by means of boundary

14

migration of the recrystallised grain boundary. The final grain size of the recrystallised structure will depend on both the nuceation rate, and growth rate of the recrystallised grains. Grain growth of recrystallised grains can occur, either during or after recrystallisation is completed, by migration of grain boundaries in order to reduced the overall grain boundary surface energy. The migration of boundaries is thus an important phenomenon.

A grain boundary can be defined as a layer of distorted material created by atomic mismatch between two differently oriented crystals of the same phase. An important principle in many models of grain boundary structure is that the interfaces of relative low energy may be maintained by networks of dislocations[18]. The grain boundaries are normally considered to be high angle interfaces which have the ability to migrate rapidly. Various models exist for the structure of the grain boundary :-

        (i)   the dislocation model,

        (ii) the island model,

        (iii) the coincident-site model.

2.3.1 The Dislocation Model

The dislocation model is based on an extension of the structure of simple tilt or twist boundaries to high misorientation. This model was proposed by Read and Shockley[18] but the concept breaks down at misorientation $>10°$ because of the interaction of the closely adjacent dislocations, which changes the core structure, and the boundary is no longer simple. At somewhat higher angles, $\sim15°$, dislocations would be so closely spaced that they would lose their identity and the dislocation model becomes of little or no value in describing the structure of such a grain boundary[19].

2.3.2 The Island Model

Mott[20] suggested that if two crystals are in contact but cannot fit together owing to the different orientations, the area of contact is divided in to islands where the fit is reasonably good separated by areas where the fit is poor. It was assumed that the basic process of

grain boundary migration involves the "melting" of a group of atoms
belonging to the bad-fit boundary region to allow migration to occur.
To remove an atom from such a region requires an energy equivalent to
the latent heat of fussion. As will be seen later, this model has some
similarities conceptually with the coincident site model.

2.3.3. The Coincidence-Site Model

Extensive investigations on simple grain boundaries in zone refined
materials showed that the migration rate of the boundary was
orientation dependent[21]. It was observed that the lattices of the two
grains had a common sublattice across the boundary, referred to as a
coincidence lattice, and comprising an array of sites which occurred on
the lattices of both grains. There is periodic repetition of these
structural units, and such boundaries can have low energies. Models of
grain boundaries which involve coincident site concepts, usually imply
a sequence of ledges in the boundary, and deviations from regular ledge
spacing can lead to increasing boundary energy. A high density of
coincident sites confers high mobility on the boundary.

2.4 Mechanism of Grain Boundary Migration

Turnbull[22] developed the grain boundary migration concept on the
basis of absolute reaction rate theory. It was assumed that the atoms
are transferred singly across the migrating boundary. This leads to a
relationship between the rate of migration (G), the activation energy
(Q), and the absolute temperature (T) of the form

$$G = G_o \exp - \frac{Q}{RT} \qquad\qquad 8$$

where G_o is a function of :-
   a. the extent of local boundary movement when an atom is
      transferred from one grain to another,
   b. the lattice parameter,
   c. the driving force,
 and d. the temperature.

Li[19], using a dislocation model, suggested that migration of a grain

boundary can be regarded as a diffusion process where the diffusion along the core of the dislocation controls the rate of migration. In fact vacancy interractions at both sides of the core are responsible for the movement, and it has been suggested and assumed that all atoms at the grain boundary have the same jump frequency and moreover always find a free site on the adjoining grain surface.

Several investigators[21] have observed that growth selectivity can produce preferred orientation in recrystallised alloys, but this does not imply that the different mobilities of various boundaries are responsible for the selective growth of grains with preferred orientation. It has also been shown that twinning during the growth of recrystallised grains can result in the replacement of a migrating boundary by a second boundary whenever, thereby, the total interfacial energy is lowered. The interfacial energy of grain boundaries varies with relative orientation and therefore grains oriented so that they have low-energy boundaries may well be favoured during the nucleation or the growth stage of their development.

Aust and Rutter[23] suggested that differences in impurity segregation at grain boundaries of different structure were responsible for the very specific orientation selectivity of growth mobility. They based their model for this effect on the concept that the lattices of the new and old grains have a common sublattice, i. e. a coincident site model. As the density of the coincidence sites increases the degree of good fit increases. Good fit boundaries adsorb considerably less impurity than bad fit boundaries or random boundaries. The tendency to adsorb impurities also is affected by the temperature; at low temperatures impurities segregate at boundaries strongly, but at high temperature the impurity atmosphere tends to evaporate. Thus at high temperatures there was little difference between the migration rates of their special and random boundaries since neither adsorbed significant amounts of impurity. At low temperatures however the random boundaries became impurity laden, and the migration rates fell below those of relatively impurity-free special boundaries. The introduction of dislocations into the coincidence sites boundaries can increase the vacancy concentration and in consequence the rate of boundary movement.

2.5 Effect of Solute on Grain Boundary Migration

It has been assumed[24] that a boundary is a sink for solute atoms to an extent that depends on the size difference between the solute and solvent atoms. The segregation of solute atoms also depends on the temperature and the structure of the grain boundary. Such segregations of impurities play an important role in the mechanism of boundary migration. Many investigators have proposed different theories to account for the effect of solutes on grain boundary migration.

2.5.1 Lucke and Detert's Theory of Solute-Dependent Growth

Lucke and Detert[24] proposed that the grain boundaries are energetically favoured sites for segregation of solute atoms. The degree of segregation of solute atoms to boundaries is dependent on the interaction energy between the two constituents, and the temperature

$$C = C_o \exp \frac{U}{KT} \qquad\qquad 9$$

where C = concentration of solute atoms in the boundary;

C_o = the average solute concentration;

U = interaction energy between boundary and a solute atom;

K,T are Boltzmann's constant and absolute temperature respectively.

They assumed that the interaction between the solute and the boundary was elastic in nature, and that it was dependent on the elastic stress field surrounding the solute atom. The larger the solute atoms with respect to solvent, the greater the interaction energy and the greater the retardation of grain boundary migration.

Using solutes of different sizes in copper-based alloys, it was found that the increase in the recrystallisation temperature was directly proportional to the solute:solvent atom diameter ratio. In the presence of solute atoms, the driving force for boundary migration during the growth stage of recrystallisation was taken to be the difference in the line tensions of the dislocation in the grains on either side of the boundary, i.e. inhomogeneity in the dislocation density between grains.

The attractive force (P_a) between solute atoms and a boundary is given by :-

$$P_a = f_a n_a C \qquad\qquad 10$$

where f_a is the attraction force per solute atom,

   n_a is the number of atoms per unit boundary area.

This attractive force exerts a drag effect on the boundary migration such that when a boundary moves at a constant velocity the driving force is balanced by the attractive force.

The condition for boundary migration is given by :-

$$(\rho - \rho_0)\mu b^2 = f_a n_a C_0 \exp \frac{U}{KT} \qquad\qquad 11$$

where $(\rho - \rho_0)\mu b^2$ is driving force for boundary migration,

   μ is the shear modulus,

   b is Burger's vector of the dislocations,

   ρ and ρ_0 are the dislocation densities in the deformed and
   unrecrystallising grains respectively ($\rho_0 \ll \rho$).

This leads to an expression for boundary velocity V

$$V = V_0 \exp - \frac{Q_D + U}{KT} \qquad\qquad 12$$

Where Q_D is the activation energy for volume diffusion,

   and U is the interaction energy between the solute atoms and
   the boundary.

and where

$$V_0 = \frac{\mu r^2 \rho a^2 D_0}{\sqrt{2KTC_0}} \qquad\qquad 13$$

where :- μ is the shear modulus,

   r is the solvent atom radius,

   ρ is the dislocation density in the deformed grain, but
   $\rho \gg \rho_0$,

19

D_o is the pre-exponential factor for the basic volume
diffusion equation,

a is the lattice parameter.

The controlling mechanism depends on the volume diffusion of solute
atoms behind the boundary. During the migration of the boundary which
is retarded by the solute atoms, Lucke and Detert calculated that the
maximum velocity was :-

$$V_{max} = \frac{f_o D_o}{KT} \ exp - \frac{Q_D}{KT} \qquad\qquad 14$$

where f_o is the maximum interactive force between solute atom and
migrating grain boundary.

Grain boundaries having velocities greater than that given in equation
(14) will have broken away from solute atoms. Figure 8 shows the
solute-limited grain boundary velocity and breakway conditions for the
three different concentrations where, $C_1 > C_2 > C_3$. The curves show that as
the temperature is increased the concentration of foreign atoms in the
grain boundary decreases, Eqn. 9, and a critical temperature is reached
where the retarding force is less than the driving force and hence
breakway occurs. The temperature at which breakway occurs will be lower
as the average concentration of solute C_o is decreased. The dotted
lines represent V_{max} condition according to Eqn. 14.

A more concise representation of the theory is shown in Fig. 9. At low
temperature Eqn. 12 applies and the slope of the line represents volume
diffusion of solute atoms. However at very high temperatures the
smaller slopes corresponds to an activation energy for grain boundary
diffusion which is the rate controlling process. The breakway stage is
not associated with any activation process. The different slope and
therefore the different activation energies explain why published value
of activation energy for recrystallisation often differ widely.

Gordon and Vandermeer[25] modified Lucke and Detert's migration
relationship as a result of the re-interpretation of the nature of the
lattice in which foreign atoms migrate. Lucke and Detert assumed that

the separation distance between the boundary and the solute atoms was large enough for the boundary not to influence the diffusion of the solute atoms. However they[25] stipulate that this separation distance is less for the maximum restraining force, which means that the boundary energy is lower than the maximum. Therefore the solute atoms must move within the distorted material. Hence the mobility factor can not be expressed by the volume diffusion coefficient as described by the Lucke and Detert model but by some lower value of activation energy for diffusion.

Gordon and Vandermeer[21] obtained the following relationship for the velocity of solute-dependent grain-boundary migration rate V_{SD} at a given temperature,

$$V_{SD} = G_o^i \exp - \frac{Q^i + U}{RT} \qquad\qquad 15$$

where $G_o^i = \dfrac{P_a D_o^i}{RT\lambda A C_o}$

where D_o^i and Q^i represent pre-exponential factors and the

activation energies respectively for the

diffusion of solute in a region of distorted

lattice adjacent to the grain boundary,

λ is the relevant boundary width,

A is the change in entropy when an impurity atom

is exchanged with a solvent atom in the grain

boundary,

U is the internal energy gained by replacing

solvent atoms in the grain boundary by solute

atoms,

P,R,T, and C_o as previously described.

At high temperatures growth is controlled by the grain-boundary movement which is independent of the impurities. On the other hand at low temperatures growth is controlled by the diffusion of solute

atoms. The growth is much lower than in the previous case and decreases rapidly as the temperature falls. The same effect was observed by Sheard and Nutting[26] using photoemission electron microscopy to study the recrystallisation phenomena in plain carbon steels.

Lucke and Stuwe[27] have suggested that Eqn. 9 inadeqately represented the high solute concectration. They proposed a more realistic equation in which when V is finite and C represents a dilute solution, then assuming a constant diffusion coefficient, the concentration at a point (x) relative to the grain boundary is given by:-

$$C(x) = C_o \exp - \frac{U(x)}{kT} \left[1 - \frac{V}{D_i} H(x) \exp - \frac{Vx}{D_i} \right] \qquad 16$$

$$\text{where } H(x) = \int_{-\infty}^{+\infty} \exp \frac{Vx}{D_i} \left[1 - \exp \frac{U(x)}{kT} \right] dx \qquad 16a$$

where C is the boundary solute concentration,

C_o is the average solute concentration,

V is the velocity of the boundary,

D_i is the diffusion coefficient for atom in the potential field of the grain boundary,

and U(x) is the interaction energy between boundary and solute atoms.

It can be seen that as the temperature increases, C approaches C_o, which results in the disappearance of the solute atmosphere. Further C(x) will decrease as the velocity increases, and the reduction in C will be less for negative x values, behind the moving boundary, than for positive x values in front of the moving boundary. Lucke and Stuwe[27] were able to derive an expression for the attractive force between solutes and the moving boundary. This was achieved by combining Eqn. 16 with an equation for the total force on unit grain boundary area by solute atoms. Thus the attractive force was :-

$$P_a = - nkT \frac{V}{D_i} \left(I - \frac{V}{D_i} J \right) \qquad 17$$

where n is the number of atoms per unit volume

$$I = \int_{-\infty}^{+\infty} \exp \left[(- \frac{U(x)}{2kT}) - \exp \frac{U(x)}{2kT} \right]^2 dx \qquad 17a$$

$$J = \int_{-\infty}^{+\infty} \exp - \frac{Vx}{D_i} \exp - \frac{U(x)}{kT} - 1 \; H(x) dx \qquad 17b$$

When the boundary velocity V is zero then P_a is zero; for a finite value of V however, P_a increases. But this increase is not continuous with increasing V, but decreases and approaches zero for large values of V. The approach of P_a towards zero means that the solute atmosphere is in effect left behind by high boundary velocities. At this point the authors distinguished between two types of grain boundary mobility. Microscopic mobility (m) was taken as a theoretical intrinsic property of the boundary and is the property which determines the velocity V_m of a small segment of the boundary. The force acting on this boundary segment is P. Thus the macroscopic driving force for migration to occur P is :-

$$P = \frac{V}{m} - P_a(V) \qquad 18$$

where V is the overall velocity of boundary,

   m is the microscopic mobility of grain boundary.

Lucke and Stuwe[27] considered a further contribution to inhomogeneous movement of the grain boundary. The macroscopic movement consists of several microscopic movements which are not migrating at the same speed. This phenomenon will be important when, during deformation, serrated or corrugated grain boundaries are formed.

At low V values, V becomes proportional to P

$$V = \frac{P}{\alpha Nb \frac{kT}{D_m} + nI \frac{kT}{D_i}} \qquad 19$$

Where α is the proportionality factor $= 1$

    N is the total number of atoms/unit volume,

    n is the number of solute atoms/unit volume,

    b is the distance moved by the boundary per jump per atom,

    D_m is the diffusion coefficient for transfer of atoms
       across the boundary.

At high solute concentration, a transition range is shown where V temporarily increases with increasing P. Such a region is equivalent to the breakway stage in the Lucke and Detert theory and a similar transition region exists in Gordon and Vandermeer's theory.

The predicted grain boundary velocity is shown in Fig. 10, as a function of temperature for various conditions. Curve (c) represents the linear behaviour between V and T for unsegregated boundaries. Curve (a) represent the the condition for low solute content such that the $nI(kT/D_i)$ (Eq. 19) is small. Conversely when the solute content is high this term has a significant effect on the velocity as shown by curve (b). Thus for low solute concentration the behaviour represented by curve (a) approaches that predicted by Gordon and Vandermeer[25].

2.5.2 Cahn's Theory

Cahn's[28] appproach was similar to that Lucke and Stuwe[27] where diffusion is considered to occur normal to the boundary. From a knowledge of the composition variation, the drag force exerted by impurities was calculated, which enables the boundary velocity to be formulated as a function of driving force, impurity concentration, and temperature. Cahn considered U(x) to be negative for the absorption of solute atoms at the boundary, the opposite to Lucke and Detert[24]. Other workers have also suggested that the grain boundary is a region across which the interaction energy and diffusion coefficient varies as a function of distance x from the boundary. Developing the equation describing the concentration across a migrating boundary, the total force in relation to composition is given by:-

$$P_i = -N_i \int_{-\infty}^{+\infty} (C-C_o) \frac{dU}{dx} \, dx \qquad\qquad 20$$

where N_i is the number of atoms per unit volume,

   C is the concentration of solute at the boundary,

   C_o is the average solute concentration,

   U(x) is the interaction energy between solute and
      boundary.

In order to find P_i the value of C must be known and also the values of U(x). Limiting cases have been considered :-

i. For the high velocity limit the impurity drag is given by:-

$$P_i \simeq \frac{C_o N_i}{kTV} \int_{-\infty}^{+\infty} U^2 D \, dx \qquad\qquad 21$$

where D is the diffusion coefficient of solute normal to the grain
      boundary,

   P_i is proportional to D, but inversely proportional to V,

   V the grain boundary velocity, which is in disagreement with
      the Lucke and Detert model.

ii. For the low velocity limit :-

$$P_i = 4N_i C_o VKT \int_{-\infty}^{+\infty} \frac{\sinh^2 [\, U(x)/2KT \,]}{D(x)} \, dx \qquad\qquad 22$$

Comparing equations 21 and 22 indicates important
similarities and differences:

   (a) Equation 22 reduces to equation 14 if U(x) is large
      enough and negative at the grain boundary and if D(x)
      is constant and equal to the bulk diffusion.

   (b) Equation 22 is independent of the sign of U and predicts
      that the drag for the impurities which avoid the
      boundary is the same as that for the impurities which
      are adsorbed. The former are pushed ahead of the
      boundary; the latter are dragged behind the boundary.

By comparing Eqns. 21, 22 it is possible to construct a relationship

for the drag effect which fits both the high and low velocity requirements :-

$$P_i = \frac{\alpha V C_o}{1 + \beta^2 V^2}$$

23

Where α and β are constants which can be calculated from the interraction potential between the solute, the boundary and the diffusion coefficient of solute as :-

$$\alpha = 4N_i kT \int_{-\infty}^{+\infty} \frac{\sinh^2 [\ Ux/2kT\ ]}{D(x)} dx$$

23a

$$\alpha/\beta^2 = \frac{N_i}{kT} \int_{-\infty}^{+\infty} \left(\frac{dU}{dx}\right)^2 D(x)\ dx$$

23b

Furthermore Cahn[28] considered the effect of the grain boundary velocity as a function of temperature, composition and driving force. For impure material the intrinsic drag, $P_o(V)$, is the difference between the actual driving force $P(V, C)$ which gives a velocity V in a material with impurity concentration C, and the impurity drag $P_i(V, C_o)$. Cahn also assumed that the composition dependence of P_o is negligible compared to P_i, and :-

$$P(V, C) = P_o(V) + P_i(V, C_o)$$

24

Assuming that P_i is given by the Eqn. 23 and that $P_o = \xi V$, Eqn. 24 becomes :-

$$P = \xi V + \frac{\alpha C_o V}{1 + \beta^2 V^2}$$

25

Where ξ_i is intrinsic drag coefficient and is the reciprocal of the intrinsic mobility and is related to diffusion at grain boundary for

26

pure metals. The limiting conditions for Eqn. 25 becomes :-

(a) For low velocity and low driving force when $V \ll 1/\beta$:-

$$V = \frac{P}{\xi + \alpha c_o} \qquad 25a$$

(b) For high velocity and when $V \gg 1/\beta$ Eqn. 25 becomes,

$$P = \xi V + \frac{\alpha c_o}{\beta^2 V} \qquad 25b$$

i. for high velocity and high driving force:

$$V = \frac{P}{\xi} \left(1 - \frac{\alpha \xi c_o}{\beta^2 P^2} \right) \qquad 25bi$$

ii. for high velocity and low driving force:

$$V = \frac{P}{\xi} \left(1 - \frac{\alpha c_o}{\xi} \right) \qquad 25bii$$

At very low driving forces, the transition between pure and impure boundary behaviour should be continuous with no inflection point. At higher driving forces the boundary is capable of migrating at such velocities that the impurity drag shows an inflection point, Fig. 11. At intermediate velocities, however, there is an unstable situation. If the boundary momentarily accelerates, it will lose enough impurities so that the total drag will decrease, allowing the boundary to accelerate still further. Similarly if the boundary slows down momentarily, the total drag will increase, slowing the boundary still further.

2.5.3 Machlin's Model

Machlin[29] proposed a model for the motion of a grain boundary enriched with solute atoms in which the mechanism varied as the solute concentration at the grain boundary varied. Three processes were considered to control grain boundary migration. At very low solute concentrations the boundary moves but the solute atoms act to reduce the net driving force on the boundary by inducing local reversed curvature, this is known as mechanical breakaway. As the solute concentration is increased solute atoms diffuse together with the boundary movement, so that both the boundary and solute atoms can

migrate together and the boundary velocity is determined by the rate at which solute atoms diffuse. At still higher solute concentrations the occurrence of thermal breakway of the boundary from the solute atoms is possible.

The most important assumption is that the boundary velocity is limited by the diffusion of solute atoms. Machlin arrived at this conclusion by considering the change in shape of a grain boundary caused by the adsorption of solute atoms. Free- energy considerations in the regions of the boundary at which solute atoms are situated, are thought to create a cusp between the fast moving parts of the boundary on either side of the solute affected region. Lucke and Stuwe[27] suggested that the model of the cusp formation by solute atoms is too restrictive, since diffusion parallel to the boundary and normal to the boundary is needed. This can only be justified by the assumption that the solute atoms are larger than the boundary width. Furthermore there is evidence that atoms smaller than the solvent atom[30] can cause delay in recrystallisation and the assumption that the solute must be larger than the grain boundary width appears to be invalid.

2.5.4 Li's Theory

Li[19] assumed that the impurity segregated to the boundary to reduce the vacancy concentration in the boundary. This leads to saturation effects on the migration rate at some concentration of solute atoms. An approximate treatment led to the following expression for boundary velocity :-

$$\text{Ln} \frac{G_o}{G} = \frac{A(V_o - V) KC}{RT (1 + KC)} \qquad 26$$

Where G_o and V_o are the mobility and vacancy concentration
of the boundary in the pure metal,

G and V are the coresponding values when is completely
saturated with impurity atoms,

A is a proportionality constant,

K is the equilibrium constant for segregation

28

and C is the average composition.

The reduction in vacancy concentration caused by the segregation of solute atoms will discourage individual atomic movement and will also increase the activation energy of grain boundary migration, which will always be reduced by solute atoms.

2.5.5. The Electronic Interaction Theory of Solute-Dependent Growth

Abrahamson and Blakeney[31] working on iron with solute addition up to 1 atomic per cent found a linear relationship between recrystallisation temperature and the solute content the slope of which changes at some critical solute concentration. It was possible to relate the initial rate of change of recrystallisation temperature, and these critical concentration values, to the electronic structure of the solvent atom in the ground state.

The results obtained for iron provided a good example of these effects, and it was also found that the solute which produced the greatest initial rate of increase of the recrystallisation temperature also had the lowest critical concentration. Figure 12 shows how the electronic structure of the solute influenced the initial rate of increase of the recrystallisation temperature with solute content. This can be summarised as follows :-

(i)   For solutes having a given number of s-shell electrons the rate of increase of recrystallisation temperature with composition is increased as the number of d-shell electrons increases.

(ii) For solutes having a given number of d-shell electrons, the fewer the s-shell electrons the greater the rate of increase of recrystallisation temperature with composition.

(iii) As the number of inner shell electrons increases a greater increase in recrystallisation temperature occurs with increase of solute content.

Similar correlations between electronic structure and recrystallisation have been found for other transition metals. Therefore experimental evidence strongly suggests that electronic interactions either between solute and solvent atoms or between solute atoms and grain boundaries, have a greater influence on recrystalisation than the elastic interactions, at least for the transition metals.

2.5.6 Further Comments

A number of theories to account for the effect of solute atoms on recrystallisation have been presented, in each recrystallisation is retarded as the solute concentration increases, but there is no simple linear relationship between the two variables. It is well accepted that the presence of solute elements can affect both the nucleation and the growth stages of recrystallisation.

In all theories of solute-dependent growth after nucleation, boundary migration is considered to be controlled by absorbed solute atoms. However Lucke and Detert's[24] original theory seems applicable although some additional observations have enabled the theory to be refined. To refine the theories further necessitates much more knowledge of the structure and properties of grain boundaries.

2.6 Effect of Second Phase Particles on Primary Recrystallisation

Many commercial alloys, such as steels, are phase mixtures rather than homogeneous solid solutions. Their recrystallisation behaviour depends on whether the alloy is deformed in the single phase state or in the two-phase condition. If a supersaturated alloy is deformed and then recrystallised, recrystallisation may be influenced by precipitation of the second phase particles. If the particles are present before deformation, recrystallisation behaviour depends on the nature and size of the precipitates.

2.6.1 Theoretical Treatment of Precipitation in Relation to Recrystallisation

In a supersaturated solution alloy which is deformed and then annealed,

30

second phase particles can precipitate in the same temperature range over which recrystallisation occcurs. Precipitation and recrystallisation mutually influence each other. The precipitates hinder both the rearrangement of dislocations to form recrystallisation fronts and the migration of the latter, while the defects present in the crystal lattice accelerate the nucleation of precipitating phases, which themselves can also affect dislocation rearrangement and grain boundary migration.

The start of recrystallisation[35] can be described by:-

$$t_r = A \exp \frac{Q_r(N)}{RT} \qquad\qquad 27$$

where A is a factor containing the driving force for the
reaction, an entropy term and geometric factors.

Q_r is the activation energy for the formation of a
recrystallisation front. It depends on the dislocation
density, N.

The incubation period for precipitation is given by the equation:

$$t_p = B \exp \frac{Q_N(C,T)+Q_D}{RT} \qquad\qquad 28$$

Where B is a factor containing an entropy term and geometric
factors.

$Q_N(C,T)$ is the activation energy for nucleation of the second
phase. It depends strongly on the supercooling below the
equilibrium temperature. $Q_N(C,T)$ is small compared with
the activation energy for the diffusion Q_D.

Curves showing both relationships in equation 27 and 28 are shown in Fig. 13. On the basis of this diagram three temperature ranges in the recrystallisation behaviour can be distinguished:-

1. $T > T_1$ Recrystallisation is influenced by solute segregation
as no precipitation occurs.

31

2. $T_1 > T > T_2$ Recrystallisation is influenced only by segregation; precipitation occurs after completion of recrystallisation.

3. $T < T_2$ Precipitating particles influence both the rearrangement of dislocations to form recrystallisation fronts and the migration of the latter.

The transition at T_2 is not sharp since a certain period of time is necessary for the completion of recrystallisation. In this transition region the behaviour characteristics of the ranges (2) and (3) occur simultaneously at different sites in the specimen. Furthermore the deformation structure of the deformed alloy is not homogeneous. There are regions with much higher dislocation density, e.g. deformation bands. Precipitation is generally accelerated in this more heavily deformed region, and consequently the start and finish of the recrystallisation may be delayed.

In the temperature range (3) precipitation and recrystallisation processes influence each other. In a supersaturated and deformed alloy the volume fraction of precipitates before the start of recrystallisation increases with decreasing temperature, from f=0 at T_2, and these precipitates pin dislocations and thus decrease dislocation mobility. Simultaneously the precipitate particle size decreases with decreasing temperature. Therefore, dislocation rearragement and the migration of grain boundaries are hindered increasingly with decreasing temperature.

An increase in solute concentration at constant dislocation density will shorten the incubation time for precipitation, but it is assumed that this change in solute concentration has little effect on the initiation of recrystallisation. At higher solute concentrations T_1 and T_2 are shifted to higher temperatures due to the general acceleration of the precipitation reaction with increasing supersaturation.

2.6.2 Influence of Dispersed Particles on Recrystallisation

The overall recrystallisation characteristics of alloys reflect the infuence of the dispersed particles on the recrystallisation behaviour in two ways:-

32

(i)   Dispersed particles influence the distribution of
        dislocations in the matrix after deformation. Precipitates
        aid the creation of dislocation sources and act as
        barriers to dislocation movement[32,33]. It has also
        been suggested that in the over-aged condition precipitates
        tend to activate large numbers of slip systems. Barnby and
        Smith[34] have shown that widely-spaced particles promote the
        formation of a dislocation cell structure since they act as
        dislocation sources. On the other hand fine particles appear
        to inhibit dislocation movement.

(ii)   Quite independently, it is possible that the presence of
        dispersed particles may physically modify the nucleation and
        growth of recrystallised grains for a given deformation
        structure.

The parameters   influence   the recrystallisation are volume
fraction f, mean particle radius r, and the interparticle spacing d. It
is now well recognised[36,37,38] that nucleation of recrystallisation
may occur in the vicinity of large second phase particles. Particle-
stimulated nucleation has been observed in-situ in the high voltage
electron microscope[4,5]. It is found[4], that recrystallisation
originates at a pre-existing subgrain within the deformation zone
surrounding the particle, although the subgrain is not always at the
particle-matrix interface. The subgrain grows by rapid sub-boundary
migration until the deformation zone is consumed, and thereafter may
either grow into the matrix or may remain as a small grain apparently
nucleated at the particle[38]. The number of nuclei formed increases as
the particle size increases. Humphrey[40] rarely found more than one
recrystallisation nucleus for particles <5 µm diameter, whereas English
and Backofen[16] observed multiple nucleation at particles >10 µm
diameter. The strain is also likely to effect multiple nucleation at a
particle because of the more complex and inhomogeneous strain
distribution in the deformation zone near to the particle. Particles
which are close together may form joint deformation zones. If a nucleus
occurs within this zone, it can grow to a larger size than would be the
case for a single particle[41].

It is difficult to separate the effects of the particle size and

particle spacing because in much of the published work these parameters are not varied independently. A detailed list of investigations has been compiled by Cotterill and Mould[42], and these authors[43] combined their data for recrystallisation in aluminium-iron alloys with that of Doherty and Martin[44] for recrystallisation of aluminium-copper alloys, Fig. 14, to construct a fairly complete set of data for alloys containing particles.

A detailed examination by Davidson and West[45] showed that recrystallisation in steels is retarded by fine particles of Nb(CN) which were close together, Fig. 15, particularly if less than 0.01 μm in diameter. These investigations assumed that the second phase particles were non-deformable. On the other hand Kamma and Hornbogen[46] have shown different effects using a hypo-eutectoid steel. If the particles were small they shear at intermediate strains of 50-70 per cent. This further refined the particles and recrystallisation of such structures was further delayed, Fig. 16. The shearing of small particles can lead to microscopic inhomogeneity of strain by the concentration of the strain into deformation bands. This effect favours the formation of nuclei for recrystallisation. At higher strains $\varepsilon \simeq 80\%$ deformation bands broaden and the strain becomes more homogeneous so that recrystallisation is retarded still more in comparison with medium size particles.

2.6.3 Recrystallisation in Iron and Steels

It has been reported[47] that commercial purity iron recrystallised more slowly when heated to higher temperature prior to cold deformation. Leslie et al[48] observed that aluminium nitride in steel retarded recrystallisation. This occurred only if precipitation has taken place prior to or during the very early stages of recrystallisation.

Le Bon et al[49] showed that precipitation of niobium carbonitrides from the austenite in HSLA steels reduced the recrystallisation rate after straining at temperatures corresponding to those of industrial hot working processes. The rate of recrystallisation in austenitic stainless steel increases

CHAPTER 3 **GRAIN GROWTH**

The process of primary recrystallisation is considered to be completed when the recrystallised grains have impinged. At this stage the metal has a minimum grain size, but the relatively high internal energy of the deformed state has been removed by primary recrystallisation. The resulting structure is however still metastable and a further reduction in overall energy can be achieved by a reduction of the total grain boundary area. A continuation of annealing thus leads to further migration of grain boundaries, thereby resulting in grain growth. Grain growth can be classified as :-

(i) normal or continous grain growth, characterised by the maintenance of an approximately uniform grain structure, in which the distribution of the grain size and shape remains constant throughout the specimen, but in which the average grain size increases.

(ii) abnormal or discontinuous grain growth, also known as secondary recrystallisation, characterised by the growth of selective grains at the expense of their neighbours.

3.1 Normal Grain Growth

It has long been recognised that grain boundaries tend to migrate during grain growth so as to decrease their curvature. Normal grain growth occurs by the migration of grain boundaries consistent with the need to minimise the resultant boundary tensions. Curved grain boundaries migrate towards their centres of curvature during grain growth, contrary to the direction which occurs during the growth stage of primary recrystallisating grains.

3.1.1 Kinetics of Normal Grain Growth

Beck et al[50,51] were the first to show experimentally that during isothermal annealing conditions grain growth was described by :-

$$D_g = Kt^n \qquad\qquad 29$$

36

where D_g is the average grain diameter at any time t, during grain growth, and K and n are constants which depend on the alloy composition and on the annealing temperature but which are independent of the grain size. This relationship applies best if the initial (pre-growth) grain size is small compared with the grain size which is being measured during growth. Beck et al[50,51], in order to avoid the uncertainty of the time at which grain growth started, suggested that the phenomenon could better be expressed in a more general form :-

$$D_g^{1/n} \quad - \quad D_{g(o)}^{1/n} \quad = \quad ct \qquad\qquad 30$$

where $D_{g(o)}$ is the initial pre-growth grain diameter,
  and c is a constant which contains a temperature dependent
      mobility term and the grain boundary energy.

An alternative derivation has been suggested by Burke[52] who formalised the concept that grain boundary curvature is the controlling factor in normal grain boundary migration because:-
  1. grain boundary migration occurs by the transfer of atoms
      across the boundary,
  2. the rate of migration is proportional to the reciprocal of
      the boundary's radius of curvature,
  3. the radius of curvature of a boundary is proportional to
      the grain diameter,
and 4. the specific interfacial energy of a migrating grain
      boundary does not vary during the course of grain growth.

In Burke's[52] analysis the temperature dependence of normal grain growth arises from the temperature dependence of the grain-boundary mobility and includes a temperature factor within the rate constants of the isothermal growth equation :-

$$\frac{dD_g}{dt} = \frac{C_1}{D_g} \exp - \frac{Q_g}{RT} \qquad\qquad 31$$

and

$$D_g^2 - D_{g(o)}^2 = 2 C_1 t \exp - \frac{Q_g}{RT} \qquad 32$$

where C_1 is a constant which includes the grain boundary specific interfacial energy, and Q_g is the activation energy of migration. A careful analysis suggests the need for the introduction of a velocity independent drag component[53] into the grain boundary migration equation. This drag was found to depend on the composition of the metals and on the annealing temperature, and it accounts for the observed deviation from the ideal behaviour predicted by the equation 29, i.e. n is not constant.

3.1.2 Hillert's Theory of Normal Grain Growth

Hillert[54] gave a theoretical treatment of grain growth in terms of the behaviour of individual grains within a distribution of grain sizes. The analysis was based on the following assumptions :-

1. the grain boundary migration rate is proportional to the pressure difference caused by its curvature and hence is proportional to the reciprocal of its radius of curvature,
2. the rate of grain growth is proportional to the rate of grain boundary migration,
3. there is a critical grain size for the grain growth to occur, such that grains larger than this size will grow and grains smaller than this size will be eliminated,
4. the grain size of any particular grain can be described by the radius of an equivalent circle or sphere having the same area or volume as the grain.

On the basis of these assumptions, the following expression was developed for the rate of grain growth:-

$$\frac{dR}{dt} = \alpha M \gamma \left(\frac{1}{R_{cr}} - \frac{1}{R} \right) \qquad 33$$

where α is a dimensionless constant,

  M is the grain boundary mobility,

  γ is the grain boundary specific interfacial energy,

R   is the radius of the growing grain, and

R_{cr} is the critical grain radius for growth to occur.

Hillert[54] also suggested a more simple relationship for normal
grain growth :-

$$\frac{d(R_{cr}^2)}{dt} = 0.5 \, \alpha \, M \, \gamma \qquad\qquad 34$$

Hillert's theory predicts that stable growth occurs in a steady-state
grain size distribution which is maintained as the average grain size
increases. For practical purpose the average grain size, compared with
the maximum grain size, is about 1.8R in a three-dimensional system and
1.7R in a two-dimensional system. If the initial grain size range lies
wholly within Hillert's distribution, grain growth will occur uniformly
through the specimen. However if the initial grain size range is wider
than Hillert's distribution, those grains having a radius which is
larger than 1.8 times the average value will be unstable and will grow
abnormally at the expense of the remainder until impingement takes
place. This suggests that abnormal grain growth may sometimes be
necessary in the development of normal grain growth.

3.2   Abnormal Grain Growth

Abnormal grain growth or secondary recrystallisation is a deviation
from normal grain growth such that a small number of selective grains
tend to grow by consuming their neighbours. The growth is non-uniformly
distributed within the specimen. The resultant structure prior to
abnormal grain growth may be produced by some normal grain growth,
which should continue until all the grain boundaries had been removed,
but in practice usually ceases when one of the various forms of grain
boundary pinning becomes operative.

3.2.1   Kinetics of Abnormal Grain Growth

The driving force for grain growth, normal or abnormal, in an alloy
containing dispersed particles effectively consists of two components;

a term which represents the reduction in the total interfacial energy associated with the grain boundaries and a term which represents the pinning effect of the dispersed particles.The former acts to promote grain growth whilst the latter opposes it. Normal grain growth is therefore inhibited when grain boundary pinning by the dispersed particles exceeds the driving force for grain growth. This interaction was first considered by Zener, and subsequently analysed further by Hillert[54] and Gladman[57].

In an attempt to offer a quantitative treatment of grain growth in dispersion containing alloys, Smith[55] suggested that if a moving boundary encounters a rigid and insoluble particle it will locally cling to it, causing a cusp in the surface , until the motion of the grain boundary elsewhere has proceeded sufficiently to cause it to break away. If there is a sufficient number of particles, the grain boundary will be unable to move. Several theoretical models have been proposed:-

    1. Zener's model [56]
    2. Hillert's model[54]
    3. Gladman's model[57].

3.2.2 Zener's Model

The driving force (P_r) for grain growth is provided by surface tension :-

$$P_r = \frac{\gamma}{R} \qquad\qquad 35$$

where γ is the surface tension

   R is the radius of curvature of the grain boundary.

The retarding force exerted by a particle of radius r is:-

$$P = 2\pi r \gamma \sin\theta\cos\theta \qquad\qquad 35a$$

where θ is the angle between the average surface of the grain boundary and the surface at the point where it joins the inclusion. For the

maximum restraining force, $\theta=45^{\circ}$ and $\sin\theta\cos\theta = 0.5$. Therefore :-

$$P_{max} = \pi r \gamma \qquad\qquad 35(c)$$

If N is the number of particles of radius r randomly distributed per unit volume, the volume fraction of these particles is $f/(4/3\ rN)$ where f is the fraction of the total volume occupied by the particles within the volume 2rN. Hence the number of particles intersecting per unit boundary area (n), is given by :-

$$n = \frac{3f}{2\pi r^2} \qquad\qquad 36$$

So the retarding force, P_u per unit area of boundary is

$$P_u = \frac{3f\gamma}{2r} \qquad\qquad 37$$

If the boundary is migrating under the influencing of its own interfacial tension and has a radius of curvature R_o, then the driving force for grain growth is $2/R_{crit}$. At equilibrium, a balance of forces occurs and Zener[56] proposed the relationship :-

$$R_{crit} = \frac{4r}{3f} \qquad\qquad 38$$

The assumptions made in this model are that the particles are randomly distributed as uniform spheres, that the particle-matrix interfacial energy is independent of matrix orientation, the boundaries are randomly positioned and that each particle exerts the maximum restraining effect on the movement of the boundary.

Zener[56] derived equation 38 for condition in which the driving force is the reduction of total grain boundary energy. It was suggested that

41

growth will eventually cease when the retaining force exerted by the particles on the boundary equals the driving force for boundary migration.

3.2.3 Hillert's Model

When a grain boundary moves through the matrix containing second-phase particles, there is a tendency for the grain boundary to adhere to the particles. Zener[56] suggested that for particles of uniform size r and a total volume fraction f, a hypothetical back stress would act at the grain boundary of magnitude $P_u = 3f/4r$ or $P_u = Z$ which is independent of the boundary curvature. Z is the ratio of the growing grains (R) to that of the matrix (R_o). According to Hillert[54] this may not be true. Taking into account the effect of the particle, the rate of grain growth becomes

$$\frac{dR}{dt} = M\left(\frac{1}{R_{cr}} - \frac{1}{R} \overset{+}{\underset{-}{}} \frac{Z}{\alpha}\right)$$

39

α = a dimensionless constant.

The sign must be chosen in each such that the back stress P_u is acting against the movement of the grain boundary. The negative sign holds when $1/R < 1/R_{cr} - Z/\alpha$ and the positive sign when $1/R > 1/R_{cr} + Z/\alpha$. Within this range dR/dt = 0. A steady state solution cannot be found because the second phase particles become ever more important as the grain size R_{cr} increases. For grain growth to occur the driving force should be positive. This is given by $1/R < 1/R_{cr} - Z/\alpha$ therefore $1/R_{cr} - 1/R > Z/\alpha$. There will be a range of grain radii R_1 and R_2 for which grains will neither grow nor shrink. In a dispersion containing alloy grain growth is restricted to those grains larger than R_2 (which is larger than the minimum radius for growth in the absence of dispersed particles, i.e. R_{cr}). R_2 increases as normal grain growth proceeds and fewer grains are able to grow. However, for any given average grain size the value of R_2 will increase if either the particle volume fraction is decreased or the particle size is increased. If normal grain growth has been inhibited and the particle dispersion characteristics are altered in

42

either or both ways mentioned above, then grains larger than R_{2cr} will be able to grow, the remainder will not.

3.2.4 Gladman's Model

While Hillert[54] assumed that the grains could be represented as spheres, Gladman's[57] treatment was based on the more realistic tetrakaidecahedral grain shape. Gladman considers the energy of the system to be increased by the increase in grain surface area as the grain boundary pulls away from its pinning particles and also that the energy of the system is decreased by the elimination of the interfaces of the grains which are absorbed by the growing grain. The area of grain boundaries eliminated, by growth of the grain from a radius R to a radius R+s is:-

$$A_e \simeq \frac{3s}{2R_o} \qquad\qquad 40$$

where R_o is the mean radius of the grains or radius of the inscribed circle in the tetrakaidecahedron. The grain also increase its own area of boundary

$$A_c \simeq \frac{2s}{R} \qquad\qquad 41$$

The net change in area A_n is given by:-

$$A_n = s\left(\frac{2}{R} - \frac{3}{R_o}\right) \qquad\qquad 42$$

when $R/R_o < 1.33$ there is an increase in boundary area and when $R/R_o > 1.33$ there is a decrease in grain boundary area. Therefore if $R/R_o = Z$, the energy during grain growth is :-

$$E_n = \frac{S\gamma}{R_o}\left(\frac{2}{Z} - \frac{3}{2}\right) \qquad\qquad 43$$

If the migrating grain boundary encounters a dispersed particle, there will be $2rn_u$ particles per unit grain boundary area, where n_u is the number of particles per unit volume. The energy release per particle due to grain growth, E_1 is:-

$$E_1 = E_n/2rn_u \qquad\qquad 44$$

or

$$E_1 = \frac{2S\alpha r^2\gamma}{3R_o f}\left(\frac{2}{Z} - \frac{3}{2}\right) \qquad\qquad 44a$$

where f is the volume fraction of the particles of radius r and $f = 4/3n_u\pi r^3$.

Thus the total energy change associated with the unpinning from a single particle, E_T, is:-

$$E_T = E_P + E_1 \qquad\qquad 45$$

where E_P is the pinning energy. He further suggested that the grain boundary will be able to migrate if the energy released per particle by the migration is equal to or greater than the energy released which is associated with the boundary-particle unpinning process. The magnitude of the energy released, during the unpinning process is a function of the particle size and volume fraction of the precipitates. It becomes inevitable to assume that there is a critical particle radius for unpinning the grain boundaries at which thermally initiated grain boundary release can occur.

Thus the critical particle size r_{cr} may be calculated if the boundary migration is completely particle inhibited. Gladman[57] showed r_{cr} to be :-

$$r_{cr} = \frac{6Rf}{\pi}\left(\frac{3}{2} - \frac{2}{Z}\right)^{-1} \qquad\qquad 46$$

It can be seen from Eqn 43, the controlling factor for grain growth is the value Z. In normal grain growth, all grains which produce negative

energy changes per unit boundary area per unit distance travel, will grow. As all grains are pinned initially and as the Ostwald ripening of the particles is a continuous process, the largest grain will be unpinned first. The rate of growth will then accelerate as Z increases.

In summary, each theory described, predicts a relationship between the overall grain structure, the size and quantity of dispersed paricles and the occurrence of abnormal grain growth. According to Hillert's[54] theory abnormal grain growth arises from the selective growth of the largest grains, within a non-uniform grain size distribution which has been produced as the result of the influence of the dispersed particles on normal grain growth; the growth process being selective as the particle volume fraction decreases and or as the particle size increases. Alternatively, according to Gladman's[57] theory abnormal grain growth is controlled by the ability of a grain boundary to migrate away from the dispersed particles which are larger than a critical minimum size, whether the initial grain-size distribution is uniform or not.

Gladman and Pickering[58] have shown that the particle dispersion characteristics associated with the onset of grain coarsening in aluminium and Nb steels correspond very closely with those predicted by Gladman's unpinning theory. The unpinning mechanism is controlled by particle growth rather than by particle dissolution.

In recent work on Al-killed vanadium steels Amin and Pickering[59] found close correlation between the calculated and observed grain coarsening temperature,but the controlling factor was the growth of vanadiun nitride at temperatures below $1000^{\circ}C$ whereas for temperatures greater than $1000^{\circ}C$ the growth of aluminium nitride was the controlling factor.

A major problem in the study of austenite deformation in plain carbon steels is the allotropic transformation which renders it difficult to observe readily the austenite structure present during and after the thermo-mechanical treatments. Consequently many investigators have used a direct method for studying the deformation and restoration processes, based on the load measurement during hot deformation. The three major methods[60] used are the hot compression, hot tensile, and hot torsion test, the result being translated into true-stress true-strain curves with the aim of relating these to the behaviour[61] of steel during the thermo-mechanical processing.

The relative influence of microalloyed additions, the nature of precipitation prior to deformation, deformation above and below the transformation temperature, and precipitation during or after deformation, on the primary or secondary recrystallisation has been under dispute for some time[62-65]. The effect of thermo-mechanical processing and recrystallisation should be carried out in such a way that it can be utilised during the austenite/ferrite transformation and on subsequent cooling to obtain the finest ferrite grain size. Factors which are likely to affect the microstructure prior to or during transformation are the reheating temperature before deformation, the amount and rate of deformation, the rate of recrystallisation of austenite, and the finishing deformation temperature.

4.1   Re-Heating Prior To Deformation

The whole purpose of controlled rolling is to condition the austenite such that there are very many nuclei for ferrite nucleation, so that during the subsequent transformation of the austenite, a very fine ferrite grain size is produced. It is now accepted that a fine austenite grain size prior to controlled rolling is beneficial because :-

(i)   even when controlled rolled so that recrystallisation of
       the deformed austenite takes place, the recrystallised
       grain size is very fine due to the fact that

recrystallisation occurs predominantly at the deformed
austenite grain boundaries. Hence the subsequent ferrite
grain size is fine.

(ii) if the steel is rolled in the regime where austenite
recrystallisation does not take place, the elongated or
'pancaked' grains are very thin and hence result in fine
ferrite grains after transformation.

Thus it is essential to understand the factors which control the
austenite grain size during reheating, and in particular the austenite
grain coarsening temperature. In the absence of carbide/nitride
particles which pin the austenite grain boundaries, the austenite grain
size inceases progressively with increasing temperature. If however the
grain boundaries are pinned by carbide/nitride particles of the
microalloying additions such as Nb, V, Ti, or Al, the grain size
remains fine until the grain coarsening temperature at which some
boundaries become unpinned and localised grain growth occurs. This is
sometimes called secondary recrystallisation. It is normally observed
that this grain coarsening temperature often occurs below the
temperature at which the carbides/nitrides are fully dissolved[66-68],
because of the growth of the particles by Ostwald Ripening which
reduces their pinning potency. A model has been proposed[58], based
upon the Gladman model[57] for grain boundary pinning which allows the
grain coarsening temperature to be estimated.

A demonstration of the complex conditions which govern the grain size
during reheating before deformation is demonstrated by Webster and
Allen[69] Fig. 17. During the reheating of low alloy vanadium steel,
the precipitates both dissolve and coarsen. With rapid heating the
resulting fine precipitates can pin the austenite grain boundaries and
produce a fine austenite grain size. At slower heating rates more
dissolution of precipitates takes place as equilibrium is more nearly
achieved, but the precipitates also have more opportunity to grow so
that grain coarsening is observed at lower temperatures. At even slower
heating rates which allows the precipitates to coarsen even more
readily, marked secondary recrystallisation is observed. This example
can simulate an industrial practice in which a fast heating rate is

applied on the surface and a much slower heating rate occurs in the centre of the large ingot hence producing wide variations in the prior austenite grain size.

4.2 Amount of Deformation

It is well accepted that the main sites for ferrite nucleation are the austenite grain boundaries. Apart from the deformation temperature, the amount of deformation contributes to the maximising of the grain boundary area and thus of the number of ferrite nucleation sites.

It has been shown that at high deformation temperatures above the recrystallisation temperature, the recrystallised grain size depends on the amount of deformation[70,71]. DiMiccio and Davenport[72] examined the effect of rolling reduction on the austenite grain size with microalloy additions of V, Nb, Al and nitrogen, and showed that in agreement with other workers[73] increasing the reduction per pass above the recrystallisation temperature caused the austenite grain size to be refined even further. Thus, the austenite grain size decreases as the amount of reduction increases[74] Fig. 18. A critical amount of deformation, however is required to initiate recrystallisation, otherwise strain induced boundary migration will commence giving rise to abnormal grain growth in certain places[75] and the formation of inhomogeneous microstructures which can not subsequently be eliminated. Additions of microalloying elements increases the critical amount of deformation and its dependence on grain size and deformation temperature. The critical amount of deformation required for completion of recrystallisation[74] in plain carbon and niobiun steels is shown in Fig. 19.

Complete recrystallisation at low temperatures leads to refined austenite structures. Further deformation leads to highly elongated austenite grains if the deformation temperature is below the recrystallisation temperature. It has also been shown[76] that in vanadium steels deformed at low temperature and then held, recrystallisation increases as time proceeds. Increasing the amount of deformation increase the volume fraction of austenite recrystallised at any given time and temperature. On the other hand increasing nitrogen

48

content decreases the rate of austenite recrystallisation. At lower reheating temperatures, increases in nitrogen and the amount of deformation have the same effect. Lower reheating temperatures increase the area of grain boundary per unit volume, $S_{V\gamma}$[59] and consequently increase the number of recrystallisation nucleation sites and thus the volume fraction of recrystallised austenite.

A recent application of the control of the austenite grain size prior to controlled rolling is the so called recrystallisation rolling treatment in which very fine particles of highly stable TiN are used to produce a fine austenite grain size[77]. This initial structure can then be rolled at fairly high temperatures and recrystallised to very fine austenite grains which do not grow due to the pinning effects of the TiN particles. Moreover the structure, not being developed in the non-recrystallised or partially recrystallised regime, (see later) does not produce the detrimental inhomogeneous or mixed grain sizes.

4.3 Recrystallisation of Austenite

The conditioning of austenite by thermo-mechanical processing prior to transformation is a major aim in order to produce the finest possible ferrite grain size after transformation. Conditioning of austenite involves not only control of the austenite grain size and shape but also the defect structure resulting from deformation, recovery or recrystallisation which may be influenced by the addition of microalloyed elements. The recrystallisation of plain C-Mn steel is very rapid, even at low temperatures, and conditioning prior to transformation can be extremely difficult. The addition of microalloyed elements can retard recrystallisation by either, at high temperatures, a solute drag effect or at lower temperature by precipitation of microalloy carbides/nitrides, which may be influenced by the strain rate[78]. Recrystallisation can occur either under dynamic or static conditions.

The effect of vanadium on the recrystallisation of austenite will be discussed in relation to :-

        (i)   rate of recrystallisation,

        (ii)   nucleation,

and (iii) growth of recrystallised austenite.

4.3.1 Rate of Recrystallisation

The rate of recrystallisation of austenite is determined by the
microstructure which is developed, and is controlled by the temperature,
strain, strain rate and the presence of carbide/nitride forming
elements. High temperature deformation is associated with a marked
increase in the recrystallisation rate and as a consequence uniform
recrystallised grains are produced. On the other hand low temperatures,
in the presence of microalloying elements, are associated with much
retarded recrystallisation rates and the formation of highly elongated
unrecrystallised austenite grains.

Varying the homogenisation temperature varies the amount of microalloy
in solution and subsequently the initial austenite grain size. Amin[76]
and Amin and Pickering[79] have shown that raising the reheating
temperature prior to deformation by increasing the austenite grain size
and dissolving microalloying carbides/nitrides, retards
recrystallisation, but increasing the amount of microalloying element
delays recrystallisation even further. Similar work showed that
increasing the amount of deformation accelerates the recrystallisation
rate.

In the early stages of the development of microalloyed steels[80, 81]
it was observed that regions of large ferrite grains occurred in a
matrix of very fine grains. This was attributed to partially
recrystallised austenite produced during the initial rolling. Mixed
ferrite grain sizes can be eliminated by using higher temperatures for
the roughing-hold-finishing rolling sequence with increased holding
time to allow for complete recrystallisation to occur. During high
temperature rolling (roughing) recrystallisation takes place to form
large recrystallised grains, but with lower temperature rolling partial
recrystallisation occurs at the large prior-deformed austenite grain
boundaries. Because of the retarded rate of recrystallisation, and the
insufficient holding between rolling passes for complete
recrystallisation to occur, mixed austenite grain sizes are developed
which result in a mixed ferrite grain size.

The sluggish recrystallisation of austenite in Nb steels below 1100°C was associated with the precipitation of NbC in the austenite[81]. This precipitation was much coarser than that observed in ferrite and appeared as networks which cut across ferrite boundaries. The coarse precipitates were thought to occur at recovered sub-boundaries in the deformed austenite, and to retard recrystallisation by inhibiting the migration of the sub-boundaries.

Smaller initial austenite grain sizes[82] markedly increase the recrystallisation rate due to the increased number of nuclei, consequent upon the increased grain boundary area. Increasing niobium content also increased the rate of recrystallisation by particle stimulated recrystallisation resulting from large undissolved Nb(CN) precipitates. Similar effects were observed in vanadium steels[76] but an increase in vanadium content above 0.14% had little further effect on the recrystallisation rate.

4.3.2 Nucleation

Recrystallisation mainly nucleates at the prior austenite grain boundaries as shown by Kozasu et al[71] who found that, nucleation can also take place at non-coherent twin boundaries, deformation bands and at the interface between recrystallised and unrecrystallisation regions (sympathetic nucleation)[71, 76, 83]. It was observed that not all the grain boundaries acted as nuclei.

In aluminium killed C-Mn steel, it has been shown that nucleation can occur by many mechanisms, including sub-grain coalecence[84], strain-induced boundary migration[76, 85, 86] and bulge nucleation[12]. During deformation a concentration of dislocations occurs adjacent to grain boundaries, forcing the grain boundary to become serrated. The serrations may act as nucleation sites[87]. Strain induced boundary migration has been observed[86] with low reduction less than 8%, whilst other investigators[85] have suggested that large austenite grain sizes accompanied by large deformations produce the same effect at high temperature.

51

Substitutional solute elements delay recrystallisation[78] by
inhibiting the migration of dislocations, i.e. recovery. Cordea and
Hook[88] examined systematically the effect of vanadium on the
recrystallisation of austenite. The inhibition of austenite
recrystallisation decreased with increasing holding temperature from
825°C to 930°C at 0.059%V. Decreasing homogenisation temperature
increased the recrystallisation rate. This was attributed to smaller
grain sizes, produced by lower heat treatment temperatures,
accelerating recrystallisation.

Vanadium in solution[87, 89] delays dynamic recrystallisation.
Recrystallisation at 900°C in 0.1%V steels was initially rapid but
slowed down after isothermal holding due to the formation of fine VC/VN
precipitates. A further increase in vanadiun content to 0.2% suppressed
static recrystallisation. Increasing the deformation temperature
increased the recrystallisation rate, which was still slower than for
plain carbon steels. This latter decrease was attributed to vanadium in
solution, no precipitation being observed.

Akben et.al.[78] have studied the recrystallisation kinetics and the
effect of solute and precipitation in more detail. It was shown that
the strengthening due to dynamic precipitation can be separated from
that of solute by employing different strain rates. A dynamic
precipitation time temperature (PTT) diagram was constructed, Fig. 20,
together with a recrystallisation diagram, Fig. 21. When the two
diagrams are combined, Fig. 22, it is possible to separate
precipitation effects from recrystallisation and show that
recrystallisation became retarded when it is preceded by precipitation.
They also showed that precipitation of VN takes place just below 900°C,
but this temperature depends on the carbon, nitrogen and vanadium
contents.

Similar conclusions were reached by Yamamoto et. al. [90] who showed
that vanadium in solution retarded recovery in deformed austenite and
consequently delayed the onset of recrystallisation, but did not greatly
influence the progress of recrystallisation once it had started.

4.3.3   Growth of Recrystallised Austenite

The austenite grains produced by recrystallisation will naturally grow unless accelerated cooling is employed. The growth will depend on the holding temperature, and whether the microalloying elements are in solid-solution or as precipitates in the recrystallising matrix. Particles precipitated prior to deformation will offer little or no barrier to the growth of recrystallised grains, but if precipitation has taken place during or after deformation, the precipitates will control the grain growth until coarsening of precipitates takes place as explained in section 3.

The study of grain coarsening during isothermal holding after rolling was investgated by Amin[76]. He showed that the presence of niobium inhibited the coarsening of the recrystallised austenite grain size. This inhibition was more pronounced at lower holding temperatures. The coarsening time depended on the niobium content and the amount of deformation prior to isothermal holding. A similar effect was observed for vanadium steels, in which grain coarsening occurred progressively up to a holding time of 15 minutes at high temperature, but at lower temperature no grain coarsening was observed. This latter effect might have been due to the presence of AlN[59, 91] because the steels used were Al-killed.

A critical microalloying content is known to exist at which grain coarsening can be inhibited for short times at the recrystallisation temperature. Amin[76] found that, a high niobium content was needed for low carbon low manganese steels compared with the results of Tanaka[86] who used higher carbon higher manganese steels. Similar effects can be achieved by addition of a second microalloyed element, e.g. vanadium.

Tanaka[86] and Dimiccio and Davenport[72] both show that recrystallisation only occurs above a certain amount of applied deformation, which depends on the initial austenite grain size and on the deformation temperature. With small deformations however, so few recrystallised nuclei are formed such that very large grains may result, which can persist during rolling and on subsequent transformation form bainite rather than polygonal ferrite, with a

consequent detrimental effect on the mechanical properties.

4.4 Finishing Deformation Temperature

Microalloyed additions give rise to three kind of regimes in which controlled rolling can take place[61-65]:-

      1 Recrystallisation at high temperatures,

      2 Partial recrystallisation,

      3 No recrystallisation at low temperatures.

Although there is no clear borderline between the three regimes due to inhomogeneity of deformation, it is accepted that high temperature recrystallisation takes place rapidly whilst at low temperatures just above the α/γ transformation temperature, recrystallisation is quite slow. At intermediate temperatures, partial recrystallisation occurs, the recrystallised grains being observed mainly around deformed austenite grain boundaries.

Rolling in the high temperature regime results in the complete and rapid recrystallisation of austenite in the C-Mn stels, and whilst solute drag effect due to microalloying additions may retard recrystallisation somewhat, the effect is not large. Thus even microalloyed steels, using Nb or V, are completely recrystallised during rolling at high temperatures. In the low temperature rolling regime, again in the absence of microalloying additions, i.e. in plain C-Mn steels, recrystallisation is also rapid, but of course not so rapid as at high temperatures. It is in this regime, when microalloying additions give rise to strain induced precipitation and retard greatly recrystallisation, that rolling can produce completely unrecrystallised austenite which exists as very elongated grains.

In the intermediate temperature range between these two extremes, partial recrystallisation can occur during rolling and give rise to fine recrystallised austenite grains, at the boundaries of coarse, elongated unrecrystallised grains. It is this latter condition which can be deleterious and must be avoided, because it gives rise to a mixed ferite grain size originating from transformation of the two separate type of austenite morphology, i.e. recrystallised and non-recrystallised. A mixed ferrite grain size is particularly detrimental

to toughness. Even lower rolling temperatures can cause ferrite to form during rolling, giving rise to elongated bands of ferrite which may or may not themselves be recrystallised depending on the rolling conditions and whether the steel contains microalloying additions which delay the recrystallisation of the deformed ferrite. Again this type of rolling, within the critical range, can lead to very mixed grain sizes, as shown by Amin[79].

4.5 Inhomogeneity of Microstructure During Hot Working

The microstructural inhomogeneity of a controlled rolled steel will depend on the deformation reduction, temperature and strain rate which control the time required for recrystallisation. In addition the form and distribution of the second phase particles such as microalloyed carbides/nitrides will be important in controlling the rate of recrystallisation. Inhomogeneity of both composition in the steel and of deformation during controlled rolling will also play a significant part in the homogeneity of the resulting structure[92].

At high deformation temperatures austenite refinement can only be attained at high deformations which result in complete rather than partial recrystallisation[86], for a given initial austenite grain size. Holding at such a temperature, allows the recrystallised austenite grains to grow and with longer holding times some abnormal grain growth occurs as certain grain boundaries become unpinned due to coarsening of any pinning precipitates. The critical time for the onset of abnormal grain growth decreases with decreasing grain size as indicated by grain coarsening theories[57] but may be increased with increasing volume fraction of pinning precipitate particles.

With reductions less than the critical value for partial recrystallisation, grain coalescence instead of grain refinement occurs and so few recrystallisation nuclei are produced, that grains larger than the initial grains can be formed. Once large grains are formed, they may persist throughout the whole of rolling, whereas, smaller grains tend to recrystallise. Hence the inhomogeneity of grain size is perpetuated.

During deformation the austenite forms elongated grains with serrated grain boundaries and containing deformation bands. Strain distribution within these deformed grains has been investigated[92-94] and a satisfactory model for the formation of recrystallisation nuclei under such conditions has been proposed[95]. It is possible to observe where recrystallisation nuclei are formed in the inhomogeneously deformed structure by studying the progress of recrystallisation during holding after rolling. The initial recrystallisation nuclei appear to be highly localised[82], forming predominantly at the austenite grain boundaries[16, 78, 82] and frequently being observed at the intersection of the three grains. Deformation bands, deformed twin boundaries and inclusions may also provide effective nucleation sites[59,96]. Sometimes highly serrated austenite boundaries are found, which also act as nucleation sites for recrystallised grains[59, 82].

During the early stages of recrystallisation, growth of the recrystallising grains occurs along the original deformed grain boundaries but at a later stage, when impingement prevents continual growth along the grain boundary the recrystallised grains become equiaxed. Fine strain induced precipitates, which occur inhomogeneously in the matrix and mainly at the most highly deformed regions within the deformation bands or near to the original deformed grain boundaries, will inhibit growth of the recrystallising grains. Consequently new recrystallisation nuclei are observed to be activated on the surfaces of existing recrystallised grains[59], and because these grow into regions where there are no strain induced precipitates they tend to grow to larger sizes and give rise to a further form of the inhomogeneous recrystallised structure.

5.1   Solubility of Vanadium Carbide/Nitride

The great affinity of vanadium for carbon and nitrogen and the limited solubility of these phases in austenite and particularly in ferrite can be exploited to influence the properties and transformation characteristics of steels. Many of the effects observed have been explained fully in recent reviews[97, 98]. The effects observed are related to the temperature dependence of the solubility of the phase[99, 100], the formation of precipitates in the austenite during thermo-mechanical treatment and its effect upon austenite recrystallisation, the solubility for the phase between austenite and ferrite, the precipitation of vanadium carbides/nitrides during or after the transformation of the austenite, and of course to the intrinsic difference in solubility between VC and VN, the latter being much smaller than the former[106].

5.1.1 Solubility of Vanadium Carbide

The high solubility of vanadium carbide in austenite leads to precipitation during and after transformation of austenite, which gives precipitation strengthening. In addition, due to decreasing solubility of VC with decreasing temperature, VC may be strain induced to precipitate in austenite during and after thermo-mechanical treatment, but only at the relative low temperature of 850°C[77]. Even in steels quenched from the austenite region, to form martensite, VC precipitates during tempering at 550-600°C to produced the well known secondary hardening effect.

The solubility of V_4C_3 in austenite was determined by Bungart et. al.[99], using the then accepted formula of V_4C_3:-

$$\log [V] [C]^{0.75} = - \frac{7670}{T} + 4.92 \qquad\qquad 47$$

Graphical representation of this equation is given in Fig. 23. Narita[100] gave a slightly different solubility relationship in high purity iron:-

$$\log [V] [C] = - \frac{9500}{T} + 6.72 \qquad 48$$

Based on experimental values Wriedt and Hu[101] used a thermodynamic analysis method to calculate the solubility of V_4C_3 in austenite which was :-

$$\log [V] [C]^{0.75} = - \frac{6560}{T} + 4.45 \qquad 49$$

The solubility of V_4C_3 in ferrite has been determined by Sekine et. al.[102] as :-

$$\log [V] [C]^{0.75} = - \frac{9404}{T} + 4.65 \qquad 50$$

and also by Chino and Wada[103] as :-

$$\log [V] [C]^{0.75} = - \frac{10000}{T} + 7.06 \qquad 51$$

Roberts and Sandberg[106] reported the solubility as in γ that of VC :-

$$\log [V] [C] = - \frac{9500}{T} + 6.72 \qquad 52$$

Calculation of the heats of solution of vanadium carbide in alpha and gamma iron have been made by Chino and Wada[103] from the solubility measurements and are reported to be :-

$$\Delta G_{(\alpha)} = - 119662.2 + 89.96T \quad KJ/mol$$
$$\Delta G_{(\gamma)} = - 81169.6 + 92.93T \quad KJ/mol$$

Alloying additions which decrease the activity coefficient of carbon, increase the solubility of vanadium carbide. This is shown in the case of manganese by work of Kogan and Entin[104].

5.1.2. Solubility of Vanadium Nitride

Vanadium Nitride has a considerably lower solubility in austenite than vanadium carbide, and thus can produce grain refinement effects. The

solubility was originally investigated by Fountain and Chipman[105]
in α and γ iron.

The solubility of vanadium nitride in γ-iron was :-

$$\log [V] [N] = - \frac{7070}{T} + 2.27 \qquad\qquad 53$$

Narita[100] however determined a different relationship :-

$$\log [V] [N] = - \frac{8700}{T} + 3.63 \qquad\qquad 54$$

Irvine et. al.[66] on the other hand found the solubility
relationship to be intermediate between the above two values :-

$$\log [V] [N] = - \frac{8330}{T} + 3.46 \qquad\qquad 55$$

The lower solubility of VN in alpha iron compared with the gamma
iron was shown by Fountain and Chipman[105], who obtained the
relationship :-

$$\log [V] [N] = - \frac{7830}{T} + 2.45 \qquad\qquad 56$$

Roberts[106] calculated the solubility relationship for VN in
austenite using the results obtained by Irvine et.al.[66] and
obtained :-

$$\log [V] [N] = - \frac{7840}{T} + 3.02 \qquad\qquad 57$$

The solubility of VN is shown in Fig. 24.
The addition of manganese increases the solubility of vanadium
nitride[66] as is also the case for vanadium carbide. The quantitative
effect of manganese is depicted by :-

$$\log [V] [N] = - \frac{8330}{T} + 3.40 + 0.12\%Mn \qquad\qquad 58$$

The addition of 1% Mn increases the solubility product at a given
temperature by about 30 percent. It has been suggested that the
increase in solubility of vanadium nitride is a result of the activity

coefficient of nitrogen in austenite being lowered by manganese, just as in the case for the activity coefficient of carbon.

It is obvious from the above relationships that there are discrepancies in the published data. The solubilty of vanadium carbide and vanadium nitride however is much lower in ferrite than in austenite, thus the precipitation can be used either at low temperatures in austenite as a barrier to grain boundary movements or as a precipitation strengthener in ferrite when . . VC/VN is precipitated during γ/α transformation, or from supersaturated ferrite. Typical solubility curves for VC and VN in austenite are shown in Figs 23 and 24 respectively.

5.2 Methods of Precipitation Extraction

Several attempts have been made to extract microalloy carbides/nitrides either by mechanical means[107] or to analyse the phases in situ using X-Ray microanalysis coupled with either Scanning or Transmission electron microscopy. However the most effective method of separating and concentrating a particular phase is by selective dissolution of the matrix. This may be done in two ways, namely by simple chemical dissolution, . usually in an appropriate acid, or by electrolysis.

5.2.1 Chemical Extraction Methods

Chemical extraction methods[108,109] have been widely used to study the solubilities of NbC and TiC in 18%Cr 12%Ni stainless steel. Preferential chemical solution of the matrix, leaving the precipitates as an insoluble residue, was achieved in boiling 20% H_2SO_4 solution refluxed to prevent acid concentration. The risk of precipitate attack was thereby minimised, and this was aided by the use of suitable heat treatments to coarsen the precipitate particle size, and by keeping the separation time to a minimum.

Brown[110] dissolved steel turnings in 10 v/v aqueous hydrochloric acid solution to which aluminium chips had been added. The dissolution was carried out at 38°C under an argon atmosphere. After dissolution, separation of the residue is accomplished normally by centrifuging, and the residue is then washed with dilute hydrochloric acid and isopropyl

alcohol, finally being dried under argon. Analysis for carbon and nitrogen used DTA-EGA analysis, whereas for vanadium and aluminium a wet chemical method was used.

5.2.2 Electrochemical Extraction Methods

The electrochemical conditions, particularly the composition of the electrolyte and the potential, are chosen so that the matrix dissolves leaving the required phase adhering to the surface, from which it can be removed either by ultrasonic vibrations or simply by brushing. The early work in this field[111, 112] used galvanostatic methods for high alloy steels. It was recognised that potential was most important in controlling the dissolution but it was not until later that potentiostatic methods were developed.

Klinger and Koch[113] developed a more refined cell in which a specimen could be dissolved evenly and under very careful control[107, 114]. Andrews and Hughes[115, 116] suggested that optimum separation of precipitate from the matrix using the potentiostatic method occurred best at lower current densities and maximum separation voltage. The effective use of potentiostatic methods requires a provision of standard polarisation curves for the phases present in the alloy. Edeleanu[117] used potentiostatic polarisation techniques for metallographic etching and Steigerwald and Greene[118] used it for anodic dissolution of phases in binary alloys.

Pure iron exists in two allotropic forms:- the bcc α and δ iron whose solid solution is called ferrite and fcc γ-iron whose solid solution is austenite. The α form of pure iron exists below 910°C and above 1400°C whereas γ-iron is stable between 910°C and 1400°C.

Alloying elements show widely different solubilities in each of the two forms of iron, and moreover have marked effects on the temperature ranges over which the α and δ forms of iron are stable. In pure iron transformation occurs at a single temperature, but in iron alloys the two forms of $\alpha(\delta)$ and γ can occur over a range of temperatures. Alloying elements can broadly be classified into two types, namely the austenite forming elements which increase the temperature range of stability of the fcc-γ solid solution, and ferrite forming elements which increase the temperature range of stability of the α-iron solid solution.

(i) Austenite forming elements :-
     These have been classified into two types[119], Fig. 25
     both of which expand the temperature range of austenite
     stability by depressing the γ—α transformation
     temperature and raising the γ—δ transformation temperature.
     In the first type there is no intermetallic compound
     formation, and such types are formed with the elements Mn,
     Ni, Co. The second type of austenite forming element,
     however, forms a compound with iron so that a eutectoid
     transformation occurs, e.g. C, and N. Other elements which do
     not form a compound can also show a eutectoid transformation,
     e.g. Cu.

(ii) Ferrite forming elements :-
     All ferrite forming elements decrease the temperature range
     for stability of austenite, and again there are two main
     types. Some, such as Cr, Si, V, W, Mo, etc, form a closed γ-
     loop and result in the alloy becoming fully ferritic above
     certain alloy contents. Other ferrite forming elements
     strongly contract the γ phase field, but the γ-loop is not

fully closed due to the intervention of an intermetallic compound, e.g. B, S, Ta, Nb and Zr.

Andrews[120] described the overall behaviour of alloying elements thermodynamically, in terms of the difference in the enthalpy change per cent concentration of solute dissolving in γ and α.

In practice binary alloys are very rarely used, and alloying elements are added in conjuction with carbon. Vanadium, which is particularly the subject of the present work, is a strong ferrite forming element which contracts the γ-phase field to form a closed γ-loop. But vanadium is a strong carbide and nitride forming element and the VC or VN phase can be in equilibrium with either ferrite or austenite over wide temperature ranges.

6.1 Austenite Formation and Growth

Heat treatment of steel usually requires that initially it is heated to a temperature within the austenite phase field. The temperature and time of austenitising treatment is controlled so as to achieve homogeneity of composition and a specific austenite grain size.

Austenite forms during heating at three main sites[121, 122], namely :-

        (i)   from the pearlite on heating above the A_1 temperature,

        (ii) at ferrite grain boundaries,

and (iii) at the interface between ferrite and isolated or spheroidised carbides.

Growth of the austenite occurs by diffusion, and there is a partitioning of carbon to the austenite.

The formation of austenite has received little attention, and particularly the factors which lead to maximum refinement of the austenite grain size produced by heating. The relatively small amount of published information shows that austenite nucleation mainly takes place at the ferrite grain boundaries[122 - 124] in high purity

iron and in commercial mild steels. The interface between ferrite and Fe$_3$C also acts as a nucleus for the formation of austenite[122]. During heat treatment the first formed austenite nuclei are rich in carbon, the carbon content being that of the eutectoid and being achieved by partitioning of carbon to the austenite often due to the solution of the carbide at which nucleation occurs. Simultaneously the carbides also dissolve in the ferrite to achieve a ferrite composition which can be in equilibrium with the austenite. It is reported that manganese decreases the rate at which austenite is formed[123], but by depressing the A$_1$ temperature manganese can lower the temperature at which austenite forms. Growth of the austenite grains tends to be non-equiaxed, possibly due to orientation relationships developed between the austenite and the ferrite which leads to a lath-like form of the austenite grains[124]. Eventually however, impingement of the austenite grains allows an equiaxed austenite grain structure to be developed.

Other workers[125] have examined austenite formation in vanadium steels using initial ferrite or martensitic structures. Nucleation of austenite in martensite and bainite seems to occur at the prior austenite grain boundaries and also at the lath boundaries of the martensite grain or bainitic ferrite. This latter form of nucleation, results in a lath-like regions of austenite between the original bainite/martensite laths. At faster heating rates, which produce more superheating, there is greater driving force for nucleation, i.e. more austenite nuclei which results in a finer eventual austenite grain size. As the austenite grains grow and consume the ferrite, they impinge and the grain boundaries assume low energy configurations which result in a fine equiaxed austenite grain size when austenitisation is completed. Thus the greater the number of austenite nuclei, the finer will be the resultant austenite grain size, but these austenite grain sizes can then grow unless their growth is restricted by the presence of fine precipitates, e.g. AlN, which may have been formed during the $\gamma-\alpha$ transformation, or left undissolved from the original ferrite structure, e.g. NbC or VN.

In order to obtain as fine austenite grain size as possible at the austenitising temperature, and thereby good toughness and ductility in the transformed product, the grain growth of austenite should be

minimised and the grain coarsening temperature increased. The important effect of vanadium in this context has long been recognised. However, relatively little work has been reported on this effect. Erasmus[126] has studied the effect of vanadium on the austenite grain size at a constant nitrogen content, Fig. 26, and showed that only above a critical vanadium content was there marked grain refinement and a clearly defined grain coarsening temperature. Above this critical vanadium content, the grain coarsening temperature increased with increasing vanadium and at any temperature above the grain coarsening temperature the austenite grain size was refined with increasing vanadium content, Fig. 26.

The effects were attributed to growth and solution of the VN precipitates, and the increased grain coarsening temperature with increased vanadium content was attributed to the higher solution temperature of the VN. However, it was emphasised that the unpinning of the austenite grain boundaries and consequent grain coarsening always occurred below the VN solvus temperature and was attributable to the growth of the VN particles. Due to its much increased solubility and more rapid growth rate, VC was not responsible for the observed grain size effect. A similar effect was observed by Amin and Pickering[59] in vanadium steels containing both low and high nitrogen contents. These results are in agreement with the work of Konig[91] who showed the strong interaction between aluminium, vanadium and nitrogen, and indeed VN precipitation may be replaced by AlN precipitation. In fact Amin[59] attributed the apparent effect of the vanadium content on the grain coarsening temperature to a simultaneously varying aluminium content. It is clear that, the understanding of the grain coarsening characteristics in V-Al-N steels is not completely understood.

6.2 Mechanism of Austenite Transformation

Austenite is not stable at temperatures below the Ar_1 on cooling. Several different transformation mechanisms, and resulting products, may occur during continuous cooling, depending upon the steel composition and cooling rate. The most frequently encountered transformation under relatively slow rates of cooling in low alloy steels is the pro-eutectoid ferrite transformation which frequently is

followed by the formation of pearlite. At faster cooling rate, upper
bainite and then lower bainite may be formed whereas at the most rapid
cooling rates the formation of these structures is supressed and
martensite is the predominant transformation product. The
transformation of austenite in steels can be studied during either
continuous cooling or under isothermal transformation conditions at
temperatures below A_3

6.2.1 Pro-Eutectoid Ferrite Reaction

Pro-eutectoid ferrite is formed in hypo-eutectoid steels and
predominantly nucleates at the austenite grain boundaries. These are
high energy regions which offer preferential nucleation sites by
virtue of the ferrite eliminating grain boundary surface energy. The
growth of pro-eutectoid ferrite depends on the nature of the
ferrite/austenite interface, the degree of undercooling which controls
the supersaturation and also carbon diffusion away from the interface.
Pro-eutectoid ferrite can occur in two basic morphologies, grain
boundary nucleated polygonal ferrite and widmanstatten ferrite which
often can nucleate within the austenite grains, depending on the
driving force as controlled by the degree of undercooling which in turn
influences the degree of supersaturation and the transformation
temperature.

Grain boundary ferrite tends to exhibit a morphology depending on the
degree of coherency between the ferrite and austenite. The ferrite is
of lenticular shape when both interfaces are non-coherent, due to the
equilibrium developed between the interfacial tensions. On the other
hand when semi-coherent interfaces are present the ferrite grows as
laths into both adjoining austenite grains, and this is an incipient
form of widmanstatten ferrite (i.e. side-plates) which are formed with
increasing driving force at relative low transformation temperatures in
the ferrite range.

The most frequent type of grain boundary ferrite nucleation is where
the interface with one of the austenite grains is semi-coherent whereas
the other is non-coherent. The semi-coherent interface is of lower
energy than the non-coherent interface. It is usually observed that a

non-coherent interface can grow normal to itself in a non-crystallographic manner, although such an interface can attempt to lower its energy by developing facets showing some degree of semi-coherency. On the other hand, semi-coherent interfaces are relatively immobile (except at very high driving forces for the transformation) and can only move by the migration of steps or ledges along the interface. This ledged semi-coherent interfaces, typical of the planar interfaces of widmanstatten ferrite laths, result in a well developed orientation relationship between the ferrite and the austenite in which it is forming. On the other hand non-coherent interfaces show no crystallographic relationship across them.

With a small degree of undercooling, it is difficult to nucleate the ferrite because of the small driving force. Thus, ferrite nucleates at the austenite grain boundaries, and part of the energy is supplied by the elimination of the austenite grain boundary itself. However, the growth of ferrite takes place along the boundaries and also into the austenite grains with which the ferrite has a non-coherent interface (i.e. with which there is no orientation relationship) to give a well defined structure generally referred to as equi-axed ferrite.

With higher degrees of undercooling the driving force for nucleation is much higher, consequently ferrite can nucleate within the austenite grains, and form an intragranular widmanstatten lath. Such a form of nucleation will attempt to lower the energy of the system by forming semi-coherent interfaces with the austenite which accounts for the parallel sided laths, the lath interfaces being semi-coherent and thus relatively immobile. The growth of such widmanstatten plates occurs mainly lengthwise. These immobile interfaces are the habit plane of the transformation which show the Kurdjumov-Sachs orientation relationship with the austenite matrix,

$$\{110\}_\alpha \ // \ \{11\bar{1}\}_\gamma$$

$$\langle 11\bar{1}\rangle_\alpha \ // \ \langle 110\rangle_\gamma$$

The habit planes are $\{110\}_\alpha \ // \ \{111\}_\gamma$.

Widmanstatten ferrite is encouraged by large austenite grain sizes which restrict the number of grain boundary nucleation sites, and at the same time ferrite grains cannot so readily grow to impinge with other ferrite grains nucleated on the opposite austenite grain boundary. If the carbon content is greater than 0.4%, the pearlite regions are sufficiently large to prevent widmanstatten ferrite laths growing[127]. However, if the carbon content is below 0.2%, impingement of grain boundary nucleated ferrite across γ-grains again minimises the growth of widmanstatten ferrite. The widmanstatten ferrite form is enhanced during continuous cooling, by the fact that lower transformation temperatures and higher supersaturation increases the frequency of intra-granular nucleation. The lower transformation temperature the finer is the widmanstatten ferrite morphology for a given austenite grain size.

In general, many separate nuclei will occur along any austenite grain boundary, each nucleus being semi-coherent with one grain and non-coherent with the other. The growth of these nuclei will depend on the supersaturation conditions. At low supersaturation the non-coherent interface will grow but at high supersaturations the semi-coherent interface will grow. Growth by movement of the non-coherent interface will give rise to a grain boundary network of ferrite grains comprising many individual grains which are of two different orientations,in view of the fact that they have the Kurdjumov-Sachs orientation relationship with one of the two adjoining austenite grains. At high supersaturation the movement of the semi-coherent interface occurs in preference to the non-coherent ones, giving rise to a saw-tooth or side-plate morphology which is an incipient form of widmanstatten ferrite.

6.2.2 Precipitation During Transformation (Interphase Precipitation)

In many alloy steels containing strong carbide forming elements the γ-α transformation is accompanied by the precipitation of an alloy carbide. This is particularly evident for steels containing Cr, Mo, V, W, Nb and Ti. The alloy carbide often precipitates at the interface between the growing ferrite and the austenite, but may also form after the pro-eutectoid transformation as a form of alloy pearlite[128]. In microalloyed H.S.L.A. steels, with alloy contents less than 0.2 wt%,

alloy carbide precipitation largely occurs during the $\gamma - \alpha$ transformation, but may occur in the ferrite after transformation is complete, particularly during continuous cooling. The solubility of microalloy carbides, NbC, VC and TiC, in austenite is at least an order of magnitude greater than that in ferrite so that precipitation during the transformation from austenite to ferrite is to be expected.

Whilst the morphology of precipitation is very complex it is possible to classify the precipitates into[129]:-

        (i) interphase precipitation,

        (ii) precipitation from supersaturated ferrite.

Interphase precipitation is associated with the transformation front and is nucleated periodically at the γ / α interface[130]. The precipitates form in bands which are closely parallel to the interface. These bands are often associated with planar, low energy interfaces, and the spacing between bands is determined by the height of ledges which move along the semi-coherent interface. The nucleation of the carbide particles occurs normally on the low energy planar interface, rather than on the non-coherent higher energy ledges, and was first observed in high chromium steels[131, 132] in which the precipitates occur on a much coarser scale than in microalloyed steels. On the other hand, high energy planar interfaces are associated with bands of precipitation which are curved, as would be expected from the lower degree of coherency of a curved α / γ interface. It was suggested[132, 133] that the high energy γ / α boundaries do not migrate step by step, but the boundary escapes locally from precipitate particles by bowing between them.

The step height and, therefore, the band spacing of the precipitates is dependent on the transformation temperature and on the steel composition. As the transformation temperature decreases the band spacing is reduced. At high transformation temperatures slower rates of reaction lead to coarser band spacings. Similarly, if the reaction is slowed down by the addition of alloying elements such as Ni and Mn, the precipitate dispersion coarsens. The scale of dispersion varies from steel to steel, being coarsest, in chromium tungsten and molybdenum steels, where the reaction is relatively slow, and much finer in

vanadium niobium and titanium steels in which the transformation is more rapid.

Although the nucleation of interphace precipitation takes place at the γ/α interface their growth is in a direction normal to the boundary. Transformation under nearly equilibrium conditions, in association with interface precipitation mode, leads to fibrous precipitates observed frequently within the same ferrite grain[134, 135]. Fibrous precipitation occurs at the higher supersaturation or with the addition of Mn and Ni which slow down the $\gamma-\alpha$ reaction. During isothermal transformation at high temperatures fibrous precipitation is observed more frequently than interface precipitation, which also tends to be coarse.

On the other hand, at lower transformation temperatures, precipitation does not necessarily take place at the γ/α boundary during transformation but may occur at a later stage within the ferrite. Precipitation mainly takes place on dislocations introduced by the volume change during transformation. It can occur side by side with interface precipitation but becomes more significant as the transformation temperature decreases[136, 137].

During isothermal transformation of austenite to ferrite, ferrite can nucleate within a few seconds but transformation may not be completed for several minutes depending on the temperature and composition of the alloy. The first ferrite to form may be supersaturated and precipitates later form from it on dislocations, whereas, the ferrite which forms later may exhibit interface precipitation even within the same grain. Similar considerations apply to alloys transforming during continuous cooling, in which case the ferrite and precipitate can nucleate and grow over a wider temperature range.

6.2.3 Pearlite Reaction

Pearlite is the transformation product of iron-carbon austenite of eutectiod composition (0.8%C) at temperatures below A_1. The formation of pearlite occurs by the co-precipitation of ferrite and cementite from austenite and nucleation occcurs predominantly at the austenite

grain boundaries, giving a structure of alternative lamellae of ferrite and Fe_3C. Although the events leading to the formation of pearlite are not fully understood the following features are observed :-

i   Nucleation is mainly at the austenite grain boundaries but in hypo- or hyper-eutectoid steels, nucleation can occur on the grain boundary of ferrite or cementite. Additionally, pearlite may nucleate heterogeneously at non-metallic inclusions. As pearlite is a two phases transformation product, a viable nucleus must also be two-phase.

ii The pearlite, once nucleated, grows as colonies within which the lamellae are roughly parallel and have a common orientation relationship with one another. Each colony is roughly spherical in shape and often a new colony can nucleate onto a pre-existing one.

iii Neither the carbide, nor the ferrite, form extensive flat sheets or lamellae. Rather, the lamellae are more like wide ribbons, which bend, wave, twist and branch giving candelabra-like growths.

iv Due to the complex structure of pearlite, the interlamellar spacing between the ribbons is not precisely constant within a colony, except over short distances. Nevertheless the average interlamellar spacing normal to the plane of the ribbons is more constant for all the colonies provided that they form at the same constant temperature. Decreasing the transformation temperature causes a pronounced decrease in the interlamellar spacing. It has been shown both experimentally and theoretically by Zener[137(a)], that the relationship between interlamellar spacing and transformation temperature is of the form :-

$$S \simeq \frac{1}{T_e - T} \qquad\qquad 59$$

where S = interlamellar spacing

      T_e = eutectoid temperature(A_1)

v   At high temperatures near the A_1 the growth rate is very
slow but each nucleus can grow to large dimensions and even
may consume the whole austenite grain or cross into another
grain.

vi In pearlite of eutectoid compositon the smaller the
interlamellar spacing the thinner are the carbide lamellae
forming the lamellae. In general the relationship between the
interlamellar spacing of eutectoid pearlite and the thickness
of the carbide lamellae (t) is :-

$$t \sim 0.12S \hspace{4cm} 60$$

6.2.3.1 Nucleation of Pearlite

As already mentioned, the viable pearlite nucleus must be two-phased.
The first phase to nucleate, depends upon the composition of the
austenite, being either ferrite or cementite in lower and higher carbon
steels steels respectively. In the case of cementite being the first
phase to nucleate, carbon is depleted on either side of the cementite
and these carbon depleted regions then form the nuclei for ferrite. In
this way a duplex nucleus is developed and the same (but inverse)
process would apply if ferrite was the first to nucleate. This implies
side-by-side nucleation of the two phases in pearlite. However, as the
pearlite nucleates on austenite grain boundaries, the two phases
(ferrite and cementite) must grow together into the same austenite
grain. They thus must have non-coherent interfaces with the same
austenite grain, which implies that they equally have semi-coherent
interfaces with the other contiguous austenite grain into which they do
not grow. Having semi-coherent interfaces with the same grain, also
implies that the two phases have orientation relationships with the
same austenite grain (into which they do not grow) and thus an
orientation relationship with one another. The orientation relationship
between ferrite and austenite is Kurdjumov-Sachs, whilst that between
Fe_3C and austenite is the Pitsch[138] relationshp :-

$$(100)_{Fe_3C} \text{ // } (1\bar{1}1)_\alpha$$
$$(010)_{Fe_3C} \text{ // } (110)_\alpha$$
$$(001)_{Fe_3C} \text{ // } (\bar{1}12)_\alpha$$
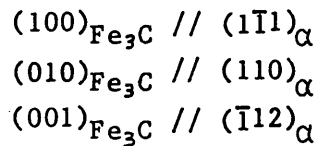
Because . . pearlite comprises interpenetrating single crystals of ferrite and cementite which have orientation relationships with the austenite grain into which they do not grow, they have mutual orientation relationship with each other. In eutectoid pearlite, forming on "clean" austenite grain boundaries in which there is no pro-eutectoid phase this is the Pitch/Petch orientation relationship[127] :-

$$(001)_{Fe_3C} \text{ // } (5\bar{2}\bar{1})_\alpha$$
$$(001)_{Fe_3C} \text{ 2-3}^\circ \text{ from } [11\bar{3}]_\alpha$$
$$(001)_{Fe_3C} \text{ 2-3}^\circ \text{ from } [13\bar{1}]_\alpha$$
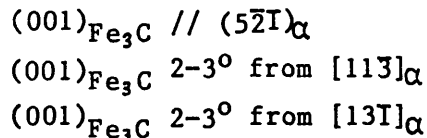
Where there is pro-eutectoid Fe_3C on the austenite grain boundary, it is reported that a different orientation relationship is obeyed because the ferrite will be isolated from the austenite grain into which it does not grow and thus have a simple epitaxial relationship with the cementite, i.e. the Bagaryatski relationship :-

$$(100)_{Fe_3C} \text{ // } (0\bar{1}1)_\alpha$$
$$(010)_{Fe_3C} \text{ // } (1\bar{1}\bar{1})_\alpha$$
$$(001)_{Fe_3C} \text{ // } (211)_\alpha$$
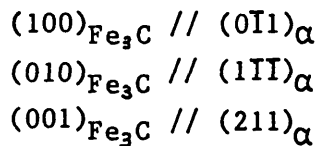
6.2.3.2 Growth of Pearlite

There is now a general agreement that pearlite growth occurs by edge-wise growth of the ferrite and cementite lamellae. For such growth to occur, carbon must diffuse cross-wise with respect to the pearlite austenite interface, from positions in advance of the ferrite to positions in advance of the Fe_3C. However, the nature of the interface plays an important part in the growth of pearlite, since different colonies of pearlite grow at different rates. This is probably due to the misorientation between the α or the Fe_3C and the austenite grain into which they grow, which will alter the structure of the interface and, therefore, the rate of interface diffusion. The rate of growth of pearlite at any given temperature is constant, and is inversely proportional to a function of the interlamellar spacing. With decreasing transformation temperature, the rate of growth $\dot{G}$ increases

73

to a maximun and then decreases at lower temperature. This may be due to the competition between increasing driving force, ΔG_o and decreasing diffusion rate as the temperature of transformation decreases.

6.2.4 Bainite Reaction

Bainite is a nucleation and growth reaction involving shear transformation to form the ferrite. The bainitic ferrite is formed by a shear of the austenite lattice in low carbon steels, but the growth of the shear trnsformation products is controlled by the diffusion of carbon. Bainite comprises a duplex structure of ferrite and carbide, the ferrite occurring as laths. In general there are two forms, upper and lower bainite with different morphologies, different α/Fe_3C orientation relationship, and different kinetics of formation.

With decreasing transformation temperature the bainite laths become narrower and occur by more pronounced nucleation within the austenite grains. Also, carbon can no longer diffuse so readily and the ferrite formed from the austenite will have a higher carbon content. Formation of bainite is promoted by the free energy change of the $\gamma - \alpha + Fe_3C$ reaction which provides the driving force which must be sufficient to provide the interfacial energies of the transforming products with austenite, and the associated strain energy of the transformation. As the transformation temperature decreases the carbon concentraton increases in the untransformed austenite, the strain energy increases and the mode of nucleation and growth of the carbide changes giving rise to upper and lower bainite. The formation of upper and lower bainite also depends on the carbon content of the steel.

6.2.4.1 Upper Bainite

In low carbon steels the first stage is the formation of a ferrite lath by shear, giving surface relief effects. In high carbon steels Fe_3C needles may form first. At high temperatures nucleation is often at the prior austenite grain boundaries, but intra-granular nucleation takes place more readily with decreasing transformation temperature. A co-operative side-by-side formation of the ferrite laths by sympathetic nucleation often

74

occurs, which becomes more frequent with increasing carbon content or decreasing temperature. This results in a colony or sheaf of parallel bainitic ferrite laths.

Growth of the ferrite laths occurs by rapid migration of their non-coherent end faces, i.e. lengthwise direction. Lateral growth or thickening of ferrite laths must occur by a ledge migration mechanism, accompanied by diffusion of carbon into the austenite, infront of the thickening ferrite lath. Thus, the carbon concentration builds up between the ferrite laths until Fe_3C can precipitate from this carbon enriched austenite at the ferrite/austenite interface. Decreasing the transformation temperature leads to smaller carbides which are closer together. Also the ferrite laths become more narrow due to the more limited carbon diffusion, whereas, the axial length of laths remains the same, (i.e. often the entire austenite grain diameter or the size of the untransformed austenite regions)

Increasing the carbon content also causes the bainitic ferrite lath to become more narrow, and the carbides more numerous. At carbon contents higher than 0.6% the carbides between the bainite ferrite laths become continuous and the structure develops a lamellar type structure not dissimilar from pearlite.

Due to the shear nature of the ferrite transformation the bainitic ferrite laths contain a higher dislocation density in which increases with decreasing transformation temperature.

6.2.4.2 Lower Bainite

In the fully transformed structure, Fe_3C forms as small rods oriented at 55/60° to the long axis of the bainite ferrite lath. Initially in lower carbon steels the nucleus seems to be a supersaturated bainitic ferrite lath, but this rapidly precipitates the typical oriented Fe_3C rods within it. Side-by-side nucleation is rarely so apparent as in upper bainite but the lateral growth of lower bainitic ferrite laths is restricted. The nucleation is more often intra-granular than at the austenite grain boundaries, and the structure shows more a clearly defined "acicular" aspect.

Decreasing the transformation temperature causes the bainite ferrite laths to be thinner and the carbides to be smaller but more numerous. The dislocation density in the ferrite laths is higher than in upper bainite. Increasing the carbon content does not seem to alter the structure greatly except to increase the number of carbide particles.

6.2.5 Martensite

Martensite is a metastable structure which forms at low transformation temperatures, and comprises a supersaturated solid solution of carbon in α-iron, which has a body centred tetragonal (bct) structure. This structure, a distorted form of bcc α-iron is mainly formed in low alloy steels during continuous rapid cooling of austenite at cooling rates in excess of critical cooling velocity, which is the slowest cooling rate at which the ferrite, pearlite or bainite trasformations can be supressed. The transformation is athermal, i.e. it progresses with a continuous decrease in temperature. Unlike pearlite, martensite is a diffusionless transformation, the atoms moving less than one interplanar spacing, and the carbon atoms occupying the same position relative to the iron atoms in both austenite and martensite. The driving force for the transformation is high, consequent upon the low transformation temperature, and must be sufficient to provide the appropriate strain and interfacial energy. Thus, the undercooling at which this criterion is met, occurs at a certain temperature, below which martensite can form, the M_s temperature. With increasing degrees of undercooling more martensite crystals nucleate, and the martensite transformation is completed at a specific lower temperature, M_f. The austenite transforms to the body centred tetragonal lattice by a shear process, which is highly crystallographic in nature.

The tetragonality of martensite changes with changes in carbon concentration :-

$$\text{tetragonality ratio } \frac{c}{a} = 1 + 0.045 \text{ wt\% C} \qquad 61$$

At 0 wt% C, the martensite exhibits no tetragonality, but simply has a bcc structure.

The M_s temperature depends upon the alloy content of the austenite, and all common alloying elements depress M_s, and consequent M_f temperature. Only cobalt increases M_s and M_f. Various empirical equations have been experimentally determined to describe M_s and M_f in terms of alloy content. A typical one from British Steel Corporation Atlas of Continuous Cooling Transformation Diagrams[139] is :-

$$M_s(^oC) = 539 - 423(\%C) - 30(\%Mn) - 18(\%Ni) - 12(\%Cr) - 8(\%Mo) \qquad 62a$$

$$\text{and} \quad M_f(^oC) = M_s - 215 \qquad\qquad\qquad\qquad\qquad\qquad 62b$$

Because of the shear nature of the transformation the interface between the martensite and austenite is semi-coherent, and this leads to a preferred and often a specific orientation relationship between the parent and the product phases. Nucleation of martensite occurs intragranularly in the austenite and not at the austenite grain boundaries. The orientation relationship and the morphology of martensite changes progressively with increasing carbon content, Fig. 27. In low carbon steels, up to 0.5%C, the martensite forms as laths often in packets, in which there is a high dislocation density, $10^{11}/10^{12}$ cm^{-2}, induced by the shear transformation and low transformation temperature. These laths are a few microns wide and those formed first at temperatures just below M_s may extend completely across the austenite grain in which they form. They have relatively straight or planar interfaces with the parent austenite, which defines the the habit plane $\{111\}_\gamma$, usually referred to the parent phase. The orientation relationship is Kurdjumov-Sachs :-

$$\{111\}_\gamma \ // \ \{110\}_{\alpha'}$$
$$\langle 110 \rangle_\gamma \ // \ \langle 11\bar{1} \rangle_{\alpha'}$$

With increasing carbon content above 0.5% the Kurdjumov-Sachs orientation relationship is maintained, but the habit plane alters to $\{225\}_\gamma$ and the morphology changes from laths to lenticular shaped plates. Moreover these lenticular martensite crystals do not occur in packets but as much more isolated crystals or as zig-zag arrays formed by a cataclysmic "burst" of the transformation. In addition the internal structure is changed from one of a high dislocation density to

77

one comprising many fine internal twins, 5-10 nm wide. These twins are most prevalent towards the centre of each martensite crystal, often defining what can be seen in the optical microscope as a "mid-rib". The lenticular shape crystals often meet at their tips in the "zig-zag" array. The internal microtwinning occurs on the $\{112\}_\alpha$,[140, 141]. Towards the center region of the lenticular crystal, the twinning may often be replaced by dense dislocation tangles. In the lower carbon martensites, comprising a heavy internal dislocation density, the high M_s may allow some rearrangement of the dislocations to form cells or sub-boundaries.

At still higher carbon contents, especially above 1.4%, the morphology generally remains as internally twinned lenticular plates, again occurs as "zig-zag" arrays formed by the "burst" phenomena, but the crystallography is changed. In these high carbon steels, the M_s may be close to or even below room temperature, so that large amounts of retained austenite are present which can only be transformed by sub-zero cooling. The orientation relationship is generally found to be the Nishiyama-Wasserman[127] relationship :-

$$\{111\}_\gamma \; // \; \{110\}_{\alpha'}$$
$$\langle 211\rangle_\gamma \; // \; \langle 110\rangle_{\alpha'}$$

and the habit plane is now $\{259\}_\gamma$.

It is sometimes believed that this orientation relationship is more precisely described by the Greninger-Troiano relationship in which the habit plane lies between $\{3.10.15\}_\gamma$ and $\{9.22.33\}_\gamma$.

In general the change in habit plane as carbon content increases is :-

$$\{111\}_\gamma - \{225\}_\gamma - \{259\}_\gamma$$

and as the carbon content increases so does the c/a ratio of the martensite, i.e. it becomes more tetragonal. The change in crystallography occurs gradually with increasing carbon content, and not sharply at specific compositions.

6.3 The Effect of Alloying Elements on the kinetics of the
γ/α Transformation

Alloying elements may be either austenite or ferrite formers, and within each group they may be carbide or non-carbide formers. Consequently, partitioning of alloying elements to austenite, ferrite or carbide can occur during the transformation and so influence the transformation kinetics and the structure of the transformed product, e.g. interphase precipitation.

6.3.1 Effect of Alloying Elements on the pro-eutectoid
Ferrite Reaction

There is little information available on the effect of alloying elements on the pro-eutectoid reaction in a multicomponent system. However, the pro-eutectoid ferrite reaction in iron-carbon alloys is affected by the third element in the ternary alloy system, in two ways[142].

i   The growth of ferrite occurs with partitioning of the alloying element X between α and γ under local equilibrium conditions. The ferrite therefore grows slowly at a rate which is determined by the diffusivity of alloying element in the γ-phase. This behaviour is sensitive to alloy composition, and Mn and Ni particularly show the effect of partitioning during transformation.

ii The situation where partial-partitioning occurs is more common. This involves a narrow zone of enrichment or depletion depending on whether X is a α or γ-stabiliser, which moves ahead of the α/γ interface. Aaronson and Domian[142] showed this to occur for ternary alloys in which the third element is Si, Mo, Co, Al, Cr or Cu. In the non-partitioning regime the observed growth rates are relatively high, being mainly determined by the diffusivity of carbon, which is several orders of magnitude faster than that of the metallic alloying elements[143].

Manganese shows the widest temperature range over which partitioning occurs, nickel having a rather smaller temperature range. In general the rate of ferrite formation, particularly its growth rate, is faster when there is no partitioning of alloying between the ferrite and austenite.

6.3.2 Effect of Alloying Elements on the Pearlite Reaction

The nucleation of pearlite in hypo-eutectoid steels is a consequence of the enrichment in carbon at the transformation front due to the rejection of carbon by the pro-eutectoid ferrite. The nucleation rate will be influenced by alloying elements due to them influencing the diffusion of carbon. This will decrease the nucleation rate irrespective of whether the alloying element segregates to the ferrite or cementite phase in pearlite. For example, Mo and Ni[127] both tend to decrease the nucleation and growth rate of pearlite whereas Co increases them. Chromium additions in the eutectoid steels also lower the growth rate of pearlite.

It is possible to distinguish between situations in which partitioning, or non-partitioning occurs[144]. Both situations are composition and temperature dependent. Austenite forming elements depress the eutectoid temperature and retard the pearlite growth rate, e.g Mn. Strong carbide forming elements, which are usually also ferrite formers, raise the eutectoid temperature and are likely to exhibit a partitioning effect between the ferrite and carbide at higher transformation temperature , e.g. Cr, Mo[127] and V[136, 145].

Growth of pearlite in the non-alloy partitioning regime is controlled by diffusion of carbon, and it is usually believed that this occurs along the pearlitic ferrite/austenite interface. This diffusivity is reduced by the presence of substitutional alloying elements such as Ni which accounts for the observed slow rate of pearlite growth. Mn retards pearlite formation, partitioning preferentially to the cementite phase. The extent of partitioning increases with increasing transformation temperature, which leads to cementite containing a higher Mn content. Furthermore, other elements are soluble in the cementite e.g. Cr and Mo which can replace iron atoms by up to 20% and

up to 4% respectively. The change in cementite composition, whilst not affecting the crystal structure, will influence the interlamellar spacing of pearlite, the detailed morphology, and the tendency to spheroidise[127]. Alloying elements have an inherent effect on the pearlite interlamellar spacing by virtue of their effect on the pearlite growth rate which is inversely proportional to the interlamellar spacing. This means that, because alloying elements decrease the pearlite growth rate, at constant transformation temperature they actually increase the interlamellar spacing. When the alloy element concentration reaches a critical level, cementite will be replaced by an alloy carbide. As the transformation temperature decreases, the pearlite colonies, as well as the pearlite interlamellar spacing, becomes finer due to the decreased diffusion rate.

6.3.3 Martensite and Bainite Transformation

The effect of alloying elements on the martensite reaction is to reduce the M_s temperature, with the exception of Co which raises the M_s. The interstitial elements, carbon and nitrogen are much more effective in reducing the M_s than the substitutional elements. The relative effects of the alloying elements on the M_s temperature are given by Andrews[146], as :-

$$M_s(^oC) = 539-423(\%C)-30.4(\%Mn)-17.7(\%Ni)-12.1(\%Cr)-7.5(\%Mo) \quad 63$$

Alloying elements also decrease the B_s temperature for the bainite reaction, and in so doing develop a metastable austenite bay between the pro-eutectoid ferrite/pearlite reaction and the bainite reaction. This is a clearly defined feature of the T.T.T. diagram of alloy steels. A typical empirical equation for the depression of B_s by alloying elements is :-

$$B_s(^oC) = 830-270(\%C)-90(\%Mn)-37(\%Ni)-70(\%Cr)-83(\%Mo) \quad 64$$

Alloying elements also decrease the nucleation and growth rate of bainite. This is due to alloying elements retarding diffusion, which is necessary for the bainite reaction to take place, but the transformation temperatures in the bainite range are usually much too

81

low for the partitioning of substitutional solutes.

Because the experimental steels which form the basis of the work described later in the thesis, contain Mn, Si, N and V, a brief summary of their effects on the transformation will be given. Mn retards the formation of pro-eutectoid ferrite[147] and pearlite without markedly changing the nature of the transformation or the transformed structure. Both Ac_1 and Ac_3 temperatures are depressed by Mn, which decreases the nucleation and growth of pro-eutectoid ferrite and pearlite reactions. At constant transformation temperature, Mn increases the interlamellar spacing. The bainite reaction is very markedly retarded by Mn.

Silicon, being a ferrite forming element, raises Ac_1 and Ac_3, which tends to increase the amount of pro-eutectoid ferrite formed at a given cooling rate, even though Si retards the rate of formation of ferrite. These effects, particularly associated with the increase in Ac_3 by silicon, tend to cause pro-eutectoid ferrite apparently to form more rapidly with increasing Si, but this is only the case at very high transformation temperatures at which ferrite would not form in low Si materials. Hence it is sometimes observed[148, 149, 142] that Si decreases the incubation period for pro-eutectoid ferrite. Another important effect of Si is that it decreases the solubility of carbides, particularly VC, in austenite[150].

Balliger[136] has investigated the effect of nitrogen on the transformation characteristics of vanadium bearing steels and has shown that there is a partitionig effect prior to transformation, above the nose of the ferrite C curve. The transformation rate is faster in nitrogen bearing steels over the entire temperature range studied where interface precipitation was found to occur. This leads to a finer interparticle spacing of the interphase precipitates.

Vanadium is a strong ferrite former, and may therefore behave similarly to silicon in terms of the pro-eutectoid ferrite transformation. However it has been reported that V in small amounts can actually lower the Ac_3[151]. When dissolved in austenite, vanadium retards the formation of pro-eutectoid ferrite, but there is some confusion because if there are undissolved VC or VN precipitates, the ferrite reaction

82

may be accelerated, and this effect can apparently be exacerbated if the grain refining effect of VC/VN is not taken into account. During the pro-eutectoid ferrite transformation, VC/VN can form as an interphase precipitation, and a similar effect has been reported in the pearlite transformation.

7.1 Structure of Martensite

Martensite, being an unstable phase in which carbon is in enforced solid
solution in the bcc (b.c.tetragonal) lattice, is both hard and brittle.
Except for the lowest carbon martensites, it is not used as an
engineering material without subsequent heat treatment. The heat
treatment or tempering process involves heating the martensite at
higher temperatures up to the A_1 to allow carbide precipitation and the
structure to recover partially or completely to the equilibrium
condition. The brittleness is largely removed, albeit with some loss of
strength. Apart from carbide precipitation, tempering also involves
clustering of carbon atoms at low temperatures and at high tempering
temperatures the recovery, recrystallisation and grain growth of the
original martensite structure. These structural changes are greatly
influenced by the alloying elements in the steel which can both
influence the types of carbides formed during tempering and also the
rates of various tempering reactions. During tempering certain
embrittlement phenomena may occur, predominant amongst which is temper
embrittlement which is associated with impurity elements such as P, Sn,
Sb etc.

7.1 Tempering of Plain Carbon Martensite

During the martensite transformation the first formed martensite
crystals, which formed just below M_s, can themselves undergo tempering
even during the quenching operation if the M_s is high enough, i.e.
usually with low carbon steels. This phenomenon is called auto-
tempering. On the other hand if the M_f is below room temperature
retained austenite occurs.

Clustering of carbon atoms occurs rapidly even at room temperature,
around individual dislocations and cell walls. Normally these are low
energy sites for carbon atoms to segregate to, compared with normal
interstitial lattice sites[127, 152, 153]. It has been suggested[152]
that in martensite containing less than 0.2%C, most of the carbon atoms
are segregated to some form of defects, but with higher carbon content

martensites which contain fewer dislocations, but are internally twinned, clustering of carbon atoms occurs along 100 planes of the martensite. The driving force for this clustering effect is believed to be the reduction of total strain energy of the lattice. This stage is really the first stage of tempering, but _ it does not involve actual precipitates of carbide. The normal definition of the first stage of tempering is associated with iron carbide(Fe_3C or ϵ-carbide) precipitation. In general there are three stages of the tempering process which are identified[127], but particularly in alloy steels of specific compositions, two further stages can be distinguished, namely those associated with alloy carbide precipitation which often leads to secondary hardening, and also a stage associated with intermetallic compound formation.

7.2.1 First Stage of Tempering

This occurs at temperatures between 80-250°C. In low carbon steels containing up to about 0.25% C. It is associated with further clustering of the carbon atoms[152, 153]. In medium and high carbon steels (0.3-1.5%C), the removal of carbon from interstitial solid solution, from clusters or from association with dislocations, occurs by the precipitation of ϵ-carbide which has a c.p.hex. structure of the general composition $Fe_{2.4}C$. ϵ-carbide does not form in low carbon martensite because the energy of carbon atoms segregated to dislocations is stated to be lower than that of carbon atoms as ϵ-carbide[154]. During the precipitation of ϵ-carbide in the higher carbon steels however, the carbon content remaining dissolved in the matrix is reduced to about 0.20/0.25% at which tetragonality is difficult to observe.

ϵ-carbide precipitates in the martensite with an orientation relationship[127] :-

$$(101)_{\alpha'} \text{ // } (10\bar{1}1)_{\epsilon}$$
$$(011)_{\alpha'} \text{ // } (0001)_{\epsilon}$$
$$[1\bar{1}]_{\alpha'} \text{ // } [12\bar{1}0]_{\epsilon}$$

The habit plane is $\{100\}_{\alpha'}$ and the ϵ-carbide seems to grow as thin plates, on one of the three sets of $\{100\}_{\alpha'}$ planes[154]. Other workers[127] suggest that ϵ-carbide grows as narrow laths or rodlets on

85

matrix cube planes. These plates or needles of ϵ-carbide form in a crosshatched arrangement within the martensite grains but not on the twin boundaries within the martensite. The observed orientation relationship leads to coherency straining of the matrix around the ϵ-carbide, there being about 0.5% misfit between $(101)_\alpha$ and $(10\bar{1}1)_\epsilon$, and this is believed to be responsible for the increase in hardness observed during the first stage of tempering, Fig. 28.

7.2.2 Second Stage of Tempering

There is a general agreement that the second stage of tempering is the result of the transformation of retained austenite. This only occurs in steels in which the M_f temperature is below room temperature, and/or in which there has been considerable stabilisation of the austenite. In plain carbon steels, this stage becomes apparent above 0.35% C at tempering temperatures in the range 230-280°C. This temperature range can be altered either by alloying additions or by the rate of heating. The breakdown of retained austenite is generally believed to occur by normal transformation processes to produce bainite. In high carbon steels the Fe_3C_2-Hagg carbide (monoclinic) is apparently formed[155], whereas in low carbon steels it is uncertain whether the Hagg carbide is present.

7.2.3 Third Stage of Tempering

This stage of tempering in plain carbon steels is regarded to occur over the tempering temperature range 250°C to A_1. It is associated with the precipitation and growth of Fe_3C and is accompanied by a decrease in volume as the Fe_3C precipitates, and also a decrease in hardness. In addition this stage is associated with :-

    (i) the growth of Fe_3C, and spheroidisation, which is
          associated with a continuing decrease in hardness,

    (ii) the recovery and recrystallisation of the matrix
          structure, which also is associated with the continuing
          decrease in hardness.

In the low carbon martensites, $\lesssim 0.2\%$ C, the carbide Fe_3C which is orthorhombic in structure, occurs as needles within the martensite laths and as more lenticular particles at the grain boundaries of both

the martensite laths and the prior austenite grains. The Fe_3C within the martensite laths appears as a widmanstatten structure with an orientation relationship described by Bagaryatski[127] :-

$$(211)_{\alpha'} \text{ // } (011)_{Fe_3C}$$
$$(011)_{\alpha'} \text{ // } (100)_{Fe_3C}$$
$$[111]_{\alpha'} \text{ // } [010]_{Fe_3C}$$

It is frequently observed that the Fe_3C precipitates in a "dendritic" form due to precipitating along $\langle 111 \rangle_{\alpha'}$ directions as bundles of fine rods and needles, and the growth direction is $\langle 11 \rangle_{\alpha'}$ // $[010]_{Fe_3C}$.

In high carbon martensite, in which there are many fine twins, and in which there is pre-existing ε-carbide, it has been shown that the Fe_3C is nucleated separately and its formation is accompanied by the solution of ε-carbide. Nucleation of Fe_3C takes place on the twin interfaces and grows by destroying the twin interface, finally coalescing into films with $(101)_{Fe_3C}$ parallel to the $\{112\}_{\alpha'}$ twin plane.

With increasing tempering temperature the rods and "dendritic" plates of Fe_3C thicken to form plate like slabs and globular carbides within the grains. The grain boundary precipitates grow faster at the expense of those within the grains, which dissolve. The rate controlling mechanism for this growth of Fe_3C is the self diffusion of iron and the growth process is described by an Ostwald Ripening equation :-

$$r_t^3 - r_o^3 = \frac{k}{RT} V_m^2 \, D \quad t \qquad\qquad 65$$

where r_o = the mean particle radius at time zero

r_t = the mean particle radius at time t

D = diffusion coefficient of solute in the matrix

= interfacial free energy of particle/matrix interface

V_m = molar volume of precipitates

k = constant

The above equation assumes that carbides approach perfect spheres to minimise the surface energy.

During the third stage of tempering, apart from the nucleation and growth of iron carbide, recovery and recrystallisation of matrix takes

place. During recovery annihilation of the dislocations occurs together with polygonisation into sub-cells within the tempered martensite grain. Fe_3C particles tend to pin polygonised boundaries, stabilising the structure. De-stabilisation occurs by the coarsening of Fe_3C particles unpinning the sub-grain boundaries and allowing them to migrate. Recrystallisation occurs between $600^{\circ}C$ and $700^{\circ}C$ and grain growth of the polygonal ferrite thus formed occurs with increasing temperature. Recrystallisation is faster in low carbon steels than in high carbon steels.

7.2.4 Fourth Stage of Tempering

The addition of alloying elements which are strong carbide formers, the carbides of which have greater negative enthalpies of formation than Fe_3C, leads to the phenomenon of secondary hardening or the fourth stage of tempering. At low tempering temperature, $450^{\circ}C$-$500^{\circ}C$, the rate of formation of alloy carbides is very slow due to the low rate of diffusion of alloy elements. Consequently Fe_3C forms but is replaced at higher temperatures by the alloy carbide. Due to their low solubilty, and consequent high degree of of supersaturation compared with Fe_3C, they tend to nucleate more generally, often on dislocations, and thus form widespread and fine dispersions which cause precipitation strengthening.

The alloy carbides tend to grow much more slowly than Fe_3C and hence preserve the strengthening effects to higher tempering temperatures at which in some cases e.g. Cr, Mo and W steels the carbide type may alter. In addition the slow diffusion of alloy solute atoms and the fine precipitates, retards recovery and recrystallisation of the matrix, thus preserving a higher base hardness to higher tempering temperatures. This effect of secondary hardening means that for a given strength a higher tempering temperature can be used, and moreover the steel maintains its strength to higher temperatures. In all cases, the carbide which gives rise to secondary hardening is formed by separate nucleation in the matrix and its formation is accompanied by the solution of existing Fe_3C. There is always a degree of semi-coherency between the secondary hardening carbide and the matrix, which results in a well defined orientation relationship specific to the alloy carbide.

7.3 Effect of Alloy Elements on Carbide Precipitation

It is known[127] that silicon can stabilise ε-carbide up to 400°C compared with 250°C in the absence of increased silicon contents, and even higher temperatures if the silicon is further increased. Silicon enters into the ε-carbide which influences its nucleation and growth and slows down the precipitation process. Some alloying elements e.g. Cr, Mo, W, V, Ti, Si tend to retain the tetragonality of martensite up to $400/500^{\circ}$C, whereas the tetragonality is lost during tempering at 300°C in plain carbon steels. On the other hand, Mn and Ni decrease the stability of the martensite, so that the tetragonality is lost at lower tempering temperatures than for plain carbon steels.

Alloy elements also retard the coarsening of cementite in the range $400-700^{\circ}$C. Several alloy elements such as Si, Cr, Mo and W cause cementite to remain as fine particles during tempering by either dissolving into the cementite or by segregating to the carbide-ferrite interfaces. The retention of fine precipitates slows down the recovery process involving the dislocations in the martensite, and causes pinning of the ferrite grain boundaries[57], so that grain growth is inhibited.

Alloying elements not only affect the nucleation and growth of iron carbide but cause the Fe_3C to be replaced by alloy carbides. The enthalpies of formation of some alloy carbides are given in Fig. 29 in which iron carbide is the least stable compound. The alloying elements Cr, Mo, V, W and Ti all form carbides and nitrides while the elements Ni, Co and Cu do not form alloy carbide phases. The diffusion of the interstitial elements is several orders of magnitude greater than that of substitutional elements. Consequently higher temperatures are needed for the diffusion of alloying elements prior to nucleation and growth of alloy carbides.

Precipitation of carbides in steels has been examined by many workers over a period of years[156, 157]. As already described the coarsening of alloy carbides occurs by Ostwald Ripening, the approach of Lifshitz and Wagner[157], being commonly applied so that the solute diffusion coefficient has a major effect, Eq. 65. However, it is probable that it

89

is the effect of solute atoms on vacancy diffusion which mainly controls the growth rate of alloy carbides because of the different specific volumes of the various carbides and the iron matrix.

Maximum secondary hardening occurs at a critical dispersion of the precipitates, or of the zones which are sometimes believed to preceed the true carbide precipitates. At tempering temperatures or times in excess of those required for maximum secondary hardening, the strength decreases. The tempering process is therefore time and temperature dependent, and for plain carbon and low alloy steels time and temperature of tempering can be combined into one parameter known as the Holloman Parameter(P) :-

$$P = T (K + \log t)$$ 66

Where T is the absolute temperature, t is time in seconds, minutes or hours and k is constant for different steels.

P is the Holloman Parameter which is normally plotted against the hardness value to give master curves for a particular steel as shown Fig. 30. The use of Holloman parameters is less effective for the illustration of master tempering curves if the steel is heavily secondary hardened.

7.4 Tempering of Steels Containing Vanadium

It has been known for sometime[156] that additions of vanadium to plain carbon steel produce secondary hardening. A systematic examination of the effects of increasing vanadium content has been made by Irvine and Pickering[158], and Pickering[159]. It has been shown that secondary hardening increases as the vanadium content increases up to the stoichiometric ratio, Fig. 31, and decreases at hyper-stoichiometric compositions. This has been attributed to the fact that there is a maximum temperature dependence of the alloy carbide solubility at the stoichiometric composition[176].

Tekin and Kelly[160] have studied the secondary hardening process in low alloy steels containing vanadium, using Electron Microscopy. In the early stages of secondary hardening, zone formation was observed in the matrix in addition to precipitation on dislocations. The possible

formation of zones is now postulated by several workers. Dense dislocation tangles persist until well after the maximum hardness together with very small cloud-like precipitates. Often the precipitates, which are VC, are associated with dislocations. At the onset of secondary hardening a number of straight dislocations were observed implying that recovery was about to commence. Precipitates have been observed to occur on dislocations possibly due to segregation effects and at a later stage of tempering discrete vanadium carbide particles are also seen to lie often on dislocations.

At a later stages of tempering[160], it has been observed that distinct platelets of vanadium carbide are present and associated with strain fields. These strain fields indicate a high degree of coherency with the matrix and may well indicate that the VC could have been developed from vanadium enriched zones, similar to G-P zones. At higher temperatures of 650°C well developed dislocation networks have been found, suggesting the commencement of sub-grain formation. Clear evidence of precipitation on such dislocations has been observed[160] at 700°C. The breakdown of coherency and the growth of vanadium carbide was indicated by the sharpening of the electron diffraction spots.

The precipitates obey the Baker and Nutting[161] orientation relationship, as also reported by Smith[162] :-

$$\{1\bar{0}0\}_{\alpha Fe} \; // \; \{100\}_{VC}$$

$$\langle 1\bar{1}0 \rangle_{\alpha Fe} \; // \; \langle 100 \rangle_{VC}$$

CHAPTER 8 **EXPERIMENTAL TECHNIQUES**

8.1 Experimental Steels

Three series of 1.6% Mn steels were made, the compositions of which were as follows :-

(a) A series of base steels, free from vanadium, containing 0.1% and 0.2% C with varying nitrogen contents of 0.006%, 0.010% and 0.020%.

(b) A series of low carbon steels containing 0.12% C, with vanadium contents of 0.15% and 0.40% at nitrogen contents of 0.006%, 0.010% and 0.020%.

(c) A series of higher carbon steels containing 0.20% C, with vanadium and nitrogen contents as in (b) above.

(d) An extra low carbon steel containing 0.055% C, 0.15% V and 0.020% N.

All these steels were silicon killed and contained no addition of aluminium. This was to eliminate any interaction effects between Al-V-N. The steels were air melted as 15Kg melts in a 50KW-3KHz induction furnace, lined with basic magnesite refractory (Thermax G10). The base materials used to make the steels were :-

(i) Electrolytic iron for the low C - low N melts.

(ii) High purity iron for the higher C-N melts.

(iii) Warner pig iron to achieve the necessary carbon content.

(iv) Commercial high purity silicon, to eliminate the aluminium present in normal ferro-silicon.

(v) Commercial purity vanadium, also to eliminate contamination by aluminium. For the low vanadium steels ferro-vanadium was used as this could be accommodated without introducing more than 0.01% Al.

(vi) Low carbon ferro-manganese.

(vii) High carbon ferro-manganese.

(viii) High nitrogen ferro-manganese.

The ferro-manganese contained less than 0.01% Al, and was therefore deemed suitable for the manufacture of the alloys. The analyses of these base materials are given in Table 1.

In view of the use of silicon deoxidation, rather than the more conventional deoxidation by ferro-silicon which contains aluminium and/or aluminium, a number of trials were needed to developed a satisfactory melting procedure. A standard melting method was then adopted, on the basis of these trials, as follows:-

(a) The base charge comprised either of electrolytic or high purity low carbon iron with the appropriate amount of pig iron.

(b) During the melting down, 65g of silicon metal, was added when the charge was appoximately 50% molten, the charge then being melted out and the temperature raised to 1570/1600°C.

(c) A further addition of 18g of silicon metal, together with the appropriate amounts of the different forms of ferro-manganese, was then made. It was found important to add low carbon ferro-manganese before high carbon ferro-manganese, in order to achieve the requisite carbon content, and the final addition was the high nitrogen ferro-manganese when required. The melt was then slagged off.

(d) Finally the vanadium metal was enclosed in an iron foil and plunged into the melt, the melt being stirred until the vanadium had dissolved. This was a rapid process because the vanadium metal itself was in the form of foil.

As soon as possible after the vanadium was melted in, in order to minimise vanadium loss, the melt was cast into an ingot, nominally 7.7 cms square x 45 cms long, using an exothermic feader head compound to minimise piping. The actual compositions of the alloys which were made by this technique, together with the aim analyses, are shown in Table 2.

8.2 Rolling to Initial Dimensions Required for Experimental Work

An initial diameter of 19 mm was chosen for the experimental work, which was the maximum diameter which could be consistently ice-brine quenched to martensite.

Prior to rolling, up to 15 cms was cut from the top of each ingot to remove pipe and segregation, and the ingot surfaces were milled to minimise surface defects. The ingots were then rolled from 1150°C in 17 passes from 75 mm square to 19 mm round bar, the finishing temperature being 750-850°C.

8.3 Homogenisation Treatment

In order to homogenise the bars and to have a constant initial condition for the subsequent experiments, a treatment of 1250°C was used to take all the V(CN) into solution. Electron Microscopy showed that after 15 minutes at 1250°C, there were no undissolved V(CN) particles present. To minimise oxidation and decarburisation, heating for homogenisation was carried out in a high purity argon atmosphere.

8.4 Solubility Studies

8.4.1 Heat Treatment

Specimens, 110 mm long x 12 mm diameter, were enclosed in silica tubes under 140 torr high purity argon. The encapsulated samples were heat treated at various temperatures from 900°C to 1250°C at 50°C intervals for times between 1 hour and 8 hours, followed by iced-brine quenching. All specimens were surface skimmed to a depth of 0.5 mm prior to the extraction of the precipitates. The specimens were then degreased and dried, and two methods were employed for extraction of the VN and VC precipitates.

8.4.2 Chemical Extraction

After the predetermined heat treatments the solid specimen was machined to millings, to increase the surface area and also to accelerate the chemical dissolution process, which was accomplished by the use one of the following solutions :-

(a) 20% Sulphuric acid at 60/70°C, refluxed to maintain a constant acid concentration.

(b) 6 N Hydrochloric acid at room temperature.

(c) 10% Hydrochloric acid at 50°C. High temperature dissolution
    is faster and reflux condensation was used to maintain the
    acid concentration.

8.4.3 Electrochemical Extraction

Any given alloy has a critical potential above which it is in an active
state but below which the alloy is passive. The same phenomenom occurs
for compounds such as VC and VN. An investigation into the
passive/active state for the materials under examination, C-Mn steel,
vanadium carbide and vanadium nitride, led to the construction of
polarisation curves. Further details are given in Appendix II.

Using the experimentally determined polarisation curves the following
extraction conditions were used :-

(a) Electrolytic solution of the steel in 3% HCl, 7% $FeCl_3$ 3%
    ethyl glycol, $(HO.(CH_2.CH_2.O)_n.CH_2.CH_2.OH)$, (n = 7 to 8)
    solution using potentiostatic control at 0.2 V (SCE) at room
    temperature. A current density of 50 mA/cm^2 was used but this
    varied as dissolution proceeded.

(b) Electrolytic solution of steel in 10% HCl solution using
    potentiostatic control at 0.2V(SCE). The initial current
    density was 50 mA/cm^2.

Extraction in all the processes used continued until the whole of the
specimen was dissolved. The extracted residues were separated from the
mother liquor by centrifuging, and were washed several times with fresh
extraction solution to ensure they were free from contamination by the
mother liquor. The wash solution was added to the original mother
liquor, which was chemically analysed for vanadium and nitrogen. The
extracted and washed residue was then further washed in alcohol,
separation again being accomplished by centrifuging, and finally the
extacted residue was dried at ~50°C under a continuous flow of high
purity argon. The extracted residues were then analysed for vanadium,
carbon and nitrogen.

8.5 Austenite Grain Coarsening

The grain coarsening characteristics were determined for all the steels listed in Table 2. Specimens 12.5 mm in diameter x 10 mm long were encapsulated in silica tubes under 140 torr high purity argon. Heat. treatment was carried out for 1, 2, 4 and 8 hours at 900 to 1250°C at 50°C intervals. After heat treatment all the specimens were quenched in iced-brine solution.

Prior austenite grain boundaries were revealed initially by electrolytically etching in a solution containing 10g Cr_2O_3 dissolved in 40ml of distilled water and 40ml H_3PO_4 made up to 100 ml by further addition of distilled water. A Struers Electropol was employed at a current density of 4-6 mA/mm^2.

Grain boundary etching was improved by tempering the quenched specimens at 500°C for up to 8 hours. This tempering treatment did not affect the prior austenite grain size. Intermediate polishing during etching on 1/4 micron diamond cloth further improved the etching of the prior austenite grain boundaries. The mean linear intercept of the austenite grain size was was determined by a standard quantitative metallographic technique. The method of estimating the errors is given in Appendix I.

8.6 Isothermal Transformation Characteristics

In order to provide a basis against which the transformation characteristics, in terms of ferrite nucleation and growth, after various thermo-mechanical treatment can be compared, the TTT diagrams were determined for steels 1, 3, 5, and 14. Specimens of 19mm diameter and about 4mm thick, were homogenised for 16 ± 2 minutes at 1250 ± 5°C prior to quenching into a constant temperature salt bath. The isothermal transformation behaviour was determined at temperatures between 500°C and 850°C at 50°C intervals. The accuracy of the salt bath temperature was better than ± 5°C. Isothermal holding times of 2, 4, 7, 10, 20, 40, seconds, 1, 2, 4, 7, 10, 20, 40, minutes and 1, 2, 4, 7, and 24 hours were used. The accuracy of the transformation times was better than 10% for times up to 20 seconds and better than 2% for longer times.

After heat treatment at the predetermined temperatures and times the specimens were quenched into iced-brine. All the specimens were mounted in cold resin, polished to 1 micron diamond using standard metallographic techiques and etched in 2% Nital. The determination of volume fraction of the transfomed product was carried out by point counting.

8.7 Tempering Studies

8.7.1 Tempering Martensite

In order to study V(CN) precipitation during tempering martensite, specimens 19 mm diameter and 5 mm in thickness were homogenised at 1250°C or 1075°C, (error ∓ 5°C) in a continuous flow of high purity argon, for 16 ± 2 minutes and iced-brine quenched followed by tempering in a salt bath at temperature between 500 to 700°C (± 5°C) at 50°C interval. Tempering times were 24, 47, 94, 375, 750, minutes, 25, 50, 100 hours.

Hardness measurements were used to study the tempering characteristics of the steels, and in particularly the secondary hardening.

8.7.2 Tempering of Non-Martensitic Products

Hardness measurements were also used to study the precipitation in polygonal ferrite structures obtained from modified Jominy end-quenched specimens. Modified end quenched specimens, of 18mm diameter and 100 mm long were homogenised at 1250°C and 1075°C for 30 minutes. The specimens were water quenched from one end, using standardised conditions. To determine the cooling rates, at various distances from the quenched end, thermocouples were inserted into the specimen at various distances from the quenched end. The cooling curves were constructed and the rate of cooling over the temperature interval 800-600°C was determined. After quenching the specimens were sliced into quadrants. The first quadrant was kept in the as quenched condition whilst the others were tempered at 550°C, 600°C and 650°C for 30 minutes and one hour followed by air cooling. The variation in hardness along the specimen was determined after 1 mm has been ground from the surface.

8.8 Effect of Austenite Morphology on the Nucleation and Growth of Ferrite

The effect of morphology on the conditioning of the austenite as produced by various thermo-mechanical treatments, was examined on the transformation to ferrite. The following austenite structures were investigated :-

A. Fully recrystallised austenite of varying grain size, without any strain induced precipitation.

B. Unrecrystallised austenite of varying grain size and grain elongation with strain induced precipitation.

C. Unrecrystallised austenite of varying grain size and grain elongation with deformation bands and strain induced precipitates.

The thermo-mechanical treatments designed to produce the above initial austenite structures are shown in Fig. 32. All thermo-mechanical treatments were carried out using 15 mm diam. X 22.5 mm high cylinders deformed in a forging press. Specimens thermo-mechanically treated to give the appropriate initial austenite structures were quenched directly to the isothermal transformation temperature of 750°C and the transformation kinetics were determined using optical metallographic techniques. The formation of ferrite nucleated at different sites in the thermo-mechanically conditioned austenite, was studied in relation to the volume fraction of ferrite and to the final ferrite grain size observed.

8.9 Metallographic Techniques

A description of the etching proceedures to reveal the prior austenite grain size, has already been given. In the case of the thermo-mechanically processed specimens, these were sectioned parallel to the deformation axis, mounted in cold setting resin and polished using standard metallographic techniques. The transformed ferrite and ferrite grain boundaries were revealed by etching the specimens in 2% Nital and

measurements were made of the volume fraction of ferrite, Appendix III, together with the ferrite particle size, Appendix I. Large numbers of ferrite particles were counted to minimise the error.

Whenever possible the ferrite grain size was measured :-

     (a) near to prior austenite grain boundaries,

     (b) in the deformation bands,

     (c) within the prior austenite grain.

Complementary to optical microscopy, electron microscopy was used to study the precipitation of V(CN) in the transformed structures. Carbon extraction replicas and thin foils were used. Carbon replicas were prepared by lightly etching the specimen in 2% Nital followed by the standard technique. For thin foils 3 mm diameter rods, were machined or spark eroded from solid specimens, and slices 250 μm in thicknes were cut from the rods, mechanically polished on 600 grade emery paper down to   150 μm in thickness and then electropolished using a twin jet Struers automatic polishing equipment and a solution of 10% perchloric acid in methanol at -50°C.

CHAPTER 9 **EXPERIMENTAL RESULTS**

9.1 **SOLUBILITY STUDIES**

Extraction of VC/CN precipitates was carried out using the methods
outlined in section 8.4. Chemical extraction in 10% HCl at 50°C and
electrolytic extraction in 7% $FeCl_3$, 3% HCl, 3% Ethylene Glycol
solution was used. In preliminary work to compare the methods,
specimens solution treated at 900°C were used, in which condition a
large amount of undissolved precipitates in the austenite would be
obtained. The results, including where available the particle size
measurements of the extracted carbides/nitrides, are given in Table 3.
A comparison of the extraction methods is shown in Table 4.1 for the
0.12% C, 0.13% V, 0.010% N steel. The carbon and nitrogen contents of
the precipitates using electrolytic extraction appear to be higher
than those present in the steel itself, but in the chemical extraction
technique the carbon and nitrogen contents are much lower and more
conformable with the contents present in the steel. The vanadium
content of the precipitates did not seem to be influenced by the
extraction method. On the basis of these results, it was decided to
standardise using the chemical extraction technique, and this will
be discussed later.

9.1.1 Comparison of Precipitates

The compositions of the precipitates after solution treatment at 900°C
are given in Table 4, for steels containing varying carbon, nitrogen
and vanadium contents. It was apparent that a high V:N ratio in the
steel, i.e. a low nitrogen content in the steel, gave precipitates
which had a low N:C ratio, i.e. were much richer in carbon, Fig. 33,
and Table 5, and the converse was apparent. Thus it seems that the
composition of the precipitates was largely dictated by the
composition of the steel and the higher the N:C ratio in the steel the
greater was the N:C ratio of the precipitates, Fig. 34. In Table 6, it
is also apparent that in the high vanadium, low nitrogen steel the
precipitate are rich in carbon and the carbon content of the
precipitates becomes greater as the carbide solvus is approached, the
nitride disolving at lower temperatures due to the low nitrogen

100

content of the steel. Increasing the nitrogen to 0.020% in the high
vanadium steel however produced precipitates richer in nitrogen which
increased with increasing solution treatment temperature. This
indicates that the N-rich carbides/nitrides are much more stable than
the carbon rich carbides/nitrides, as indeed is well known[106, 136].
However the analytical data does not differentiate between carbides
and nitrides, and it may well be that a carbo-nitride is formed. In
that case it is suggested that with increasing temperature the
precipitate becomes richer in nitrogen as the carbon is dissolved out
of it.

9.1.2 Solubility Products

The solubility of vanadium, carbon and nitrogen in austenite, for
temperatures between 900°C and 1250°C is given in Table 6. Typical
examples of the results, for steels Nos 6, and 11 are shown in Figs 35
and 36. All the steels showed increasing solubility with increasing
temperature. From the results, solubility product equations were
calculated for temperatures up to where the measured vanadium, carbon
and nitrogen contents levelled out, i.e. at the solvus temperature. It
is suggested that when, as occurs in some cases in Table 6, the
apparent solubility exceeds the nominal steel composition, this may be
due to segregation effects. Indeed, microstructural work on the
transformations in these alloys which will be reported later, confirmed
that some segregation effects were present. In fact relatively small
segregation effects can lead to considerable scatter in the solubility
data as it often seen in published results.

The solubility equations were calculated on the assumption that VC and
VN did not interact with one-another, i.e. were not mutually soluble.
This undoubtedly is an over simplification but does follow indications
from a recent thermodynamic analysis, Roberts[106]. In every steel,
the solubility product of VC was much greater than that of VN, as
might be expected, typical examples being shown in Figs 37 and 38,
which show the average lines (least squares fit) through the
experimental data.

The solubility determined for VC in the austenite is given in Fig. 39,

for the steels examined, and is compared with published data, which indicates the wide scatter which has been reported. The present results all fall within the published scatter band. However, the results also show systematic effects. At a constant carbon content in the steel, increasing the nitrogen content decreases the solubility of VC. Also at a constant nitrogen content in the steel, increasing carbon also decreases the solubility of VC. There also seems to be an effect of increasing vanadium decreasing the solubility of VC. These effects will be discussed later. With respect to the solubility of VN, Fig. 40, the results show much less scatter and fall well within the band of published results. The effects of varying steel composition were much less marked than those for VC solubility but the solubility product was at least one order of magnitude smaller. However it seems that increasing the carbon content in the steel, i.e. decreasing the N:C ratio, decreases the solubility of VN. The effects of other compositional variables are not great. Again these effects will be discussed later.

Futhermore, as it is uncertain to what extent vanadium would be combined either with carbon or nitrogen, it is reasonable to assume that vanadium would be combined with carbon and nitrogen to form V(CN) in a variable carbon to nitrogen ratio. To validate this assumption results of the solubility product of [V] [C + (12/14) N] were plotted as shown in Fig. 41. As the vanadium content increased from 0.15% to 0.415% the solubility product increased. Increasing carbon content caused the solubility product of [V] [C + (12/14) N] to decrease, whereas increasing the nitrogen content from 0.005% to 0.020% caused the solubility product to decrease. This indicates that the higher nitrogen content of the V(CN) the lower is its solubility, but a calculation of the solvus temperature based on Fig. 41 gives much too low temperatures. Consequently the assumption made by Roberts[106] that VC and VN form independently is probably very viable.

9.2 GRAIN COARSENING

A comprehensive study of the effects of carbon, nitrogen and vanadium on the grain coarsening characteristics was undertaken, the steels

being examined comprising those listed in Table 2. Whilst there was no decarburisation, analysis showed a progressive loss of nitrogen from the surface layer, particularly the half millimeter in which the nitrogen content in the 0.020% N steel had decreased to about 0.014% N. This occurred at 1250°C under a partial pressure of 0.14 atmospheres argon, and the effect would be much smaller with decreasing austenitising temperature. However, this surface loss of nitrogen did not affect the observed austenite grain size, which was measured well away from the surfaces. This loss of nitrogen has been reported in other work[136].

9.2.1 Effect of Austenitising Temperature and Time

In the 0.12% C, V-free steel, the austenite grain size increased monotonically with increasing temperature in the steel, Fig. 42(a), and also increased with increasing austenitising time, in the low N (0.005%) steel. Increasing the nitrogen to 0.020% in this steel caused a much less temperature dependance of grain growth up to 1100/1150°C, Fig. 42(b), but between 1150°C and 1250°C the grain size increased very rapidly. A similar effect was observed with the higher C (0.20%) steel, Fig. 42(c), and when rapid grain growth occurred the effect of time at temperature became more pronounced.

In the steels containing 0.13/0.15% V, at the low nitrogen content of 0.005%, the grain growth characteristics were very similar to those of the V-free steel, Fig. 43(a), but the general level of grain size was smaller. Increasing the nitrogen content however in this 0.13/0.15% V steel to 0.020%, Fig. 43(b), changed the grain growth characteristics and resulted in a constant grain size up to 1000°C and only slow grain coarsening at higher temperatures with relatively little effect of austenitising time.

These two general effects were exhibited with minor modifications by all the steels, and the effects of composition will now be discussed. Because the compositional effects were similar irrespective of austenitising time, they will be illustrated by examples drawn from the 1 hour austenitising treatments. Where rapid grain coarsening occurred at some particular temperature, i.e. there was a grain

coarsening temperature, the effect of increasing austenitising time was to lower the temperature at which grain coarsening occurred, as expected. Furthermore, grain growth did not occur uniformly, as the effect of grain boundary pinning particles usually leads to inhomogeneous grain coarsening due to variations in the local volume fraction of the pinning particles. This effect is illustrated by the typical histogram in Fig. 44, which show that with increasing austenitising time a wider distribution of grain size is developed, and particularly some very coarse grains are introduced as the grain boundary pinning process becomes less effective. This effect was quite generally observed.

9.2.2 Effect of Vanadium

Vanadium additions cause refinement of austenite grain size due to the formation of grain boundary pinning particles of which V(cN) is more effective than V(Cn) due to the greater stability of the former, but the effect is also greatly dependent on the volume fraction of precipitates.

In the 0.12% C, 0.005% N steels the addition of 0.13/0.14% V, whilst decreasing the grain size compared with the V-free steel did not alter the overall grain coarsening characteristics, Fig. 45(a), the grain size still increasing monotonically with increasing temperature. A large addition of 0.35/0.45% V however, caused the grain size to remain almost constant up to 950/1000°C, and thereafter the grain size again increased monotonically with temperature but at a still lower level of grain size than for the 0.13/0.14% V addition, Fig. 45(a). In the same 0.12% C steels but containing 0.010% N, the addition of 0.13/0.19% V produced no grain growth up to 950/1000°C and considerably retarded grain growth between 1000°C and 1150°C, above which grain coarsening became rapid, Fig. 45(b).

Increasing the vanadium further to 0.35/0.41% in this steel, accentuated these effects, causing an overall smaller grain size at all temperatures above 950°C but still showing marked retardation of grain growth between 1000°C and 1150°C. With 0.020% N in the 0.12% C

steels, the high nitrogen markedly retarded grain growth and refined the grain size compared with the lower nitrogen contents in the V-free steel, Fig. 45(c), whilst still allowing the grain size to increase more or less regularly with temperature. The addition of 0.13/0.19% V and 0.35/0.41% V refined the grain size compared with the V-free steel and up to 1000°C no grain growth occurred at any vanadium content. At above 1000°C, grain growth commenced but was less apparent at 0.35/0.41% V than at 0.13/0.19% V due to the higher vanadium steels having the highest apparent grain coarsening temperature. An unusual feature was the fact that at the highest temperature of 1200/1250°C, the 0.13/0.19% V steel showed a smaller grain size than the 0.35/0.41% V steel.

In the 0.20% C steels at the 0.005% N level, the effect of vanadium was very similar to that observed in the 0.12% C steels, Fig. 46(a). In the 0.20% C steels containing 0.010% N, the V-free steel showed slower grain coarsening up to 1150°C than did the 0.005% N steeel. In the 0.010% N steel, addition of 0.13/0.15% V or 0.35/0.45% V refined the grain size below 1050°C and caused slower grain growth than in the V-free steel, Fig. 46(b), but it can be seen that the 0.13/0.15% V steel had a higher grain coarsening temperature and therefore a finer grain size than did the 0.35/0.45% V steel. This effect will be discussed later. In the 0.35/0.45% V, 0.017/0.020% N, 0.20% C steels the effects of vanadium were reversed compared with the 0.010% N steels in that the grain coarsening temperature increased and the grain size decreased with increasing vanadium content, Fig. 46(c).

9.2.3 Effect of Nitrogen

In the 0.10% C, V-free steels, increasing nitrogen from 0.005% to 0.020% refined the grain size appreciably at all temperatures and caused slower grain coarsening, Fig. 47(a), but the grain size still increased progressively with increasing temperature. With 0.15% V however, a grain coarsening temperature was introduced which increased with increasing nitrogen content and at the same time the overall level of grain size decreased with increasing nitrogen content, Fig. 47(b). Similar general effects for nitrogen were observed in the 0.35/0.41% V steels, the grain size being further decreased. However

there was a tendency at the highest temperatures of 1200/1250°C for the 0.010% N steel to have a slightly smaller grain size than the 0.020% N steeel, Fig. 47(c), and this feature became more clearly apparent with increasing austenitising time, Fig. 47(d). These effects will also be discussed later.

In the 0.20% C steels free from vanadium, increasing nitrogen refined the grain size and decreased the rate of grain growth with temperature, Fig. 48(a), but at 1250°C a sudden grain coarsening occurred in the 0.020% N steel compared with a similar sudden grain coarsening at 1150/1200°C in the 0.010% N steel. In the 0.20% C, 0.15% V steels, 0.005% N did not cause any marked grain boundary pinning because there was no sudden grain coarsening effect but the rate of grain growth with increasing temperature was reduced and was even further reduced as the nitrogen content increased up to 0.010%. However, at 0.020% N the grain size was rather coarser than at 0.010% N and in both the 0.010% and 0.020% N steels there was rapid grain coarsening at 1250°C, Fig. 48(b). The effects were therefore different than for the 0.12% C steels, probably due to the increased volume fraction of carbo-nitrides. At 0.40/0.45% V, Fig. 48(c), the effect of increasing nitrogen was to refine the grain size at all temperatures and to markedly increase the grain coarsening temperature.

9.2.4   Effect of Carbon

In the V-free steels, increasing carbon at 0.020% N had no effect on the grain coarsening characteristics up to 1200°C but at 1250°C the higher carbon steel coarsened more rapidly than the lower carbon steel, Fig. 49(a). No comparable data was available for 0.005% and 0.010% N steels. In the 0.13/0.16% V steels at 0.005/0.006% N, carbon had no effect on the grain size which progressively increased with increasing temperature, Fig. 49(b), whilst at 0.010% N the high carbon steel only had the smaller grain size above 1050°C and there was a grain coarsening temperature which increased with increasing carbon content, Fig. 49(c). In the 0.13/0.15% V steels containing 0.020% N, increasing carbon had virtually no effect on the grain size up to 1150°C but the 0.12% C steeel maintained a finer grain size at 1250°C than either the 0.055% or 0.20% C steels, Fig. 49(d). However carbon

did not apparently affect the grain coarsening temperature which was
about 1000°C, but had an effect on high temperature grain coarsening
at 1150/1250°C. These complex effects of carbon are related to the
composition, volume fraction and coarsening/dissolution rate of the
pinning particles, and will be discussed later.

9.3 TEMPERING STUDIES

9.3.1 Hardness of As Quenched and Tempered Martensite

A survey has been carried out of the effect of vanadium, nitrogen and
carbon on the tempering characteristics of 0.10/0.12% C steels
austenitised at 1075°C and 1250°C, followed by iced-brine quenching.
At 1250°C, both VC and VN would be dissolved, whereas at 1075°C the VC
only would be completely dissolved whilst some VN would remain
undissolved.

The hardness of the as quenched martensite, Table 7, is related to its
composition. Increasing nitrogen increases the hardness of as quenched
martensite, Fig. 50(a), whereas the addition of vanadium became more
effective when the nitrogen level exceeded 0.010%, Fig. 50(b). There
was also evidence that increasing the austenitising temperature tended
to decrease the as quenched martensitic hardness due to an increased
austenite grain size and therefore an increased martensitic grain
size.

Isothermal tempering curves showed that for the V-free steels the
hardness progressively decreased with increasing time and temperature,
Fig. 51(a), but at the highest tempering temperature and longest times
the hardness remained constant due to the tempered martensite having
recrystallised and subsequent ferrite grain growth being small. On the
other hand, the vanadium steels all showed retardation of tempering up
to 500/550°C and then secondary hardening the intensity of which
depended on composition and austenitising temperature. A typical
series of isothermal tempering curves are shown for the 0.10% C,
0.35% V, 0.005% N steel, Fig. 51(b).

The large amount of isothermal tempering data made it necessary to depict it by constructing Holloman type "Master tempering Curves" in which hardness is plotted against the parameter T(20+logt) where T is the temperature in Kelvin and t the time. Typical master tempering curves for a V-free and V-containing steels are shown in Fig. 52, which illustrates the typical scatter which was obtained. This type of scatter has been shown in previous literature but the average lines through the many data points allows comparison to be made between steels of different composition. In presenting the results, the master tempering curves will be used.

Only a small amount of electron microscopy was carried out, the general microstructural changes in low carbon vanadium steels having been well described in the literature. Some typical micrographs for a 0.12% C, 0.15% V, 0.020% N steel, using carbon extraction replicas are shown in Fig. 53, the presence of small VC/VN precipitates being clearly apparent particularly at the higher tempering temperatures.

9.3.2 The Tempering Characteristics

The hardness values obtained at different tempering times and tempering temperatures were plotted against the Holloman Parameter to give master tempering curves for all the alloys. Such a curve is shown in Fig. 52, together with the scatter in hardness about the mean tempering curve as shown previously. This scatter was very small at low tempering parameters, but much greater at higher tempering parameter values. As will be explained latter additions of vanadium, carbon and nitrogen raised the level of the tempering curve but vanadium was responsible for the introduction of secondary hardening.

9.3.2.1 Effect of Vanadium

The effect of vanadium on the tempering characteristics is shown in Figs 54-55. Figs 54(a) and 54(b) show the effect of increasing vanadium in 0.11% C, 0.005% N steels austenitised at 1075°C and 1250°C respectively. After austenitising at 1250°C the base composition without vanadium showed progressive softening as the tempering parameter increased. Introducing vanadium (0.14%) to the steel, apart

from raising the level of the tempering curve to higher hardness values, also producing a marked retardation of softening at tempering parameters up to 19000 (1-3 hours at 600°C). This effect was more pronounced at the higher vanadium content of 0.35% at which marked secondary hardening also occurred. The level of hardness decreased after secondary hardening but the hardness level in the overaged condition increased as the vanadium content increased. Austenitisation at 1075°C, Fig. 54(b), had no significant effect on the level of hardness or the secondary hardening compared with austenitising at 1250°C, except that in the overaged condition the steels showed more resistance to softening, possibly due to finer recrystallised ferrite grains which were observed.

Similar characteristics were observed for the 0.010% N and 0.020% N steels containing additions of vanadium, as shown by Figs 55(a) and 55(b) for austenitising temperature of 1250°C. The overall pattern of the results show that increasing vanadium content at any given nitrogen content increased the low tempering temperature resistance, increased the intensity of secondary hardening and increased the overaged hardness. However, at the higher tempering parameter (highest temperature longest time) the advantage conferred by vanadium on the overaged hardness became less pronounced. An interesting feature shown by changing the austenitising temperature from 1075°C to 1250°C, Fig. 56, was the greater intensity of secondary hardening produced in the vanadium steels, and the lower overaged hardness. This will be discussed later but is associated with the extent of the solubility of VC/VN and the presence of undissolved particles at 1075°C which resulted in a finer recrystallised ferrite formed at the highest tempering parameters, and consequently a higher overaged hardness.

9.3.2.2 Effect of Nitrogen

The effect of increasing nitrogen on the master tempering curves at vanadium contents up to 0.415% is shown in Figs 57 and 58. Increasing the nitrogen content from 0.005% to 0.020% in the vanadium free steel, Fig. 57(a), slightly raised the hardness at all values of the Holloman parameter. Increasing the austenitising temperature from 1075°C to 1250°C, had little effect at the lower Holloman parameter values, but

at the high parameter values there was a tendency for slightly lower hardness due probably to the coarser grain size.

Increasing the nitrogen to 0.010% at a constant vanadium content of 0.13/0.15%, Fig. 57(b), raised the hardness curve, particularly at lower tempering temperatures, but the effect of nitrogen became less pronounced with increasing tempering temperature. At 0.020% N steel, Fig. 58, there was a slight indication of increased secondary hardening. Increasing the austenitising temperature from 1075°C to 1250°C had no effect on the secondary hardening but low austenitising temperature, Fig. 58(a) caused more resistance to overaging softening compared with a higher austenitising temperature.

Further increasing the vanadium to 0.35/0.41%, caused a pronounced secondary effect, Fig. 58, and increasing nitrogen content raised the whole of the tempering curve. The effect of nitrogen decreased at the highest tempering parameter. There was no effect on nitrogen on the intensity of secondary hardening. There was a tendency for increasing the austenitising temperature to cause the maximum secondary hardening to occur at a lower tempering parameter, possibly due to the greater supersaturation giving more rapid precipitation. Again it was observed that the higher austenitising temperature led to less resistance to overaging in the most heavily tempered conditions, and also the intensity of secondary hardening was increased.

9.3.2.3 Effect of Carbon

Figure 59 shows the effect of carbon on the tempering characteristics of 0.41/0.43% V, 0.018/0.020% N steels. Increasing carbon from 0.126% to 0.195% raised the level of hardness prior to secondary hardening but in the overaged condition there was virtually no effect of carbon content. Carbon had no effect on the intensity of secondary hardening, Table 8. Increasing the austenitising temperature had similar effects at both carbon contents, increasing the intensity of secondary hardening and giving higher hardness values in the overaged condition.

9.4 ISOTHERMAL TRANSFORMATION STUDIES

Isothermal Transformation Diagrams have been determined for the base
steel containing 0.12% C, 1.6% Mn, 0.010% N, and for the same steel
with 0.13% V. In addition isothermal transformation diagrams were
determimed for the 0.13% V steels containing 0.005% and 0.020% N. The
isothermal transformation behaviour was examined, after quenching from
an austenitising temperature of 1250°C. The main purpose of this work
was to investigate the formation of pro-eutectoid ferrite for
comparison with a similar study in thermo-mechanically conditioned
austenite. A comparison will be made of the effect of adding 0.15% V to
a steel containing 0.126% C and 0.010% N, and the effect of increasing
nitrogen from 0.005% to 0.020% in a 0.15% V will be presented.

The curves showing the progress of transformation with time were
plotted for temperatures of 500°C to 850°C, and at temperatures where
the polygonal ferrite formed, i.e. above 650°C, the transformation
curves all showed a similar form, Figs 60 and 61. This comprised two
apparent stages, the first of which (region A in Fig. 60 (a) and (b),
and Fig. 61 (a) and (b)), was associated with ferrite nucleation and
growth at the austenite grain boundaries and the later stage (region B
in Fig. 60 (a)and (b), and Fig. 61 (a) and (b)), being associated
with ferrite nucleation and growth within the austenite grains and
eventually with the pearlite transformation below A_1. However the two
stages of ferrite formation were also observed at temperatures
above A_1.

In interpreting the kinetics of ferrite formation, the period of
induction has been used as an indication of the general rate of
nucleation of ferrite, whilst the initial slope of the ferrite volume
fraction versus time curve has been used to indicate a measure of the
growth rate of ferrite.

The results were also used to determine the transformation temperature
which would be used to investigate ferrite formation in the thermo-
mechanically processed austenite, which will be described later. It
was concluded that 750°C would be the optimum temperature for such
investigation because ferrite nucleation and growth was sufficiently

slow and because transformation did not go to completion i.e. above A_1, so that the austenite structure could clearly be observed at all stages of the transformation. In the presentation of the isothermal transformation results, a temperature of 750°C will mainly be used for illustrative purposes.

9.4.1   Effect of Vanadium

The effect of an addition of 0.14% V on the transformation characteristics of a 0.12% C, 0.010% N steel was to accelerate the nucleation and to decrease the growth rate of ferrite, as typified by the curves for the transformation temperature of 750°C, shown in Fig. 60. It was observed metallographically that in the early part of stage A in Fig. 60 (a) and (b), and Fig. 61 (a) and (b) ferrite nucleation at the austenite grain boundaries was the predominant effect whereas in the later part of stage A when saturation of the austenite grain boundaries by ferrite nuclei had occurred, growth of the ferrite was the main process.

As previously explained in stage B, ferrite formed within the austenite grains, but also at existing austenite-ferrite interfaces. The acceleration of ferrite transformation by 0.13% V, which is clearly shown by the T.T.T. diagrams in Fig. 62 and 63 could be due to the vanadium refining the austenite grain size from 175 um to 90 um. However, plotting the volume fraction of ferrite per unit of austenite grain boundary area indicates that it is largely the growth of ferrite which is retarded by the vanadium addition, Fig. 60. The effect of vanadium in accelerating the ferrite transformation became less as the transformation temperature decreased. Another effect of the vanadium addition was to increase the amount of ferrite at a given time and temperature where transformation was not complete, due to accelerating the transformation, and also it was clear that the vanadium increased somewhat both the A_1 and A_3 temperatures. These overall effects have also been shown by Hoogendoorn and Spanraft[164]. It was also observed, Figs 62 and 63, that vanadium seemed to be more effective in accelerating the completion of transformation below A_1 than the start of transformation.

112

The microstructures in the V-free steel showed grain boundary nucleation of ferrite at temperatures between 800°C and 550°C, Fig. 64 (a) and (b), and at 700°C and below a saw-tooth form of grain boundary ferrite often was observed, Fig. 64(c). At a later stage at these temperatures, ferrite started to nucleate within the austenite grains, Fig. 64 (d) and (f), some of which grew as polygonal grains, Fig. 64 (e) and (g). Between 650°C and 550°C widmanstatten ferrite also formed within the austenite grains, Fig. 64 (e) and (g), and became prevalent with decreasing transformation temperature. Below 550°C, a typical bainite structure was formed without pro-eutectoid or widmanstatten ferrite, Fig. 64(h).

The effect of the vanadium addition was largely to refine the grain boundary nucleated ferrite, Fig. 65, and the structure generally. The grain boundary nucleated ferrite remained fine during the transformation, but was engulfed by the ferrite which nucleated within the austenite grains or at the ferrite · austenite interfaces and which grew rapidly, Fig. 65 (c) and (d). It was also observed that much of the ferrite etched relatively darkly, indicating precipitationof V(CN) probably in an interface mode, Fig. 65(d). In addition, there was an almost complete absence of widmanstatten ferrite in the vanadium steel. As in the V-free steel, bainite with no polygonal ferrite occurred below 550°C.

9.4.2 Effect of Nitrogen

The effect of increasing N up to 0.020% on the T.T.T. diagram of the 0.12% C, 0.14% V steel was negligible in terms of the rate of formation of ferrite at the nose of the ferrite C curve, compare Figs 66 with 63 and 67. However, with increasing transformation temperature the effect of nitrogen became more apparent in retarding the formation of ferrite, see Fig. 61(a), for a temperature of 750°C. This retardation of ferrite formation by nitrogen was despite a refinement of the austenite grain size from 198 um at 0.005% to 90 um at both 0.010% N and 0.020% N. It is clear that increasing nitrogen from 0.010% to 0.020% markedly retarded ferrite formation, and it can clearly be inferred from Fig. 61(a), that in fact progressively increasing nitrogen from 0.005% to 0.020% progressively retarded ferrite

formation. From Fig. 61(a) it may also be inferred that increasing
nitrogen decreased both the rate of nucleation and rate of growth of
grain boundary nucleated ferrite. The major form of the T.T.T. diagram
did not appear, however, to be significantly altered by nitrogen
content.

The microstructures produced by increasing nitrogen content were very
similar to those already described for the 0.010% N, 0.14% V steel.
However there was a clear indication that the higher nitrogen contents
refined the grain boundary nucleated ferrite, Figs 68(a) and 69(a).
Some examples were also observed, particularly in the low N (0.005%)
steel, of the grain boundary nucleated ferrite only growing into one
austenite grain, Fig. 68(c) and also developing a marked saw-tooth
morphology, Fig. 68(a). Below 550°C, typical bainite stucture were
formed, Fig. 68(d). With the higher nitrogen content (0.020%) the
precipitation in the ferrite was clearly developed, Fig. 69(b).
Nitrogen did not inhibit intragranular ferrite nucleation in the
austenite grains, Fig. 69(c), and indeed many of these nuclei seemed
to developed into fine widmanstatten ferrite, causing the formation of
a very fine microstructure, Fig. 69(d).

9.5 TRANSFORMATION DURING CONTINUOUS COOLING

9.5.1 Hardenability

9.5.1.1 Effect of Vanadium

The effect of an addition of 0.14% V on the jominy hardenability
curves for a 0.12% C, 1.60% Mn, 0.010% N steel, austenitised at 1075°C
or 1250°C are shown in Fig. 70.

In the V-free steels, there was little significant effect of varying
the austenitising temperature from 1075°C to 1250°C, the slightly
higher hardenability after austenitising at 1075°C being due to the
steel used for this test containing slightly higher Mn and C contents,
although the N was somewhat less. The hardenability curves were
generally within the scatter band experienced from specimem to

114

specimen. The major effect of vanadium, at both austenitising temperatures is not in terms of the martensitic hardenability as measured by the distance to the point of inflexion, but is associated with the marked increase in hardness of the non-martensitic products. As will be shown later, this is due to vanadium refining the structure, and also due to some interphase precipitation in the polygonal ferrite. It can be seen that there are small increases in the hardness at distances about 30-40 mm from the quenched end. This is believed to be due to precipitation, but it is interesting that there was a consistent trend for this small maximum hardness to be nearer the quenched end when austenitised at 1075°C compared with 1250°C. This is due to the higher transformation temperatures produced for a given distance from the quenched end for the lower austenitising temperature, i.e. a slower rate of cooling, augmented by the smaller prior austenite grain size.

9.5.1.2 Effect of Carbon

Increasing carbon from 0.055% to 0.12% increased the martensitic hardenability, Fig. 71, in the 0.14% V, 0.020% N steels, but only slightly increased the hardness of the non-martensitic transformation products. Again small increases in hardness were observed due to precipitatiion effects, and after austenitising at 1075°C the lower carbon steel produced the precipitation effects at distances nearer the quenched end. This precipitation effect however was not so pronounced in the lower carbon steel after austenitising at 1250°C. In the higher nitrogen steels there was little effect of increasing the austenitising temperature from 1075°C to 1250°C on the martensitic hardenability.

9.5.1.3 Effect of Nitrogen

Increasing nitrogen from 0.005% to 0.020% caused a small but progressive trend for increasing martensitic hardenability at austenitising temperatures of both 1075°C and 1250°C, but there was virtually no effect of varying the austenitising temperature. Increasing nitrogen increased progressively the hardness of the non-martensitic transformation products, Fig. 72, due to a lowering of the

115

transformation temperature on cooling. After austenitising at 1075°C, there was a consistent increase in hardness at about 35-40 mm from the quenched end, but with the higher austenitising temperature this increase in hardness occurred at a greater distances from the quenched end.

9.5.1.4   Effect of increased V and C simultaneously

The effect of simultaneously increasing the carbon content to 0.20% and the vanadium to 0.43%, in 0.020% N steels after austenitising at 1250°C is shown in Fig. 73. Apart from the increase in martensitic hardness, resulting from the higher carbon content, increasing carbon and vanadium markedly increased the martensitic hardenability and also the hardness of the non-martensitic transformation products. This latter effect was not only due to a lower transformation temperature, but also due to a considerable increase in the intensity of precipitation of VC/VN. It should be noted that after about 30 mm from the quenched end the hardness progressively increased with increasing distance from the quenched end, due to the precipitation strengthening effect.

9.5.2. Microstructures Developed During End Quenching

An end-quenched specimen was austenitised at 1250°C for 30 minutes, and the rate of cooling was measured at various distances from the quenched end. The cooling curves are shown in Fig. 74, and the rates of cooling over the temperature interval 800-600°C are shown as a function of distance from the the quenched end in Fig. 75. The hardenability curve for the end quenched specimen of the 0.12% C steel without V, austenitised at 1250°C is shown in Fig. 76, together with selected microstructures in Fig. 77. At the quenched end, the martensite structure was predominant, Fig. 77(a), followed by the formation of bainitic ferrite which sometimes nucleated at the pior austenite grain boundaries. At some distance from the quenched end the formation of grain boundary ferrite took place, Fig. 77(b), followed by the bainitic ferrite transformation and eventually by the formation of pearlite, Fig. 77(c). The presence of pearlite was associated with polygonal ferrite and occurred mainly in regions near to the prior

austenite grain boundaries, whereas the interior of the austenite grains had often transformed to bainitic ferrite. This mixture of microstructures persisted with increasing distance from the quenched end, but with increasing amount of pro-eutectoid ferrite.

The addition of 0.15% V at the high nitrogen content of 0.020% increase the martensitic hardenability, Fig. 76, largely due to the higher nitrogen content as shown earlier. Microstructures are shown in Fig. 77 (d) and (e), and were very similar to those already described. An interesting feature remote from the quenched end was the fairly large amount of polygonal ferrite which etched darkly to indicate some precipitation, Fig. 77(f). In the steel containing higher carbon (0.195%) and higher vanadium (0.43%) the hardenability had been considerably increased and the structures are shown in Fig. 77 (g) and (h). These show the martensitic structures near to the quenched end and the much reduced amount of pro-eutectoid ferrite in association with bainite at a considerable distance from the quenched end. Also the structures were much refined due to the greater amount of V(CN) keeping the austenite grain size small. In addition the higher the carbon and vanadium contents the lower the transformatiom temperature for any position on the jominy curve. A possible additional reason for the higher hardenability, and particularly the higher hardness of the non-martensitic transformation products could be the presence of precipitates pinning ferrite austenite interfaces and allow less growth of the pro-eutectoid ferrite, i.e. the smaller amounts of ferrite which were observed.

9.5.3 Tempering of the Jominy Bars

Because of the evidence for precipitation effects in the non-martensitic transformation products formed remote from the quenched end of the jominy specimens, it was decided to temper the jominy specimens at temperatures between 550°C and 650°C for times of 30 minutes and 1 hour in order to examine more closely the possible changes which could occur. Due to the many results obtained, only selected illustrations will be given in relation to the general effects observed.

In the V-free steels, tempering at 550°C for 30 minutes slightly decreased the hardness at all positions along the jominy bar. The hardness became lower with increasing tempering temperature, Fig. 78, and also with increasing tempering time from 30 minutes to 1 hour. There was no significant effect of increasing the austenitising temperature on the response of these steels to tempering at various tempering temperatures.

9.5.3.1 Effect of Vanadium

0.13/0.15% V was added to the 0.010% N, 0.12% C steel, and the as quenched jominy curves showed that in the vanadium steel the hardness of the non-martensitic transformation products was about 50 H.V. greater than in the V-free steel, Fig. 78. Tempering the vanadium steel at 550°C caused little effect on the hardness in the 1075°C austenitised condition, but tempering at 600°C and 650°C eliminated the peak in hardness observed in the as quenched specimen and after tempering at 550°C. Tempering at 650°C also tended to increase the hardness to a level above the peak hardness shown in the tempering 550°C condition, Fig. 78. Increasing the austenitising temperature to 1250°C had little effect on the influence of tempering on the hardness values of the jominy curve,but the overall level of hardness of the non- martensitic transformation products was slightly lower due to the coarser grain size produced, Fig. 79. Increasing the tempering time from 30 minutes to 1 hour for both austenitising temperatures, had relatively little effect on the hardness curve, but did eliminate the peak in hardness obtained in the as quenched specimen, even after tempering at 550°C.

9.5.3.2 Effect of Nitrogen in 0.13/0.14% V Steels

There was a general effect of increasing nitrogen from 0.005% through 0.010% to 0.020% to increase the hardness of the non-martensitic products, and this occurred at all tempering temperatures and at both austenitising temperatures. At 0.005% N there was a small peak in hardness on the jominy curve at ~30/40 mm from the quenched end, and this peak increased in intensity as the nitrogen content increased from 0.005% to 0.010% but remained at more or less the same position

on the jominy curve. Tempering at 550°C did not eliminate this peak in hardness, but tempering at 600°C and 650°C did eliminate the peak in the 0.005% and 0.010% N steels, Fig. 80. At 0.020% N however tempering at 600°C and 650°C caused a second peak to be observed on the hardness curve at an increased distanced of some 60/70 mm from the quenched end, Fig. 80. This double peak only occurred after austenitising at 1250°C, but not after austenitising at 1075°C. Moreover the general hardness level of the non-martensitc transformation products after tempering at 650°C was appreciably higher in the 0.020% N steel than at lower nitrogen contents.

9.5.3.3 Effect of Carbon

The effect of increasing carbon content from 0.055% to 0.12% was studied in the 0.15% V, 0.020% N steels, Fig. 81. Increasing the carbon content increased the level of hardness of the non-martensitic transformation products at all tempering temperatures, but this hardness level was lower with increasing austenitising temperature from 1075°C to 1250°C. The lower carbon content of 0.055% still produced the single hardness peak at 30-40 mm from the quenched end after tempering at 550°C. After tempering at 600°C and 650°C the two hardness peaks observed in the 0.12% C steel were not produced at the lower carbon content of 0.055%.

9.5.3.4 Effect of Carbon and Vanadium

Using a 0.020% N steel, the efect of a further increase in carbon to 0.20% with a simultaneous large increase in vanadium to 0.43% was examined, Fig. 82. The potential for precipitation in this steel was clearly enhanced particularly after austenitising at 1250°C and in the as quenched condition the hardness of the non-martensitic products increased appreciably at positions greater than 60 mm from the quenched end. Tempering at 550°C had little effect but tempering at 600°C and 650°C caused a further appreciable increase in the hardness of the non-martensitic structures, 650°C producing greater hardening than 600°C. Moreover a peak in hardness was developed at 60 mm from the quenched end after tempering for 30 minutes at 650°C,. Whilst these general effects were maintained on increasing the tempering time

119

from 30 minutes to 1 hour, the peak in hardness after tempering at 650°C was no longer observed, but was observed at the lower tempering temperature of 600°C. This suggests some overaging effect at 650°C. Material was not available to study the effect of a lower austenitising temperature (1075°C) in this steel.

9.6 THERMOMECHANICAL PROCESSING

The block diagram showing the proposed thermo-mechanical treatments to produce the different morphologies of austenite is shown in Fig. 32. The austenite morphology, is classified in terms of the end product after quenching and prior to isothermal transformation :-

1. Recrystallised austenite of either fine or coarse grain size to vary the austenite grain boundary surface area,

and 2. unrecrystallised austenite, with either small or large grains elongated to different extents, to vary the grain boundary area and to introduce intra-granular nucleation of ferrite during isothermal transformation.

Four steels were selected for this work, namely the V-free steel containing 0.12% C and 0.010% N, and 0.14% V steels containing 0.005%, 0.010% and 0.020% N. The effects of temperature and reduction during deformation were studied in both the recrystallised regime and in the unrecrystallised regime in order to established the thermo-mechanical processing conditions which would be used to investigate the transformation to ferrite from the different austenite morphologies.

9.6.1 Deformation in the Recrystallised Regime

9.6.1.1 The V-Free Steel

Recrystallisation of the V-free steel occurred at deformation temperatures of 875°C and above. At 825°C however, virtually no recrystallisation was observed. As shown in Fig. 83(a), increasing the deformation reduction from 30% through 50% to 70% at any given temperature caused a marked refinement of the recrystallised austenite

grains, Table 9.1. Similarly, for a constant reduction, decreasing the deformation temperature down to 875°C progressively decreased the recrystallised grain size. Some typical micrographs are shown in Fig. 84, which also shows the unrecrystallised austenite after deforming at 825°C.

9.6.1.2 Effect of Vanadium

Adding 0.13/0.19% V to a 0.12% C, 0.010% N steel refined the recrystallised austenite grain size for all temperatures and reductions in the recrystallised regime, Fig. 83(b). Some typical micrographs are shown in Fig. 85, from which it can be seen that at 925°C and below full recrystallisation did not occur. With *increasing* the reduction and *decreasing* deformation temperature the recrystallised austenite grain size decreased, Table 9.2.

9.6.1.3 Effect of Nitrogen

The effect of increasing nitrogen from 0.005% to 0.020% in the 0.12% C, 0.13/0.19% V steel is shown in Fig. 86. It was observed also that as nitrogen increased the temperature below which recrystallisation did not occur increased. For example, at 0.005% N, recrystallisation was complete for all deformations at 925°C but with 0.010% and 0.020% N, recrystalisation did not occur completely immediately after deforming at 925°C, but only at 1025°C and above. As will be shown later, however, in the 0.010% and 0.020% N steels, recrystallisation was complete at 925°C in about 10 seconds after deformation. From Fig. 86, it can be seen that for all nitrogen levels, decreasing the temperature and increasing reduction during deformation in the recrystallised regime, decreased the recrystallised austenite grain size, Tables 9.3 and 9.4. Increasing the nitrogen content from 0.005% to 0.010% refined the recrystallised grain size for all deformation conditions, but a further increase in nitrogen to 0.020% caused the recrystallised grain size to increase slightly. Thus the smallest recrystallised grain was shown by the 0.010% N steel. However, because the 0.005% N steel had such a coarse austenite grain size (198 um) prior to thermo-mechanical processing, the effect of such processing in changing the grain size was much larger in the 0.005% N

steel than in the 0.010% and 0.020% N steels. Some typical
microstructures are shown in Fig. 87 and Fig. 88, for 0.005% N and
0.020% N steel respectively.

9.6.1.4 Growth of Recrystallised Austenite Grains

In order to investigate the growth of recrystallised grains, and the
possible influence of precipitated VN, specimens were held for times
up to 10000 seconds at 925°C after deformation at higher temperatures,
Table 10.

In the V-free steel containing 0.010% N there was little grain growth
after deformation at either 1200°C or 1050°C, but in the 0.19% V,
0.010% N steel some growth did occur after deformation at 1200°C but
not after deformation at 1050°C, Fig. 89(a), and Table 10. For all
holding conditions the vanadium steel maintained a finer grain size
than the V-free steel.

Increasing nitrogen from 0.005% to 0.020% in 0.14/0.19% V steels had
little effect on the growth of the recrystallised grains after
deformation at 1200°C, Fig. 89(b), but with a lower deformation
temperature of 1050°C but a higher reduction of 70%, increasing
nitrogen decreased the rate of grain growth and in the 0.010% N steel
the grain size remained almost constant. Again it can be seen that
the 0.010% N steel had the finest grain size after deforming at
1050°C and more over this steel was most effective in resisting grain
growth of the recrystallised austenite.

9.6.2 Deformation where Recrystallisation is Absent or Incomplete

As already indicated the 0.12% C, 0.10% N steel free from vanadium
recrystallised at temperatures at and above 875°C for deformation of
30%, 50% and 70% reduction. Only at 825°C was recrystallisation
incomplete. Some micrographs illustrating the unrecrystallised
austenite have been showm in Fig. 84(d).

In steels containing 0.12% C, 0.13/0.19% V with nitrogen contents of
0.005%, 0.010% and 0.020%, the deformation temperature was lowered to

875°C and 825°C with 30%, 50% and 70% deformation. In the steel
containing 0.005% N there was no recrystallisation immediately after
deformation at 875°C, Fig. 87(d), and increasing the reduction caused
the austenite grains to become more elongated, as expected. Similar
effects were observed in the 0.010% and 0.020% N steels, Fig. 85(d)
and Fig. 88 (c) and (d). In general the elongation of the
unrecrystallised grains was only dependent on the amount of
deformation, and did not appear to change significantly with changing
temperature.

In order to investigate the effect of nitrogen on the
recrystallisation of the deformed austenite, the 0.010% and 0.020% N
steels were deformed to 50% and 70% reduction at 925°C, under which
conditions partial recrystallised had taken place. The results in
terms of the % recrystallisation are shown in Fig. 90(a), from which
it can be seen that increasing nitrogen content decreased the amount
of recrystallisation. In addition, Fig. 90(b) shows that increasing
deformation reduction increased the amount of recrystallisation, i.e.
accelerated the recrystallisation process as expected.

9.6.3 Austenite Boundary Area per Unit Volume (Svγ)

Svγ will be an important parameter in controlling the number of
nucleation sites for ferrite during the transformation of austenite
and therefore in controlling the rate of ferrite formation. When the
austenite was fully recrystallised, increasing reduction and
decreasing temperature caused Svγ to increase for all the steels,
Table 11, as the recrystallised austenite grain size was progressively
refined. Typical examples are shown in Fig. 91(a) and Fig. 91(b), for
V-free and vanadium steel. The addition of 0.13/0.19% V at 0.010% N
caused a marked increase in Svγ, Fig. 92(a), due to vanadium
decreasing the recrystallised austenite grain size. In the presence of
0.13/0.19% V, the effect of increasing nitrogen on Svγ is shown in
Fig. 92(b). It can be seen that the 0.010% N steel had the greater Svγ
value, which agrees with the smallest recrystallised grain size in
this steel as shown in Fig. 86.

In the case of the incompletely recrystallised structures, Svγ was

123

difficult to measure because the retained deformation increased the Ar_3, temperature so that transformation to ferrite occurred during or immediately after deformation. However, despite the inability to make accurate $Sv\gamma$ measurements on those structures, there was an indication that at the lowest deformation temperature of $825^\circ C$ the $Sv\gamma$ value decreased. The reason for this is not understood, but as will be shown later, this tentative observation correlates with a retardation of ferrite nucleation after deformation at $825^\circ C$ compared with higher deformation temperatures.

9.6.4 The Effect of Initial Grain Size

Because the recrystallised grain size depends on the initial grain size prior to deformation, a parameter has been used which indicates the effect of thermo-mechanical processing on the increase in the area for ferrite nucleation during subsequent transformation. This parameter will tend to indicate possible nucleation potency irrespective of the initial austenite grain size itself. The parameter is:-

$$RSv\gamma = \frac{Sv\gamma \text{ of thermo-mechanically processed structures}}{Sv\gamma \text{ of initial structures}}$$

The results show that increasing deformation and decreasing temperature increase $RSv\gamma$ for all the steels, which means that those processing changes will increase the number of ferrite nucleation sites. As shown in Fig. 93(a), vanadium had little effect on $RSv\gamma$ at 0.010% N although in the V-free steel decreasing the deformation temperature from $925^\circ C$ to $825^\circ C$ markedly increased $RSv\gamma$, i.e. would be expected to increase the number of ferrite nucleation sites. The effect of increasing nitrogen at 0.13/0.19% V as shown in Fig. 93(b), and increasing the nitrogen from 0.005% to 0.010% decreases $RSv\gamma$ at all temperatures, but there was no further effect on increasing the nitrogen from 0.010% to 0,020%. It seems therefore that increasing nitrogen from 0.005% to 0.010% would decrease the nucleation potential for ferrite formation during transformation, but that above 0.010% N there would be no further effect. Again, despite the difficulty of measuring the $Sv\gamma$ values at low

deformation temperatures where recrystallisation was incomplete, there was an indication that the RSvγ value decreased, and this narrowed the apparent effect previously reported for the Svγ value itself.

9.6.5 Transformation Studies on Thermo-mechanically Processed Austenite Structures

Based on the results presented in the previous section, five different thermo-mechanical processing conditions were selected to produce different austenite morphologies, namely:-

(a) Heat 1250°C, deformed 30% at 1200°C to give large recrystallised austenite grains, the size of which depended on composition but were in the range 56-107 μm.

(b) Heat 1250°C deformed 70% at 1050°C to give fine recrystallised austenite grains, the size of which again depended on composition but were in the range 14-40 μm.

(c) Heat 1250°C, deformed 50% at 925°C to give partially or fully recrystallised austenite, the fully recrystallised grains being in the 0% V steel or 0.005% N-0.13% V steels with grain sizes in the range 30-50 μm.

(d) Heat 1250°C deformed 30% at 875°C to give unrecrystallised austenite grains which were only slightly elongated.

(e) Heat 1250°C, deformed 50% at 825°C to give heavily elongated unrecrystallised austenite grains containing some deformation bands.

Specimens which had been thermo-mechanically deformed using the above conditions were quenched directly after deformation into a salt bath at 750°C, and the progress of transformation with time was determined, Table 12. As already stated, the isothermal transformation curve showed two stages, the initial stage of formation of ferrite occurring at the prior austenite grain boundaries and the second stage being due to ferrite nucleated within the austenite grains. Actual measurements

of the nucleation rate and growth rate of the different ferrite grains
were not made. However, the period of induction was obtained, and the
shorter the period of induction the faster it can be assumed that
nucleation occurs. Also the average size of the ferrite particles, ie
grains, as a function of time was measured. Whilst this does not give
the actual growth rate of the ferrite particles, the rate of increase
in ferrite particle size always being less than the actual growth
rate, it can be assumed that the faster the average ferrite particle
size increases with time then the faster is the ferrite growth rate
provided the measurements are made before impingement of the ferrite
grains occurs. Thus the rates of growth of the ferrite particle size
may be compared only at small volume fractions of transformation.

9.6.5.1 Effect of Thermo-mechanical Working of the V-Free Steel

The effects of the five different thermo-mechanical treatments on the
progress of transformation in the 0.12% C, 0.010% N, V-free steel are
shown in Fig. 94. Treatments (a)-(d) gave recrystallised austenite of
the grain sizes and $Sv\gamma$ values indicated. In treatment (e) incomplete
recrystallisation occurred and so only $Sv\gamma$ values for two reductions
of 50% and 70% are given. It can be seen that in the recrystallised
condition, decreasing grain size gave faster ferrite nucleation, but
after 30% reduction at 875°C there was an apparent anomaly in that
ferrite nucleated faster than would have been expected from the
austenite grain size. This indicates that at this low deformation
temperature and reduction the austenite was in fact not completely
recrystallised but that this had not been apparent in the optical
micrographs.

On lowering the deformation temperature to 825°C, at which
recrystallisation was incomplete, it can be seen that ferrite
nucleation was accelerated, the effect being more pronounced as the $Sv\gamma$
increased, i.e. as the deformation increased. Some typical
microstructures are shown in Fig. 95. The finer the recrystallised
austenite grain size, in general the finer was the ferrite nucleated
at the austenite grain boundaries, but it is clear that the ferrite
which forms within the austenite grains at the later stage of
transformation is coarser and appears to grow more rapidly probably

126

due to segregation effects. The microstructure of the specimen
deformed 30% reduction at 875°C does - show that recrystallisation
was in fact incomplete, ferrite forming on the deformation bands in
some austenite grains, Fig. 95(d), but this intragranular nucleated
ferrite grew rapidly.

The ferrite nucleated from the unrecrystallised austenite was also
very fine, but again the intragranularly nucleated ferrite grew
rapidly. The effect of thermo-mechanical treatment on the ferrite
particle size is shown in Fig. 96, which confirms the above
observations. It can be seen that after 30% reduction at 875°C the
ferrite particle size became very large due to the rapid growth of the
intragranular nucleated ferrite. In general however the data in Fig.
96 and Table 13, was inconclusive with regard to any indication of the
growth of the ferrite in the early stages of formation, and infact the
thermo-mechanical working conditions which produce substantially
recrystallised austenite all gave apparently similar ferrite growth
rates.

9.6.5.2   Effect of Vanadium

The effect of vanadium was studied by means of an addition of
0.13/0.19% to the 0.12% C, 0.010% N steel. In all the thermo-mechanical
worked conditions, the ferrite transformation at 750°C was considerably
accelerated compared with the unworked specimens. This in largely due
to the refinement of the recrystallised austenite grain size, or an
increase in the Sv_γ in the thermo-mechanically worked condition, Fig.
97. An interesting feature in the very small Sv_γ in condition (d) in
which recrystallisation had not occurred, the Sv_γ reflecting the coarse
austenite grains at 1250°C which had been little elongated by 30%
reduction at 875°C. Yet the transformation did not show any significant
retardation compared with other thermo-mechanically worked conditions,
because the retained deformation caused the ferrite formation to be
accelerated. In the unrecrystallised condition after working at 825°C,
there was very little acceleration of ferrite formation with increasing
reduction and despite an appreciable increase in Sv_γ. This may be due
to the retained deformation accelerating the ferrite nucleation and
masking the effect of Sv_γ.

127

Typical microstructures observed in the thermo-mechanically worked vanadium steel are shown in Fig. 98. In the fully recrystallised condition (a)-(c), decreasing the austenite grain size refined the ferrite particle size. However, when the ferrite nucleated within the grains it showed a coarser ferrite particle size than that nucleated at the austenite grain boundaries, and at the longer transformation times bands of this coarse intragranularly nucleated ferrite were observed, the bands being largely the results of segregation. The coarse intragranularly nucleated ferrite particles engulf the more rapidly · nucleating grain boundary ferrite particles, but do not absorb them. Hence a very variable ferrite grain size is developed. In the unrecrystallised austenite produced by thermo-mechanical working at 875°C and 825°C, the rapidity of nucleation of ferrite did not follow the Sv_γ indications for reasons which have been suggested, but the grain boundary nucleated ferrite continued to be considerably refined. An interesting feature of Fig. 98(e) is the ferrite nucleating effect clearly shown by small second phase particles, the nuclei often occurring within the austenite grains.

The vanadium addition accelerated ferrite formation for all thermo-mechanically worked conditions producing fully recrystallised austenite, Fig. 99, due to the refinement of the recrystallised austenite grain size. In the austenite produced in condition (d), vanadium had little or no effect on the rapidity of ferrite formation. In fact the V-free steel was largely recrystallised (Sv_γ = 31 mm^{-1}) whereas the vanadium steel was completely unrecrystallised and showed little elongation of the austenite grains due to the low elongation, (Sv_γ = 7 mm^{-1}). It might be expected that an Sv_γ of 7 mm^{-1} would retard ferrite formation compared with an Sv_γ of 31 mm^{-1}, but this was not observed due it is believed to the accelerating effect of deformation in the unrecrystallised structure of the vanadium steel. When both the V-free and and the vanadium steel were unrecrystallised at 825°C, and had experienced the same deformation (50%), the ferrite formation in the vanadium steel was accelerated compared with the V-free steel. This follows the trend indicated by the Sv_γ values, the differences in which were due to differences in the original reheated austenite grain size.

The ferrite particle sizes are shown as a function of transformation time in Fig. 100, Table 13. If one considers the very early stages of ferrite transformation, it seems that in the fully recrystallised austenite structure, vanadium decreases the initial growth rate of the ferrite particles, and in fact a similar effect is seen in the unrecrystallised austenite. This effect was possibly due to the formation of interphase precipitates pinning the ferrite/austenite interface or the result of the vanadium partitioning to the growing ferrite and hence decreasing its growth rate. It should also be noted in Fig. 100, that in the recrystallised austenite structures there was little evidence of intragranular ferrite nucleation (other than due to segregation) but in the unrecrystallised austenite there was clear evidence for intra-granularly nucleated ferrite (I) which grows to larger particle size than the grain boundary nucleated ferrite (G.B.)

From these results it is possible to summarise the effect of the 0.13/0.19% V addition. Vanadium accelerates the ferrite formation due largely to it refining the recrystallised austenite grain size or the original austenite grain size which was not recrystallised by thermo-mechanical working. On the other hand, vanadium seems to slow down the growth of ferrite by interphase precipitation or partitioning mechanisms.

9.6.5.3 Effect of Nitrogen

The effect of increasing nitrogen from 0.005% through 0.010% to 0.020% has been studied in 0.12% C, 0.13/0.19% V steels. At all nitrogen contents, the thermo-mechanically processed materials started to transformed more rapidly than the material not thermo-mechanically treated, Fig. 101, 97 and 102. In the low nitrogen steel, 0.005%, this effect was much smaller than in the 0.010% and 0.020% N steels. In general, in the recrystallised austenite structures this effect was largely due to the refinement of the austenite grain size by thermo-mechanical working, and was greater in the 0.010% and 0.020% N steels than in the 0.005% N steels because the latter showed less refined austenite. In the unrecrystallised austenite condition similar effects were also observed, but now the acceleration of transformation in the

low nitrogen steel (0.005%) was increased due to the retention of deformation. At all nitrogen contents, increasing the deformation in the unrecrystallised austenite condition accelerated the ferrite transformation.

Typical structures for the 0.010% N steel have been shown in Fig. 98, and already have been described. Microstructures for the 0.005% N and 0.020% N steels are shown in Figs 103 and 104. The general effects observed were similar at all nitrogen contents but the ferrite particle size in the recrystallised austenite conditions showed slightly smaller values at the 0.020% N level, possibly due to the smaller austenite grain size developed especially in condition (a). Other features which were observed were:-

    i the occurrence of precipitates at the prior austenite grain boundaries in the 0.020% N steel, and also marked darkening of the ferrite due to interphase precipitation.

   ii the much finer grains nucleated on the austenite grain boundaries compared with intragranularly nucleated ferrite, especially in the high nitrogen steel.

  iii the coarse intragranularly nucleated ferrite engulfed the grain bounday nucleated ferrite but did not absorb it, and often formed bands due to segregation effects.

In particular the ferrite formed from recrystallised austenite was observed to produce a uniform ferrite grain size, whereas that formed from unrecrystallised austenite had a much more variable ferrite grain size.

A comparison of the effect of nitrogen is shown in Fig. 105. Increasing the nitrogen content from 0.005% to 0.010% in recrystallised austenite caused ferrite to nucleate more rapidly, but a further increase in nitrogen to 0.020% caused a retardation of ferrite nucleation. The acceleration of ferrite as nitrogen increases from 0.005% to 0.010% is undoubtedly due to a refinement of the austenite grain size. But the retardation of ferrite formation when

the nitrogen increases from 0.010% to 0.020% occurs with a still further, if smaller, refinement of the austenite grain size. It seems that the high nitrogen content itself can retard ferrite formation. In the unrecrystallised austenite in which only 30% deformation has been used at 875°C (condition (d)) similar effects of nitrogen are observed, but at in condition (e) where 50% deformation has been used at the lower deformation temperature of 825°C, the effect of the increased retention of deformation obscures the effect of nitrogen and in fact the transformation is generally the most rapid for all the thermo-mechanically worked conditions. In Fig. 106 is shown the volume fraction of ferrite per $Sv\gamma$ as a function of $Sv\gamma$, which indicates that the increasing nitrogen content decreases the volume fraction of ferrite formed. This is confirmed by the results shown in Fig. 105.

The effect of nitrogen on the ferrite particle sizes for all the thermo-mechanically treated conditions is shown in Fig. 107. It can be seen that the highest nitrogen content produces the finest ferrite particles for all deformation conditions, and it seems the ferrite growth rate is lowest for the high nitrogen steel. This effect may well be due to increased pinning of the ferrite/austenite interface by either an increased volume fraction and/or a decreased particle size of the interphase V(CN) precipitates. In the recrystallised austenite, (conditions (a)-(c)) refining the austenite grain size produces smaller ferrite particles.

An interesting feature is the intra-granular nucleation of ferrite at the highest nitrogen content, possibly due to the nucleating effect of V(CN) precipitates. In the unrecrystallised austenite, there is always intra-granular nucleation of ferrite, and the intra-granular ferrite is always coarser than the grain boundary nucleated ferrite, as indeed was shown by the microstructures in Fig. 98, 103 and 104. It is interesting to note that after only after 30% reduction at 875°C, the ferrite particles were larger than 30% and 50% reduction at the lower temperature of 825°C. It may be suggested that ferrite experiences more dificulty in growing in more heavily deformed austenite, although the intra-granular nucleation rate may be increased. The evidence in Fig. 107, does not show clearly whether increasing nitrogen decreases the apparent growth of the ferrite in recrystallised austenite.

However in unrecrystallised austenite there seems to be a systematic effect of increased nitrogen causing a slower initial ferrite growth rate, possibly due to strain inducement of more precipitates in the austenite which impede the movement of the ferrite transformation front.

9.6.6 Effect of Continuous Cooling on the Ferrite Grain Size

Thermo-mechanically processed specimens were cooled between 800°C and 500°C at rates in the range of 2.5 to 4.5 °C/sec, Table 14, to investigate the effect of vanadium and nitrogen on the ferrite grain size which was developed. Large (30% reduction at 1200°C) and small (70% reduction at 925°C) recrystallised austenite grain sizes were selected from the recrystallised regime and 50% and 70% reduction at 825°C from the unrecrystallised regime. Results are shown in Fig. 108. With increasing $Sv\gamma$, i.e. increasing nucleation potential for ferrite, the ferrite grain size in the continuously cooled transformation specimen was markedly refined and this effect was more pronounced for the vanadium steel compared with the V-free steel, as expected. However, it can be seen from Fig. 108(a) that at small $Sv\gamma$ values below 25 mm^{-1}, vanadium had no effect on the ferrite grain size. In Fig. 108(b) it can be seen that there was no systematic effect of nitrogen on the ferrite grain size irrespective of $Sv\gamma$, possibly because of changes in the transformation temperature during continuous cooling obscuring any effect of nitrogen.

CHAPTER 10 **DISCUSSION**

10.1 **SOLUBILITY STUDIES**

10.1.1. Preliminary Work to determine Extraction Method

The solubility products for VC[(99-103)], Fig. 23 and
VN[(65,100,105,106)], Fig. 24, show that all the vanadium, carbon and
nitrogen will be in solution at 1250°C in all steels listed in Table
2. The minimum temperature at which VC and VN will be in equilibrium
in the absence of ferrite is 900°C, as some ferrite was observed at
850°C during isothermal transformation studies, section 9.4. Specimens
for preliminary work to determine the best method for precipitation
extraction were austenitised at 900°C. Table 3 shows the results
together with particle size where available.

Two main methods were initially employed for preliminary
investigation, the chemical method in which millings of specimens were
immersed in the solution concerned, either at room temperature or at
higher temperatures until the millings were completely dissolved.
Using the electrochemical method, in the solution concerned, a
potentiostat was used to maintain a constant voltage until the sample
was dissolved. Chemical extraction in 20% H_2SO_4 at 60°C took about 8
hours to dissolve a similar amount of millings as was dissolved in 6N
HCl in 3 to 4 weeks. Decreasing the concentration to 10% HCl, but
raising the temperature of the solution to 50°C accelerated the
reaction and reduced the dissolution time to 2-3 days. On drying the
extracted residue, in a high purity argon atmosphere after washing in
fresh mother liquor, distilled water and alcohol, the residues in 6N
HCl resulted in a solid cake, whereas the other solutions resulted in
a powder, as expected. Analysis of the extracted residue showed high
sulphur concentrations in the residue extracted in 20% H_2SO_4.

Furthermore, the electrochemical method using 10% HCl suffered from
similar disadvantages to that of extraction in 6N HCl, i.e. on drying
the residue resulted in a solid cake. Electrochemical extraction of
precipitates using 7% $FeCl_3$, 3% HCl and 3% Ethylene Glycol solution,
gave residues which showed larger concentrations of carbon and

133

nitrogen than those present in the steel itself, Table 4.1, but in the chemical extraction techique using 10% HCl at 50°C the carbon and nitrogen contents were much lower and conformable with those present in the steel. The vanadium contents of the precipitates were unaffected by the method of extraction. In the light of the difficulties mentioned, it was decided that chemical extraction in 10% HCl at 50°C should be used throughout for precipitation extraction. This method has the advantage of dissolving any Fe_3C[165] formed during quenching specimens from the austenitising temperature.

10.1.2 Comparison of Precipitates

All the steels used in the present investigation were silicon killed to avoid the formation of AlN. Whatever aluminium was present was in very small quantities, less than 0.010%, and is unlikely to form any AlN[91, 166]. However it is known that some elements can dissolved in VC[167], and when wet analysis was not possible due to small quantities of residues extracted from steels, flourescence spectroscopy revealed not only the presence of vanadium, but also the presence of silicon which of course may be due to silicate inclusions. However, various silicon nitrides can be formed[168] and silicon has been reported to dissolve in various microalloying nitrides[169] so that silicon may occur in complex (VSi)(CN) precipitates. Quantitative analysis for silicon content was not carried out on the residues.

The effect of increasing austenitising time at 900°C on the composition of the precipitates is given in Table 4. At a low N:C ratio in the steel i.e. low nitrogen content in the steel, increasing austenitising time had no effect on the composition of the precipitates, Table 4.2.1.

Increasing the nitrogen content to 0.010% in 0.12% C, 0.13% V steel increased the N:C ratio in the precipitates with increasing austenitising time from 0.14 to 0.29, Table 4.1. It can be suggested that the first to precipitate out were VC with nitrogen diffusing into them with increasing time, forming V(CN). Alternatively the VC and VN nucleated separetely with the former nucleating first from supersaturation considerations. However increasing the nitrogen

134

content from 0.005% to 0.010% did not have any effect on the final average composition of the V(CN). Increasing the vanadium content to 0.41% in the 0.10% C, 0.010% N steels, caused austenitising time to have no effect on the composition of the precipitates, but the overall nitrogen content of the precipitates was reduced, Table 4.2.3. Further increasing the nitrogen content to 0.020% in the 0.12% C, 0.15% V steel apparently caused nitrogen rich precipitates to form first due to the higher nitrogen content of the steel with subsequent diffusion of carbon into the V(CN) with increasing time or the nucleation of VC (low in nitrogen) at the longer times. This latter suggestion is in agreementwith Roberts and Sandberg[106] who suggested that VN should form first in a vanadium H.S.L.A. steel, especially at high nitrogen contents in the steel.

Increasing the V:N ratio in the steel by either increasing the vanadium or more usually by decreasing the nitrogen content, gave precipitates which had a low N:C ratio i.e. were much richer in carbon, Fig. 33, Table 5, as the potential of nitrogen for precipitation was much smaller than that for carbon. However at lower V:N ratios in the steel, i.e. high nitrogen contents in the steel, the N:C ratio in the precipitates increased. Thus it seems that the higher the N:C ratio in steel the greater was the N:C ratio in the precipitates, Fig. 34, which is in good agreement with the published data[165].

It seems that in a high vanadium-low nitrogen steel the first to form were rich in carbon followed by nitrogen diffusing into them to become V(Cn). The stability of such precipitates is less than that of V(CN)[136] and this is indicated by the increase in carbon content in the precipitates as the carbide solvus temperature was approached, Table 6, the nitride dissolving at lower temperatures due to lower nitrogen in the steels. Increasing the nitrogen in the high vanadium steel caused the stability of V(cN) rich in nitrogen to increase as the solution treatment temperature increased. This indicates that the stability of V(cN) rich in nitrogen is much greater than the V(Cn) rich in carbon, as indeed is well known[106, 136, 137].

In the present investigation it was found that if the V:N in the steel

is greater than the stoichiometric ratio the V(CN) precipitates are rich in nitrogen. From the results shown below the present data are in reasonable agreement with that published.

steel composition V:N	composition of precipitates V:N	source of data
6.7	5.45	Kopernikova[163]
4.75	3.35	Robert and Sandberg [106]
7.50	3.37	Present

In summary it has been shown that increasing the V:N ratio in steel produced precipitates rich in carbon due to the lower nitrogen content. However at lower values of V:N ratio in the steel, by increasing the nitrogen in the steel, the precipitates were rich in nitrogen. In general as the N:C ratio in steel increased the corresponding N:C ratio in the precipitates increased greatly. Furthermore, the stability of V(cN) rich in nitrogen was much greater than the stability of V(Cn) rich in carbon.

10.1.3 Solubility Product

The solubility of vanadium, carbon and nitrogen is influenced by the presence of other alloying elements[66, 104, 166]. In the present investigation the slight variation in manganese content, Table 2, probably had little or no effect on the solubility.

The solubility of vanadium, carbon and nitrogen are given in Table 6. These data probably represent only an incomplete approach to equilibrium[105], but it must be emphasised that they show some systematic effects. The solubility of vanadium, carbon and nitrogen increased with increasing temperature between 900°C and 1250°C, Figs 35 and 36. The solubility of carbon is greater than the solubility of nitrogen.

The solubility equations for vanadium carbide (VC) and vanadium nitride (VN) were calculated on the assumption that there was no interaction, as indicated recently[106] in a thermodynamic analysis. Typical example of solubility curves are shown in Figs 37 and 38, which show that the solubility of VC and VN increased with increasing austenitising temperature, and the former being higher than the latter, as expected.

The solubility relationships determined for VC are given in Fig. 39. The scatter of the present results are within the scatter band of the published literature, However in the present results, at a constant carbon and vanadium content increasing nitrogen decreased the VC solubility, probably due to nitrogen forming V(CN) of greater stability than VC. Also increasing vanadium content in the steel at constant carbon and nitrogen decreased the calculated solubility for VC, as also did increasing the carbon content of the steel. These effects may be due either to the presence of a defect lattice in the predominantly VC, the extent of the defect lattice controlling the solubility, or due to V-C clustering in the austenite. A VC lattice free from vacant interstitial sites due to the introduction of nitrogen, and V-C clustering in austenite might both be expected to decrease the solubility of VC.

Published data has shown a much narrower scatter band for VN solubility, Fig. 40, compared with VC, Fig. 39. Also VN has a solubility at least one order of magnitude less that that for VC. The observed solubility data are comparable with those published and are within the published scatter band. The effect of varying composition on the solubility of the VN is less marked than in the case for VC, and no clearly defined trends could be identified, but the effects appeared to be somewhat similar to those found in studying the solubility data for VC. As it has been shown by Roberts and Sandberg[106] that the VN is more probable than VC to form first especially at the higher nitrogen contents, and the overall stability of VN is much greater than VC, it is suggested that the solubility of VN will not be influenced as greatly by the presence of carbon as that of VC is by the presence of nitrogen.

137

Theoretically it is known[106] that VC and VN are mutually soluble and in an attempt to assess the solubility of a V(CN) phase, the carbon and nitrogen were combined as (C + (12/14) N). This approach has been used in other solubility studies[109]. Such data is shown in Fig. 41. Although there is no equivalent published data, the solubility curves shown similar effects to those encountered during the examination of the solubility of VC i.e. increasing the precipitating elements in steel decreased the solubility of [V] [C + (12/14) N] in austenite. However calculation of the solvus temperature from Fig. 41 gives too low temperatures. Consequently the assumption for the formation of [V] [C + (12/14) N] is probably unjustified and the assumption made by Roberts and Sandberg[106] that VC and VN form independently is probably most viable.

The solubility equations obtained in the present study are as follows:-

a. Solubility product - log [V] [C] = - A / T + B

where T in ^{o}K and A and B as given below

steel composition			A	B
0.103% C	0.350% V	0.005% N	4509	1.70
0.120% C	0.150% V	0.020% N	9507	5.74
0.126% C	0.415% V	0.020% N	7885	3.99
0.212% C	0.145% V	0.018% N	8704	4.27

b. Solubility product - log [V] [N] = - A / T + B

where T in ^{o}K and A and B as given below

steel composition			A	B
0.103% C	0.350% V	0.005% N	7851	2.90
0.120% C	0.150% V	0.020% N	7754	2.80
0.126% C	0.415% V	0.020% N	9280	4.04
0.220% C	0.160% V	0.0058% N	3716	0.54
0.212% C	0.145% V	0.018% N	7472	2.90

In summary it has been shown that the solubility of V(CN), VC and VN increase with increasing austenitising temperature. The solubility of V(CN) is not greatly dissimilar from that of VC but the solubility of VN is much smaller at all austenitising temperatures. The solubility of VC decreases with increasing vanadium, carbon and nitrogen in the steel, and possible reasons for these have been implied. The results indicate that VN and VC largely form as separate phases.

10.2 AUSTENITE GRAIN GROWTH

In a steel in which there is no restriction of austenite grain boundary movement, the grain size increases progressively with increasing temperature. At constant temperature, the grain size increases with increasing time according to the equation (29) :-

$$D = k\ t^{\,n} \qquad\qquad 29$$

At low temperature n is less than the theoretical value of 0.5, but with increasing temperature n increases towards the theoretical value. This type of behaviour is shown by the low nitrogen steels relatively free from grain boundary pinning particles, Figs 42(a) and 43(a). It is reported that k obeys an Arhennius relationship with temperature but that the activatiom energy for the grain growth process is not constant.

On the other hand, in a steel in which the grain boundaries are pinned by second phase particles or even solutes, the grain size remains constant at the low temperatures or grows only slowly with increasing temperature or time. At some higher temperature, however, the grain size begins to grow much more rapidly due to less of the pinning effect, and this temperature is the grain coarsening temperature. Again the results in the present work show this effect for many of the steels. Below the grain coarsening temperature, the value n in equation (29) is much less than above the grain coarsening temperature[170]. This effect is also shown in the present work. The grain coarsening temperature decreases with increasing austenitising time due to growth of the pinning particles allowing the boundaries to

become unpinned at lower temperatures. This effect also has been shown by the present work. Due to inhomogeneity in the size distribution of the pinning particles, some grains can become unpinned earlier than others, leading to abnormal grain growth, and the grain size distributions in Fig. 44 indicate this effect[171].

A model proposed for estimating the grain coarsening temperature[57, 58] has shown that there is a critical pinning particle size, which increases with increasing volume fraction of particles, above which grain boundary pinning is lost. This model shows that the grain coarsening temperature is always below the solvus temperature of the pinning particles, and that grain coarsening is largely controlled by the growth of the pinning particles with either increasing temperature or time. In the present work, the solvus temperatures of the most probable pinning particles, VC and VN, can be estimated, but there does not seem to be any reliable information on the growth of VC and VN in austenite, nor has the size of the particles been determined in the present work as a function of time and temperature. It is however possible to compare the grain coarsening temperature with the pinning particle solvus temperature.

10.2.1   Effect of Nitrogen and Carbon in V-free steels

In the 0.103% C, 0.006% N steel, no grain coarsening temperature was observed, Fig. 42(a) and the grain size increased progressively with increasing temperature, i.e. the steel contained no grain boundary pinning particles. However the n values (equation 29) show very little systematic effect with increasing temperature.

Increasing the nitrogen content to 0.020% caused a different grain coarsening behaviour, Fig. 42(b). At low temperatures up to 1150°C only slow grain growth occurred, n being small, but at higher temperatures of 1150°C - 1250°C rapid grain growth occurred and at these higher temperatures n is approached the theoretical value of 0.5. Moreover, the austenite grain sizes were considerably finer than in the low nitrogen steel. These effects indicate some pinning action due to nitrogen, which will be discussed later.

Increasing the carbon to 0.20% in the high nitrogen steel caused a further change in the grain coarsening characteristics. The actual value of the austenite grain size at low temperatures was similar to that for the 0.12% C, 0.020% N steel, but at about $1000/1050^{\circ}$C, a small sudden increase in the grain size occurred, and at higher temperature of $1150/1200^{\circ}$C major grain coarsening occurred and the n value again approached 0.5. Once again, some grain boundary pinning seems to be indicated. The possibility of grain boundary pinning by increasing carbon and nitrogen in a steel containing no vanadium and 0.001/0.010% Al is unusual, especialy as the steels contained low sulphur, phosphorous and residual elements, and there was little difference between them. In the 0.10/0.12% C steels, the aluminium was 0.001% i.e. so low that if AlN had been formed it would have all been dissolved at 900°C. Consequently the effect of 0.020% N at this carbon content seems to be to cause some grain boundary pinning, but even if nitrogen segregated to the austenite grain boundaries its diffusivity would be expected to be so high as not to cause a pinning effect.

It is tentatively suggested that some clustering of nitrogen atoms might occur at the lower austenitising temperatures which could cause some boundary pinning effects, and that these clusters might thermally disperse at higher temperatures to allow more rapid grain growth to occur. This possibility has been suggested in other contexts, but only for the steels containing small vanadium contents[172]. When 0.20% C was added to the 0.017/0.020% N steel, the grain size up to 1000°C was hardly affected, and the slight increase in the grain size at 1050°C may have been due to a loss of pinning by clusters of carbon atoms, analogous to those suggested tentatively for nitrogen. But a definite grain coarsening temperature occurred at approximately 1150°C, which could have been due to some pinning by AlN at lower temperatures, the steel containing 0.01% Al which would give a calculated AlN solvus of approximately 1150°C.

10.2.2 Effect of Nitrogen in 0.13/0.19% V steels

In the steels containing 0.11% C, and 0.005% N, the vanadium steel showed very similar grain coarsening characteristics to the V-free steel, Fig. 43(a), except that at low temperatures of $900-950^{\circ}$C the

grain size was smaller in the vanadium steel. In fact VN in this steel would not dissolve until approximately 980°C, so that it might be responsible for the smaller grain size. At higher temperatures however there was little effect of vanadium on the grain size, suggesting that vanadium in solid solution had very little effect on the grain growth at this low nitrogen level.

Increasing the nitrogen to 0.021% however produced a very small grain size at 900-1000°C and the time dependence was negligible. This indicates very effective pinning by VC/VN, Fig. 43(b). Above 1000°C, grain coarsening occurred, but the austenite grain size above the coarsening temperature was much smaller than that of a comparable V-free steel. A possible explanation of these effects is that at 1000°C, the VC is all dissolved (solvus 1000°C) which allows some slow grain coarsening because there is still some VN causing pinning. It is calculated that the VN solvus is approximately 1200°C and it is significant that only at 1250°C did the grain size coarsen, and then only at the longest time, i.e. the grain coarsening temperature for VN pinning seems to be in the range 1200-1250°C. It is possible that a pinning effect could be exerted by V-N clusters, and the time exponent is low at all temperatures up to 1200°C, indicating a definite grain boundary pinning effect.

10.2.3 Effect of Nitrogen in 0.43% V steels

In the higher (0.35/0.41%) V, 0.10/0.12% C steels, increasing nitrogen increased the temperature at which grain coarsening commenced, Fig. 47 (c) and (d). In the 0.005% N steel, the solvus temperature of VC was about 900°C[99] and for the VN 1060°C[106]. The grain size was refined up to 1000°C in the presence of VN precipitates whereas on further increasing the temperature a sharp increase in grain size was observed due to the solution and growth of VN precipitates. Increasing the nitrogen content to 0.010% and 0.020% in the 0.10/0.12% C steels refined the grain size below the grain coarsening temperature with the latter steel being refined due to the increased volume fraction of VC/VN. The refinement was greater at temperatures just prior to full solution of VN. However at the higher temperatures the grain size of the 0.010% N steel was somewhat smaller than that of the higher

nitrogen steel, contrary to expectation, and this effect was more pronounced and occurred at lower temperatures when the austenitising time increased to 8 hours, Fig. 47(d). It suggested that this effect is due to more pronounced abnormal grain growth in the highest nitrogen steel due to some of the precipitates being larger because of the higher supersaturation. These larger precipitates allow local unpinning to occur so that abnormally large grains are formed which grow to consume the matrix. This effect is not inconsistant with the lowering of the grain coarsening temperature reported for higher alloy contents in niobium and vanadium steels[76].

10.2.4   Effect of Vanadium

The addition of 0.13/0.14% V to the 0.12% C, 0.005% N steels decreased the austenite grain size at all temperatures without altering the overall grain coarsening characteristics, Fig. 45(a), the grain size increasing monotonically with increasing temperature. A larger addition of 0.35/0.41% V however decreased the austenite grain size up to 1000°C due to the formation of VC and VN with solubility temperatures of 900°C[99] and 1060°C[106] respectively. On dissolution of VC/VN above 1000°C the grains grew in a manner similar to the steel with lower (0.13/0.14%) vanadium, but the grains were finer at all temperatures. The refinement of the grains was attributed to the initial grain refinement by the precipitates at the lower temperatures. In these low nitrogen steels there was no evidence of abnormal grain growth and vanadium in solution did not apparently alter the rate of grain growth with increasing temperature.

The addition of 0.13/0.19% V to the 0.10/0.12% C steel containing 0.010% N, caused a constant grain size to be observed up to 950/1000°C, Fig. 45(b), due to the larger volume fraction of VN with solvus temperatures up to 1050°C. Grain growth commenced as soon as the particle volume fraction or size departed from the critical values[57,58], i.e. the volume fraction of precipitates decreased by solution or the actual particle size increased by growth. It can be seen from, Fig. 45(b), that grain growth appeared to occur in two stages. That which occurred above approximately 1000°C was due to lack of pinning by VC (i.e. growth or dissolution of VC) whereas the

grain coarsening which occurred at the higher temperature of approximately 1100°C was due to the removal of pinning by VN. Increasing the vanadium addition further to 0.35/0.45% in the 0.010% N steels caused a much refined austenite grain size due to an increased volume fraction of pinning particles, but the general grain coarsening effects were little altered, there again being a two stage coarsening behaviour.

In the 0.020% N steels, the addition of 0.13/0.19% V markedly refined the grain size due to the introduction of a larger amount of VN, with some VC, and grain coarsening occurred just above 1000°C, although the VN solvus was greater than 1100°C. It should be noted that there was not a two stage coarsening process, presumably the coarsening characteristics in this case being controlled largely by VN. It is interesting to observe the absence of marked grain growth at 1150/1200°C, and it is suggested that this was due to the absence of any pronounced abnormal grain growth. On the other hand a still further increase in vanadium to 0.35/0.45% caused an increase in the grain coarsening temperature to approximately 1100°C due to the greater volume fraction of VN and the higher solvus temperature of approximately 1200°C. However the grain size at above 1200°C was considerably larger than for the 0.13/0.19% V steel, and this is believed to be due to localised and more pronounced abnormal grain growth for reasons discussed earlier, i.e. larger local particle sizes due to increased supersaturation.

10.2.5 Effect of Carbon

Increasing the carbon content from 0.12% to 0.20% in the V-free steel, Fig. 49(a), had little effect on the grain size characteristics, except for the larger grain size in the 0.20% C steel at 1250°C, and this has been discussed earlier, in relation to the possibility of clustering effects and the 0.010% Al present in the higher carbon steel.

In the 0.13/0.15% V steels containing low nitrogen (0.005%) there was virtually no effect of increasing the carbon content from 0.12% to 0.20%, Fig. 49(b). With the higher nitrogen content of 0.010% there

144

was again a two stage grain coarsening behaviour. This has been discussed earlier, the lower temperature coarsening being suggested as due to loss of VC pinning, whilst the high temperature was due to the loss of VN pinning. The effect of increasing carbon from 0.055% to 0.20% in the steels containing the higher 0.18/0.020% N is shown in Fig. 49(d). In these higher nitrogen steels, carbon had little effect on the grain coarsening temperature which was in the range 1000/1050°C, and was apparently controlled by VN which had a solvus temperature of approximately 1100°C.

Grain coarsening always occurs below the pinning particle solvus temperature. However there were some interesting effects at the higher temperature of 1200/1250°C in that the 0.055% C and 0.20% C steels showed coarser grain sizes than the 0.12% C steel, i.e. a two stage coarsening effect. It is tentatively suggested that this effect may have again been due to more abnormal grain growth in the low and high carbon steels, but it should also be noted that the high carbon steel contained 0.010% Al which would have allowed AlN to be present up to approximately 1150°C. Thus some complication in the grain coarsening effects seems to have been introduced by the inadvertently high aluminium content, as discussed earlier.

10.2.6 Grain Coarsening Temperature

Because of the low solubility of VN and its greater stability in comparison to VC[136, 137] it is believed that the particles pinning the austenite grain boundaries and thereby inhibiting grain growth were mainly VN. Hence it might be that the grain coarsening characteristics are controlled by the solubility and coarsening of such VN particles in austenite. It is known[126] that the grain coarsening temperature is always lower than the solvus temperature of the VN. The results shown in Table 10.2.6.1 indicate that the solvus temperature of VN was in fact actually higher than the grain coarsening temperature, as assessed by the temperature at which the grain size started to increase appreciably.

Thus the observed grain coarsening temperature was always lower than the VN solvus temperature, as expected, with the exception of steel

145

Number 8 which contained high carbon, high vanadium and very low
nitrogen contents, i.e. there was probably relatively little VN to
produce grain boundary pinning. It seems therefore, in view of this
data and the fact that the observed grain coarsening temperature was
always above the VC solvus temperature, that the grain boundary
pinning particles largely responsible for controlling grain coarsening
were VN.

TABLE 10.2.6.1

VN SOLVUS AND GRAIN COARSENING TEMPERATURES

Alloy	VN solvus TEMP.$^{\circ}$C	GRAIN COARSENING TEMPERATURE $^{\circ}$C	
		CALCULATED	OBSERVED
1	980	1075	900
2	1060	1142	1000
3	1033	1150	1000
4	1144	1260	1050
5	1112	1150	1000
6	1222	1250	1150
7	1004	1165	925
8	1054	1180	1100
9	1060	1150	1000
10	1153	1240	1075
11	1098	1220	1025
12	1214	1280	1150

Using a model proposed for the estimation of the grain coarsening
temperature[58] a calculation of the grain coarsening temperature has
been made. This used the published solubility data for VN in order to
obtain the volume fraction of undissolved VN and thus the critical
particle size above which pinning was lost. The grain size
heterogeneity factor was assumed to be $Z = 1.5$, as indicated by the
published literature[58]. No data was found for the particle
coarsening of VN in austenite, and so the equation determined for the

NbC[58] was used because of the similar stabilities of VN and NbC as indicated by their similar solubilities. The calculated grain coarsening temperatures was considerably greater than the observed grain coarsening temperature, Fig. 109, but it can be seen that there was a clear trend for the calculated and observed grain coarsening temperatures to be related to one another. A possible reason why the calculated grain coarsening temperature was always higher than the observed temperature is probably associated with the Z value being greater than 1.5, and the observed values were in fact often much above 1.5 due to abnormal grain growth. In addition the discrepancy between calculated and observed grain coarsening temperature could also be due to the calculated particle size, from the NbC coarsening equation being too small. Hence it may be concluded that VN coarsens considerably more rapidly than does NbC.

10.2.7 Activation Energy for Grain Growth

An attempt was made to calculate the activation energy for grain growth, using the approach outlined by Byrne[3]. When there was no grain boundary pinning, the activation energy was in the range 175 – 235 KJ mol^{-1}, which is slightly lower than the activation energy for diffusion of vanadium in austenite[151] or for self diffusion in iron. But it must be remembered that the activation energy for grain growth has been reported to vary[173]. However, when there was clearly defined pinning of the austenite grain boundaries in the steel the activation energy increased to values in the range 300 – 350 KJ mol^{-1}. However the errors involved in calculating the activation energies were probably quite large, and the interpretation is unclear.

10.3 **TEMPERING STUDIES**

10.3.1 Hardness of as Quenched Martensite

Increasing nitrogen content from 0.005% to 0.020%, progressively increased the as quenched martensitic hardness, Fig. 50, but the effect of vanadium was less clear. At 0.005% N and 0.010% N, increasing vanadium had little effect on the martensitic hardness, but at 0.020% N increasing vanadium progressively increased the hardness.

147

Moreover the increase in martensitic hardness per 0.010% N increased from 11 H.V. at 0% V to 38 H.V. at 0.40% V after austenitising at 1250°C at which all the VC/VN was dissolved. With a lower austenitising temperature of 1075°C at which some VN was undissolved in the 0.40% V steel, a rather different effect was observed in that at 0% V and 0.14% V the hardening effect of nitrogen was slightly increased, but at 0.40% V, where there was much VN undissolved, a much smaller effect of nitrogen was obtained.

These results indicate a synergistic effect of vanadium and nitrogen on the martensite hardness, possibly due to V – N clusters inherited from the austenite which could give increased lattice distortion in and around the cluster. An interesting effect is the smaller effect of nitrogen on the martensitic hardness at the higher austenitising temperature, under conditions where all the VN is dissolved. This might be interpreted as the dispersion of clusters at the higher austenitising temperature, as has been suggested by other work[77]. In fact it was observed that increasing austenitising temperature above the VN solvus caused a progressive decrease in the martensitic hardness, which can be interpreted to support the clustering hypothesis. When VN is undissolved in the 0.40% V steel, as expected nitrogen has less effect on the martensitic hardness.

Similar effects were obtained with increasing carbon from 0.12% to 0.20% at 0.40% V and 0.020% N steel, in that a much greater increase in martensitic hardness was obtained after austenitising at 1075°C (approximately 80 H.V.) than after austenitising at 1250°C (approximately 50 H.V.). It is suggested that this could be due to carbon clustering together with vanadium and nitrogen atoms, the clusters being thermally dispersed at the higher austenitising temperatures. Again the possibility of V – C clusters has been postulated in previous works concerned with the tempering of vanadium steels[77].

In the above discussion, no account has been taken of possible auto-tempering effects but it is well known that vanadium retards low temperature tempering[77, 174]. Also it cannot be discounted that the lower martensitic hardness after quenching from the higher

austenitising temperature could be partly due to the coarser austenite grain size, or martensitic packet size[174], but the effect is likely to be quite small.

10.3.2 Tempering of Martensite

In the V-free steels, increasing tempering time and temperature caused the hardness to decrease progressively, as expected, but at the higher tempering temperatures the hardness levelled out due to recrystallisation having occurred and ferrite grain growth being quite small, Fig. 51(a). At the higher carbon content, the greater volume fraction Fe_3C precipitated during tempering caused the recrystallisation at the higher tempering temperatures to be slower because the Fe_3C pinned the tempered martensite sub-structure. In the V-free steels decreasing the austenitising temperature from 1250°C to 1075°C decreased the hardness during tempering probably due to the finer grain size allowing more rapid coarsening of Fe_3C because of more rapid diffusion paths. This seemed to offset the slight strengthening due to the finer grain size.

The addition of vanadium led to a number of effects. At low tempering temperature the level of the hardness was increased due to vanadium increasing the tempering resistance by retarding the growth of Fe_3C. At the higher tempering temperature of 500-550°C, secondary hardening was introduced, the effect becoming more pronounced with increasing vanadium content. At still higher tempering temperatures, vanadium increased the resistance to overaging after secondary hardening because of the slow growth of the stable V(CN) precipitates. In addition, the presence of these precipitates retarded recovery of the matrix and thus a slower recrystallisation.

Increasing the nitrogen tended to raise the overall hardness level after tempering, the effect becoming less pronounced with increasing tempering especially in the vanadium steels, Fig. 57, but nitrogen did not seem to influence the intensity of secondary hardening.

There was little systematic effect of changing the austenitising temperature, which did not seem to influence the intensity (i.e. the

increase in hardness) of secondary hardening. However at the higher tempering temperatures there was an effect that the hardness was greater than with the lower austenitising temperature, Fig. 56. Possible reasons for this are the smaller initial austenite grain size giving ⁓ smaller recrystallised ferrite grain sizes, together with undissolved VN particles also restricting the ferrite grain growth.

10.3.3 Holloman-Jaffe Tempering Curves

10.3.3.1 Effect of Vanadium

In the 0.005% N steels increasing vanadium progressively increased the resistance to low temperature tempering, due to it retarding the formation and growth of Fe_3C[175]. As Fe_3C can dissolve about 10% V[167], it is possible that it is the growth rate which is most affected. This effect is well known, and the results tend to confirm the published data which shows that this retardation of tempering by vanadium increases with increasing tempering temperature up to about 500°C, Fig. 54. Vanadium also introduced secondary hardening, the intensity of which became much more pronounced with increasing vanadium content, Table 8, due to the greater volume fraction of precipitated VC. In fact as the vanadium increased up to approximately 0.40%, the steel more nearly approached the stoichiometric ratio for VC, at which secondary hardening is known to be maximised[159, 172] due to the temperature dependence of the solubility of VC also being a maximum[176].

In the overaged condition, increasing vanadium increased the hardness, and this was more apparent with the lower austenitising temperature, as discussed previously. At higher nitrogen content, the effects of vanadium were very similar, Fig. 55, and it is interesting that increasing nitrogen did not increase the effect of vanadium on the intensity of secondary hardening. A similar lack of effect of nitrogen on secondary hardening in vanadium containing steels of the 4330 type[177] has been observed and attributed to the fact that increased nitrogen gave such a small increase in the volume fraction of secondary hardening carbides that its effect was within the general scatter band of the results.

10.3.3.2   Effect of Nitrogen

The effect of nitrogen was to generally increase the hardness at all
tempering temperatures, Figs 57 and 58. This effect was much more
pronounced at the lower tempering temperatures but decreased greatly
as the tempering temperature increased, particularly in the vanadium
steels. At the lower tempering temperatures, the tempered hardness
seems to reflect the initial martensite hardness, which clearly
increased with increasing nitrogen content, and this may simply
reflect solid solution hardening which had not been destroyed entirely
by precipitation during tempering. As already discussed, nitrogen did
not affect the intensity of secondary hardening, and therefore had
little effect on the overaged hardness at the higher tempering
temperatures presumably because it produced only a small increase in
the volume fraction of V(CN). It should be mentioned however, the VN
grows less rapidly than $VC^{(136)}$ and so nitrogen may slow the growth of
V(CN) and thus give a slightly increased overaged hardness. The
general effect of nitrogen on the tempering characteristics was very
similar irrespective of the vanadium content, but maximun secondary
hardening seemed to occur at a somewhat lower tempering parameter with
increasing nitrogen content possibly due to an increase in the
supersaturation for V(CN). Nitrogen did not seem to affect recovery
and recrystallisation during the overaging of the steels, these
processes being more influenced by the predominantly VC precipitates.

10.3.3.3   Effect of Carbon

The effect of carbon was only studied in the 0.40% V, high nitrogen
steels. At the lower tempering temperatures increasing carbon
increased the hardness, Fig. 59, due to increased volume fraction of
Fe_3C. In addition although carbon increased the maximum secondary
hardness observed, Fig. 59, it actually decreased the intensity of
secondary hardening, Table 8. This latter effect can be explained in
terms of a much lower V:C ratio in the higher carbon steels compared
with the 0.10/0.12% C steels, which caused the composition to depart
significantly from stoichiometry and thus show less temperature
dependence of the VC solubility. The result was the lower intensity of

secondary hardening. In the overaged condition, the hardness was not influenced by carbon which suggests that the lower volume fraction of VC in the higher carbon steel was just about offset by excess carbon forming Fe_3C.

10.4 ISOTHERMAL TRANSFORMATION STUDIES

10.4.1 Isothermal Transformation Characteristics

The main purpose of this work was to investigate the formation of pro-eutectoid ferrite for comparison with similar studies in the thermo-mechanically processed austenite. The effect of adding 0.13% V to a steel containing 0.126% C, 0.010% N will be examined initially followed by the effect of increasing N from 0.005% to 0.020% in the presence of 0.13/0.15% V.

Specimens were quenched from austenitising temperature of $1250^{\circ}C$ and transformed isothermally at temperatures of $500^{\circ}C$ to $850^{\circ}C$. At the temperature where polygonal ferrite was formed, above $650^{\circ}C$, the transformation curves all showed a similar form, Figs 60 and 61. Such curves were comprised of two stages, in the first (A) of which ferrite nucleation and growth occurred at the austenite grain boundaries, Fig. 60 (a) and (b) and Fig. 61 (a)and (b). The second stage was associated with ferrite nucleation and growth within the austenite grains and eventually with the pearlite transformation below A_1. However these two stages of ferrite formation were also observed at temperatures above A_1.

As explained previously, in interpreting the kinetics of ferrite formation, the period of induction has been used as an indication of the general rate of nucleation of ferrite. The initial slope of the ferrite volume fraction versus time curve has been used to indicate a measure of the growth rate of ferrite. An optimum temperature at which ferrite nucleation and growth was sufficiently slow (and transformation did not go to completion) was selected to investigate ferrite formation. From thermo-mechanically worked austenite, which will be discussed later, $750^{\circ}C$ was found to be the most suitable transformation temperature.

10.4.2 Effect of Vanadium

The effect of 0.13% V in the 0.12% C, 0.010% N steels was to
accelerate the nucleation of ferrite, as typified by the curves shown
in Fig. 60. The isothermal transformation curve comprised two distinct
stages, stage A being associated with ferrite nucleation and growth at
the austenite grain boundaries and stage B with ferrite nucleation and
growth within the austenite grains, and eventually with the pearlite
transformation below A_1. These two stages became less distinct as the
transformation temperature decreased, Fig. 60 and Fig. 61, and
approached the nose of the T.T.T. diagrams, Figs 66 and 67, when the
two stages showed considerable overlap.

It was observed metallographically that in the early part of stage A,
Figs 60 (a) and (b) and Figs 61 (a) and (b), ferrite nucleation at the
prior austenite grain boundaries was predominant, Figs 64 (a) and (b)
and Figs 65 (a) and (c), for V-free and 0.13% V steels respectively.
In the later part of stage A when saturation of the austenite grain
boundaries by ferrite nuclei had occurred, growth of ferrite was the
main process. In stage B ferrite nucleated within the austenite grains
Fig. 64(d) but also on existing austenite/ferrite interfaces, and grew
to consume some of the austenite matrix, Fig. 64(e) and Figs 65(b) and
(d).

In the V-free steel at transformation temperatures between 800°C and
550°C austenite grain boundaries provide energetically favourable
nucleation sites together with faster diffusion paths to aid both
ferrite nucleation and growth[126]. At the highest temperature, at
which there was least supersaturation, growth of ferrite developed
mainly along the prior austenite grain boundaries and resulted in
blocky or semi-polygonal ferrite at longer times. At lower
transformation temperatures the amount of blocky ferrite increased due
to the increase in supersaturation but the number of ferrite nuclei
was greater and the size of ferrite particles was smaller.
Occasionally this ferrite evolved into secondary sawtooth and side
plate forms[178]. At longer transformation times ferrite started to
nucleate within the austenite grains, Figs 64 (d) and (f), some of

which grew into fairly coarse polygonal grains, Fig. 64 (e) and (g).
As the transformation proceeded enrichment of austenite with carbon
occurred allowing some of the remaining austenite to transform to a
widmanstatten type ferrite, Fig. 64(e), and this was further aided by
lowering the transformation temperature, Fig. 64(g). At still lower
transformation temperatures the predominant structure was bainite
without the formation of pro-eutectoid or widmanstatten ferrite, Fig.
64(h).

The addition of 0.13% V to the 0.12% C, 0.010% N steels accelerated
ferrite nucleation, Fig. 60. The incubation time for ferrite formation
decreased with decreasing transformation temperature as is commonly
observed, Fig. 60. This effect of vanadium increased with increasing
transformation temperature possibly due to increased mobility of
vanadium[145]. Another effect of vanadium was to increase the amount
of ferrite at a given time and temperature[179], where transformation
was not complete, due to acceleration of the transformation, and
possibly because vanadium raised both the A_1 and A_3 temeratures. This
acceleration of the ferrite transformation by 0.13% V, was also due to
vanadium refining the austenite grain size from 175 µm to 90 µm.
Plotting the volume fraction of ferrite per unit of austenite grain
boundary area indicated that the growth of ferrite was retarded by the
vanadium addition particularly around 700°C. It may be suggested that
V(CN) may precipitate at the ferrite/austenite interface and so slow
down the growth rate of the ferrite[179, 180].

10.4.3 Effect of Nitrogen

The T.T.T. diagrams are shown in Figs 63, 66 and 67. The overall
effect of increasing nitrogen addition from 0.005% to 0.020% in the
0.13/0.15% V steel was to retard ferrite formation, Fig. 61. The effect
became more apparent as the transformation temperature increased. This
effect of nitrogen in the 0.005% and 0.010% N steels might be
overshadowed by the much coarser austenite grain size in the 0.005% N
steel (198 µm), compared with the 0.010% N steel (90 µm). The slight
retardation of transformation with increasing nitrogen might be due to
refinement of the austenite grain size partially offsetting the
retardation of ferrite by the nitrogen. It is very apparent however

154

that increasing the nitrogen content from 0.010% to 0.020% decreased the transformation period of induction, especially at the higher transformation temperatures around 700/750°C, which effect was solely due to nitrogen[79] as both steels had similar austenite grain sizes of 89 μm and 90 μm respectively.

Furthermore, it can also be inferred that increasing the nitrogen content from 0.005% to 0.020% decreased both the rate of nucleation and the rate of growth of grain boundary nucleated ferrite. The nucleation of ferrite within the austenite grain seemed to be retarded (stage B) as also was the rate of growth, although at the lower transformation temperatures nucleation and growth of ferrite was very fast due to increasing supersaturation and the two stages were impossible to separate. As the transformation temperature decreased the effect of nitrogen diminished due to the general transformation rate being much increased.

Plotting the volume fraction of ferrite per unit of austenite grain boundary area, Fig. 61, indicated that increasing nitrogen retarded the growth of ferrite. This may well have been due to the larger volume fraction of precipitates[57, 58] pinning the ferrite/austenite interface, which also refined the ferrite grain size, Fig. 69 (a) and (b). Such precipitation may also have provided additional ferrite nucleation sites, and the larger amount of precipitate in the high nitrogen steel has been clearly observed. At the lower transformation temperatures where polygonal ferrite was not the predominant feature, some widmanstatten ferrite was formed, preceded by grain boundary ferrite, and pearlite occurred at later stages of transformation, Fig. 69(d). At even lower transformation temperatures of 500/550°C, bainite was formed without any grain boundary ferrite, Fig. 68(d).

10.5 TRANSFORMATION DURING CONTINUOUS COOLING

10.5.1 Continuous Cooling transformation

During continuous cooling, the microstructures were determined by the cooling rate which controls the transformation temperature and in turn which is dictated by the distance from the quenched end in the jominy

155

specimen. Such cooling curves obtained for different distances along the jominy bar are shown in Fig. 74, and the rates of cooling over the temperature interval 800-600°C are shown as a function of distance from the quenched end in Fig. 75. A representative hardness curve for the jominy specimen of the 0.12% C, V-free steel together with those for the 0.12% C, 0.14% V, 0.020% N the and 0.19% C, 0.43% V, 0.018% N steels austenitised at 1250°C are shown in Fig. 76, together with selected microstructures in Fig. 77.

In the 0.123% C, 0.010% N, V-free steel the martensite structure was predominant very close to the quenched end, Fig. 77(a) and was reflected by a high hardness, Fig. 76. At small distances from the quenched end, formation of bainitic ferrite was observed at the prior austenite grain boundaries. The formation of bainitic ferrite was reflected by the rapid decrease in hardness with increasing distance from the quenched end. The hardness levelled out as proeutectoid ferrite was formed, Fig. 77(b), together with pearlite. There was an increase in volume fraction of ferrite as the cooling rate decreased away from the quenched end, and this ferrite was formed mainly at the prior austenite grain boundaries, whereas the interior of the austenite grain transformed to bainitic ferrite, Fig. 77(c). The formation of pearlite was accompanied by a further small decrease in hardness at the very slow cooling rates.

Increasing the vanadium and nitrogen added to the base steel, i.e. 0.115% C, 0.14% V and 0.021% N steel, raised the level of hardness of the hardenability curve as a whole and also increased both the martensitic hardness and the hardenabily, Fig. 76. The increase in hardenability was due to vanadium and possibly nitrogen segregating to the prior austenite grain boundaries[136, 145, 172], whereas the increase in hardness shown by the hardenability curves was due to V(CN) refining the austenite grain size and thus the transformation products, Figs 77 (d) and (e). At some distance away from the quenched end, where large amounts of ferrite was observed, darkening of such ferrite during etching indicated some precipitation, Fig. 77(f), which also could have been responsible partly for the higher hardness observed.

Increasing further the carbon to 0.195%, and vanadium to 0.43%, increased both the hardenability and the martensitic hardness, Fig. 76. Typical microstructures are shown in Fig. 77(g) which shows a much reduced amount of pro-eutectoid ferrite at any given position on the jominy curve. The increased carbon and vanadium increased the volume fraction of V(CN) and refined the austenite grain size further, which together with them lowering the transformation temperature, refined the transformation product and gave an overall higher hardness level, augmented by more precipitation strengthening.

10.5.2 Effect of Vanadium on the Hardenability Curve

In the V-free steel, increasing the austenitising temperature from 1075°C to 1250°C increased the autenite grain size caused a reduction in the austenite grain boundary area, and thus a subsequent a reduction in the number of nucleation sites for the transformation. Such an effect might be thought to decrease the amount of grain boundary ferrite which should give a higher hardness. However the opposite effect was observed and it might be suggested that the slight decrease in the hardness after austenitising at 1250°C was due to the coarser austenite grain size and consequent coarser transformation products, together with the slightly different compositions of the steels used to determined the curves for the different austenitised conditions.

An addition of 0.13% V to the 0.12% C, 0.010% N steel raised the hardness level of the non-martensitic transformation products by 40-50 H.V. Because of the large austenite grain size after austenitising at 1250°C (261 μm) and consequent coarser transformation products, the hardness was lower than after austenitising at the lower temperature of 1075°C. The effect of increasing austenite grain size, and thus of a coarser transformation product, might be offset by the refinement of the ferrite grains by V(CN) precipitation during the transformation. Furthermore supersaturation of ferrite together with an increased dislocation density might have contributed, with the precipitation, to the strengthening shown by the slight increase in hardness at a distance of 30-40 mm from the quenched end of the jominy specimen.

The distance from the quenched end at which the small hardness peak occurred increased with increasing austenitising temperature because, it is suggested, with increasing austenitising temperature and austenite grain size, any particular transformation temperature occurs at increasing distances from the quenched end. The effect of vanadium on the hardenability was hardly apparent, especially after austenitising at 1075°C. This was due to austenite grain refinement at 1075°C by the 0.14% V addition offsetting any increase in hardenability by the vanadium itself. Increasing the vanadium to 0.43%, as will be shown later, markedly increased the hardenability.

Tempering the V-free steel for 30 minutes slightly decreased the hardness progressively with increasing tempering temperature from 550°C to 650°C at all distances along the jominy bar, Fig. 78. Increasing the tempering time to 1 hour caused only a further slight decrease in hardness as expected. This softening became less pronounced with increasing distance from the quenched end of the jominy specimen because the higher the transformation temperature, the less is the effect of tempering on the hardness, i.e. ferrite/pearlite softens less on tempering than does bainite or martensite.

Tempering the 0.13/0.15% V steel at 550°C for 30 minutes caused little or no effect of the hardness in the 1075°C austenitised condition, but increasing the tempering temperature to 600°C and 650°C eliminated the peak in hardness observed in the as quenched or tempered 550°C condition. In specimens tempered at 550°C, the peak in hardness observed in the as quenched condition was moved to slightly greater distances from the quenched end, Fig. 78. This might have been due to supersaturation of pro-eutectoid ferrite and the bainitic ferrite causing precipitation and an increased hardness on tempering.

Tempering at the highest temperature of 650°C raised the hardness level at all positions along the Jominy curve where non-martensitic transformation products were observed, and this hardness was greater than the peak hardness observed in the as quenched and tempered 550°C conditions. This indicates that at the higher tempering temperatures precipitation strengthening is occurring at all positions along the jominy curve due to secondary hardening in bainite or general

158

precipitation in ferrite.

Increasing the austenitising temperature to 1250°C caused the small peak in hardness to occur at longer distances from the quenched end, as previously discussed. However tempering at 550°C for 30 minutes eliminated the peak and lowered the hardness along the Jominy bar, Fig. 79. Increasing the tempering temperature to 600°C and 650°C increased the level of hardness with increasing tempering temperature, indicating that after austenitising at the higher temperature the transformation products become more prone to precipitation strengthening, the overall hardness level being higher than the peak hardness in the as quenched condition. Tempering for a longer time of 1 hour increased the hardness of the non-martensitic products to a greater extent. This effect of increasing the austenitising temperature might be expected from increased solution of the VC/VN at 1250°C compared with 1075°C.

10.5.3   Effect of Nitrogen on the Hardenability Curve

Increasing the nitrogen content from 0.005% to 0.020% increased the hardenability and also the level of hardness of the non-martensitic transformation products, Fig. 72. The increase in hardenability was due to nitrogen retarding ferrite formation, Fig. 61 and the effect became more pronounced with increasing austenitising temperature, as reported elsewhere[79]. The effect of increasing austenitising temperature from 1075°C to 1250°C was to increase the austenite grain size in all the steels which would be expected to decrease the transformation temperature and raise the level of the hardenability curves. However the opposite effect was observed, i.e. as the austenite grain size increased the level of hardness decreased Fig. 72, and this effect has been discussed previously.

The strengthening effect due to austenite grain refinement and subsequently the transformed structure refinement with increasing nitrogen, together with increased precipitation strengthening, caused the general hardness level to increase with increasing nitrogen content. The greatest decrease in the apparent hardness level of the hardenability curves with increasing austenitising temperature was observed in the 0.010% N steel, Fig. 72. It is suggested that some

solute clusters were present, as the austenitising temperature of
1075°C was only slightly above the VN solvus temperature. These
clusters may have slightly retarded grain growth, but the major effect
of austenitising temperature was the incresae in grain size from 78 μm
at 1075°C to 260 μm at 1250°C which caused a marked coarsening of the
transformation products, and therefore softening.

At some distance from the quenched end, especially for specimens
austenitised at 1075°C, there was a consistent increase in the
hardness to give a peak value at 35-40 mm from the quenched end, Fig.
72. Increasing the austenitising temperature to 1250°C, at which all
the VC/VN was dissolved in all the steels, caused the hardness peak to
occur at a greater distance from the quenched end. This effect has
been discussed previously.

The effect of tempering on the hardness of the jominy specimens was to
decrease the level of hardness after tempering at 550°C, although this
did not eliminate the peak, but actually slightly increased the
hardness at shorter distances from the quenched end. This was probably
due to precipitation from supersaturated ferrite and bainite.
Tempering at higher temperatures of 600°C and 650°C raised the level
of hardness along the entire length of the Jominy bar with elimination
of the hardness peaks, Figs 78 and 79. This was due to general
precipitation of V(CN) occurring in all the transformed structures
along the jominy specimen.

Austenitising at 1075°C and then tempering, gave a lower hardness
level along the entire length of the jominy specimen and
the peaks were eliminated as the general level of hardness was
increased to mask the peak effect. The general level of hardness
increased with increasing tempering temperature as more precipitation
occurred. At the higher austenitising temperature of 1250°C, above the
solvus temperature for the VC and VN, there was a greater potential
for precipitation strengthening especially in the 0.020% N steel, and
this in fact was observed. In the 0.005% N steel the strengthening
effect was observed up to 600°C whereas overaging occurred at 650°C.
In the 0.010% and 0.020% N steel the strengthening effect increased
progressively with increasing tempering temperature, Figs 79 and 80.

160

At 0.020% N however, tempering at 550°C caused the peak to occur at shorter distance from the quenched end, and these distances became even shorter with increasing tempering temperature. However tempering at 600°C and 650°C introduced a second peak at a greater distance from the quenched end. This coincided with the darkening of the ferrite during etching, Fig. 77.

In the 0.020% N steel tempered at 550°C the peak occurred at a shorter distance from the quenched end compared with the as quenched condition which indicated the the polygonal ferrite might have contained an increased dislocation density but no VC/VN precipitates in the as quenched condition. Tempering at 550°C probably caused precipitation to occur   on the dislocations. Increasing the tempering temperature to 600°C and 650°C did not alter the positions at which the peak occurred but an additional peak was introduced still further away from the quenched end. This latter peak might have been due to precipitation from less supersaturated polygonal ferrite[181]. The overall effect of tempering in the 0.020% N steel was to increase the general level of hardness by about 20-25 H.V., which indicated that there was some degree of supersaturation in the as quenched condition at all positions along the jominy specimen.

10.5.4   Effect of Carbon

Increasing the carbon content from 0.055% to 0.12% in the 0.15% V, 0.020% N steel increased the hardenability[174] and also the hardness level of the non-martensitic transformation products, Fig. 71, as explained previously. Again small increases in hardness were observed due to precipitation effects at similar distances from the quenched end. After tempering at the lower temperature of 550°C, increasing carbon content increased the level of hardness and this effect was greater for the higher austenitising temperature, Fig. 81. Tempering at 600°C and 650°C, caused any effect of austenitising temperature to be eliminated in the 0.055% C steel due to the low volume fraction of precipitates which occurred and either the precipitates coarsened rapidly or did not produce any appreciable strengthening effect. These effects in the 0.115% C steel have been explained previously.

10.5.5 Effect of Increasing Vanadium and Carbon simultaneously

The effect of simultaneously increasing the carbon content to 0.195% and the vanadium to 0.43%, in the 0.020% N steel, increased the potential for precipitation especially after austenitising at 1250°C, as shown in Fig. 73. Apart from the increase in the martensitic hardness due to the carbon and vanadium, which is in agreement with published results[175, 177, 182], increasing carbon and vanadium also markedly increased the hardenability[182, 174] and the hardness of the non-martensitic transformation products. This latter effect was partly due to the lowering of the transformation temperature with increasing carbon and vanadium, and also due to the refinement of the transformation products. An additional factor which contributed to the increase in hardness was the large volume fraction of precipitates which occurred during the transformation. It is clear from Fig. 73, that at distances greater than about 30 mm from the quenched end, the hardness progressively increased with increasing distance. This was largely due to a precipitation strengthening effect.

Tempering at 550°C caused a slight increase in hardness of the non-martensitic transformation products, Fig. 82. Tempering at higher temperatures however caused appreciable further increase in the hardness of the non-martensitic products, 650°C producing a greater hardness than 600°C. Morever a slight increase in hardness was observed at a distance of 60 mm from the quenched end on tempering at 600°C whereas tempering at 650°C, caused this to develop into a true peak. This might be caused by supersaturation together with a high dislocation density causing precipitation strengthening.

Increasing the tempering time from 30 minutes to 1 hour did not alter these general effects, but the peak was no longer observed after tempering at 650°C, which suggested some overaging effect. However the small peak observed after tempering for 30 minutes at 600°C had increased after 1 hour at 600°C which suggests that some supersaturation effects were present in non-martensitic transformation products, and that increasing tempering time caused increasing precipitation but not overaging at this lower tempering temperature of 600°C.

An interesting feature was the greater increment in general hardening during tempering in the 0.195% C, 0.43% V steel compared with the 0.12% C, 0.14% V ateel, at the same nitrogen content. This can be explained by increased supersaturation in the higher carbon, higher vanadium steel which would be accentuated by the V:C ratio being nearer to the stoichiometric ratio so as to cause the temperature dependance of VC solubility to be increased[176].

10.6   THERMO-MECHANICAL PROCESSING

10.6.1   Deformation in the Recrystallised Regime

10.6.1.1   Effect of Vanadium in the 0.010% N Steels

The way in which deformed austenite recovers and recrystallises during and after thermo-mechanical processing, controls the austenite grain size and morphology and subsequent   refinement of the transformed products. Reheating at a higher temperature of 1250°C in the V-free steel produced large austenite grains (175 μm). Deformation below the reheating temperature progressively refined the recrystallised grain size with increasing reduction and lowering of the deformation temperature, Fig. 83(a). Recrystallisation in the V-free steel occurred at deformation temperatures of 875°C and above, but deformation temperatures lower than 875°C produced virtually no recrystallisation.

Adding 0.13/0.19% V to the 0.12% C, 0.010% N steels refined the recrystallised austenite grain size at all temperatures and reductions, Fig. 83(b). Recrystallisation occurred only above 925°C, whereas deformation below 925°C caused the recrystallisation to be incomplete, Fig. 85. However recrystallisation after deformation at 925°C occurred within a very short time[89], as during the cooling to 750°C for transformation studies, recrystallisation became complete. The inhibition of recrystallisation was due to V(CN) precipitates[78] forming at the deformation temperature of 875°C and pinning the migrating sub-boundaries which delayed recrystallisation.

Grain growth of the recrystallised austenite with increasing holding
time was observed in the 0.13/0.19% V steels after 30% reduction at
1200°C but not in the V-free steels, Fig. 89(a), due to the vanadium
steels always having the smaller austenite grain size which coarsened
on holding. Decreasing the deformation temperature to 1050°C, but with
a larger reduction of 70% refined the austenite grain size in both the
V-free and V-steels, and again the grain size in the V-steels was the
finer. However grain growth was negligible at 925°C possibly due to
the large reduction raising the temperature at which V(CN) was strain
induced, which precipitates immobilised the grain boundaries and
maintained fine grain sizes.

10.6.1.2 Effect of Nitrogen in the 0.13/0.19% V Steels

The effect of increasing nitrogen from 0.005% to 0.020% on the effect
of the deformation temperature and reduction is shown in Fig. 86.
Increasing the reduction or decreasing the deformation temperature
decreased the austenite grain size at all nitrogen contents, Figs 87
and 88.

Increasing the nitrogen content from 0.005% to 0.010% reduced the
initial reheated austenite grain size from 198 μm to 90 μm, but a
further increase to 0.020% N had little or no effect. Refinement of
the recrystallised austenite grain size by thermo-mechanical working
was greatest in the 0.005% N steels due to its large initial austenite
grain size. Deformation below 925°C produced unrecrystallised
structures in both the 0.010% and 0.020% N steels, which will be
discussed later, whereas deformation at and below 875°C produced
incomplete recrystallisation in the 0.005% N steels, i.e. increasing
nitrogen content raised the recrystallisation stop temperature. For
given transformation conditions the 0.010% N steels had the smallest
recrystallised austenite grain size. It is suggested that the reasons
why the recrystallised grains size was finer in the 0.010% N steels
were :-
   (i) in the lowest 0.005% N steels, the initial austenite grain
       size was very coarse, and there were insufficient V(CN)
       precipitates to inhibit effectively grain growth of the
       recrystallised austenite grains,

(ii) in the highest 0.020% N steels, the increased supersaturation
     led to coarser V(CN) precipitates which inhibited grain growth
     less effectively.

These suggestions are supported by Fig. 89(b), which shows the slower
rate of grain growth of recrystallised austenite in the 0.010% N
steels.

10.6.2   Deformation where Recrystallisation was Absent or
         Incomplete

10.6.2.1   Effect of Vanadium in the 0.010% N Steels

Deformation at and above 875°C in the V-free steel caused
recrystallisation at all temperature, Fig. 84, whereas incomplete
recrystallisation was observed after deformation at 825°C. Additions of
0.13/0.19% V increased the recrystallisation stop temperature to
925°C. Recrystallisation at 925°C occurred in less than 10 seconds
after deformation, whereas deformed austenite remained incompletely
recrystallised at lower deformation temperatures.

Because the austenite grain boundary is the major nucleation site for
ferrite during transformation, and thus controls the rate of ferrite
formation, the austenite grain size was expressed in terms of $Sv\gamma$ as
shown in Fig. 91. When the austenite was fully recrystallised
increasing reduction and decreasing temperature caused $Sv\gamma$ to increase
in all the steels as the recrystallised austenite grain size was
progressively refined. This can increase the ferrite nucleation rate
during tansformation[71, 183].

The effects of deformation and temperature of deformation in the V-free
and the 0.13/0.19% V steels on $Sv\gamma$ are shown in Figs 91 (a) and (b)
respectively. For given reductions and temperatures, the vanadium
steels always had the larger $Sv\gamma$, as expected. In the V-free steels,
the $Sv\gamma$ markedly and rapidly increased after deformation at 875°C,
possible due to heavier deformations at this low temperature
increasing the Ar_3 and causing some ferrite to be formed during the
deformation process. Some indication of such ferrite was observed as a

heavy delineation of the austenite grain boundaries. In the recrystallised regime the larger $Sv\gamma$ values in the vanadium steels compared with the V-free steels was caused by precipitates forming during deformation. As the deformation increased more strain induced precipitation occurred and the greater elongation of the unrecrystallised grains caused $Sv\gamma$ to increase, Fig. 91(b).

The effect of the vanadium addition on the $Sv\gamma$ at 50% reduction is shown in Fig. 92(a). The effect of vanadium was most apparent at 925°C at which temperature the vanadium steel was unrecrystallised immediately after deformation but the V-free steel was recrystallised. The results show the major effect of elongation of the unrecrystallised austenite in increasing $Sv\gamma$, and subsequently its major effect on ferrite nucleation.

Due to the difference in the initial austenite grain size which affected $Sv\gamma$ in the unrecrystallised regime, the effect of deformation temperature in terms of $RSv\gamma$ was used, as explained earlier, Fig. 93(a). This again shows that the vanadium addition increased $Sv\gamma$, (and potential ferrite nucleation), but the effect of vanadium was quite small when the initial reheated grain size or $Sv\gamma$ was taken into consideration.

10.6.2.2 Effect of Nitrogen in the 0.13/0.19% V Steels

The effect of increasing nitrogen from 0.005% to 0.020% in the unrecrystallised regime, i.e. at a deformation temperature at 925°C and below, was to decrease the amount of recrystallised austenite, Fig. 90(a), and as the reduction during deformation increased the amount of recrystallisation increased (as expected). The effect of increasing nitrogen was to cause more V(CN) precipitation at 925°C, which consequently retarded recrystallisation. As the deformation temperature decreased the amount of precipitation increased, which together with the lower temperature further retarded recrystallisation and allowed more elongation of the unrecrystallised grains, together with the formation of deformation bands. Under these conditions it is perhaps more appropriate to consider $Sv\gamma$ rather than grain size itself.

The effect of nitrogen together with the effect of deformation temperature on $Sv\gamma$ is shown in Fig. 92(b), which shows that the 0.010% N steels had the largest $Sv\gamma$ value. Previous discussion has indicated the reasons why the 0.010% N steels contain more effective precipitates in terms of grain boundary pinning than the 0.005% or 0.020% N steels. This discussion can also be applied to Fig. 92(b), as the precipitates in the 0.010% N steels will also be more effective in retarding recrystallisation and allowing more elongation of unrecrystallised grains, i.e. higher $Sv\gamma$ values.

In the recrystallised regime, account needs to be taken of the initial reheated grain size on the recrystallised austenite grain size, i.e. $RSv\gamma$ is important. As shown in Fig. 93(b), increasing nitrogen decreased slightly $RSv\gamma$, because the increasing amount of V(CN) was able to prevent growth of the recrystallised austenite grain size after deformation.

10.6.3 Transformation Studies on Thermo-mechanically Processed Austenite

10.6.3.1 Transformation of Hot Worked Austenite in the V-Free Steel Containing 0.010% N

Based on the results shown in the section 9.6, five different treatments were selected to produce different morphologies of austenite. The treatments used depended on the composition, as discussed earlier. The aim in this section is to examine the transformation to ferrite from different morphologies of austenite in the V-free steels and differences with the vanadium steels containing increasing nitrogen content will be highlighted.

The microstructures in the V-free steels were recrystallised after deformation at 875°C and above, whereas recrystallisation was incomplete at 825°C. Fig. 94 shows the progress of transformation from different austenite morphologies. It can be seen that for deformation at any temperature, decreasing the austenite grain size, accelerated the austenite tranformation in comparison with the undeformed

austenite. The incubation time for nucleation of ferrite decreased with increasing $Sv\gamma$ i.e. decreasing recrystallised austenite grain size. Similar results were found by Amin and Pickering[79].

30% reduction at 875°C accelerated ferrite formation despite the larger austenite grain size. Specimens quenched immediately after deformation revealed that recrystallisation seemed to be complete although during isothermal transformation some deformation bands were observed, Fig. 95(d). This indicated that 30% reduction at 875°C might have been the threshhold for complete/incomplete recrystallisation and that some retained deformation contributed to the faster nucleation of ferrite. However at the lower deformation temperature of 825°C, at which recrystallisation of the austenite was incomplete, increasing $Sv\gamma$ · by increasing reductions from 50% to 70%, decreased the incubation time for ferrite formation due to the larger number of sites for ferrite nucleation, as expected.

Transformation of large recrystallised austenite grains produced fewer nucleation sites for ferrite formation in the early stages of transformation and consequently allowed the ferrite particles to grow larger until impingement occurred after long transformation times, Fig. 95(a). Additional intra-granular nucleation sites become available with increasing transformation time, and ferrite formed intragranularly tended to grow more rapidly. This was aided by segregation of Mn and Si[163, 184] which occasionally caused bands of ferrite. However greater numbers of nucleation sites, i.e. a smaller austenite grain size and larger $Sv\gamma$, together with shorter transformation times eliminated such inhomogeneity effects.

Increasing the amount of deformation together with decreasing the deformation temperature refined the recrystallised austenite grains and increased the potential number of nucleation site for ferrite formation, Figs 95 (a), (c) and (d), although some inhomogeneity of ferrite growth was still observed. Deformation at much lower temperatures at which recrystallisation was incomplete produced fine ferrite particle sizes due to the increasing number of nucleation sites formed from the deformation bands, i.e. increasing $Sv\gamma$, Fig. 95(e). However at a transformation temperature of 750°C, using

incompletely recrystallised austenite, despite the larger number of nucleation sites ferrite growth was very limited due to the early impingement of the ferrite particles, Figs 96 and 95(f).

The growth of ferrite particles in relation to the five different thermo-mechanical treatments is shown in Fig. 96, with that formed after 30% reduction (conditions (a) and (d)) having the largest ferrite particles size. Again these larger ferrite particles were formed from intragranular nucleation sites. However, as explained earlier, larger deformation increased the amount of intragranularly nucleated ferrite and impingement occurred at much shorter transformation times with an overall finer ferrite particles size at the end of the transformation. In general the growth of the ferrite particles seemed to be greater after small reductions, whereas the nucleation was much smaller. The deformation temperature did not have any direct effect apart from the resultant austenite grain size, which controlled the ferrite particle size.

10.6.3.2   Effect of Vanadium in the 0.010% N steels

The effect of austenite morhopology on the formation of ferrite in the 0.13/0.19% V steel was examined together with the effect of vanadium on the transformation characteristics. The effect of the deformation was to accelerate ferrite formation by refining the austenite grain size, compared with the undeformed steel, Fig. 97. Deformation at high temperature refined the recrystallised austenite grain size, increased $Sv\gamma$ and decreased the incubation period for ferrite formation. The deformation temperature or the amount of deformation, although $Sv\gamma$ had increased from 26 mm^{-1} to 143 mm^{-1}, had no effect on the ferrite incubation time. However an interesting feature was observed in that after 30% reduction, on lowering the deformation temperature from 1200°C to 875°C, $Sv\gamma$ had decreased from 22 mm^{-1} to 7 mm^{-1}, and yet the formation of the ferrite had not been retarded to any great extent. This suggested that 30% reduction at 875°C had not produced recrystallisation but, because   the austenite grains were not observed to be elongated, had resulted in some strain induced boundary migration with a consequent decrease in $Sv\gamma$. However, there must have been some residual deformation which accelerated

169

ferrite formation and offset the normal effect of retardation of
ferrite expected from a smaller $Sv\gamma$ value. It must be admitted that
30% reduction produces such small elongation of the austenite that it
is difficult to observe.

At the lowest deformation temperature of 825°C, increasing the amount
of deformation caused $Sv\gamma$ to increase without altering the incubation
period for ferrite, contrary to the general believe[76, 79].
Deformation at 825°C increased the Ar_3 and caused a thin film of
ferrite to be formed during the deformation process at the grain
boundaries, with partitioning of vanadium into the ferrite[136, 145]
causing transformation to be delayed. However once the transformation
was initiated the increased $Sv\gamma$ caused the transformation rate to
increase. There was completely unrecrystallised austenite in the
specimen quenched immediately after deformation at 925°C, but this
unrecrystallised austenite was not observed during the isothermal
transformation at 750°C, Fig. 98(c). Instead very fine ferrite was
observed which was believed to have formed from recrystallised
austenite. Similar microstructures were obtained after transformation
for very short times, Fig. 98(b), whereas at longer times the ferrite
grew, Fig. 98(a). Thus recrystallisation must have occurred rapidly
during cooling to the transformation temperature.

Deformation at a lower temperature at which recrystallisation was
incomplete, showed the effect of heterogeneity on ferrite nucleation
and growth at the grain boundaries and within the grains. Ferrite
grains nucleated at the grain boundaries and at deformation bands were
apparently restricted in growth by the V(CN) interphase precipitation.
Hence ferrite growth was very limited. However existing
ferrite/austenite interfaces were able to form additional nucleation
sites with increasing transformation times, possibly because of the
interphase precipitates[76]. Ferrite which nucleated in the interior
of the grains grew larger due to the smaller number of nuclei and the
fewer V(CN) particles available to restrict ferrite grain growth. The
resultant microstructures were very inhomogeneous, with very fine
ferrite grains delineating the prior austenite grain boundaries and
deformation bands, and larger ferrite grains formed in the interior of
the austenite grains. This effect became predominant at the

deformation temperatures where recrystallisation of austenite was
incomplete due to the presence of strain induced precipitation.

The vanadium addition accelerated the nucleation of ferrite formed
from recrystallised austenite, Fig. 99, due to the refinement of
recrystallised austenite by V(CN) precipitates. This is in agreement
with other workers[79] who showed that finer austenite grains gave
shorter incubation periods for ferrite formation. Similarly the volume
fraction of ferrite produced at any given transformation time was
greater in the vanadium steels than in the V-free steels.

For transformation of the unrecrystallised austenite (condition (d))
vanadium had neither any effect on the incubation time for ferrite
formation nor on the volume fraction of ferrite. However the austenite
in the vanadium steel was unrecrystallised with $Sv\gamma$ 7 mm^{-1} due to
insufficient deformation in the austenite to produce any
recrystallisation whereas the V-free steel was fully recrystallised
with a grain size 64 µm and $Sv\gamma$ 31 mm^{-1}. Hence the transformation
which was accelerated in the unrecrystallised austenite in the
vanadium steel, offset the effect of the smaller $Sv\gamma$ and caused there
to be no apparent difference in the transformation characteristics of
the vanadium and V-free steels. However at a lower transformation
temperatures which had a slightly larger $Sv\gamma$ (61 mm^{-1}) in the vanadium
steels compared with the V-free steels ($Sv\gamma$ = 55 mm^{-1}), and which were
both unrecrystallised, vanadium accelerated nucleation of ferrite and
increased the volume fraction at any given transformation time. This
seems to agree with the larger $Sv\gamma$ value in the vanadium steel.

The 0.13/0.19% V addition, apart from accelerating the formation of
ferrite in the recrystallised austenite reduced the growth of the
first-formed ferrite, Fig. 100. This was probably due to precipitation
of interphase V(CN) and to general precipitation. However the effect
of vanadium on the nucleation of ferrite was less clear in the
unrecrystallised austenite, due to retained deformation as explained
earlier, but reduced the initial ferrite growth in a similar way to
that occurring in the recrystallised austenite. This retardation of
ferrite growth in the vanadium steels was possibly   due to V(CN)
interphase precipitation pinning the transformation front.

171

Smaller deformations in the austenite tended to allow ferrite particles to grow larger (conditions (a) and (d)) but if V(CN) precipitates were formed during deformation these could also help to pin the transformation front and refine the ferrite particles[62-65]. At temperatures below the recrystallisation stop temperature, and after extended transformation times, ferrite formed within the austenite grains grew larger due to insufficient precipitation to pin the transformation front, Fig. 100. It seems possible that vanadium can segregate towards the austenite grain boundaries[172] and thus give less interphase precipitation in the ferrite formed intragranularly. This duplex ferrite particle size was mainly developed from the unrecrystallised austenite and would lead to inconsistent mechanical properties, which would be most undesirable especially where impact properties are concerned.

10.6.3.3 Effect of Nitrogen in the 0.13/0.19% V Steels

The ferrite formed from different austenite morphologies in 0.005% and 0.020% N steels will be discussed with the effect of nitrogen. The transformation characteristics of different morphologies of austenite in 0.005% and 0.020% N are shown in Fig. 101 and Fig. 102 together with typical microstructures in Fig. 103 and Fig. 104 respectively. The incubation time for ferrite formation in the 0.005% N-vanadium steels was slightly smaller in thermo-mechanically processed austenite than in undeformed austenite, due to decreases in the austenite grain size, Fig. 101. However the relatively small reduction in the incubation time was not accounted for by the large reduction in the recrystallised austenite grain size. It is suggested that the incubation time is controlled by the amount of precipitate formed at the grain boundaries prior to the transformation rather than by the grain size itself. In this low nitrogen (0.005%) steels the effect of nitrogen on the precipitation of V(CN) is very small, so that the vanadium steels can behave similar to V-free steels. Such behaviour was experienced in the austenite grain coarsening of the V-free steel, which was similar to that of 0.005% N, 0.13/0.19% V steels. The incubation period for ferrite formation in the 0.005% N, 0.13/0.19% V steel was therefore similar to that for the V-free steels in the

172

recrystallised regime, and such is shown by comparing Fig. 101 with Fig. 94. However, as vanadium diffusion in austenite and in ferrite is more rapid than that of iron[151] the increase in ferrite volume fraction in the vanadium steels in the absence of precipitation should be greater than in the V-free steels. This was observed in Figs 94 and 104. In unrecrystallised austenite the effect was slightly different due to the lower deformation temperature introducing strain induced precipitates which accelerated ferrite formation. Increasing deformation at 825°C decreased the incubation time for ferrite formation by increasing $Sv\gamma$, i.e. the number of ferrite nucleation sites.

In the 0.020% N steels, deformation accelerated ferrite reaction formation due to the marked decrease in the austenite grain size, Fig. 102. In the recrystallised austenite regime decreasing temperature and increasing deformation reduced the recrystallised austenite grains, increasing $Sv\gamma$ and reducing the incubation time for transformation. A similar effect was observed in unrecrystallised austenite, so that as $Sv\gamma$ increased the rate of formation of ferrite increased. The volume fraction of ferrite increased with decreasing deformation temperature. This was due to more V(CN) being precipitated during deformation which refined the recrystallised austenite grain size. Also, V(CN) interphase precipitation during transformation cause the ferrite transformation front to be pinned, and the resulting ferrite grain size to be smaller.

The major effect of increasing nitrogen was to refine the ferrite grain size formed from different morphologies of austenite, Figs 103, 98 and 104. However some specific effects were observed :-

1. The presence of nitrogen is necessary for the precipitation of V(CN), which in turn controls the progress of transformation :-

   (i) in the presence of 0.005% N in vanadium steels, insufficient nitrogen was available to delay the formation of V(CN) so that less V(CN) was available to nucleate for the ferrite (other things being equal) and so the formation of ferrite was delayed. This is further supported by the fact that

173

enough precipitates were not present to retard
the growth of the ferrite once transformation had
started. Hence in the low nitrogen 0.13/0.15% V
steels, the ferrite growth rate was rapid, Fig. 105.

(ii) When sufficient precipitation was present in the
0.010% N, 0.13/0.19% V steels, transformation
occurred somewhat faster.

(iii) In the 0.020% N-vanadiun steels, precipitation of VN
occurred first due to its greater stability, and
VC/V(CN) occurred somewhat later so that
transformation was delayed. Precipitation of a
carbon rich V(CN), by locally lowering the carbon
content may accelerate ferrite formation.

2. Much much finer ferrite grains were formed by nucleation at
the prior austenite grain boundaries and deformation bands,
particularly during the early stages of transformation. As the
transformation time increased precipitation occurred in the
ferrite nucleated at the austenite grain boundaries,
restricting the ferrite particle growth and
causing a smaller ferrite grain size[57, 58].

3. The coarser intragranularly nucleated ferrite is believed
to contain less interphase or generally formed precipitates,
possibly due to vanadium segregating towards the austenite
grain boundaries[172]. Hence there was less restriction of the
growth of ferrite. This more rapidly growing intragranular
ferrite engulfed but did not absorb the finer grain boundary
nucleated ferrite, this effect becoming very apparent after
long transformation times and being exaggerated due to
segregation[163, 184]. As already discussed, this led to
a very variable ferrite grain size.

The effect of increasing nitrogen from 0.005% to 0.010% was to
accelerate ferrite formation, Fig. 105, as explained earlier, but a
further increase in nitrogen to 0.020% caused retardation of ferrite
nucleation. The nitrogen content played a major part in the nucleation
and growth of the ferrite. It can be tentatively suggested that
nitrogen enhances the formation of V(CN) and this produces local
carbon depleted regions which allows ferrite to nucleate. With larger

nitrogen content, VN precipitates first but does not produce the local depletion of carbon and hence does not accelerate transformation in the way that VC or V(CN) does. However the growth of ferrite was controlled by the VC or V(CN) precipitation which pins the transformation front. In the 0.005% N steels the nitrogen content was too small to affect the nucleation or to impede the growth of ferrite, Fig. 107, and the ferrite initially grew faster than in any other steel, thus resulting in the largest ferrite grain size. Increasing the nitrogen content to 0.010% allowed V(CN)to form much faster which accelerated the nucleation of ferrite and reduced its growth in comparison with the 0.005% N steels. Hence the ferrite grain size was refined. A further increase in nitrogen to 0.020%, caused VN to form first, which had little effect on the start of transformation. Once the nitrogen content was reduced sufficiently, the formation of VC/V(CN) occurred which allowed transformation to take place by nucleating the ferrite by the mechanisms previously discussed.

However, deformation in the unrecrystallised regime at 825°C obscured the effect of nitrogen on the nucleation of ferrite by the acceleration due to the retained strain. However, ferrite growth was much slower in the 0.020% N steels due to the formation VN or V(CN) rich in nitrogen precipitates which pinned the ferrite transformation front. This produced a refined ferrite grain size. The effect of Sv on the ferrite is shown in Fig. 106, which suggests that from larger values of Svγ, i.e. small austenite grain sizes, small values of ferrite per Svγ was obtained. Thus, each ferrite nucleus grows but little, and the ferrite grain size is small and uniform. However at small Svγ values i.e. large austenite grain size, both small and large values of ferrite per Svγ can be obtained, which can lead to inhomogeneous grain sizes.

10.6.4   Effect of Continuous Cooling on the Ferrite Grain Size

Commercially, thermo-mechanically worked products are continuously cooled to room temperature. An attempt was made to simulate such industrial practice using large (30% reduction at 1200°C) and small (70% reduction at 1200°C) recrystallised austenite grain sizes together with the unrecrystallised austenite produced by 50% or 70%

reduction at 825°C in all steels. The results are shown in Fig. 108 in which, at larger Sv_γ values over 25 mm^{-1}, the vanadium addition (0.13/0.19%) produced a finer ferrite grain size on continuously cooling from the deformation temperature to room temperature, using a cooling rate 2.5-4.5°C/sec between 800°C and 500°C. Such an effect was mainly due to the finer austenite grain size and heavily elongated austenite, together with the precipitation during transformation, which refined the ferrite grain size. However at smaller Sv_γ values, less than 25 mm^{-1}, the ferrite grain size became larger, and approached those present in the V-free steels.

The increase in nitrogen from 0.005% to 0.020% had no systematic effect, Fig. 108(b), on the ferrite grain size. At larger values of Sv_γ there was a marked refinement of the ferrite grain size in all the steels, and at small values of Sv_γ the ferrite grain size increased considerably. This effect was largely due to the large austenite grain size (or grain size equivalent) which decreased the number of ferrite nuclei.

CHAPTER 11 **CONCLUSIONS**

11.1 Solubility Studies

1. Analysis of precipitates extracted in 10% HCl at 50°C, gave more reliable results than did extraction electrolytically in 7% Fe_3Cl, 3% HCl and 3% Ethylene Glycol solution. Vanadium in the precipitates was unaffected by the method of extraction, whereas carbon and nitrogen were higher in the residue, after extraction electrolytically, than in the steels themselves.

2. Analysis of precipitates showed the co-existence of vanadium and silicon possibly as (V, Si)(CN) precipitates.

3. In the 0.12% C, 0.13/0.15% V steel :-
    (i)   at 0.010% N the precipitate to form was VC or a V(Cn) carbon rich precipitate.
    (ii) at 0.020% N the first precipitate to form was VN or V(cN) nitrogen rich precipitate
    (iii) after long heating times the precipitates extracted form both steels had similar C/N ratios, indicating the mutual solubility of VC and VN.

4. The formation of VN required a greater nitrogen content in the steel than the stoichiometric ratio.

5. The stability of VN/V(cN) was greater than that of VC/V(Cn).

6. The C:N ratio in the precipitates was dictated by the C:N ratio in the steels.

7. The solubility of VC was greater than that of VN.

8. Increasing vanadium, carbon and nitrogen in the steels decreased the solubility of VC.

9. Due to its greater stability, VN was not influenced greatly in the presence of increasing vanadium, carbon or nitrogen in the steels.

11.2 Grain Coarsening Studies

1. The austenite grain size, at constant temperature, increased with time according to an exponential law, the exponent increasing with increasing austenitising temperature, and approaching the theoretical value at the highest temperature.

2. In the steels in which there was no restriction of austenite grain boundary movement, the austenite grain size increased monotonically with increasing austenitising temperature.

3. In the high nitrogen, high carbon V-free steels it has been suggested that grain growth can be restricted by clustering of carbon/nitrogen atoms but much more rapid grain coarsening was observed on their thermal dispersion.

4. In the absence of vanadium, AlN seemed to control grain coarsening.

5. Vanadium in solution did not restrict austenite grain growth.

6. The austenite grain coarsening characteristics were controlled by the volume fraction and stability of the precipitates which in turn were influenced by the vanadium, carbon and nitrogen contents of the steels.

7. Increasing the volume fraction of VC/VN, by increasing vanadium, carbon and nitrogen contents refined the austenite grain size.

8. The grain coarsening temperature was controlled by the solvus temperature of VN, which was more stable than VC, and the grain coarsening temperature was higher than the VC solvus but below the VN solvus.

9. Local inhomogeneity in composition allowed local coarsening or dissolution of particles, which was followed by abnormal or exaggerated grain growth. Sudden grain growth occurred during the dissolution and coarsening of VN/V(CN).

11. Relatively fine austenite grain sizes were obtained in the 0.12% C, 0.13/0.19% V, and 0.020% N steels at all austenitising temperatures.

12. The activation energy for grain growth was higher in the vanadium steels than in the V-free steels.

11.3 **Tempering Studies**

1. Increasing nitrogen in the steel, progressively increased the as quenched martensite hardness.

2. Clustering of interstitial atoms which occurred above the solvus temperatures of VN and VC, caused the hardness of as quenched martensite to increase.

178

3. In the V-free steels, increasing tempering time and temperature caused the hardness to decrease progressively, but at higher tempering temperature the hardness levelled out due to the occurrence of recrystallisation, and the restriction of the ferrite grain growth by Fe_3C. Increasing the volume fraction of Fe_3C caused the temperature and time at which recrystallisation occurred to increase.

4. Vanadium additions increased the low temperature tempering resistance by retarding the formation and growth of Fe_3C.

5. At higher tempering temperatures of 500-600°C, depending on the tempering time, secondary hardening was introduced.

6. At still higher tempering temperatures, vanadium increased the resistance to overaging after secondary hardening due to slow growth of V(CN) precipitates which restricted the recovery of the matrix and delayed recrystallisation.

7. The intensity of secondary hardening increased with increasing vanadium content possibly due to the increased volume fraction of VC and also because the V:C ratio approached the stoichiometric ratio for VC.

8. Increasing the nitrogen content raised the overall hardness level of the tempered martensite but had no effect on the effect of vanadium on the intensity of secondary hardening.

9. The greater increase in hardness with increasing nitrogen was observed at the lower tempering temperatures, which reflected the hardness of the as quenched martensite.

10. Increasing the carbon content in steels increased the hardness level, and the maximun secondary hardening, but decreased the intensity of secondary hardening due to a lower V:C ratio, and thus less temperature dependence of solubility of VC.

11.4 Isothermal Transformation Studies

1. The effect of decreasing the transformation temperature was to accelerate the formation of ferrite.

2. Vanadium additions accelerated ferrite formation and also raised the A_1 and A_3 temperatures.

3. Grain boundary nucleated ferrite did not grow very much in the vanadium steels, but the prevalence of nucleation sites

was greater. Intra-granularly nucleated ferrite grew much more rapidly in the vanadium steels than in the V-free steels. This effect has been discussed.

4. Increasing nitrogen additions increased the incubation period for ferrite formation and this effect became more apparent with increasing transformation temperature.

5. The growth of grain boundary ferrite was restricted by increasing nitrogen, by forming more V(CN) precipitates to pin the transformation front.

6. Increasing nitrogen additions increased the inhomogeneity of the ferrite grain size by refining, particularly, grain boundary nucleated ferrite, due to increasing nitrogen increasing the precipitation which pinned the transformation front. Also nitrogen increased the number of additional nucleation sites at the particles at the ferrite/austenite interface. The ferrite nucleated within the austenite grew to large grain sizes, there being less inhibition of the movement of transformation front.

11.5 Transformation During Continuous Cooling

A. The As Quenched Condition.

1. During the quenching of jominy specimens a small increase in hardness occurred at some distance from the quenched end. This was absent in the V-free steels, which indicated that it was due to precipitation of VC/VN. This small increase in hardness increased only slightly with increasing nitrogen content.

2. Increasing the austenitising temperature in the vanadiun steels, apart from lowering the hardness level along the jominy bar, caused the small increase in hardness to occur at greater distances from the quenched end.

3. Vanadium additions increased the hardenability and raised the level of hardness along the entire length of the jominy bar, as also did increasing nitrogen content.

4. Increasing carbon content increased the hardenability and raised the hardness level of the non-martensitic products, but

the effect was less pronounced at the higher austenitising temperature.

5. Increasing the carbon and vanadium content simultaneously greatly increased the hardenability and the level of hardness of the non-martensitic products. This was due to the lowering of the transformation temperature which refined the transformation products. The higher carbon and vanadium contents increased the volume fraction of precipitates, whilst the lower transformation temperature decreased the precipitates particle size. Both effects combined to increase the hardness.

B. During tempering.

6. Tempering the V-free steel caused the hardness level to decrease with increasing tempering temperature and time.

7. Tempering vanadium steels at low temperatures decreased the distance from the quenched end at which the small increase in hardness was observed but the general level of hardness was slightly lower. During tempering at higher temperatures the small increase in hardness was eliminated due to overaging but the overall level of hardness progressively increased with increasing tempering temperature and time.

8. Tempering the high nitrogen low vanadium steel at low tempering temperatures caused the small increase in hardness in the as quenched condition to develop into a peak at shorter distances from the quenched end, whereas the general level of hardness was again slightly lower. Increasing tempering temperature produced very similar effects, but a second peak was developed at a greater distance from the quenched and this peak increased in hardness with increasing tempering temperature. Increasing tempering time caused the peak to be overaged but the general hardness level along the jominy bar remained the same.

9. During tempering, increasing the nitrogen content increased the hardness level of the jominy curves. The largest increase was in the higher nitrogen steel using the higher austenitising temperatures, and this was intensified with increasing tempering time.

10. During tempering, increasing the carbon content, raised the hardness level and this was more pronounced after austenitising at the higher temperature. However the peaks which were observed in the 0.12% C vanadium steels were not present in the 0.055% C steel due to the low volume fraction of precipitates.

11. Tempering the 0.195% C, 0.43% V, 0.018% N at the lower ^steel tempering temperature only slightly increased the level of hardness. However tempering at the higher temperatures caused the level of hardness to increase progressively with increasing tempering temperature and a peak to develop at the highest tempering temperature. Tempering for longer times caused the peak to be overaged but a smaller peak was developed at longer times at the lower tempering temperature.

11.6 Thermo-mechanical Processing

1. Increasing the amount of deformation and decreasing the deformation temperature above the recrystallisation temperature refined the recrystallised austenite grain size.

2. Increasing reduction below the recrystallisation stop temperature increased grain elongation and thus increased Sv_γ.

3. Decreasing deformation temperature below the recrystallisation stop temperature increased the strain induced precipitation and assisted further grain elongation on deformation

4. Large reductions below the recrystallisation temperature raised the Ar_3 temperature and formed ferrite at the prior austenite grain boundaries and deformation bands.

5 . Vanadium additions refined the recrystallised austenite grain size and increased the Sv_γ in the unrecrystallised condition by forming $V(CN)$ precipitates which pinned the grain boundaries.

6. Vanadium additions in steel raised the recrystallisation stop temperature.

7. Increasing nitrogen content refined the recrystallised austenite grain size for all processing conditions in the recrystallisation regime, whereas in the unrecrystallised regime increasing Sv_γ by increasing volume fraction of $V(CN)$ pinning the recrystallisation front, allowed greater elongation of

182

deformed grains to occur.

8. Increasing nitrogen in the vanadium steels raised the recrystallisation stop temperature, and also decreased the amount of recrystallisation for any given processing condition.

9. Grain growth of the recrystallised austenite with increasing holding time was observed in the vanadium steels but grain growth was reduced in the presence of V(CN) precipitates.

10. Increasing holding time coarsened the recrystallised austenite more in the 0.005% N steels than in the the 0.020% N steels, the grain size being smallest in the 0.010% N steels.

11. Increasing Sv_γ, either by refining the recrystallised austenite grain size or by increasing the aspect ratio of deformed grains, increased the number of nucleation sites thus accelerating ferrite formation.

12. Transformation of large recrystallised austenite grains produced large ferrite grains due to few ferrite nuclei, which grew at a greater extent.

13 Ferrite nucleated at the grain boundaries was generally fine, due to early impingement, in comparison to intragranularly nucleated ferrite which grew into much larger grains.

14 Transformation of fine recrystallised austenite produced fine ferrite due to the increased number of nucleation sites.

15 Vanadium additions accelerated ferrite formation :-

    (i)   by refining the recrystallised austenite grain size, increasing the grain boundary area and increasing the number of nucleation sites.

    (ii)   by forming V(CN) rich in carbon whichproduced local regional carbon depletion and allowed ferrite to form.

    (iii) by side by side nucleation, i.e. V(CN) particles restricted ferrite growth by pinning the transformation front but simultaneously acted as nucleation sites for newly formed ferrite.

16. Vanadium is suggested to segregate towards the grain boundary region, leaving the interior of the grain depleted. Thus greater V(CN) precipitation occurred near to grain boundaries than in the interior of the grains.

17. Nitrogen enhanced the precipitation of V(CN) which pinned the ferrite grain boundaries and restricted their movement.

18. Precipitation of V(CN) rich in carbon seemed to control the nucleation of ferrite whereas V(CN) rich in nitrogen appeared to control its growth.

19. Increasing nitrogen in the steels controlled ferrite nucleation and growth by the following effects :-

    (i)   insufficient nitrogen delayed the formation of V(CN) rich in carbon, and consequently the formation of ferrite, whereas the initial growth of ferrite was very fast.

    (ii) more nitrogen, which accelerated the formation of V(CN) rich in carbon, also accelerated ferrite formation and the initial growth of ferrite was slower due to the presence of enough V(CN) to pin the transformation front.

    (iii) excess nitrogen delayed the nucleation of ferrite due to the formation of V(CN) rich in nitrogen, which did not cause local depletion in carbon. At longer transformation times, when most of the excess nitrogen had been precipitated mainly as nitride, V(CN) rich in carbon was formed which initiated ferrite nucleation. Growth of ferrite was somewhat slower and ferrite grain size was finer due to the abundance of V(CN) particles pinning the transformation front.

20. Growth of ferrite was restricted by V(CN) precipitation and by ferrite impingement.

21 Inhomogeneity of ferrite grain size was caused by :-

    (i)   possible segregation of vanadium around the grain boundary region.

    (ii) increasing numbers of ferrite nucleation sites at the boundaries of elongated grains.

    (iii) the depletion of vanadium and consequently the V(CN) precipitates from the interior of the grains, which allowed ferrite grains to grow larger.

    (iv) transforming large recrystallised austenite grains.

and (v)   retained deformation together with the segregation of manganese and silicon.

22. Inhomogeneity of ferrite grain size was eliminated by transforming fine uniform recrystallised austenite grains.

CHAPTER 12 **INDUSTRIAL IMPLICATIONS**

The aim of this project was to condition the austenite so that it would be possible during transformation to obtain fine uniform ferrite grain sizes by selection of a balanced composition and processing route to give maximun strength, and improved toughness and a lower impact transition temperature.

To ensure a small starting austenite grain size, a balanced composition is required in which precipitates are present pinning the austenite grain boundaries and restricting their growth. The small austenite grain size is obtained during reheating by using a low reheating temperature below the solvus temperature of VN/V(CN) rich in nitrogen. Stable nitrides and carbonitrides are of prime importance, and the homogenisation time should have little or no effect. As the outside of a large workpiece reaches temperature very quickly, grain growth should be minimum until the temperature is equilibriated through the workpiece. However homogenisation above the solvus temperature and dissolution or growth of particles occurs, followed by grain coarsening which leads to inhomogeneous austenite grain sizes and those often can not be eliminated on subsequent deformation or heat treatment.

In normal controlled rolling, in the roughing passes at high temperatures and the small reductions often used in practice, the austenite grain size is continually refined by dynamic and static recrystallisation. This is followed by delay until the workpiece is cooled to a lower temperature. Finally the austenite is deformed at lower temperature, by reductions aimed at avoiding mill overloading, in which the grains are flattened due to the absence of recrystallisation. The thickness of the flattened austenite grains normally determines the ferrite grain size on transformation

However additions of vanadium combine with inherent carbon and nitrogen to form precipitates of low and high solubility (VC and VN) respectively, which pin the recrystallised austenite grain boundaries and restrict their growth. Not too heavy pinning of grain boundaries leads to fine recrystallised austenite and repeated deformation is

185

very effective in recrystallising the austenite down to 950°C. Grain coarsening of recrystallised austenite at this temperature is very slow due to extensive strain induced precipitates pinning the grain boundary movement. Transformation of very fine recrystallised austenite leads to very fine uniform ferrite grain sizes which have improved strength and toughness. As the deformation temperature decreases, approaching the solvus temperature of VC, the load required for similar deformation increases and the austenite grains commence to flatten rather than recrystallised. This is the case with heavy pinning of the boundaries which inhibits recrystallisation. This flattening of austenite continues down to the A_3 temperature in the unrecrystallised regime. However the workpiece becomes stiffer and a further increase in load is required. As the aspect ratio of the austenite grains increases, the number of nucleation sites for ferrite formation increases. Transformation of unrecrystallised austenite grains can lead to duplex ferrite grain size as was shown earlier.

Transformation of recrystallised austenite grains has greater potential for refining the ferrite grain size due to the increased grain boundary area and due to additional nucleation sites offered by the V(CN) particles at the austenite ferrite interfaces during transformation. Recrystallised austenite has greater potential for transformation to ferrite with a greater amount of interphase precipitation, thus increasing the strength. Transformation of unrecrystallised austenite tends to lead to duplex ferrite grain sizes, particularly if the reduction does not flatten the austenite grains sufficiently, and less precipitation strengthening during transformation due to some strain induced precipitation in the austenite.

It was shown that cooling at certain rates between 500-800°C produced strengthening by refining the transformation products together with interphase precipitation whereas other cooling rates can give a supersaturated transformatin product which can be improved further by strengthening during tempering.

It was shown that it is possible to produce uniform fine ferrite grain size by staring with uniform fine austenite grain sizes, and by

186

deformation extensively just above the recrystallisation stop
temperature. This is the basis of the currently interesting
recrystallisation controlled rolling process. However transformation
from unrecrystallised austenite grain sizes can lead to a duplex
ferrite grain size with possibly inferior strength and higher impact
transition temperatures.

CHAPTER 13   SUGGESTIONS FOR FURTHER WORK

1. The precipitation of VN and VC in austenite and ferrite is very important as the former controls the grain size and coarsening characteristics, whereas the latter contributes to precipitation strengthening. Speculation exist how VN/VC affect the austenite/ferrite transformation. Work should concentrate, using electron optical techniques, to identify the role of VN and VC during the transformation.

2. A better understanding is required of how increasing nitrogen affects the transformation characteristics, of austenite. It has been shown that increasing nitrogen intensified the precipitation of V(CN) in ferrite. Does VN act as nuclei for precipitation of V(CN), or does VC and VN nucleate separately?

3. Very little is known about the rate of coarsening and rate of dissolution of V(CN) in austenite, which controls the austenite grain size and subsequently the mechanical properties after transformation. Using electron optical techniques, the coarsening and dissolution of V(CN) should be studied.

4. It was shown that increasing nitrogen increased the hardenability and raised the hardness of the transformation products. How nitrogen affects the hardenability needs further investigation, as it may well delay the transformation to ferrite or on the other hand may form VN which refines the austenite grain size and accelerates transformation. These effects required to be studied.

5. The stage of V(CN) precipitation responsible for the recrystallisation stop conditions requires to be investigated. Austenite grain growth is controlled by V(CN) below the solvus temperature. The recrystallisation stop temperature is much lower in comparison with the grain coarsening temperature. The factors influencing these temperatures need to be examined, and it may be possible so to increase the nitrogen that VN can be used instead of TiN in recrystallisation controlled rolling.

6. Evidence suggests that fine uniform recrystallised austenite grain
   sizes transform to uniform fine ferrite grain sizes with possibly
   superior properties. This needs further investigation using
   laboratory mill practices to provide specimens for tensile and
   impact data, which may well prove to be suitable for commercial
   production.

R E F E R E N C E S

1 BECKER, R., Z. Tech. Physik, 7, 1962, p.547.

2 BURKE, J.E., and TURNBULL, D., Progress in Metals Physics, 19, 3, 1952, p220.

3 BYRNE, J.G., 'RECOVERY RECRYSTALLISATION AND GRAIN GROWTH' Macmillan, Series in Mat. Sci. 1965.

4 OROWAN, E., Quoted by CAHN, R.W. in RECRYSTALLISATION, GRAIN GROWTH AND TEXTURES, Ed. H. Margolin, A.S.M., Ohio 1966, p.99.

5 CAHN, R.W., Proc. Phys. Soc. A63, 1950, p.323.

6 BECK, P.A., Journal of Applied Physics 20, 1949, p.633.

7 GAY, P., HIRSCH, P.B., and KELLY, A., Acta Cryst. 7,1954, p.41.

8 HU, H., in ELECTRON MICROSCOPY AND STRENGTH OF CRYSTALS, Ed. G. Thomas and J. Washburn, Interscience, N.Y. 1963, p.546.

9 HU, H., in RECOVERY AND RECRYSTALLISATION IN METALS, Ed. L. Himmel, Interscience, N.Y. 1963, p.311.

10 LI, J.M.C., Journal of Applied Physics, 33, 1962, p.2958.

11 BECK, P.A., and SPERRY,P.R., Journal of Applied Physics, 21, 1950, p.150.

12 BAILEY, J.E., Philosophical Magazine, 5, 1960, p.833.

13 BAILEY, J.E., and HIRSCH, P.B., Proceedings of Royal Society, 267A, 1962, p.11.

14 ROSEN, A., BURTON, M.S., and SMITH, G.V., Trans. AIME, 230, 1964, p.205.

15 HU, H., Trans. AIME, 230, 1964, p.572.

16 ENGLISH, A.T., and BACKOFEN, W.A., Trans. AIME, 230, 1964, p.396.

17 GOODENOW, R.H., Trans. ASM, 59, 1966, p.804.

18 READ, W.T., and SHOCKLEY, W., Phys. Rev., 78, 1950, p.275.

19 LI, J.M.C., Journal of Applied Physics, 32,1961, p.525.

20 MOTT, N.F., Proceedings of Royal Society, London, 60, 1948, p.391.

21 GORDON, P., and VANDERMEER, R.A., Ref. 4, p.205.

22 TURNBULL, D., J. Chem. Physics, 20, 1952, p.411.

23 AUST, K.T., and RUTTER,J.W., Quoted by Ref. 21.

24 LUCKE, K. and DETERT, K., Acta Metallurgical, 5, 1957, p.268.

25 GORDON, P. and VANDERMEER, R.A., Trans. A.I.M.E., 224, 1962, p.917.

26 SHEARD, G. and NUTTING, J., Met. Sci., 13, 1979, p.131.

27 LUCKE, K. and STUWE, H.P., Quoted by Ref. 41.

28 CAHN, J.W., Acta Met., 10, 1962, p.789.

29 MACHLIN, E.S., Trans. A.I.M.E., 224, 1962, P.1153.

30 HUGHES, E.J., PAXTON, H.W., and JOHNSON, A.A., Trans. A.I.M.E., 233, 1965, p.1186.

31 ABRAHAMSON, E.P. and BLAKENEY, B.S., Trans. A.I.M.E., 218, 1960, p.1101.

32 PRICE, R.J., and KELLY, A., Acta Met., 10, 1962, p.180.

33 JONES, R.I., Acta Met., 17, 1969, p.229.

34 BARNBY, J., and SMITH, E., Acta Met., 12, 1964, p.1353.

35 KOSTER, U., Met. Sci., 8, 1974, p.151.

36 'RECRYSTALLISATION IN THE CONTROL MICROSTRUCTURE' Iron and Steel Institute / Institute of Metals, London 14-15 Nov. 1973, Metal Science, vol.8, 1974, pp.129-196.

37 'RECRYSTALLISATION IN THE DEVELOPMENT OF MICROSTRUCTURE' University of Leeds, 4-6 April 1978, Metal Science, Vol.13, 1979, pp.101-267.

38 'METALLURGICAL FORUM 12', Metals Forum, Vol.1 No.3 , 1978, pp. 113-176.

39 MORRIS, P.L., and DUGGAN, B.J., Met. Sic., 12, 1978, p.1.

40 HUMPHREY, E.J., Acta Met., 25, 1977, p.1323,

41 GAWNE, D.T., and HIGGINS, G.T., Mat. Sci., 6, 1971, p.403.

42 COTTERILL, P., and MOULD, P.R., 'RECRYSTALLISATION AND GRAIN GROWTH IN METALS', Surrey University Press, 1976.

43 MOULD, P.R., and COTTERILL, P., J. Mat. Sci., 2, 1967, p.241.

44 DOHERTY, R.D., and MARTIN, J.W., J. Inst. Metals, 91, 1962, p.332.

45 DAVIDSON, A.P., and WEST, D.R.F., Met. Sci., 13, 1979, p.170.

46 KAMMA, C., and HORNBOGEN, E., J. Mat. Sci., 11, 1976, p.2340.

47 RICKETT, R.C., and KALIN, S.H., Quoted by Ref. 41.

48 LESLIE, W.C., RICKETT, R.L., DALTON, C.L., and WATSON, G.S., Trans. A.S.M., 44, 1954, p.1470.

49 LE BON,A., ROFES-VERNIS, J., and ROSSARD, C., Met. Sci., 9, 1975, p.36.

50 BECK, P.A., TOWER, J., and MANLEY, W.O., Trans. A.I.M.E., 175, 1951, p.634.

51 BECK, P.A., J. Appl. Phys. 19, 1948, p.507.

52 BURKE, J.E., Trans. A.I.M.E., 180, 1949, P.73.

53 GREY, E.A., and HIGGINS, G.T., Acta Met., 21, 1973, p.309.

54 HILLERT, M., Acta Met., 13, 1965, p.227.

55 SMITH, C.S., Trans. A.I.M.E., 175, 1949, P.15.

56 ZENER, C., Quoted by 55.

57 GLADMAN, T., Proc. Roy. Soc., A294, 1966, p.298.

58 GLADMAN, T., and PICKERING,. F.B., J.I.S.I., 205, 1967, P.653.

59 AMIN, R.K. and PICKERING, F.B., in 'THERMOMECHANICAL PROCESSING OF MICROALLOYED AUSTENITE',Ed. DeArdo et al., Metall. Soc. A.I.M.E., Pittsburgh, Pennsylvania, August 17-19, 1982, p.1.

60 JONAS, J.J., SELLARS, C.M. and MCG TEGART, W., Metall. Reviews, 4, Review 130, 1969, p.1.

61 MCQUEEN, H.J. and JONAS, J.J., in 'TREATISE ON MATERIALS SCIENCE AND TECHNOLOGY 6', Edit. Arsenault, R.J., 1075, p.393.

62 'MICROALLOYING 75', Conf. Proc. Oct. 1-3 1975, Washington, Union Carbide Corp. Edit. Korchinsky, M., 1977.

63 'THE HOT DEFORMATION OF AUSTENITE', Edit. Ballance, J.B., The Metall. Soc. A.I.M.E., N.Y. 1977

64 'THERMOMECHANICAL PROCESSING OF MICROALLOYED AUSTENITE', Edit. DeArdo, A.J., et al, Conf. Proc. The Metall. Soc. A.I.M.E., Pittsburgh, August 1981.

65 'INTERNATIONAL CONFERENCE ON TECHNOLOGY AND APPLICATION OF HIGH STRENGTH LOW ALLOY (HSLA) STEELS', A.S.M. Philadelphia, PA, 1983

66 IRVINE, K.J., PICKERING, F.B., and GLADMAN, T., J.I.S.I. 205,1967, P.161.

67 ARONSSON, B., in 'SYMPOSIUM ON STEEL-STRENGTHENING MECHANISMS', Zurich, 5-6 May, 1966, p.77.

68 ROBERTS, W., Controlled Rolling of Micro-Alloyed Steels, Swedish Institute for Metal Research, IM-1085, June 1975.

69 WEBSTER, D. and ALLEN, G.B., J.I.S.I., 200, 1962, P.520.

70 PHILLIPS, R. and CHAPMAN, J.A., (Ref. 1,5, and 6), J.I.S.I. June, 1966 p.615.

71 KOZASU, I. OUCHI, C., SAMPEI, T. and OKITA,T., Ref 62, p.120.

72 DIMICCIO, D.R. and DAVENPORT, A.T., Ref.64, p.59.

73 CUDDY, L.J. Metall. Trans., 12A, 1981, p.1313.

74 TANAKA, T., TABATA, N., HATOMURA, T. and SHIGA, C., Ref. 62, p.107.

75 CUDDY, L.J. BAUWIN, J.J. and RALEY, J.C., Metall. Trans. 11A, 1980, p.381.

76 AMIN, R.K., Ph.D. Thesis, Sheffield City Polytechnic, 1980.

77 PICKERING, F.B., Ref. 65, p.1.

78 AKBEN, M.G., BACROIX, B. and JONAS, J.J., Acta Met., 31, 1983, p.161.

79 AMIN, R.K. and PICKERING, F.B., Ref. 64, p.377.

80 JONES, J.D., and ROTHWELL, A.D., I.S.I., Report 108, 1968, p.78.

81 IRANI, J.J., BURTON, D., JONES, J.D. and ROTHWELL, A.B., I.S.I. Report 104, 1967, p.110.

82 HANSEN, S.S., VANDERSANDE, J.B. and COHEN, M., Metall. Trans. 11A, 1980, p.387.

83 ROBERTS, W., Swedish Institute for Metal Research, IM-1211, July 1977.

84 DEARDO, A.J. and BROWN, E.L., J. of Metals, January 1977 p.26.

85 ROBERTS, W. and AHLBLOM, B., Swedish Institute for Metal Research, IM-1279, May 1978.

86 TANAKA, T., FUNAKOSHI, T. VEDA, M., TSUBOI, J., YASUDA, T. and UTAHASHI, C., Ref. 62, p.399.

87 KOZASU, I., Trans. I.S.I.J. 11,1971, p.375.

88 CORDEA, J.N. and HOOK, R.E., Metall. Trans. 1, 1970, p.111.

89 WHITE, M.J. and OWEN, W.S., Metall. Trans. 11A 1980, p.597.

90 YAMAMOTO, S. OUCHI, C. and OSUKA, T., Ref. 64, p.613.

91 KONIG, P., SCHOLZ, W. and ULMER, H., Arch. Eisen., 32, 1961, p.541.

92 EKEBUISI, G.O., Ph.D Thesis, Sheffield City Polytechnic, 1984.

93 GRIFFITHS, G. and RILEY, J.N., Acta Met., 14, 1966, p.755.

94 GREWEN, J., HUBER, J. and HATHERLY, M., Metals Forum, Vol. 1 Pt. 3, 1978, p.115.

95 DILLAMORE, I.L., MORRIS, P.L., SMITH, C.J.E. and HUTCHINSON, W.B., Proc. Roy. Soc. 1972, A329, p.405.

96 AMIN, R.K., Discussion in 'HOT WORKING AND FORMING PROCESS', Sheffield University, The Metals Society, 1980, p.44.

97 PICKERING, F.B. Ref. 62 p.9.

98 GLADMAN, T., DULIEU, D., and MCIVOR, I.D.,Ref. 62 p.32.

99 BUNGARDT, K., KIND, K. and OLSEN, Arch. Eisen. 26, 1955,

p.61.

100 NARITA, K. Tras. I.S.I.J., 15, 1975, p.145.

101 WRIEDT, H.A., and HU, H., in 'CHEMICAL METALLURGY – A Tribute to
     Carl Wagner' Ed. by N. Agokcen, The Met. Soc. A.I.M.E., Feb.,
     1981, p.171.

102 SEKINE, H., IDUE, T. and OGASAWARA, Trans. I.S.I.J., 8, 1968,
     p.101.

103 CHINO, H. and WADA, K., Yawata Technical Report 251, 1965,
     p.75.

104 KOGA and ENTIN, Quoted by N.A. Savost'yanova and L.A.
     Shvartsman, Fizika Metallov. I. Metall. 9 1960, p.515.

105 FOUNTAIN, R.W. and CHIPMAN, J., Trans. A.I.M.E. 2, 1958,
     p.737.

106 ROBERTS, W. and SANDBERG, A., The Composition of V(C,N) as
     Precipitated in HSLA Steels Microalloyed with Vanadium.
     Swedish Institute for Metal Research, IM-1489, October 1980.

107 KOCH, W. and SUNDERMANN, H., Arch. Eisen. 28, Sept. 1957,
     p.557.

108 The United Steel Companies, Report PM 4616/4/63, April 1963.

109 The United Steel Companies, Report PM 5631/4/68D, June 1968.

110 BROWN, E.L., Ph.D. Thesis, University of Pittsburg, 1979.

111 PEMBERTON, R., The Analyst, Vol. 77, No 915, June 1952,
     p.287.

112 BROWN, J.F., CLARK, W.D., and PARKER, A., Metallurgia, Nov.
     1957, p.215.

113 KLINGER, P., and KOCH, W., Quoted by Ref. 114.

114 KOCH, W. and SUNDERMANN, H, J.I.S.I., Dec. 1958, p.373.

115 ANDREWS, K.W. and HUGHES, H. Determination of Non Metallic
     Compounds in Steel. A.S.T.M., STP 393, 1966, p.3.

116 ANDREWS, K.W. and HUGHES, H., Iron and Steel Febr. 1958,
     p.43.

117 EDELEANU, C., J.I.S.I., 185, 1957, P.482.

118 STEINGERWALD, R.F. and GREENE, N.D., J. of Electochem. Soc. Nov.
     1962, p.1062.

119 'ALLOYING ELEMENTS IN STEEL', 2nd Edition, E.C. Bain and H.W.
     Paxton, A.S.M., Ohio, 1966,

120 ANDREWS, K.W., J.I.S.I. 184, 1956, p.414.

121 PAXTON, H.W., in 'TRANSFORMATION AND HARDENABILITY IN STEELS',

Ann Arbor, Michigan, February 27-28, 1967, Climax Mol. Co., 1967, p.3.

122 SPEICH, G.R. and SZIRMAE, A., Trans. A.I.M.E. 245, 1969, p.1063.

123 JUDD, R.R.and PAXTON, H.W., Trans. A.I.M.E. 242, 1968, p.206.

124 WATANABE, S. and KUNITAKE, T., Trans. I.S.I.J. 16, 1976, p.28.

125 LAW, N.C. and EDMONDS, D.V., Metall. Trans. 11A, 1980, p.33.

126 ERASMUS, L.A., J.I.S.I. 202, 1964, p.128.

127 HONEYCOMBE, R.W.K., 'STEELS MICROSTRUCTURE AND PROPERTIES' Arnold, 1981.

128 MANNERKOSKI, M., Metal Science 3, 1969, p.54.

129 HONEYCOMBE, R.W.K., 29th Hatfield Memorial Lecture, Metal Science 14, 1980, p.201,

130 DAVENPORT, A.T., and HONEYCOMBE, R.W.K., Proceedings of Royal Society A 332, 1971, p.191.

131 CAMPELL, K. and HONEYCOMBE, R.W.K., Metal Science 8, 1974, p.197.

132 HOWELL, P.R., BEE, J.V. and HONEYCOMBE, R.W.K., Metal. Trans. 10A, 1979, p.1213.

133 RICKS, R.A., HOWELL, P.R. and HONEYCOMBE, R.W.K., Metal. Trans. 10A, 1979, p.1049.

134 BERRY, F.G. and HONEYCOMBE, R.W.K., Metal. Trans. 1, 1970, p.3229.

135 EDMONDS, D.V., J.I.S.I., 210, 1972, 363.

136 BALLIGER, N.K., Ph. D. Thesis, Cambridge University, 1977.

137 BALLIGER, N.K. and HONEYCOMBE, R.W.K., Metal Sc. April, 1980, p.121.

137(a) ZENER, C., Trans. A.I.M.E. 167, 1947, P.550.

138 PITSCH W. Act. Metal., 10, 1962, p.897.

139 ATKINS, M., 'ATLAS OF CONTINUOUS COOLING TRANSFORMATION DIAGRAMS FOR ENGINEERING STEELS' British Steel Corporation, 1977.

140 KELLY, P.M. and NUTTING, J., Proc. Roy. Soc., A259, 1960, p.45.

141 KELLY, P.M. and NUTTING, J., J.I.S.I., 197, 1961, P.199.

142 AARONSON, H.I. and DOMIAN, H.A., Trans. A.I.M.E., 236, 1966, P.781.

143 COATES, D.E., Metall. Trans. 4, 1973, p.2313.

144 RAZIK, N.A., LORIMER, G.W. and RIDLEY, N., Acta Metallurgica, 22, 1974, p.1249.

145 ABE, T., AARONSON, H.I. and SHIFLET, G.T., Metall. Trans., 16A, April 1985, p.521.

146 ANDREWS, K.W., J.I.S.I., 203, 1965, p.271.

147 KINSMAN, K.R. and AARONSON, H.I., in 'TRANSFORMATION AND HARDENABILITY IN STEELS', Ann Arbor, Michigan, February 27-28, 1967, Climax Mol. Co., p.39.

148 SMITH, Y.E., COLDREN, A.P. and CRYDERMAN, R.L., in 'TOWARD IMPROVED DUCTILITY AND TOUGHNESS' Kyoto, Inter. Conf., Climax Mol. Co., Japan, p.352.

149 KINSMAN, K.R. and AARONSON, H.I. Metal. Trans. 4, 1973, p.959.

150 WRIEDT, H.A. and HU, H., Metal. Trans. 14A, 1983, p.307.

151 WOODHEAD, J.H., Preprints of Techical Paper, 'VANADIUM 79' Seminar held in Chicago, Nov. 1979. VANITEC.

152 SPEICH, G.R., Trans. A.I.M.E., 245, 1969, p.2553.

153 ANSELL, G.S. and ARROT, A., Trans. A.I.M.E., 227, 1963, p.1080.

154 SPEICH, G.R. and LESLIE, W.C., Metal. Trans. 3, 1972, p.1043.

155 Ref. 28, and 29, Quoted by Speich G.R., and Leslie W.C., Metal. Trans. 3, 1972, p.1043.

156 'PRECIPITATION PROCESSES IN STEEL' I.S.I. Special Report 64, 1959.

157 'PRECIPITATION PROCESSES IN SOLIDS' Edited by Russel K.C. and Aaronson H.I., The Metall. Soc.A.I.M.E. 1978.

158 IRVINE, K. and PICKERING, F.B., J.I.S.I., 194, 1960, p.137.

159 PICKERING, F.B., Ref. 156, p.23.

160 TEKIN, E. and KELLY, P.M., in 'PRECIPITATION FROM IRON BASE ALLOYS', Metall. Soc. A.I.M.E., 1963, 28, p.173.

161 BAKER, R.G. and NUTTING, J., Ref. 156, p.1.

162 SMITH, E., Acta Met., 14, 1966, p.583.

163 PLATTS, J., Private Communication.

164 HOOGENDOORN, T.M., and SPANRAFT, M.J., Ref. 62, p.75.

165 KOPERNIKOVA, V.N. et. al., Metal Science and Heat Treatment, May 1980, p.865.

166 SMITH, R.P., J. Amer. Chem. Soc., 70, No 8, 1943, p.2724.

167 SHAW, S.W.K. and QUAREELL, A.G., J.I.S.I., 185, 1957, P.10.

168 JACK, D.H. and JACK, K.H., Carbides and Nitrides in Steels, Mat. Sc and Engineering, 11, 1973, p.1.

169 GOLDSCHMIDT, H., 'Interstitial Alloys', Butterworth 1967.

170 HU, H. and RATH, B.B., Met. Trans. 1, 1970, p.

171 NIELSEN, J.P., Some Laws of Grain Growth, in Ref. 4, p.286.

172 PICKERING, F.B., Vanadium as a Hardenability and Temperability Additive in Quenched and Tempered Steels, 'HSLA STEELS 85', Beijing, China, A.S.M. 1985 in press.

173 MILLER, O.O., Trans. A.S.M., 43, 1951, p.260.

174 KRAUSS, G., PRINCIPLES OF HEAT TREATMENT OF STEELS, A.S.M. 1980.

175 IRVINE, K.J., PICKERING, F.B. and GARSTONE, J. J.I.S.I., 196, 1960, p.66.

176 WADSWORTH, J., WOODHEAD, J.H. and KEOWN, S.R., Met. Sc., 10, October, 1976, p.342.

177 VASSILIOU, A.D. and PICKERING, F.B. 'The Role of Vanadium in the development of Quenched and Tempered Alloy Steels', Project Sponsored by VANITEC, 1983-1986.

178 AARONSON, H.I., 'DECOMPOSITION OF AUSTENITE BY DIFFUSINAL PROCESSES', Interscience Publishers, N. Y. 1962, p.387.

179 COCHRANE, R.C. and MORRISSON, W.B., in 'STEELS FOR LINE PIPE AND PIPELINE FITTINGS' Pro. Int. Conf., Metals Society, 1983, p.70

180 VASSILIOU, A.D., Discussion, ibid p.114.

181 PICKERING, F.B. 'Current and Potential uses of Vanadium in steels', Report to, Union Carbide Corp. 1981.

182 KRAUSS, G. in 'HARDENABILITY CONCEPTS WITH APPLICATIONS TO STEELS', Eds, D.V. Doane and J.S. Kirkaldy, A.I.M.E., Warrendale Pa, 1978, p.229.

183 OUCHI, et al, in Ref. 63, p.316.

184 GRANGE, R.A., Metal. Trans., Vol. 2, 1971, p.417.

T A B L E 1

ANALYSIS OF BASE MATERIALS (mass %)

1) Low Carbon base steel.
   0.02% C, 0.14% Mn, `0.02% Si, 0.011% S, 0.003% P, 0.04% Ni,
   0.07% Cr, 0.02% Mn, 0.01% Al.

2) Warner pig iron.
   4.17% C, 0.24% Mn, 0.21% Si, 0.032% P, 0.016% S.

3) Electrolytic iron.
   99.9% Fe, 0.005% C, 0.004% P, 0.005% S, 0.005 Si, 0.005% Mn,
   0.004% Cu.

4) Low carbon ferro-manganese.
   81.7% Mn, 0.10% C, 1.11% Si.

5) High carbon ferro-manganese.
   76% Mn, 6.74% C, 0.72% Si.

6) High nitrogen ferro-manganese.
   81.3% Mn, 0.54% Si, 0.68% C, 5.81% N.

7) Ferro-vanadium.
   53.4% V, 0.07% C. 2.1% Al.

8) Commercial purity silicon.
   98.6% Si, 0.68% Al.

9) Commercial purity vanadium.
   99+% V.

T A B L E   2

MATERIAL FOR INVESTIGATION

SERIES	STEEL NO	ANALYSIS (mass per cent)					
		C	Mn	Si	V	Al	N
LOW CARBON STEELS	1A	0.110	1.50	0.420	0.140	0.001	0.0050
	1B	0.113	1.57	0.410	0.130	0.001	0.0050
	1C	0.112	1.45	0.350	0.155	0.002	0.0040
	2	0.103	1.36	0.270	0.350	0.002	0.0050
	3A	0.120	1.58	0.240	0.130	0.009	0.0100
	3B	0.123	1.40	0.160	0.190	0.001	0.0100
	3C	0.123	1.60	0.400	0.150	0.009	0.0110
	4	0.100	1.60	0.440	0.410	0.004	0.0100
	5A	0.120	1.77	0.450	0.150	0.004	0.0200
	5B	0.115	1.85	0.480	0.140	0.004	0.0210
	5C	0.122	1.62	0.370	0.145	0.002	0.0205
	6	0.126	1.77	0.475	0.415	0.005	0.0200
HIGH CARBON STEELS	7	0.220	1.63	0.380	0.160	0.002	0.0058
	8	0.235	1.64	0.380	0.41	0.004	0.0040
	9	0.195	1.62	0.430	0.16	0.001	0.0110
	10	0.20	1.67	0.37	0.45	0.002	0.0099
	11	0.212	1.81	0.45	0.145	0.010	0.0180
	12	0.195	1.76	0.48	0.43	0.009	0.0180
BASE STEELS	13	0.103	1.59	0.38	-	0.001	0.0060
	14A	0.123	1.60	0.20	-	0.005	0.0100
	14B	0.128	1.70	0.41	-	0.004	0.0075
	15	0.12	1.64	0.134	-	0.001	0.0200
	16	0.17	1.84	0.45	-	0.009	0.0110
	17	0.20	1.80	0.38	-	0.010	0.0170
EXTRA LOW CARBON STEEL	18	0.055	1.55	0.36	0.15	0.005	0.0195

T A B L E 3

PRELIMINARY PRECIPITATE EXTRACTION RESULTS
STEEL COMPOSITION:- 0.12%C, 0.15%V, and 0.020%N
HEAT TREATMENT:- 1, 2 and 4 hours at 900°C followed
by iced-brine quenched.

TIME AT 900°C HOURS	METHOD OF EXTRACTION	PRECIPITATES EXTRACTED	PARTICLES SIZE IN
	CHEMICAL	GRAMS	ANGSTROMS
1	20% H_2SO_4 AT 60°C	0.396	150
2	20% H_2SO_4 AT 60°C	0.574	–
1	6 N HCl AT 20°C	0.549	120
2	6 N HCl AT 20°C	0.438	–
2	10% HCl AT 50°C	0.223	–
4	10% HCl AT 50°C	0.625	–
	POTENTIOSTATIC		
1	FERRIC CHLORIDE SOLUTION	0.179	70
4	10% HCl SOLUTION	0.386	–

T A B L E 4

4.1 ANALYSIS OF PRECIPITATES AND SOLUTION AFTER DISSOLUTION OF STEEL

Steel Composition:- 0.12%C, 1.58%Mn, 0.13%V, 0.010%N.
Heat Treatment:- 900°C followed by iced brine quenched.

METHOD OF EXTRACTION	TREATMENT TIME (mins)	WT % AS A PERCENTAGE IN THE STEEL					V (C N) COMPOSITION
		PRECIPITATES			SOLUTION		
		WT % V	WT % C	WT % N	WT % V	WT % N	
CHEMICAL	60	0.0091	0.0095	0.0017	0.1209	0.0083	$VC_{0.86}N_{0.14}$
	120	0.0281	0.0095	0.0043	0.1019	0.0057	$VC_{0.72}N_{0.28}$
	240	0.0334	0.0262	0.0099	0.0966	0.0001	$VC_{0.75}N_{0.25}$
	480	0.0341	0.0102	0.0048	0.0959	0.0052	$VC_{0.71}N_{0.29}$
ELECTRO-CHEMICAL	60	0.0292	0.1454	0.0418	0.1597	0.0125	
	120	0.0224	0.1106	0.0123	0.1000	0.0074	
	240	0.0253	0.1371	0.0148	0.1036	0.0058	
	480	0.0260	0.1163	0.0165	0.0747	0.0029	

201

4.2 ANALYSIS OF PRECIPITATES AND SOLUTION AFTER CHEMICAL DISSOLUTION

Heat Treatment:- Austenitising for 1 hour at 900°C

4.2.1. Steel Composition:- (1A) 0.11%C, 1.50%Mn, 0.14%V, 0.005%N

TREATMENT TIME (mins)	PRECIPITATES			SOLUTION		V (C N) COMPOSITION
	WT % V	WT % C	WT % N	WT % V	WT % N	
60	-	0.0466	-	0.2337	0.0027	
120	0.0183	0.0136	0.0057	0.1699	0.0029	$VC_{0.73}N_{0.27}$
240	0.0142	0.0061	0.0038	0.1589	0.0029	$VC_{0.65}N_{0.35}$
480	0.0076	0.0063	0.0029	0.1603	0.0029	$VC_{0.72}N_{0.28}$

4.2.2. Steel composition:- (5A) 0.12%C, 1.77%Mn, 0.15%V, 0.02%N

TREATMENT TIME (mins)	PRECIPITATES			SOLUTION		V (C N) COMPOSITION
	WT % V	WT % C	WT % N	WT % V	WT % N	
60	-	-	-	-	-	-
120	0.0267	0.0112	0.0105	0.3052	0.0093	$VC_{0.56}N_{0.44}$
240	0.0469	0.0206	0.0147	0.0692	0.0035	$VC_{0.62}N_{0.38}$
480	0.0388	0.0179	0.0115	0.1720	0.0040	$VC_{0.65}N_{0.35}$

4.2.3. Steel Composition:- (4) 0.10%C, 1.60%Mn, 0.41%V, 0.010%N

TREATMENT TIME (mins)	PRECIPITATES			SOLUTION		V (C N) COMPOSITION
	WT % V	WT % C	WT % N	WT % V	WT % N	
60	0.0699	0.0194	0.0071	0.3431	0.0004	$VC_{0.76}N_{0.24}$
120	0.1051	0.0391	0.0136	0.3281	0.0013	$VC_{0.77}N_{0.23}$
240	0.0913	0.0200	0.0075	0.3179	0.0004	$VC_{0.76}N_{0.24}$
480	0.0804	0.0272	0.0093	0.2833	0.0003	$VC_{0.77}N_{0.23}$

Note:- Wt % quoted as a percentage of that in the steel.

T A B L E   5

THE RATIOS OF V:C V:N AND N:C IN STEELS AND N:C IN PRECIPITATES AFTER HOMOGENIZATION TEMPERATURE OF UP TO 8 HOURS AT 900°C

STEEL NO	RATIO IN STEELS			N:C RATIO IN PRECIPITATES
	V:C	V:N	N:C	
1A	0.30	7.70	0.039	0.43
3A	0.25	3.57	0.071	0.31
4	0.79	11.28	0.086	0.30
5A	0.29	2.06	0.143	0.65
18	0.64	2.11	0.303	1.27

T A B L E   6

SOLUBILITY OF VANADIUM CARBON AND NITROGEN IN AUSTENITE

6.1 Steel Composition:- 0.103%C, 1.36%Mn, 0.35%V, 0.005%N
    Heat Treatment:- 8 hours at temperature stated.

TEMPERATURE °C	WT PER CENT IN SOLUTION		
	VANADIUM	CARBON	NITROGEN
900	0.2199	–	0.0013
950	0.1494	0.0473	0.0006
1000	0.3280	0.0560	0.0032
1050	0.2717	0.0289	0.0074
1100	0.3646	0.0425	0.0104
1200	0.3771	0.0565	0.0039
1250	0.3507	0.0544	0.0178

6.2 Steel Composition:- 0.12%C, 1.77%Mn, 0.15%V, 0.020%N
    Heat Treatment:- 8 hours at temperature stated.

TEMPERATURE oC	WT PER CENT IN SOLUTION		
	VANADIUM	CARBON	NITROGEN
900	0.0456	0.0420	0.0040
950	0.0923	0.0671	0.0018
1000	0.1060	0.0249	0.0074
1050	0.1274	0.0041	0.0082
1100	0.1410	0.0588	0.0062
1200	0.1093	0.0635	0.0140
1250	0.4247	0.0487	0.0108

6.3 Steel Composition:- 0.126%C, 1.77%Mn, 0.415%V, 0.020%N
    Heat Treatment:- 8 hours at temperature stated.

TEMPERATURE	WT PER CENT IN SOLUTION		
°C	VANADIUM	CARBON	NITROGEN
900	0.0456	0.0131	0.0012
950	0.1055	0.0196	0.0016
1000	0.3316	0.0552	0.0039
1100	0.3620	0.0644	0.0067
1200	0.3923	0.0676	0.0070
1250	0.3936	0.0369	0.0204

6.4 Steel Composition:- 0.22%C, 1.6%Mn, 0.16%V, 0.0058%N
    Heat Treatment:- 8 hours at temperature stated.

TEMPERATURE	WT PER CENT IN SOLUTION		
°C	VANADIUM	CARBON	NITROGEN
900	0.0940	0.0533	0.0021
950	0.0735	0.0269	0.0036
1000	0.0937	0.0267	0.0037
1100	0.1442	0.0169	0.0038
1200	0.15175	0.0721	0.0056
1250	0.0748	0.0480	.00065

6.5 Steel Composition:- 0.212%C, 1.83%Mn, 0.145%V, 0.018%N
    Heat Treatment:- 8 hours at temperature stated.

TEMPERATURE	WT PER CENT IN SOLUTION		
°C	VANADIUM	CARBON	NITROGEN
900	0.0697	0.0862	0.0044
950	0.1437	0.0163	0.0063
1000	0.1074	0.0253	0.0149
1100	0.1456	0.0617	0.0164
1200	0.1303	0.1303	0.0115
1250	0.1323	0.1425	0.0091

T A B L E 7

THE EFFECT OF VANADIUM NITROGEN AND CARBON ON THE HARDNESS ON AS QUENCHED MARTENSITE

WT % C	WT % V	HARDNESS HV$_{30}$				
		HOMOGENISED TEMPERATURE				
		1250°C			1075°C	
		0.005%N	0.01%N	0.02%N	0.005%N	0.02%N
0.10 / 0.12	–	415	434	431	418	441
	0.13/0.15	391	422	434	377	426
	0.35/0.41	402	421	459	387	415
0.2	–	–	–	465	–	477
	0.43	–	–	508	–	495

T A B L E 8

THE EFFECT OF VANADIUM NITROGEN AND CARBON ON THE INCREASE IN HARDNESS AT MAXIMUN SECONDARY HARDENING

WT % C	WT % N	HARDNESS HV$_{30}$			
		HOMOGENISED 1250°C		HOMOGENISED 1075°C	
		0.13/0.15%V	0.35/0.41%V	0.13/0.15%V	0.35/0.41%V
0.10 / 0.12	0.005	90	150	93	150
	0.010	90	150	–	–
	0.020	80	150	100	145
0.20	0.017 /0.02	–	135	–	130

T A B L E   9

THE EFFECT OF DEFORMATION ON THE RECRYSTLLISED AUSTENITE AT VARIOUS TEMPERATURES.

9.1 Steel Composition:- 0.12%C, 1.60%Mn, 0.010%N

AMOUNT OF DEFORMATION %	DEFORMATION TEMPERATURE °C			
	1 2 0 0	1 1 2 5	1 0 5 0	9 2 5
30	107.8±15.0	-	97.4±12.8	-
50	70.9±11.0	66.5±10.3	64.5± 7.9	48.0±6.3
70	63.7± 9.5	-	39.5± 4.7	40.8±4.9

9.2 Steel Composition:- 0.12%C, 1.45%Mn, 0.14%V, 0.010%N

AMOUNT OF DEFORMATION %	DEFORMATION TEMPERATURE °C			
	1 2 0 0	1 1 2 5	1 0 5 0	9 2 5
30	77.3± 6.5	-	37.0± 3.9	-
50	40.0± 4.7	24.0± 2.7	30.0± 4.2	-
70	20.0± 2.6	-	14.0± 1.4	11.6±0.8

9.3 Steel Composition:- 0.12%C, 1.58%Mn, 0.13%V, 0.005%N

AMOUNT OF DEFORMATION %	DEFORMATION TEMPERATURE °C			
	1 2 0 0	1 1 2 5	1 0 5 0	9 2 5
30	105.7±22.3	79.1±13.8	67.8±11.3	-
50	48.7± 7.0	43.5± 5.4	37.4± 4.5	30.9±3.6
70	28.1± 2.8	-	25.1± 2.5	23.7±2.5

9.4 Steel Composition:- 0.12%C, 1.77%Mn, 0.15%V, 0.020%N

AMOUNT OF DEFORMATION %	DEFORMATION TEMPERATURE °C			
	1 2 0 0	1 1 2 5	1 0 5 0	9 2 5
30	64.7± 8.6	-	56.3± 5.4	-
50	48.1± 6.3	30.9± 3.2	25.9± 2.5	-
70	24.4± 2.3	-	24.4± 2.3	12.2±1.0

T A B L E 10

GRAIN COARSENING OF RECRYSTLLISED AUSTENITE AFTER THERMOMECHANICAL PROCESSING

10.1 Steel Composition:- 0.123%C, 1.60%Mn, 0.010%N

REDUCTION AT °C	TIME AT 925 °C (SECONDS)				
	AS QUENCHED	10	100	1000	10000
30% 1200	107.8±15.0	-	104.5±5.2	-	113.5±6.2
70% 1050	39.5± 4.7	_	30.0±1.3	_	51.9±2.5

10.2 Steel Composition:- 0.12%C, 1.40%Mn, 0.19%V, 0.010%N

REDUCTION AT °C	TIME AT 925 °C (SECONDS)				
	AS QUENCHED	10	100	1000	10000
30% 1200	77.3± 3.6	86.4±5.9	95.2±4.9	100.4±5.0	106.0±5.6
70% 925	14.0± 1.3	16.0±0.7	18.5±0.9	22.5±1.0	21.0±1.0

10.3 Steel Composition:- 0.123%C, 1.57%Mn, 0.14%V, 0.005%N

REDUCTION AT °C	TIME AT 925 °C (SECONDS)				
	AS QUENCHED	10	100	1000	10000
30% 1200	105.7±22.3	100.8±7.4	114.6±9.3	126.2±9.8	120.3±10.2
70% 925	25.1± 2.5	27.5±1.3	36.6±1.9	48.3±2.1	58.3± 3.6

10.4 Steel Composition:- 0.12%C, 1.83%Mn, 0.14%V, 0.021%N

REDUCTION AT °C	TIME AT 925 °C (SECONDS)				
	AS QUENCHED	10	100	1000	10000
30% 1200	56.3±5.4	82.7±5.2	83.4±5.3	81.7±3.6	98.2±5.1
70% 925	24.4±2.3	21.1±0.9	23.8±1.1	28.0±1.2	41.1±2.4

THE EFFECT OF VANADIUM NITROGEN AND AMOUNT OF DEFORMATION ON THE FORMATION OF AUSTENITE GRAIN BOUNDARY AREA PER UNIT VOLUME Svv

DEFORMATION		ALLOY No 14	ALLOY No 3	ALLOY No 1	ALLOY No 5
TEMP°C	%	mm^{-1}	mm^{-1}	mm^{-1}	mm^{-1}
1200	30	18.55	25.87	18.92	35.51
	50	28.21	50.00	41.07	41.54
	70	31.42	100.00	71.22	81.97
1125	30	-	-	25.27	-
	50	30.07	83.33	46.00	64.77
1050	30	20.53	54.05	29.50	30.91
	50	31.01	66.67	53.49	77.22
	70	50.63	142.86	78.81	81.87
925	50	41.63	101.83	64.62	102.67
	70	49.06	-	84.39	-
875	30	31.14	7.36	5.99	27.33
	50	112.11	22.19	102.95	136.99
	70	130.63	143.47	163.89	153.26
825	30	74.22	41.51	6.72	23.75
	50	55.06	60.59	20.47	53.43
	70	141.46	114.29	27.80	100.21
925+	30	95.46	56.31	159.36	75.14
	50	130.72	165.84	118.76	70.96
	70	104.27	342.47	164.74	139.06
925#	30	-	114.94	209.64	173.01

+ 30% reduction at 1200°C then cooled to 925°C.
# 70% reduction at 1050°C then cooled to 925°C.

TABLE 12

VOLUME FRACTION OF FERRITE FORMED DURING ISOTHERMAL TRANSFORMATION AT 750°C AFTER DEFORMATION AT HIGHER TEMPERATURE

13.1 Steel Composition:- 0.12%C, 1.65%Mn, 0.010%n

REDUCTION AT TEMP. °C	TRANSFORMATION TIME (seconds)						
	50	100	500	1000	10000	12HRS	24HRS
30% 1200	–	0.29	11.80	17.40	28.80	35.30	36.06
70% 1050	initn	10.40	25.40	23.20	27.50	23.40	24.40
50% 925	initn	11.60	28.40	–	26.90	35.60	38.04
30% 875	11.96	16.72	22.66	29.40	32.37	29.77	32.91
30% 825	initn	9.70	–	–	–	–	–
50% 825	initn	13.60	31.00	26.40	29.40	34.00	39.30
70% 825	29.23*	33.45	–	–	–	–	–

* 10 secs ferrite initiation.

13.2 Steel Composition;- 0.12%C, 1.4%Mn, 0.14/0.19%V, 0.010%N

REDUCTION AT TEMP. °C	TRANSFORMATION TIME (seconds)						
	50	100	500	1000	10000	12HRS	24HRS
30% 1200	3.0 *	12.60	25.50	31.20	37.30	43.60	40.00
70% 1050	3.8 *	18.50	32.70	42.10	41.10	47.70	45.60
50% 925	5.6 *	25.00	27.40	43.70	32.70	53.20	54.40
30% 875	10.40	14.30	22.10	25.90	30.40	–	36.70
30% 825	6.30	11.60	21.80	–	–	29.30	40.38
50% 825	19.40	37.80	26.43	46.22	51.22	64.30	71.50
70% 825	42.00	49.00	–	–	–	–	–

* Transformation Time 10 seconds.

13.3 Steel Composition;- 0.12%C, 1.4/1.6%Mn, 0.13/0.15%V, 0.005%N

REDUCTION AT TEMP. °C	TRANSFORMATION TIME (seconds)						
	50	100	500	1000	10000	12HRS	24HRS
30% 1200	–	10.40	32.50	31.80	44.20	47.80	57.80
70% 1050	–	31.70	31.70	43.50	45.80	52.40	62.90
50% 925	–	28.90	40.55	44.15	43.16	48.60	50.00
30% 875	7.20	15.50	41.55	47.30	51.90	56.70	67.60
30% 825	7.50	20.8 *	–	–	–	–	–
50% 825	24.20	32.90	43.50	44.40	50.00	59.50	70.50
70% 825	40.10	53.50	31.20+	–	–	–	–

* 140 seconds transformation time
+ 10 seconds transformation time

13.4 Steel Composition;- 0.12%C, 1.6%Mn, 0.14/0.15%V, 0.020%N

REDUCTION AT TEMP. °C	TRANSFORMATION TIME (seconds)						
	50	100	500	1000	10000	12HRS	24HRS
30% 1200	–	–	4.40	7.50	11.60	18.40	17.60
70% 1050	–	3.10	6.90	14.50	19.60	32.40	36.90
50% 925	–	11.30	18.70	28.60	29.50	40.30	48.40
30% 875	–	4.45	6.00	13.30	33.40	36.78	39.03
50% 825	8.90	16.36	16.27	22.75	–	34.17	–

T A B L E 13

THE FERRITE GRAIN SIZE DEVELOPED DURING TRANSFORMATION
AT 750°C AFTER DEFORMATION AT HIGHER-TEMPERATURE

15.1 Steel Composition:- 0.12%C, 1.65%Mn, 0.010%N

% DEF n AT TEMP. °C	TRANSFORMATION TIME (seconds)						
	50	100	500	1000	10000	12HRS	24HRS
30% 1200	–	–	11.87	17.80	24.82	27.70	31.76
70% 1050	–	5.90	5.58	6.69	7.04	8.25	6.75
50% 925	–	5.60	7.54	–	5.33	6.20	6.80
30% 875	7.12	13.02	27.05	31.50	31.53	36.42	38.70
50% 825	–	5.93	4.80	5.11	6.29	5.28	5.98

15.2 Steel Composition:- 0.12%C, 1.4%Mn, 0.14/0.19%V, 0.010%N

% DEF n AT TEMP °C	TRANSFORMATION TIME (seconds)						
	50	100	500	1000	10000	12HRS	24HRS
30% 1200	–	10.87	17.70	22.40	24.66	21.30	25.07
70% 1050	–	6.97	7.70	6.35	7.84	9.04	8.51
50% 925	–	9.72	7.85	7.25	7.80	7.50	7.90
30% 875	4.90	5.49	9.09	8.55	10.01	–	9.40
	–	–	–	12.83	15.08	–	12.87
30% 825	3.33	4.46	6.01	–	–	10.85	11.82
	–	–	–	–	–	17.60	16.61
50% 825	3.86	3.81	3.30	4.63	3.66	4.80	5.61
	–	–	–	6.90	8.15	7.87	8.70
70% 825	4.06	3.69	–	–	–	–	–

211

15.3   Steel Composition;- 0.12%C, 1.4/1.6%Mn, 0.13/0.15%V, 0.005%N

% DEF n AT TEMP °C	TRANSFORMATION TIME (seconds)						
	50	100	500	1000	10000	12HRS	24HRS
30% 1200	–	9.71	14.06	14.10	19.37	20.20	17.44
70% 1050	–	4.71	8.24	6.61	7.65	5.56	5.50
	–	–	–	–	–	–	11.78
50% 925	–	5.84	5.88	5.80	5.59	6.11	7.25
30% 875	10.90	14.00	16.43	14.32	15.28	15.08	15.01
		–	–	23.63	24.04	26.47	23.66
30% 825	7.96	7.86*	–	–	–	–	–
50% 825	6.20	6.68	5.97	7.64	6.77	7.16	8.23
	–	–	7.15	9.67	12.80	13.40	15.30
70% 825	4.30	4.47	3.69+	–	–	–	–

* 140 seconds transformation time
+ 10 seconds transformation time

15.4   Steel Composition;- 0.12%C, 1.6%Mn, 0.14/0.15%V, 0.020%N

% DEF n AT TEMP °C	TRANSFORMATION TIME (seconds)						
	50	100	500	1000	10000	12HRS	24HRS
30% 1200	–		14.14	13.46	12.56	13.65	13.80
70% 1050	–	2.29	4.24	6.57	3.90	6.16	7.25
	–	–	–	–	7.41	7.35	7.90
50% 925	–	–	4.57	4.75	5.63	6.97	10.60
	–	–	–	–	7.88	14.50	16.60
30% 875	–	–	7.60	4.93	5.43	7.47	7.34
	–	–	–	–	11.83	8.80	11.08
50% 825	2.94	3.62	5.21	4.20	–	4.64	–
	–	–	–	9.60	–	13.25	–

TABLE 14

THE EFFECT OF THERMO-MECHANICAL TREATMENT AND COOLING RATE ON THE FERRITE GRAIN SIZE

STEEL No	PER CENT REDUCTION AT $^{\circ}$C		Svv mm^{-1}	COOLING RATES 800-500°C	
				2.2~3.2°C	4.0~5.0°C
V-FREE	30	1200	18.55	11.40±2.24	10.40±2.50
BASE	70	925	49.06	6.13±0.63	5.84±0.80
STEEL	50	825	55.06	6.94±0.92	8.05±1.75
0.010%N	70	825	141.46	5.07±0.87	5.43±0.63
VANADIUN	30	1200	25.87	12.28±2.40	9.76±1.50
STEEL	70	925	172.11	3.50±0.63	3.44±0.40
0.010%N	50	825	60.59	2.50±0.60	4.70±0.60
	70	825	114.29	3.23±0.30	4.20±0.20
VANADIUM	30	1200	18.92	13.60±4.70	9.20±2.15
STEEL	70	925	84.39	7.60±1.60	4.84±0.70
0.005%N	50	825	20.47	6.42±0.70	6.24±0.90
	70	825	27.80	5.86±0.70	4.90±0.85
VANADIUN	30	1200	35.51	5.55±0.80	7.88±1.14
STEEL	70	925	163.70	4.66±0.57	4.40±0.90
0.020%N	50	825	53.43	4.90±0.54	5.35±0.93
	70	825	100.20	3.90±0.45	3.96±0.93

213
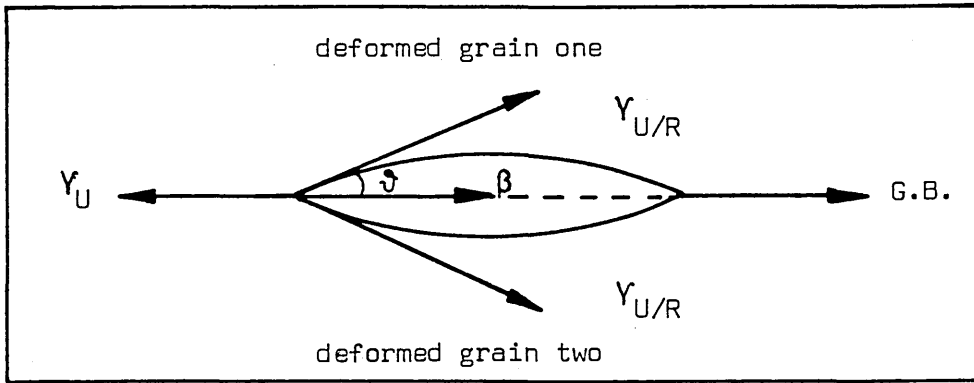
FIG, 1   THE FORMATION OF A β NUCLEUS OF A RECRYSTALLISED
STRUCTURE ON THE GRAIN BOUNDARY BETWEEN TWO DEFORMED
GRAINS.
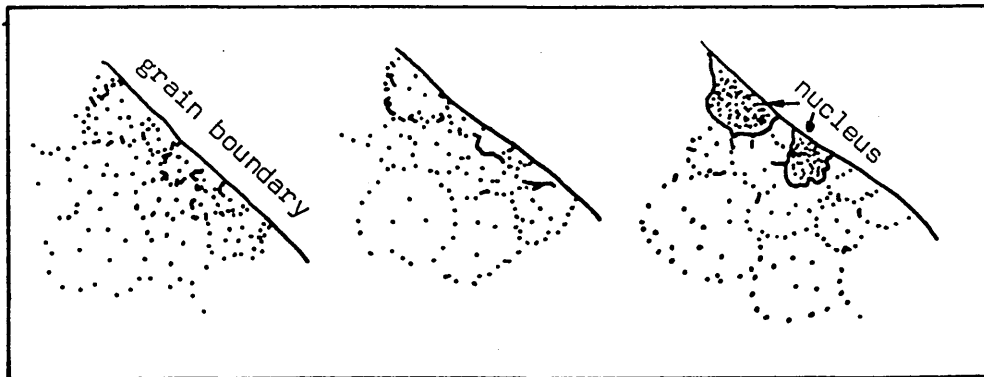
FIG. 2   NUCLEATION AND SUBGRAIN GROWTH (SHEMATIC).   SUBGRAIN
BOUNDARIES THICKLY POPULATED BY DISLOCATIONS (DOTS)
HAVE A HIGH MISORIENTATION ANGLE AND ARE MOST LIKELY
TO MIGRATE.

a. THE ORIGINAL
   SUBGRAIN STRUCTURE
   BEFORE COALESCENCE

b. ONE SUBGRAIN IS
   UNDERGOING A
   ROTATION

c. THE SUBGRAIN STRUCTURE
   JUST AFTER COALESCENCE

d. THE FINAL SUBGRAIN
   STRUCTURE AFTER SOME
   SUBBOUNDARY MIGRATION.
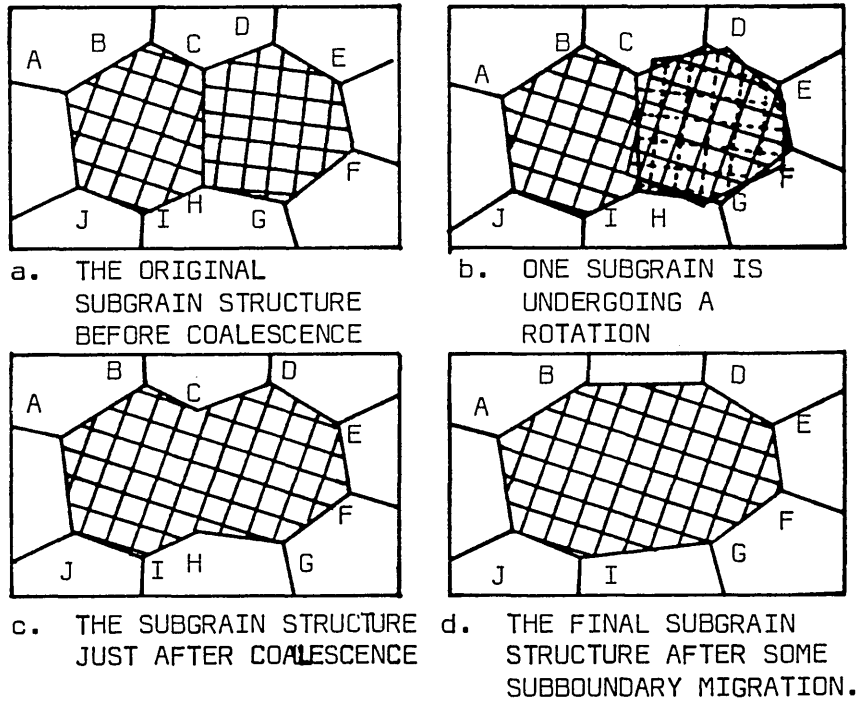
FIG. 3   SHEMATIC REPRESENTATION OF SUBGRAIN COALESCENCE
         BY SUBGRIAN ROTATION.

a. SUBGRAIN STRUCTURE
   BEFORE NUCLEATION

b. COALESCENCE OF
   SUBGRAINS A AND B
   AND C AND D.

c. FURTHER COALESCENCE
   OF SUBGRAINS B AND C

d. FORMATION OF A NUCLEUS
   WITH HIGH ANGLE
   BOUNDARIES
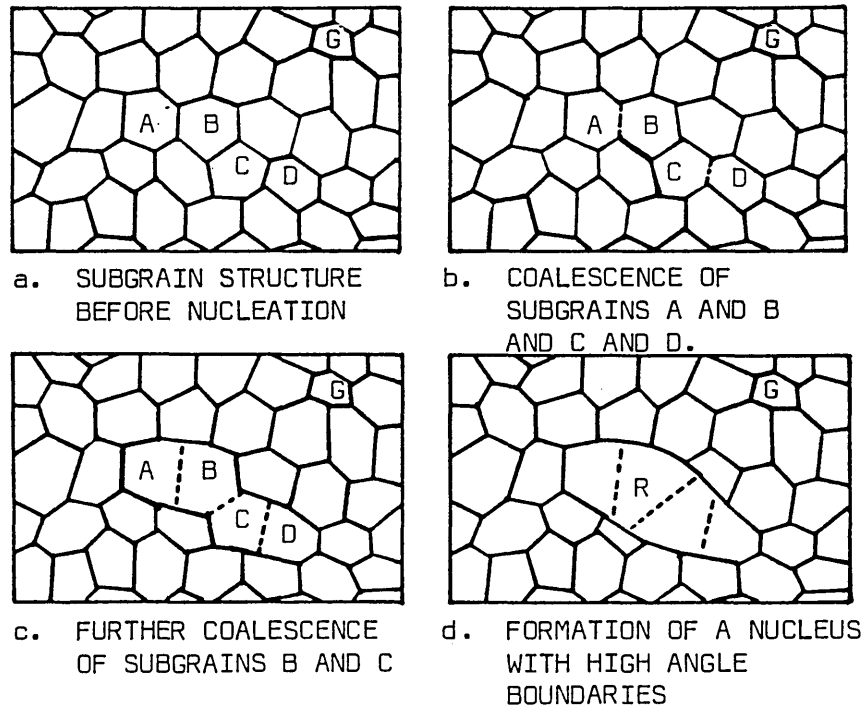
FIG. 4   SCHEMATIC REPRESENTATION OF THE FORMATION OF A
         PRIMARY RECRYSTALLISATION NUCLEUS BY SUBGRAIN
         COALESCENCE.

215
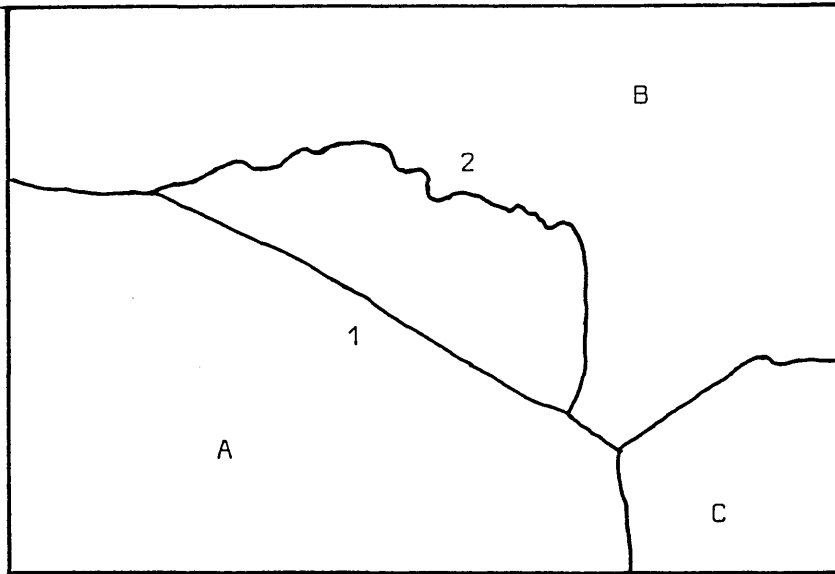
FIG. 5 OUTLINE OF A MICROGRAPH SHOWING STRAIN-INDUCED BOUNDARY MIGRATION IN ALUMINIUM
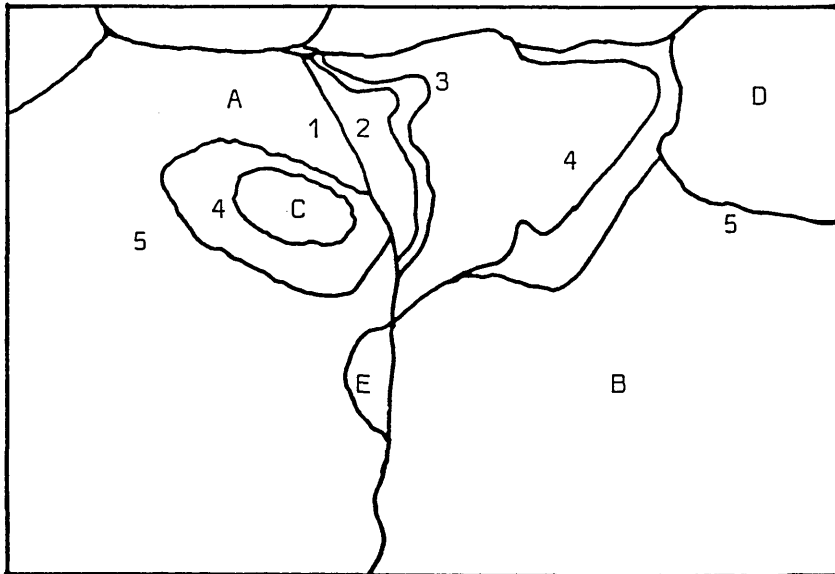
FIG. 6 OUTLINE OF A MICROGRAPH SHOWING STRAIN-INDUCED BOUNDARY MIGRATION. STRAIN INDUCED GROWTH OF A AT THE EXPENSE OF B. DIFFERENT ANNEALING TIMES CAUSED THE BOUNDARY TO MIGRATE AT (1<2<3<4<5) LONGER ANNEALING TIMES. C, D AND E RECRYSTALLISED GRAINS.
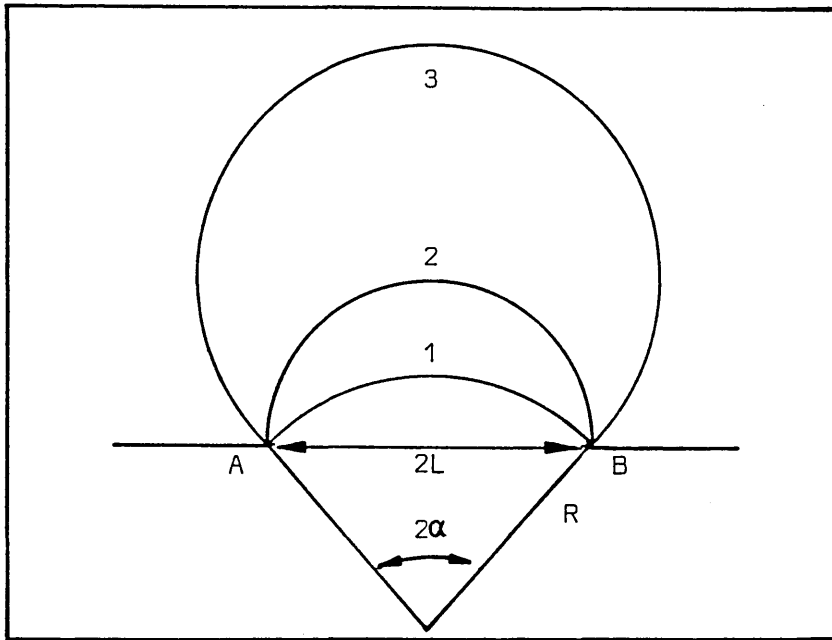
FIG. 7 SCHEMATIC REPRESENTATION OF GRAIN BOUNDARY
          BULGING.
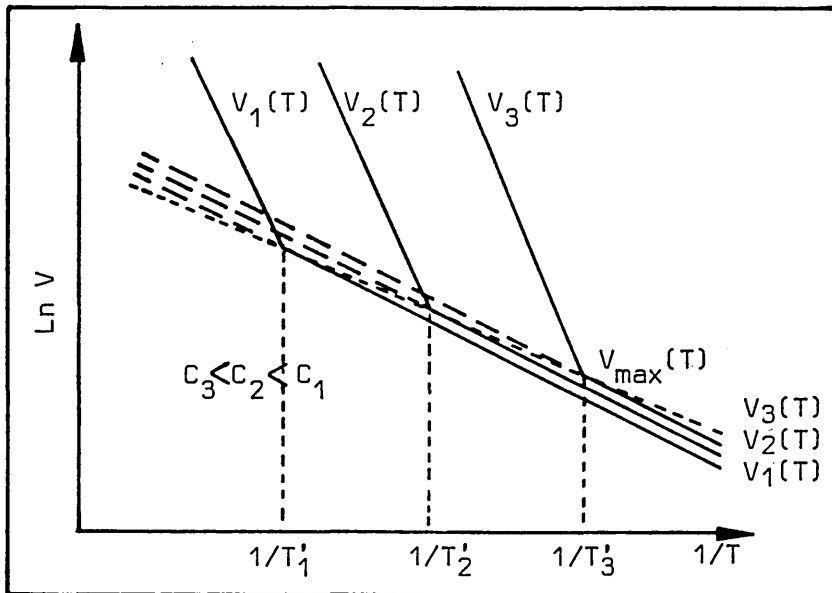
FIG. 8   SCHEMATIC REPRESENTATION OF THE TEMPERATURE
           DEPENDENCE OF THE GRAIN-BOUNDARY VELOCITY (V)
           FOR VARIOUS SOLUTE CONCENTRATIONS (C) DURING
           PRIMARY RECRYSTALLISATION.

217
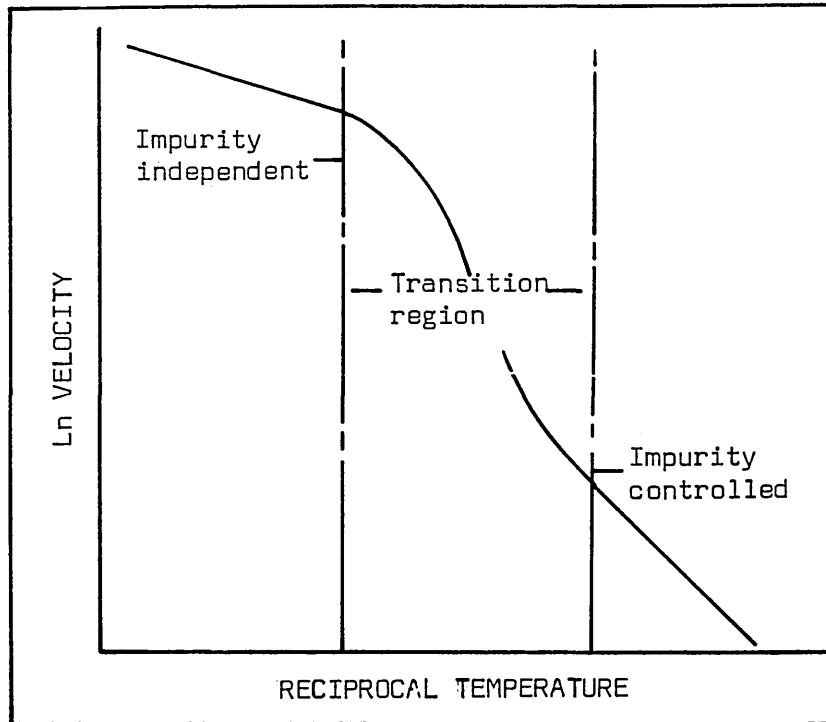
FIG. 9.   SCHEMATIC REPRESENTATION OF THE EFFECT OF THE TEMPERATURE
          ON THE GRAIN-BOUNDARY VELOCITY (V) DURING PRIMARY
          RECRYSTALLISATION.
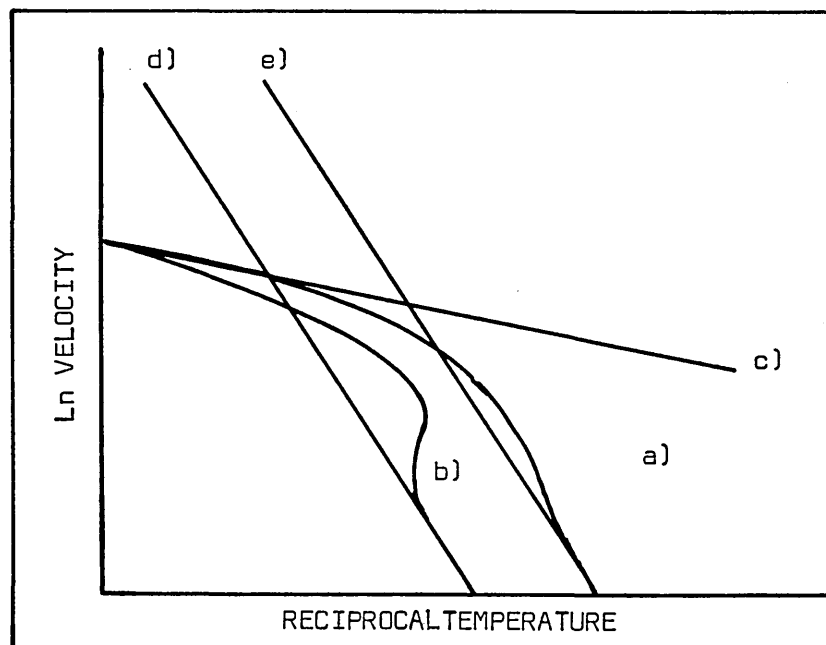
FIG. 10. SCHEMATIC REPRESENTATION OF THE GRAIN BOUNDARY VELOCITY (V)
          AS A FUNCTION OF TEMPERATURE (T) FOR TWO SOLUTE CONTENTS
          (a b), CURVE c REPRESENTS A BOUNDARY HAVING NO SOLUTE
          ATMOSPHERE. CURVES d AND e REPRESENT THE LIMITING CASES
          IN EQUATION 11.

218
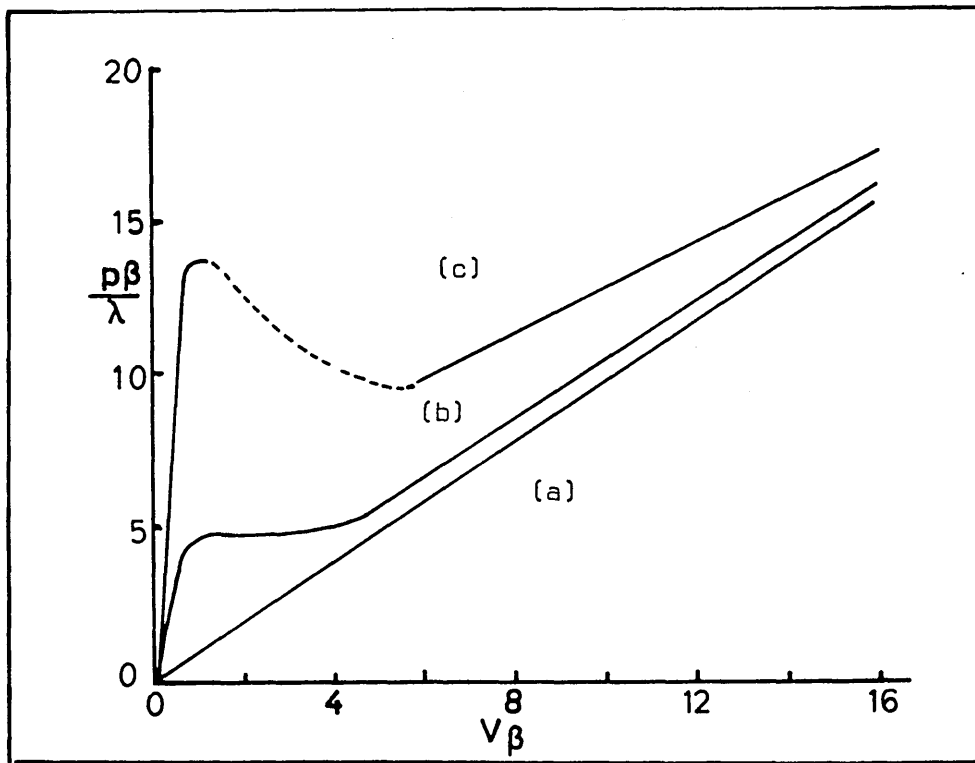
FIG. 11   THE DRIVING FORCE FOR GRAIN BOUNDARY MIGRATION AS A
          FUNCTION OF THE BOUNDARY VELOCITY. CURVE (a)
          REPRESENTS A PURE METAL. CURVES (b) AND (c) REPRESENTS
          SOLID SOLUTION ALLOYS OF INCREASING SOLUTE CONTENT.
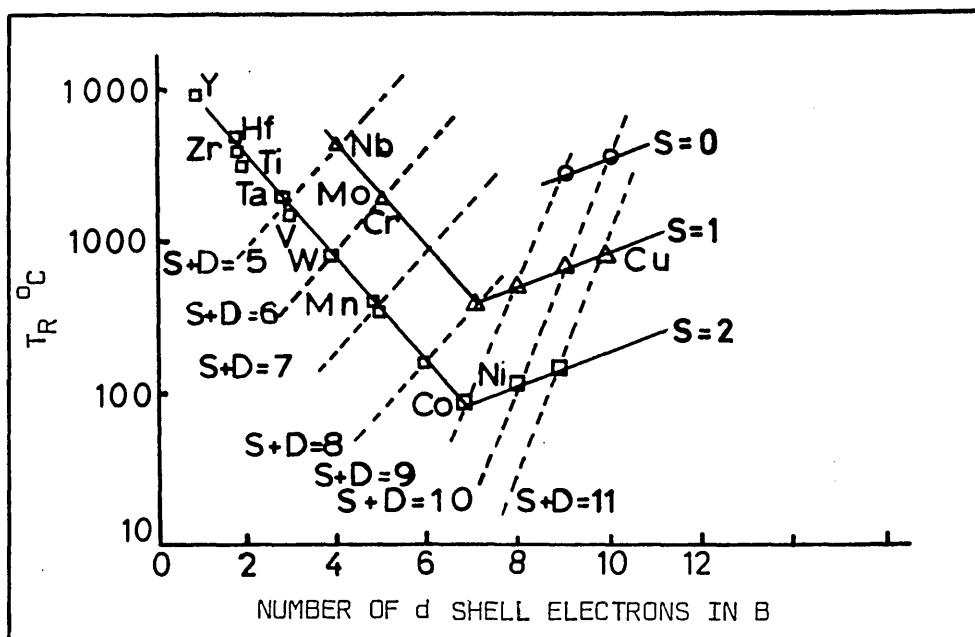
FIG. 12   RATE OF CHANGE OF RECRYSTALLISATION TEMPERATURE PER
          ATOMIC % SOLUTE ELEMENT (T_R) IN IRON AS A FUNCTION OF
          THE NUMBER OF OUTERSHELL ELECTRONS OF THE SOLUTE ELEMENT.

219
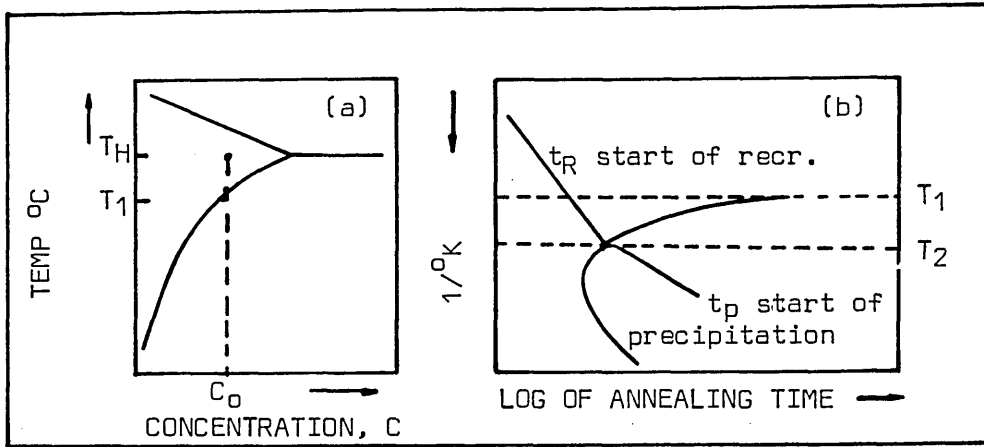
FIG. 13   OCCURRENCE OF RECRYSTALLISATION AND PRECIPITATION
a)   SCHEMATIC PHASE DIAGRAM: AN ALLOY OF CONCENTRATION
C_0 IS HOMOGENISED AT T_H QUENCHED TO T_R AND PLASTICALLY
DEFORMED IN THE SUPER SATURATED STATE.   b)   TEMPERATURE
DEPENDENCE OF THE START OF PRECIPITATION t_p AND
RECRYSTALLISATION t_R
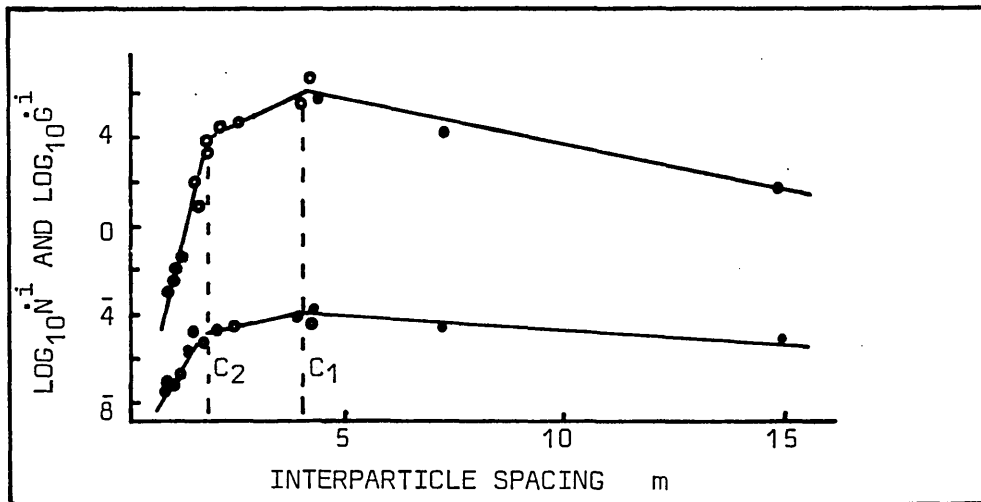
FIG. 14   APPARENT NUCLEATION $\dot{N}^i$ AND GROWTH $\dot{G}^i$ RATE AS A FUNCTION
OF INTERPARTICLE SPACING FOR Al-Cu ALLOYS (o) AND
Al-Fe ALLOYS (●) C_1 = 4 μm, C_2 = 1.8 μm.
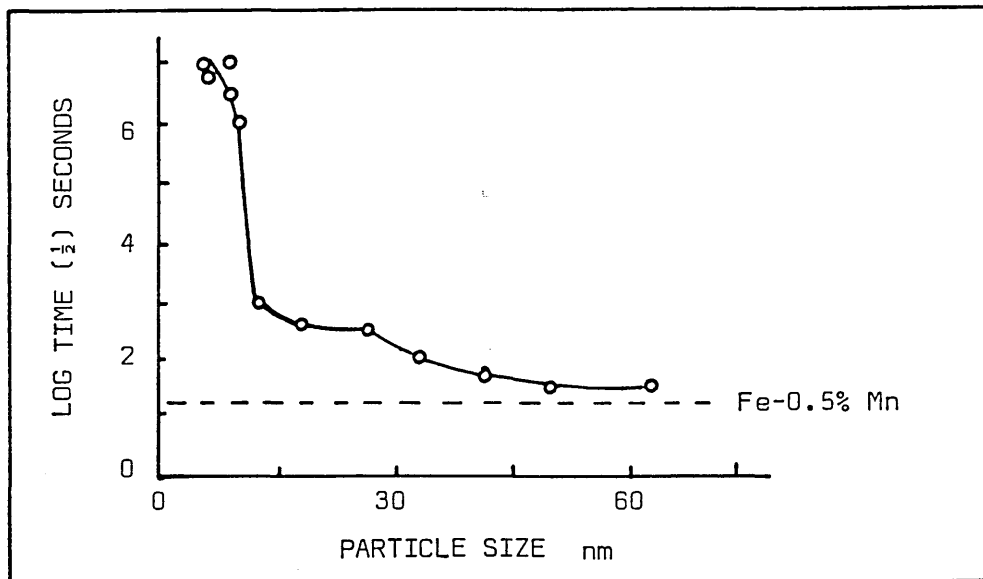
FIG. 15   THE TIME FOR 50% RECRYSTALLISATION AS A FUNCTION OF
PARTICLE SIZE.

SAMPLE	THERMAL PRETREATMENT
M300	870°C, 40 min; H$_2$O; 300°C, 1 hr; H$_2$O
M550	870°C, 40 min; H$_2$O; 550°C, 1 hr; H$_2$O
M650	870°C, 40 min; H$_2$O; 650°C, 980 hr; H$_2$O
P	870°C, 40 min; 650°C, 20 min; air
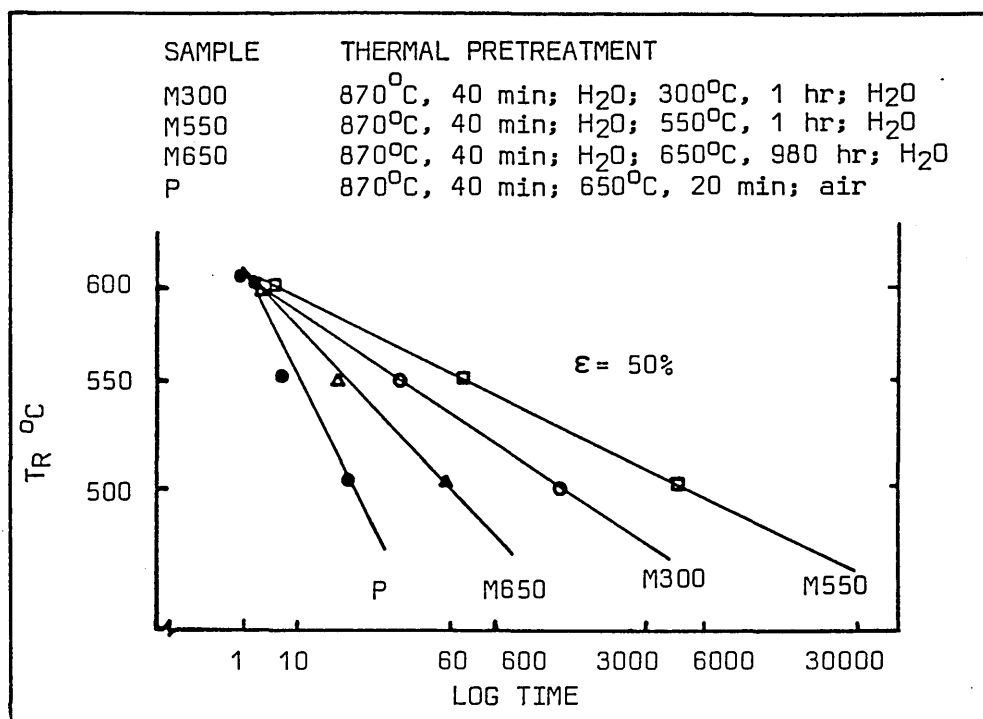
FIG. 16   TIME TO INITIATION OF RECRYSTALLISATION AS A FUNCTION
OF TEMPERATURE T$_R$ AND PRETREATMENT MT.   AMOUNT OF COLD
WORK ε = 50%
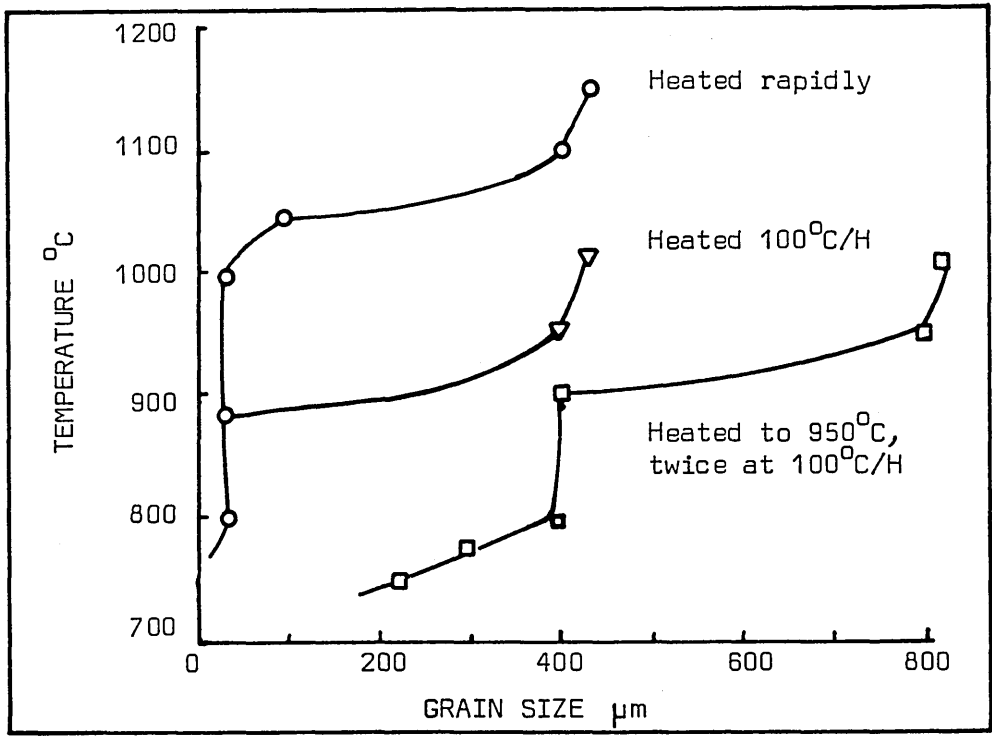
FIG. 17 GRAIN SIZE ON REHEATING C-Mn VANADIUM STEEL
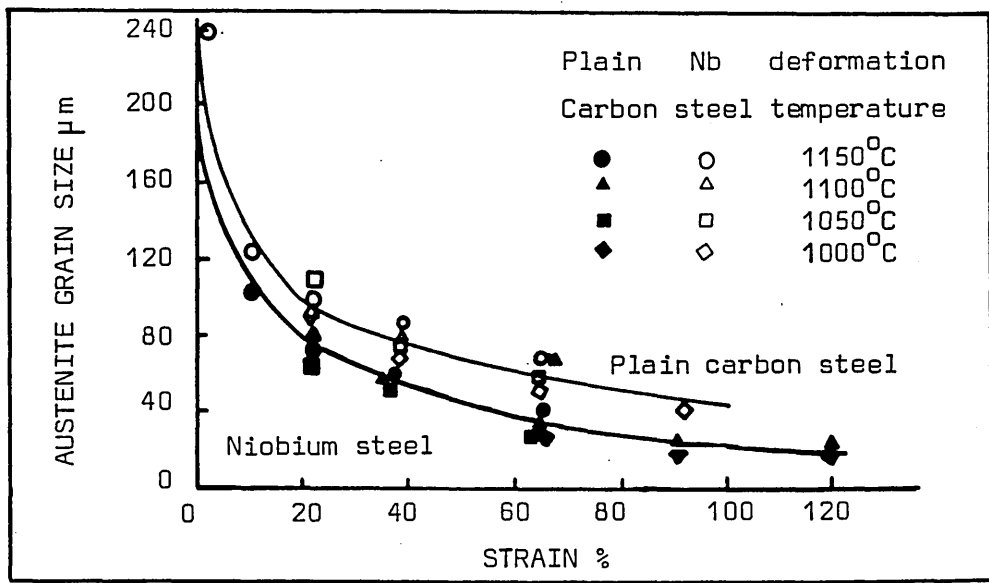
FIG. 18 INFLUENCE OF THE AMOUNT OF SINGLE-PASS DEFORMATION
AND DEFORMATION TEMPERATURE ON RECRYSTALLISED AUSTENITE
GRAIN SIZE IN PLAIN CARBON AND NIOBIUM STEELS

222
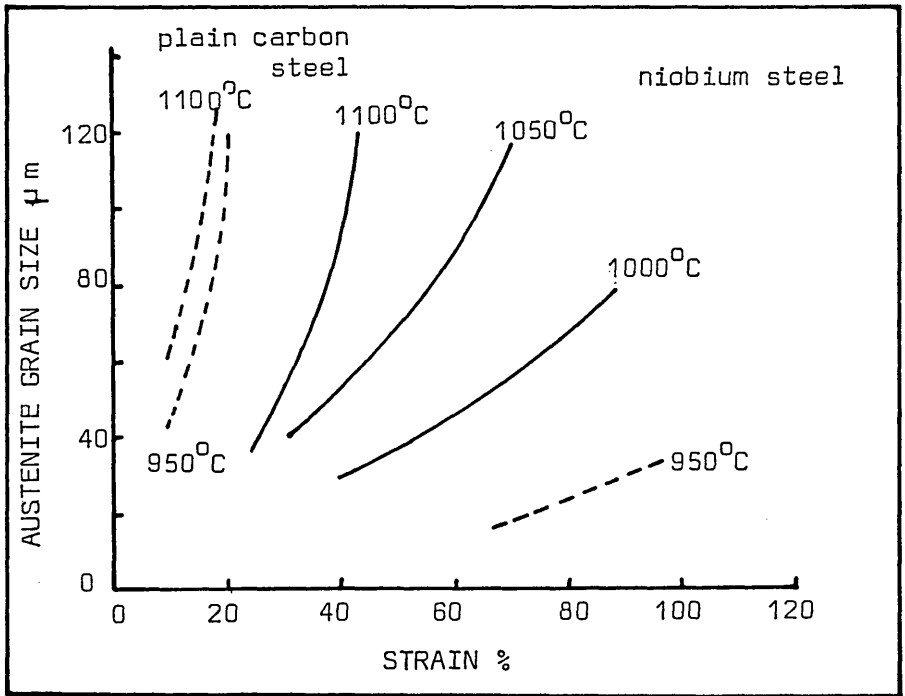
FIG. 19   EFFECT OF DEFORMATION TEMPERATURE AND INITIAL
GRAIN SIZE ON CRITICAL AMOUNT OF DEFORMATION REQUIRED
FOR COMPLETION OF RECRYSTALLISATION IN THE PLAIN
CARBON AND NIOBIUM STEELS.
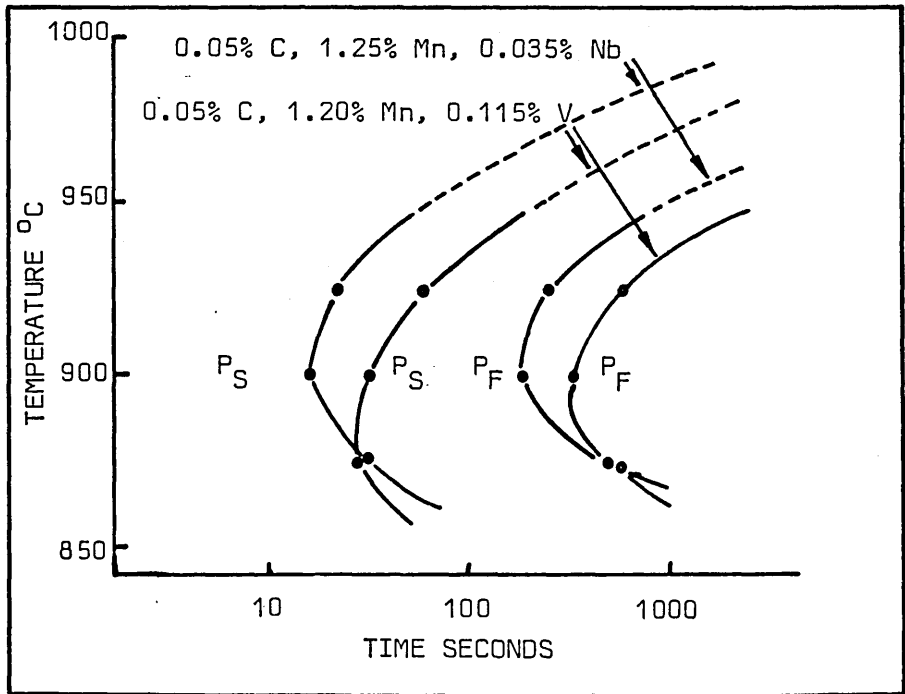
FIG. 20   DYNAMIC PRECIPITATION TIME TEMPERATURE DIAGRAM (PTT)

223
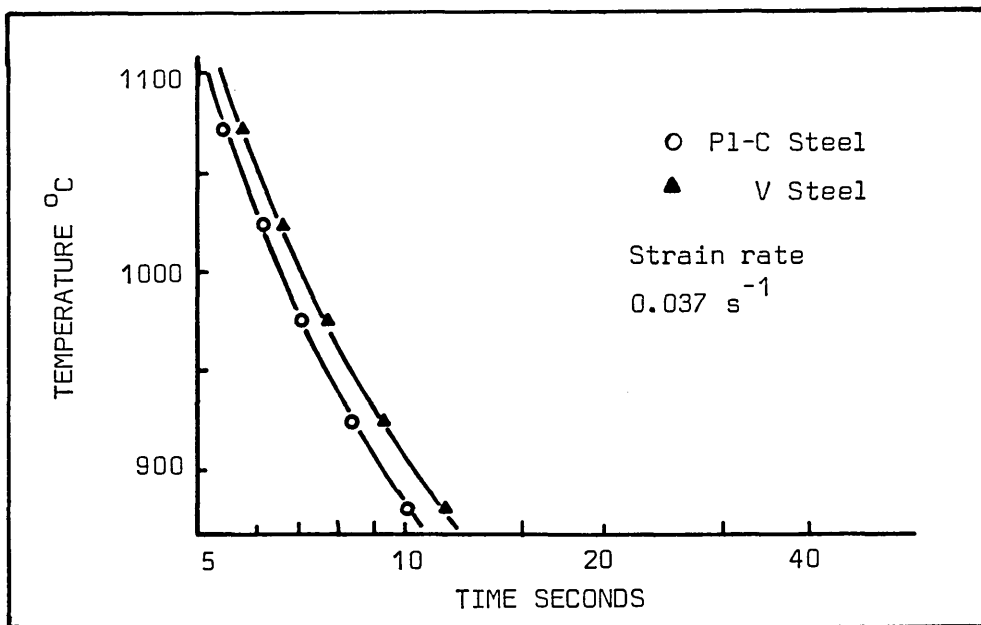
FIG. 21   DYNAMIC RECRYSTALLISATION TIME TEMPERATURE DIAGRAM (RTT)
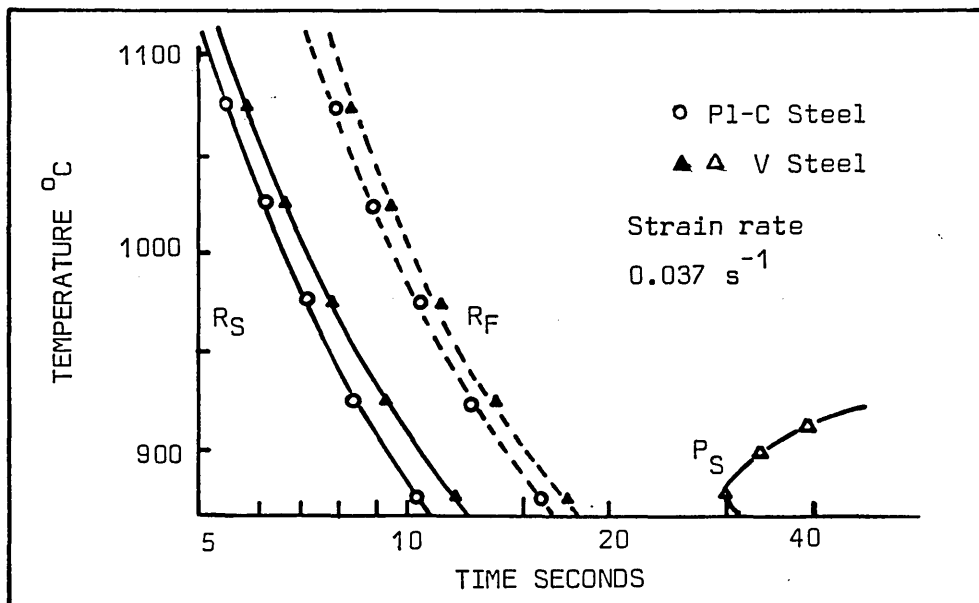
FIG. 22   DYNAMIC RECRYSTALLISATION AND DYNAMIC PRECIPITATION
           TIME TEMPERATURE DIAGRAM
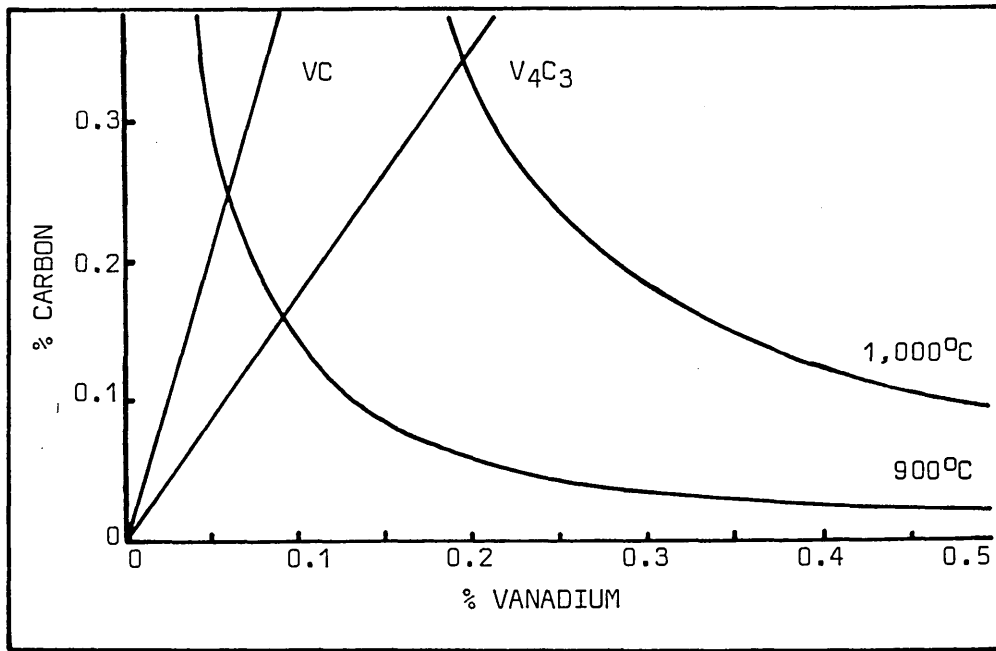
FIG. 23   SOLUBILITY OF VANADIUM CARBIDE IN AUSTENITE
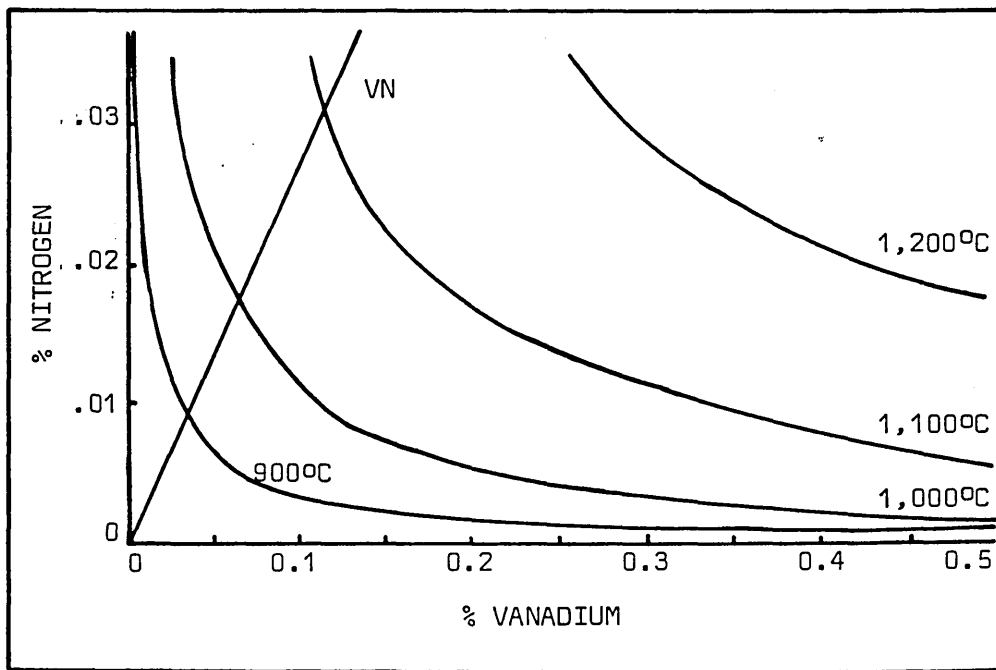
FIG. 24   SOLUBILITY OF VANADIUM NITRIDE IN AUSTENITE
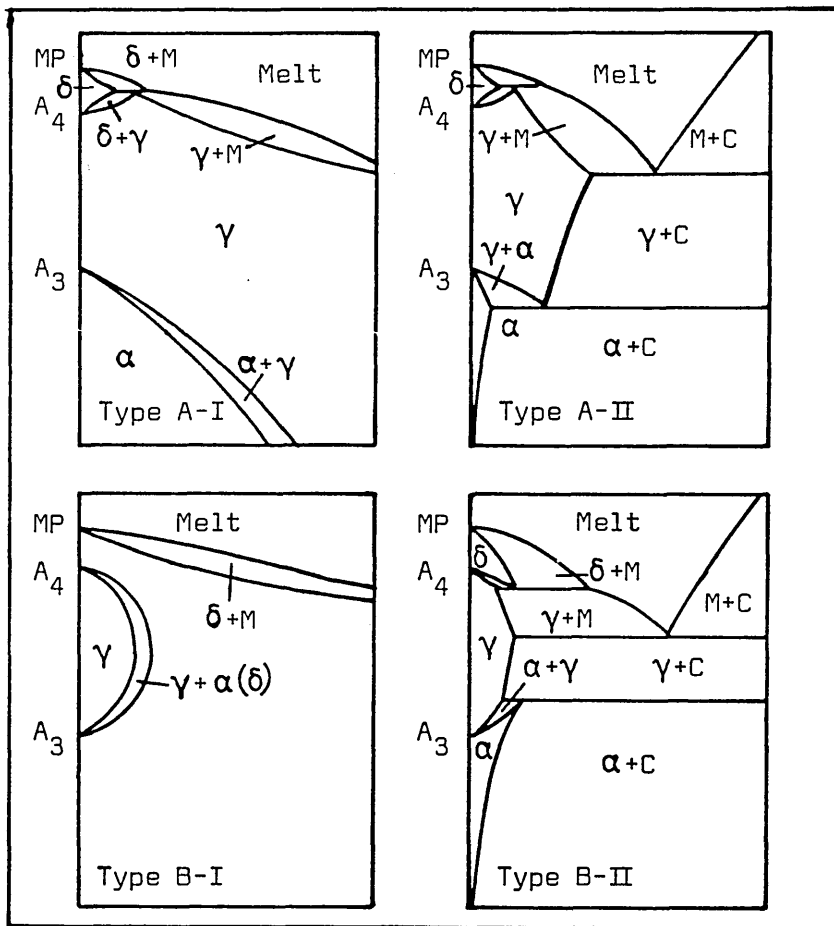
FIG. 25 TWO POSSIBLE TYPES, A AND B, AND THE SUBDIVISIONS
I AND II, OF PHASE EQUILIBRIUM DIAGRAMS FOR IRON
ALLOYS.
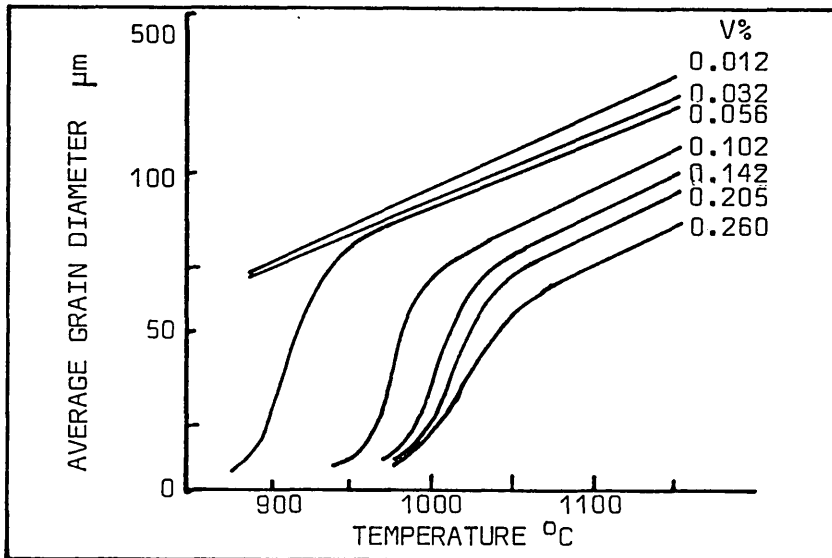
FIG. 26 AVERAGE AUSTENITIC GRAIN DIAMETER OF 0.2%C STEEL
CONTAINING VARYING AMOUNTS OF VANADIUM.

225
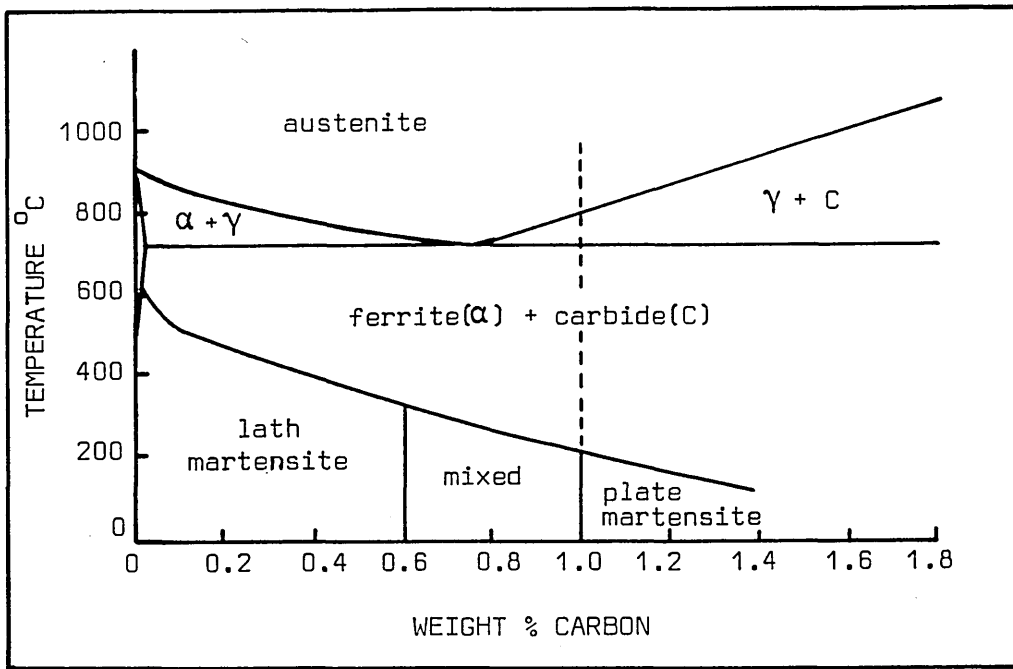
FIG. 27   RANGES OF LATH AND PLATE MARTENSITE FORMATION IN
         IRON CARBON ALLOYS
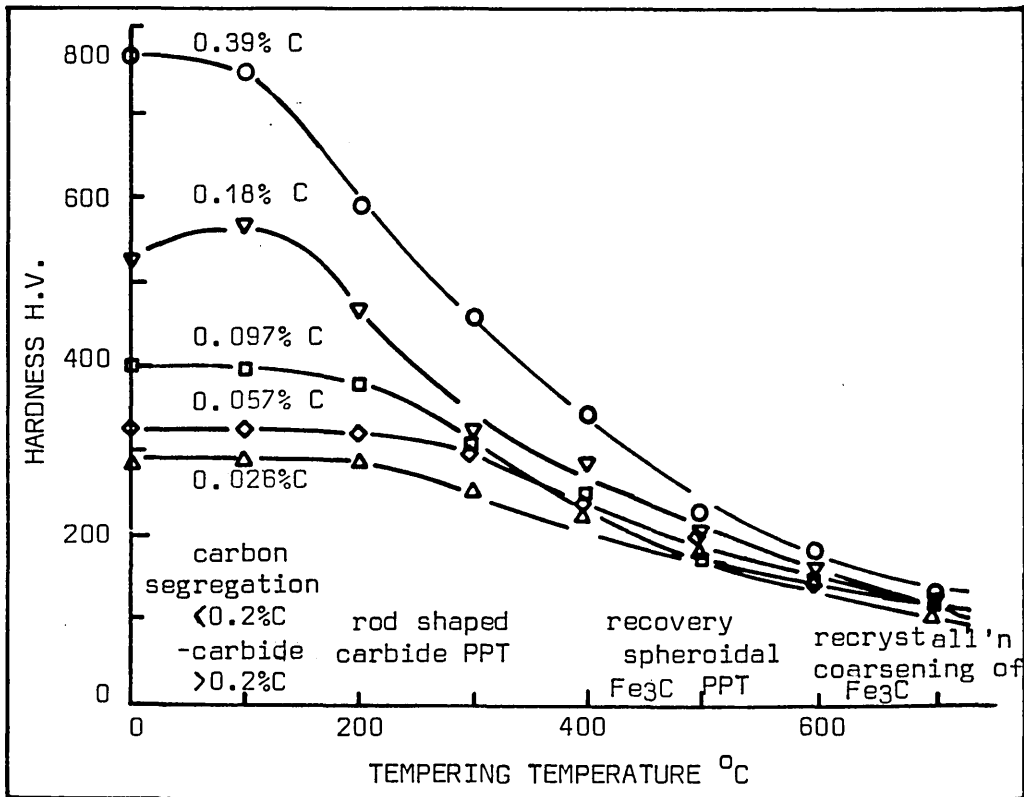
FIG. 28   HARDNESS OF IRON-CARBON MARTENSITES TEMPERED ONE
         HOUR AT 100-700°C

226
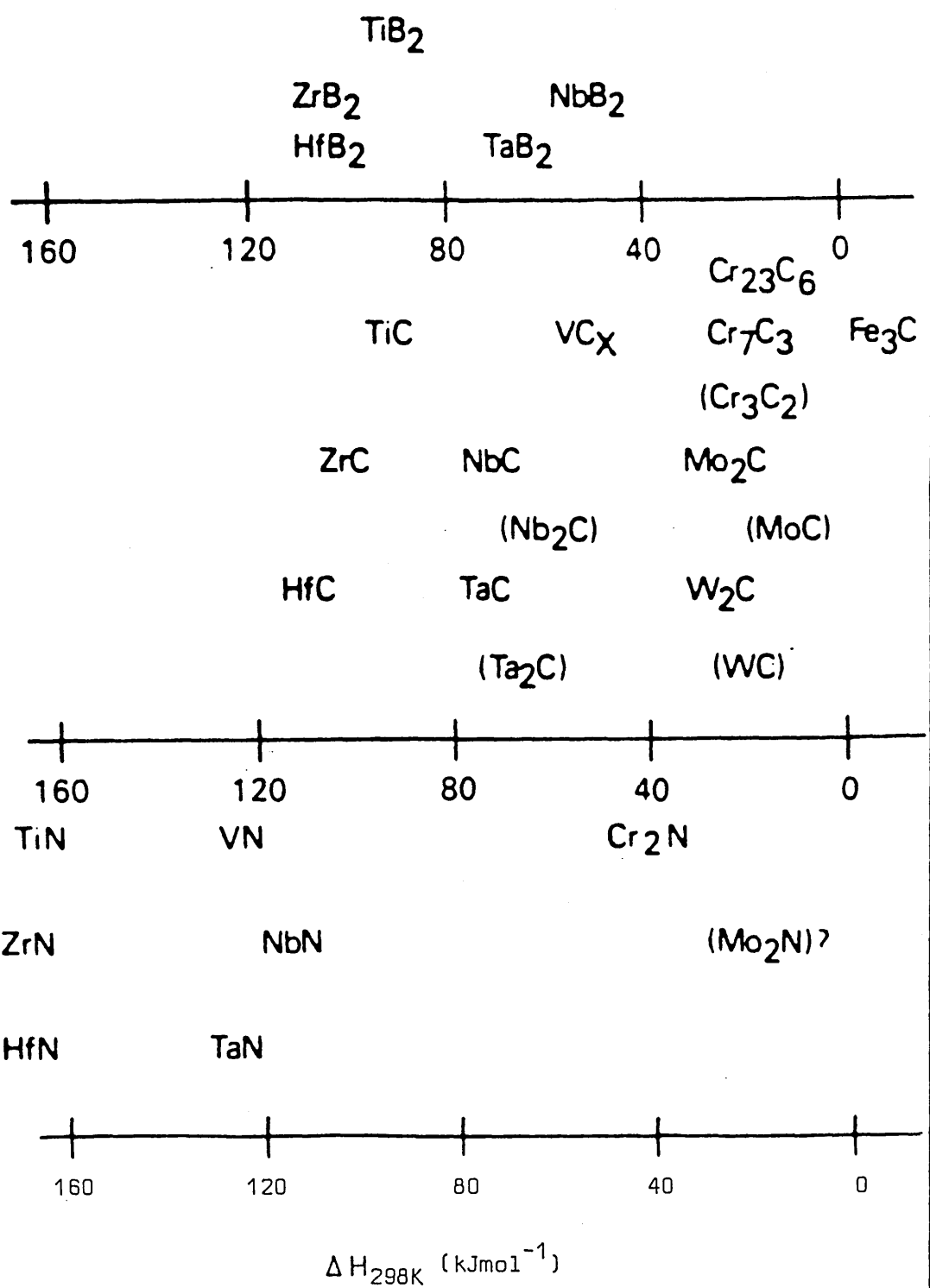
FIG. 29   ENTHALPIES OF FORMATION OF CARBIDES, NITRIDES AND BORIDES

227
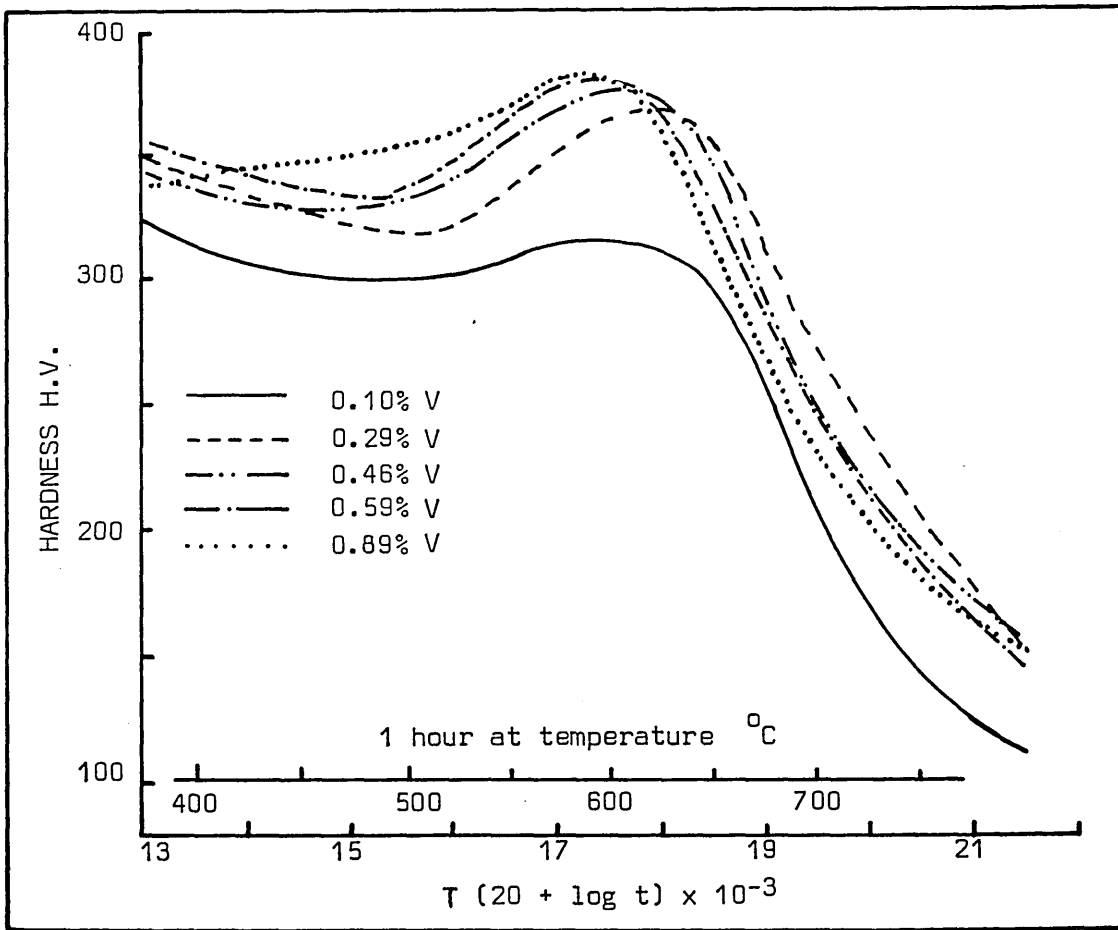
FIG. 30   THE EFFECT OF VANADIUM ON THE TEMPERING CHARACTERISTICS
OF WATER QUENCHED STEELS
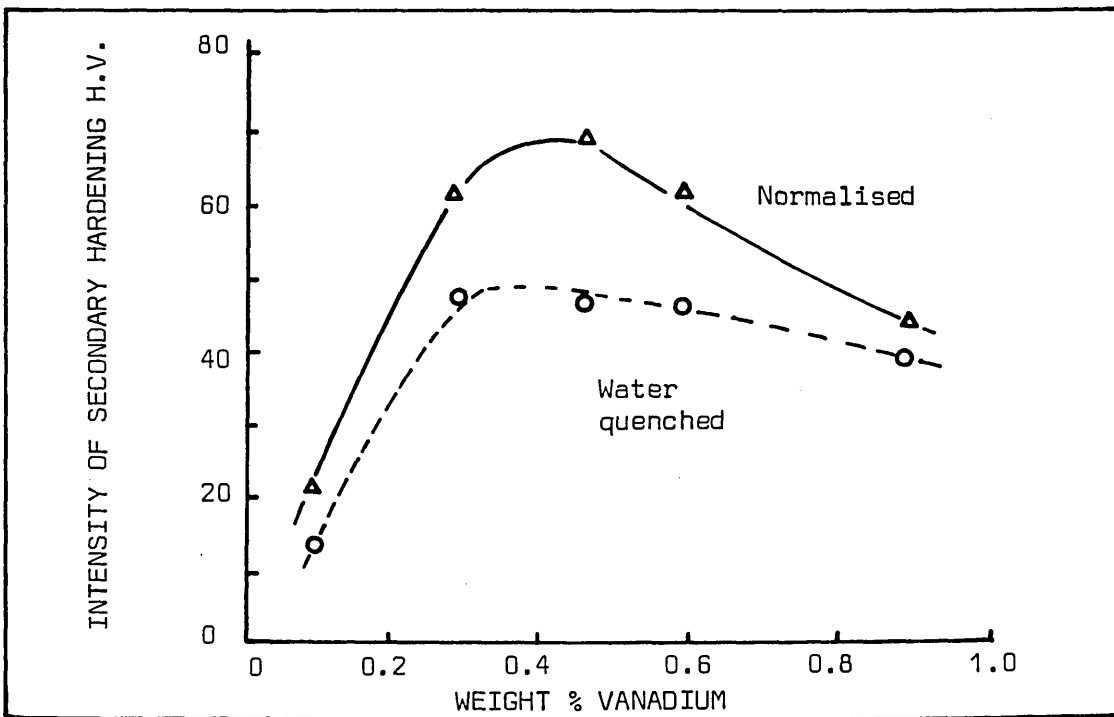
FIG.31   THE EFFECT OF VANADIUM ON THE INTENSITY OF SECONDARY
HARDENING

The specimens were coated in silica glass powder prior to homogenisation, homogenised for 30 m, removed from the furnace and cooled in still air until they reached the deformation temperature, which took between 4 and 32 s depending upon the temperatures of homogenisation and deformation. Deformation was carried out by upset forging between plattens heated at 500°C, and was immediately followed by quenching into a salt bath at 750°C.

```
AUSTENITISATION AT 1250°C -30 MINS
RECRYSTALLISED AUSTENITE -NO PRECIPITATION

   30% RED'N    50% RED'N    70% RED'N         30% RED'N    50% RED'N    70% RED'N
      AT           AT           AT                AT           AT           AT

  1200°C  1125°C  1050°C  925°C            875°C        825°C

  FULLY RECRYSTALLISED              UNRECRYSTALLISED AUSTENITE
       AUSTENITE                        VARYING ELONGATION
                                   STRAIN INDUCED PRECIPITATION
     CONDITION  'A'                  AND/OR DEFORMATION BANDS

                                     CONDITION 'C''D' & 'E'

  COOL TO 925°C                     QUENCHED TO 750°C
  HOLD TO PRODUCE                      ISOTHERMAL
   PRECIPITATION                     TRANSFORMATION
     OF V(CN)                           STUDIES

  CONDITION 'B'

                          30% RED'N          70% RED'N
                          AT 1200°C          AT 1050°C
  GRAIN COARSENING
      STUDIES                                          Schedules only used
                                                       in preliminary work
                          COOL TO 925°C                to establish
                            FURTHER                    temperature at which
                                                       recrystallisation did
  QUENCHED TO 750°C                                    not occur.
     ISOTHERMAL
   TRANSFORMATION    30% RED'N   50% RED'N   70% RED'N
      STUDIES

  UNRECRYSTALLISED AUSTENITE        EXTRA REDUCTION IN SECOND
  GRAINS VARYING ELONGATION            PASS UNRECRYSTALLISED
  STRAIN INDUCED PRECIPITATION           STRAIN INDUCED
                                       PRECIPITATION AND
     CONDITION 'C'                      DEFORMATION BANDS

                                         CONDITION 'D'
```

FIG. 32   SCHEMATIC DIAGRAM FOR THE PRODUCTION OF VARYING AUSTENITE
          STRUCTURES BY THERMO-MECHANICAL TREATMENT
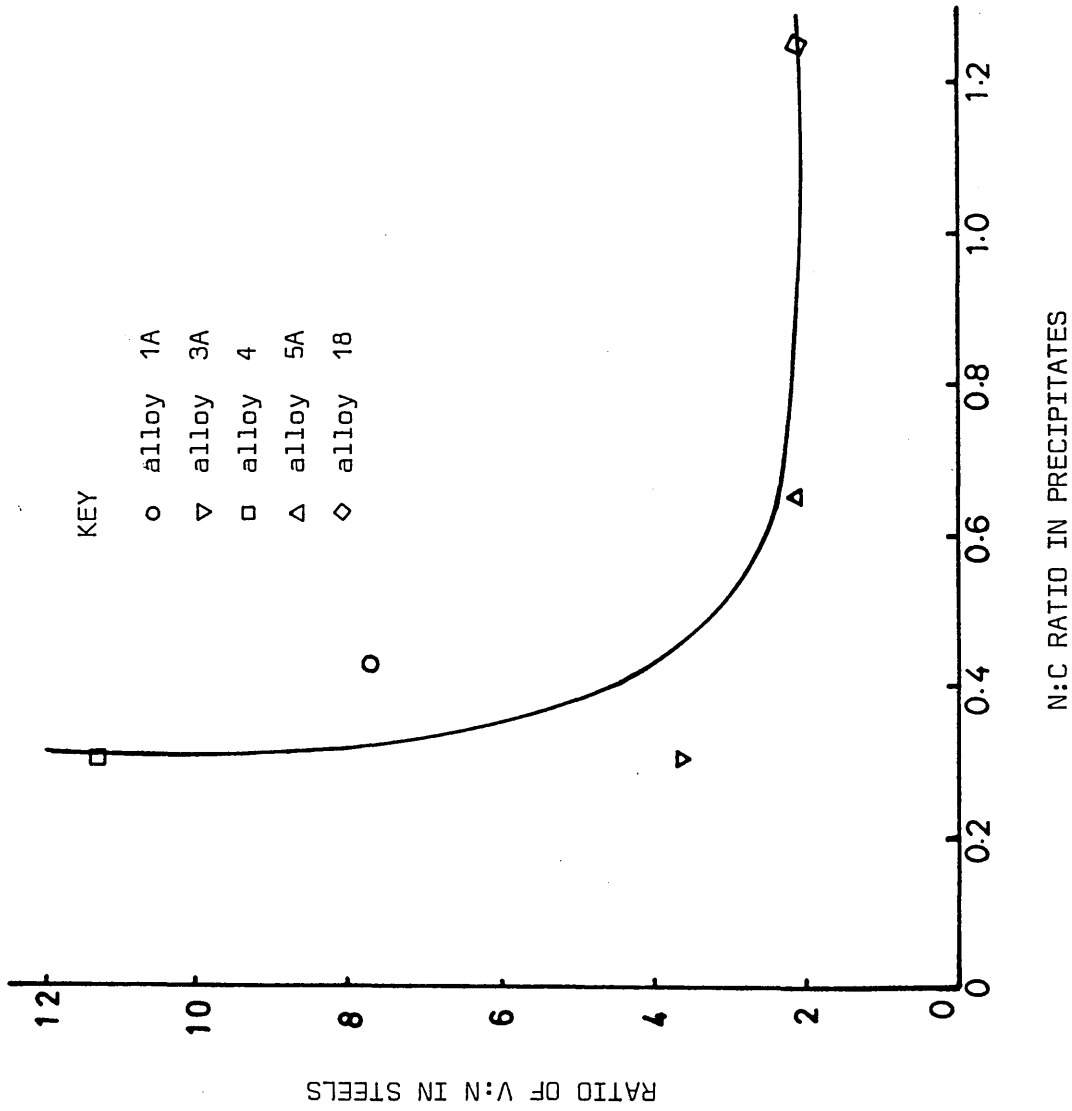
FIG. 33   RELATIONSHIP BETWEEN N:C RATIO IN PRECIPITATES AND V:N
RATIO IN STEEL AFTER AUSTENITISING AT 900°C
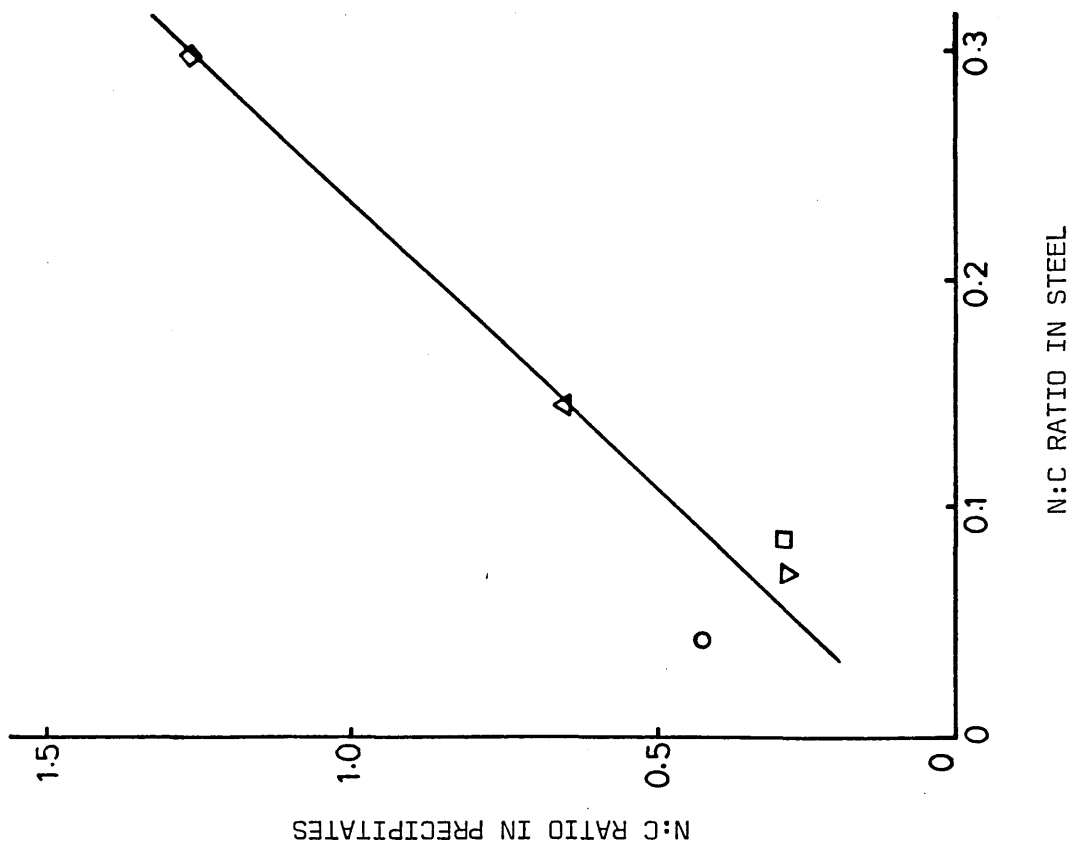
FIG. 34   RELATIONSHIP BETWEEN N:C RATIO IN STEEL AND
N:C RATIO IN PRECIPITATES AFTER
AUSTENITISING AT 900°C
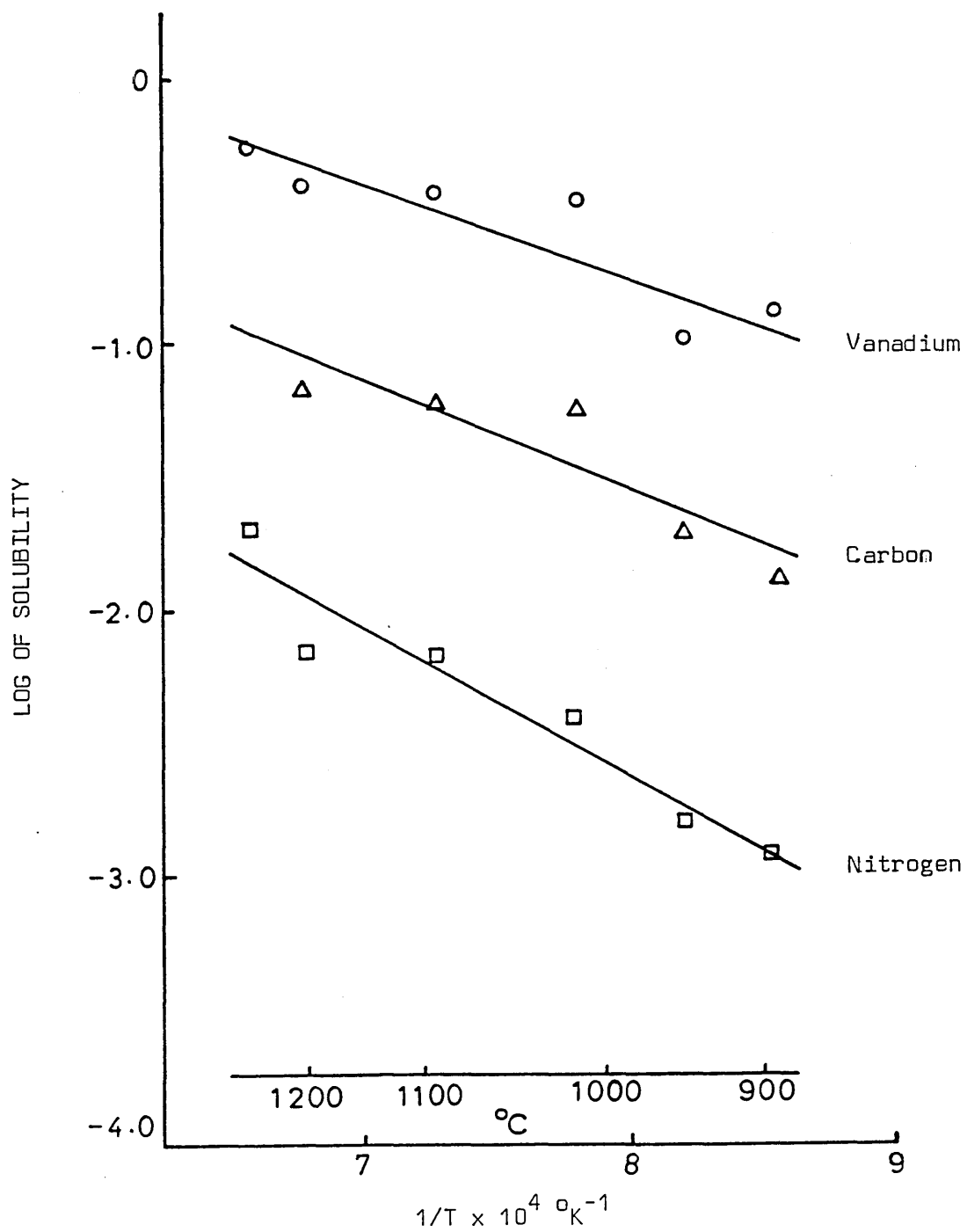
FIG. 35   EFFECT OF SOLUTION TREATMENT TEMPERATURE ON THE SOLUBILITY
OF VANADIUM, CARBON AND NITROGEN IN 0.126%C 1.77%Mn
0.415%V 0.020%N STEEL
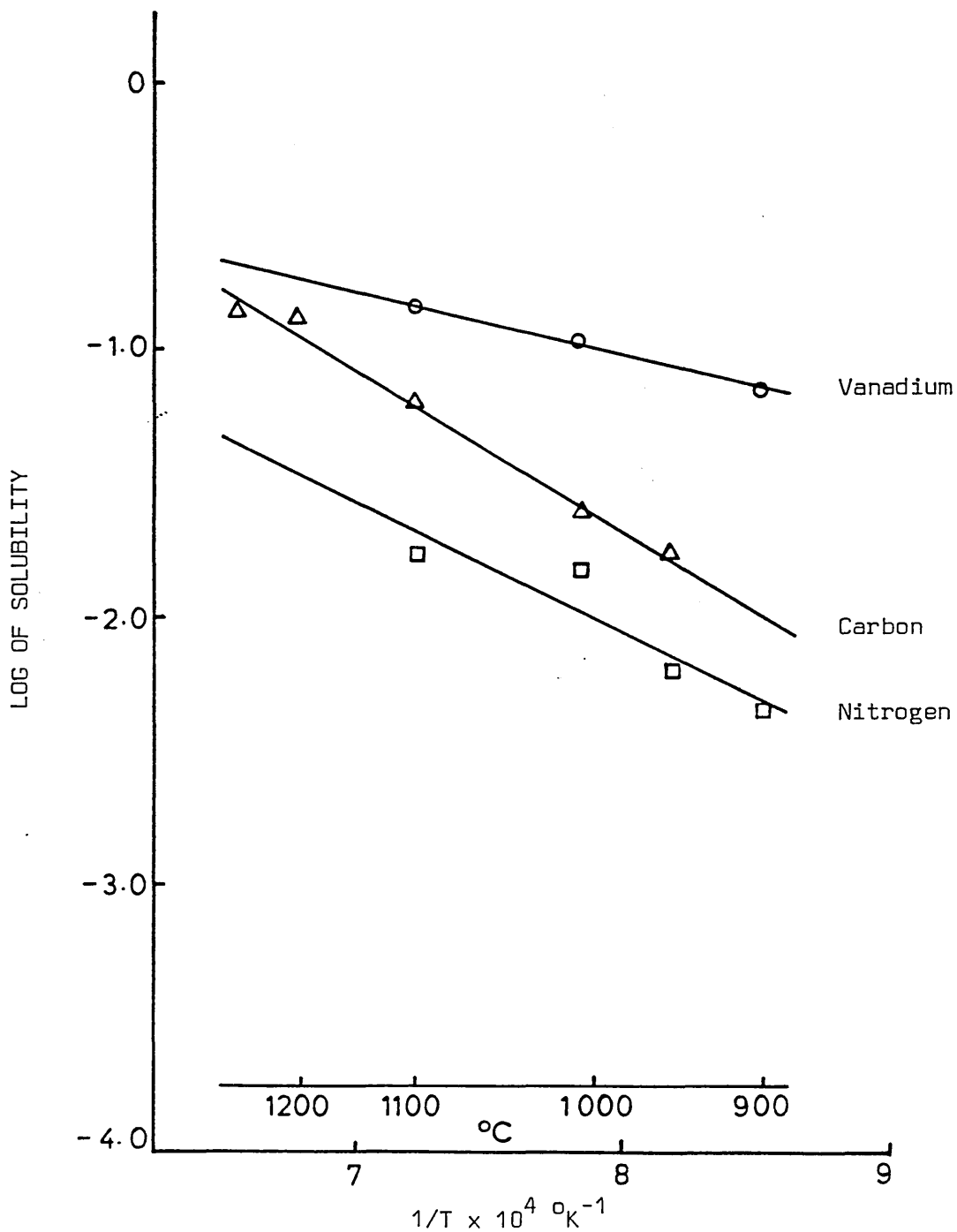
FIG. 36 EFFECT OF SOLUTION TREATMENT TEMPERATURE ON THE
SOLUBILITY OF VANADIUM, CARBON AND NITROGEN IN
0.212%C 1.83%Mn 0.14%V 0.018%N STEEL
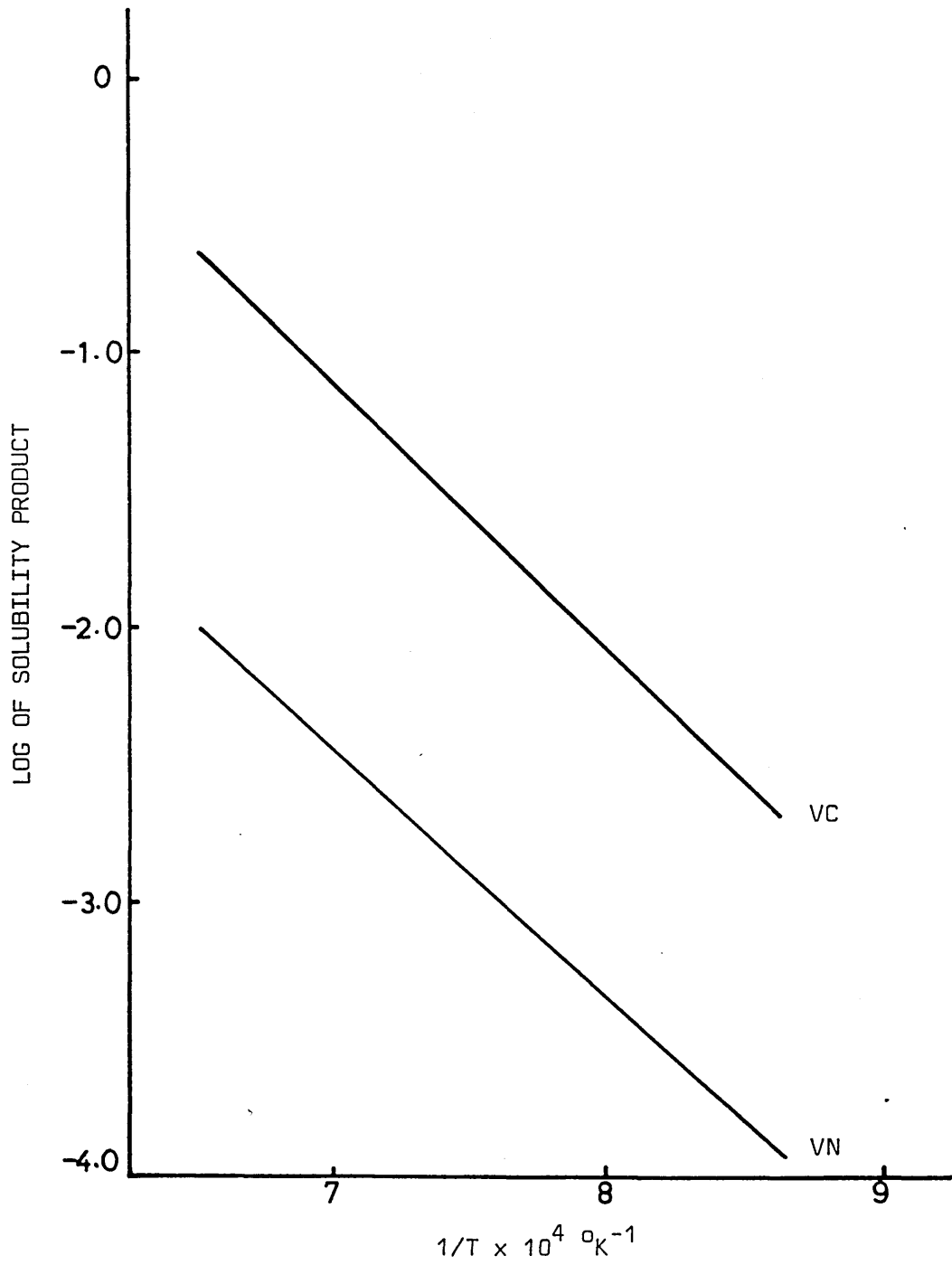
FIG. 37 SOLUBILITY PRODUCT - TEMPERATURE RELATIONSHIP OF
VANADIUM CARBIDE AND VANADIUM NITRIDE IN 0.12%C,
1.77%Mn, 0.15%V, 0.020%N STEEL
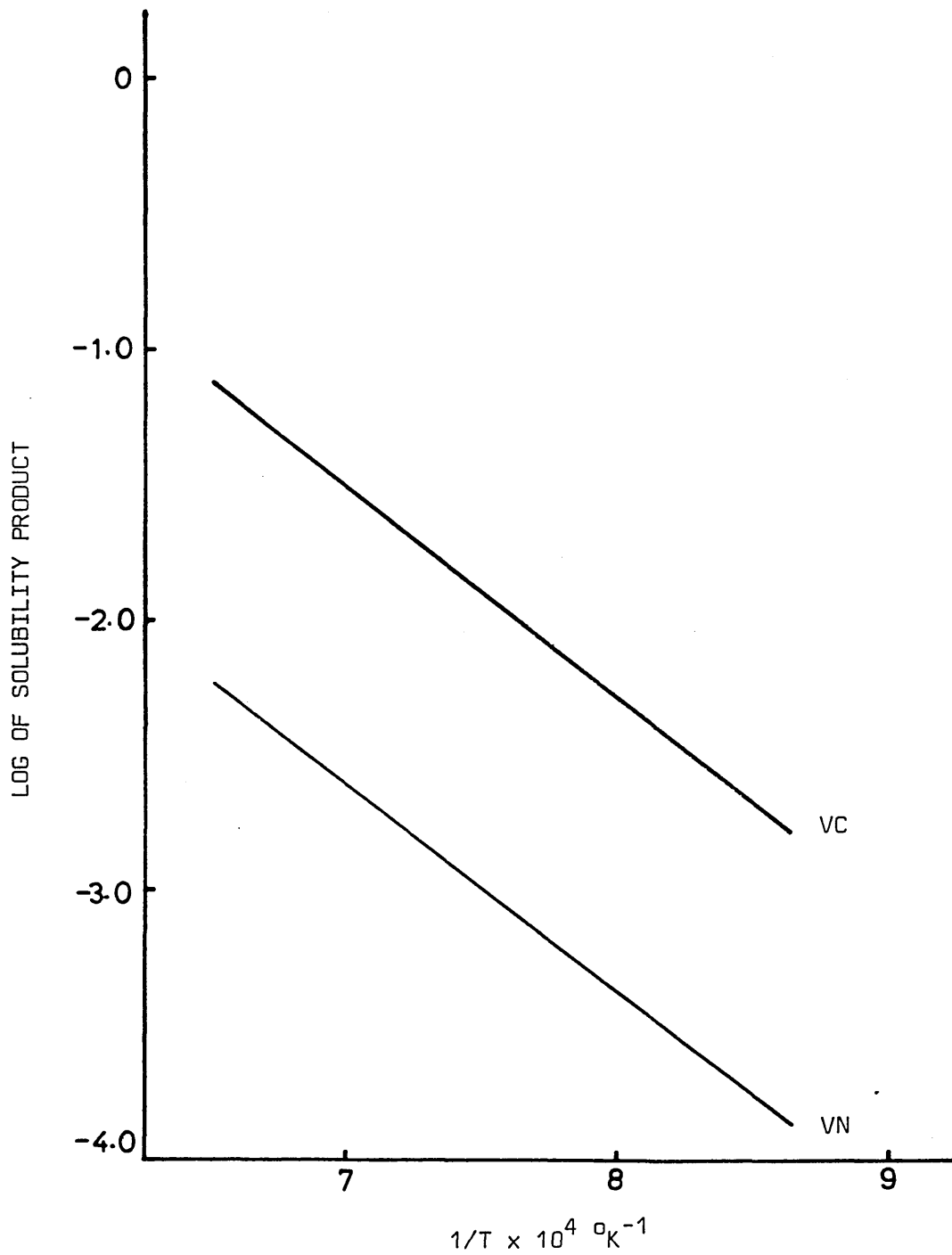
FIG. 38   SOLUBILITY PRODUCT - TEMPERATURE RELATIONSHIP OF
VANADIUM-CARBIDE AND VANADIUM NITRIDE IN 0.126%C,
1.77%Mn, 0.415%V, 0.020%N STEEL

234
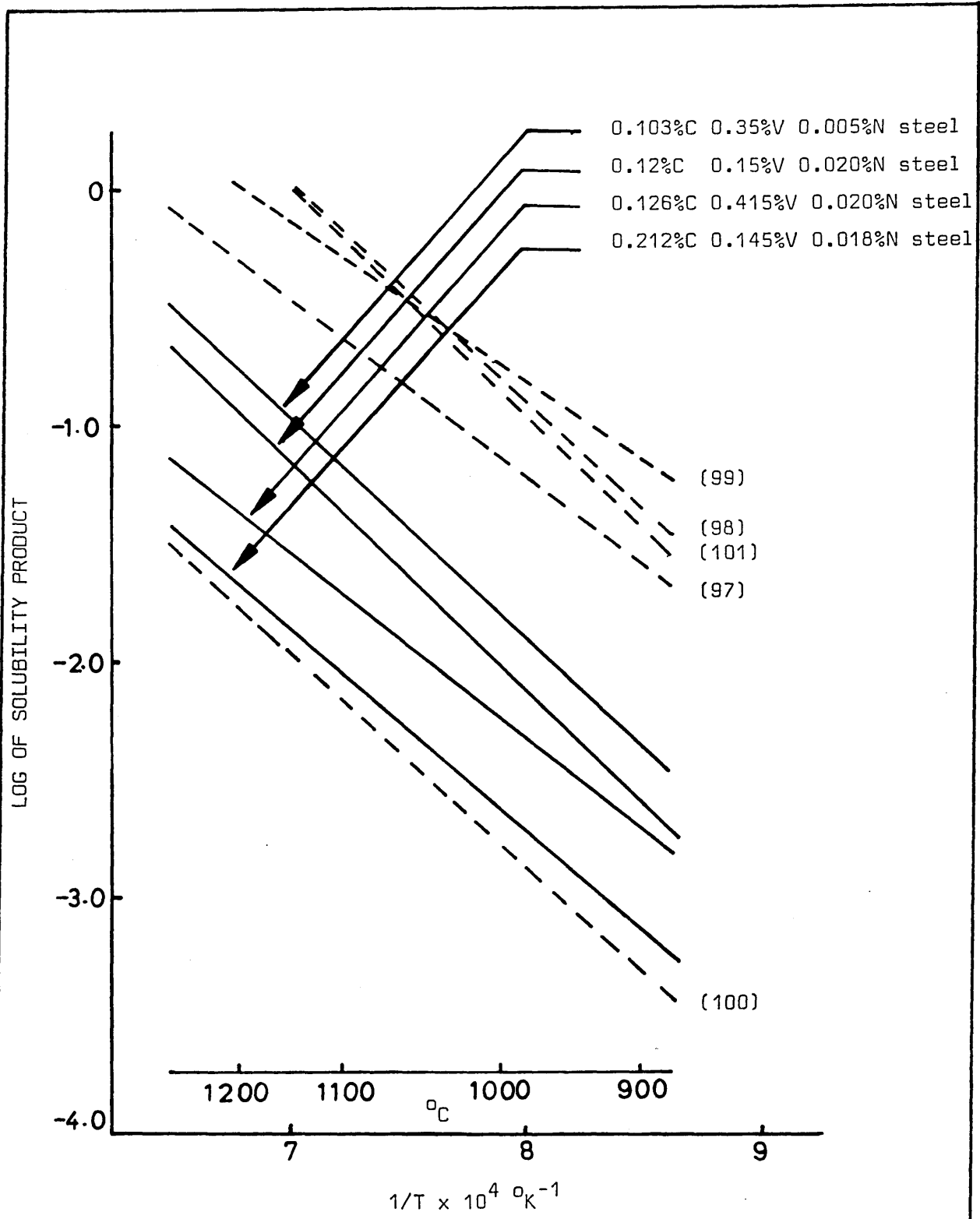
FIG. 39   SOLUBILITY OF VANADIUM CARBIDE IN AUSTENITE

235
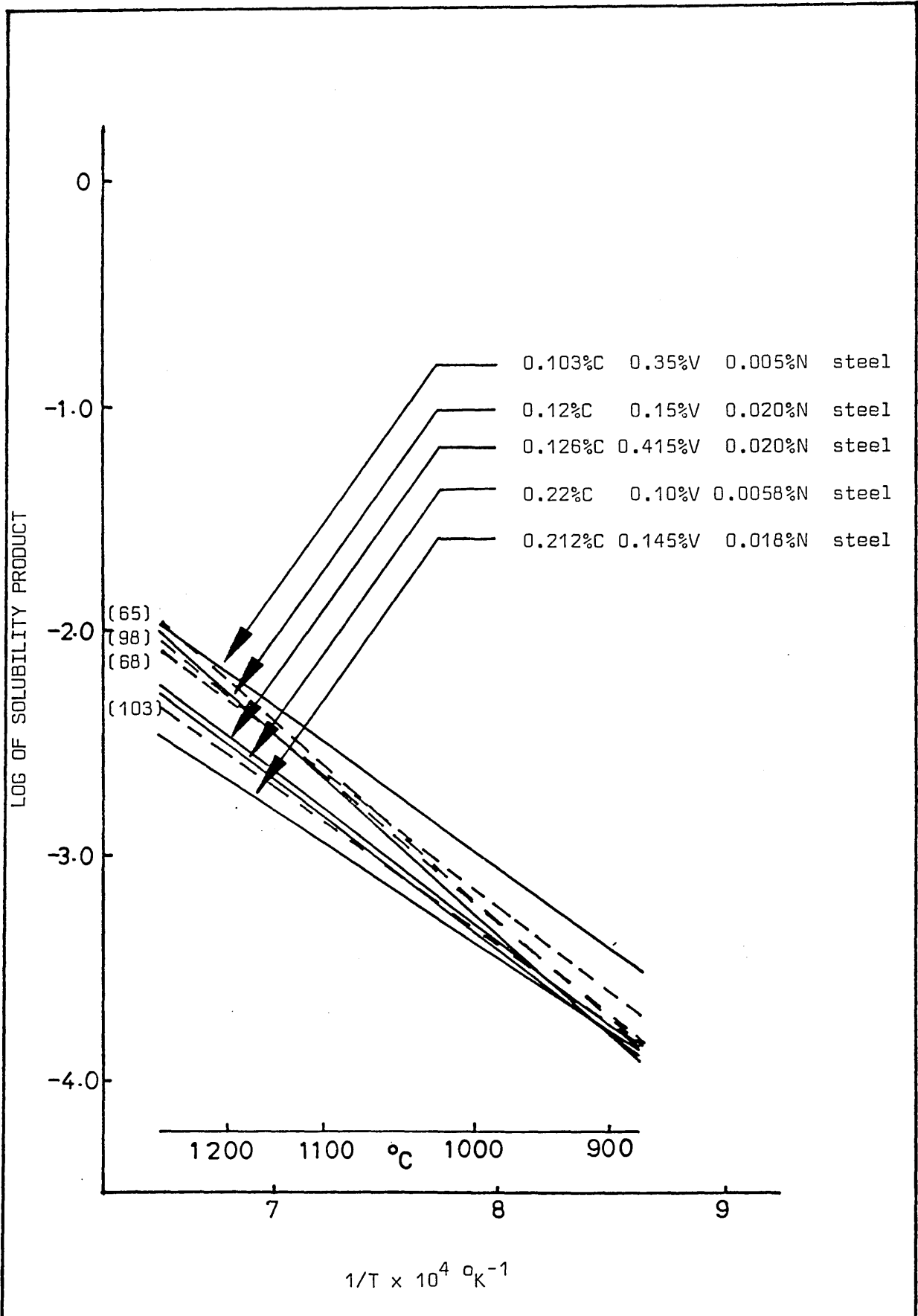
FIG. 40 SOLUBILITY OF VANADIUM NITRIDE IN AUSTENITE

236

FIG. 41   SOLUBILITY OF (V)(C + $\frac{12}{14}$ N) IN AUSTENITE

The figure plots LOG OF SOLUBILITY PRODUCT (V)(C + $\frac{12}{14}$ C) versus $1/T \times 10^4 \; {}^{\circ}K^{-1}$, with a temperature scale in ${}^{\circ}C$ (1200, 1100, 1000, 900) and the $1/T$ axis marked at 7, 8, 9.

Legend:
0.103%C 0.35%V   0.005%N steel
0.126%C 0.415%V 0.021%N steel
0.212%C 0.145%V 0.018%N steel
0.12%C   0.15%V   0.020%N steel
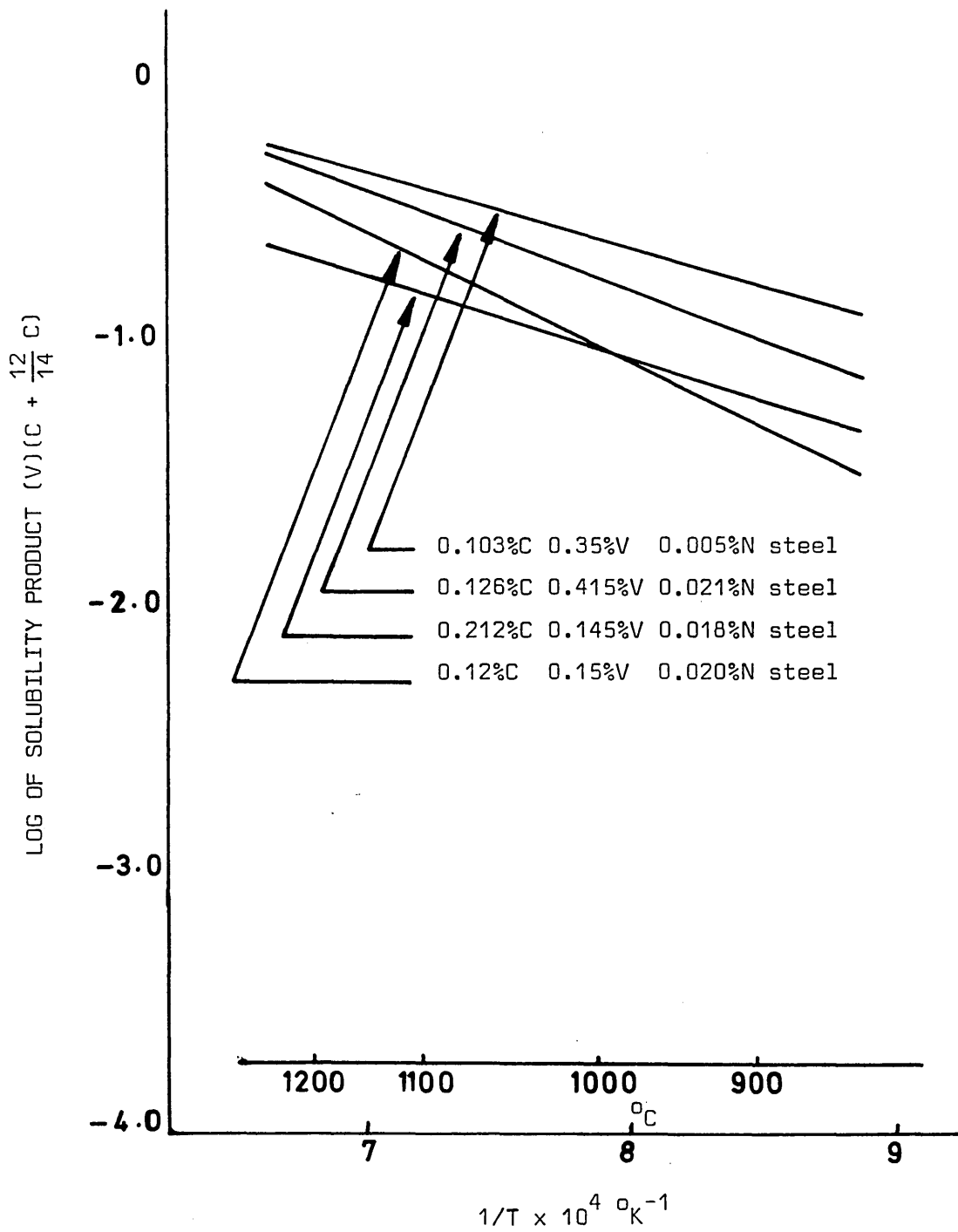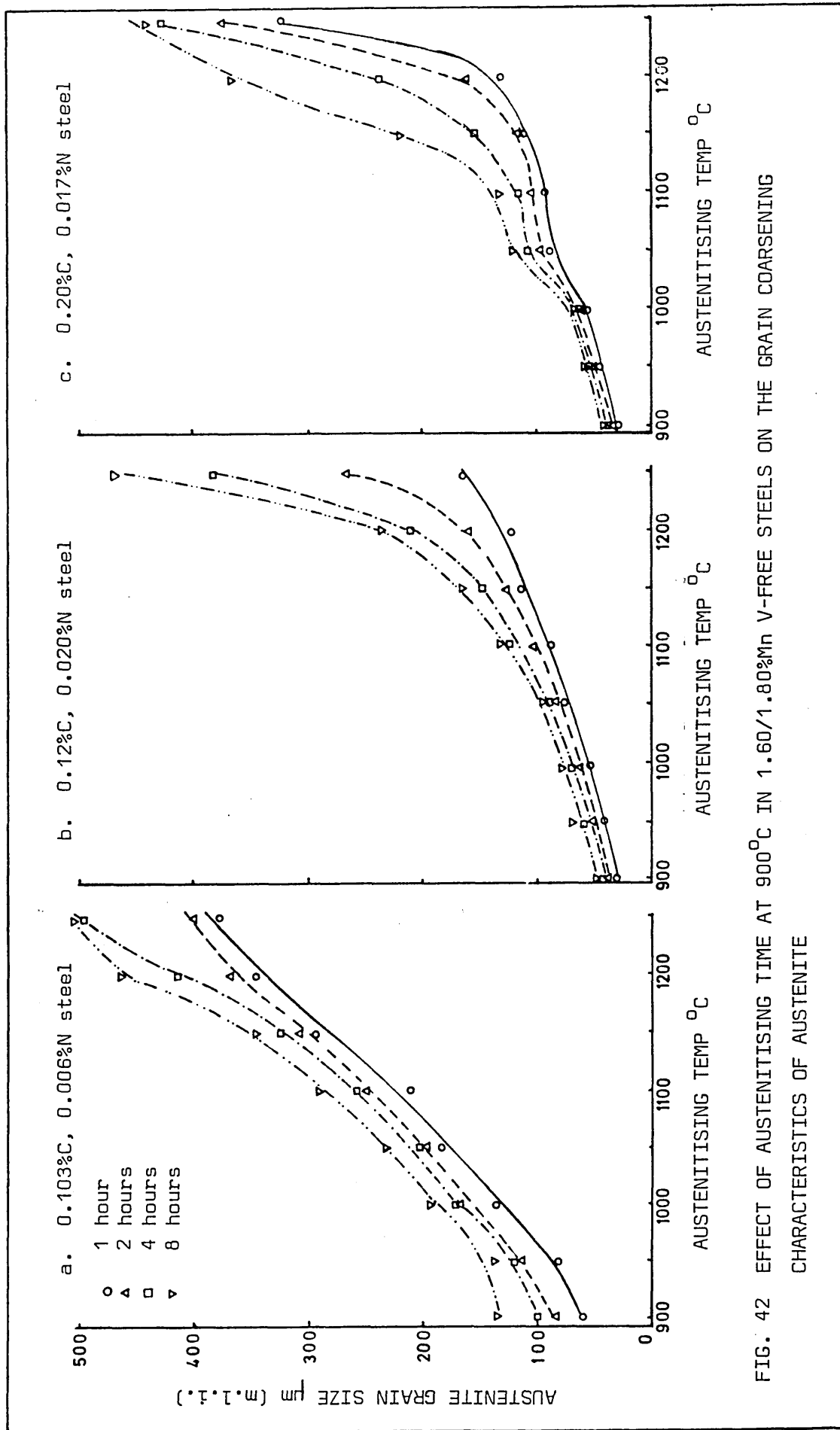
FIG. 42 EFFECT OF AUSTENITISING TIME AT 900°C IN 1.60/1.80%Mn V-FREE STEELS ON THE GRAIN COARSENING CHARACTERISTICS OF AUSTENITE

238

a. 0.005% Nitrogen steel

b. 0.021% Nitrogen steel

KEY

1 hour	○	○
2 hour	△	△
4 hour	□	□
8 hours	▷	▷

AUSTENITISING TEMPERATURE °C

AUSTENITE GRAIN SIZE μm (m.l.i.)
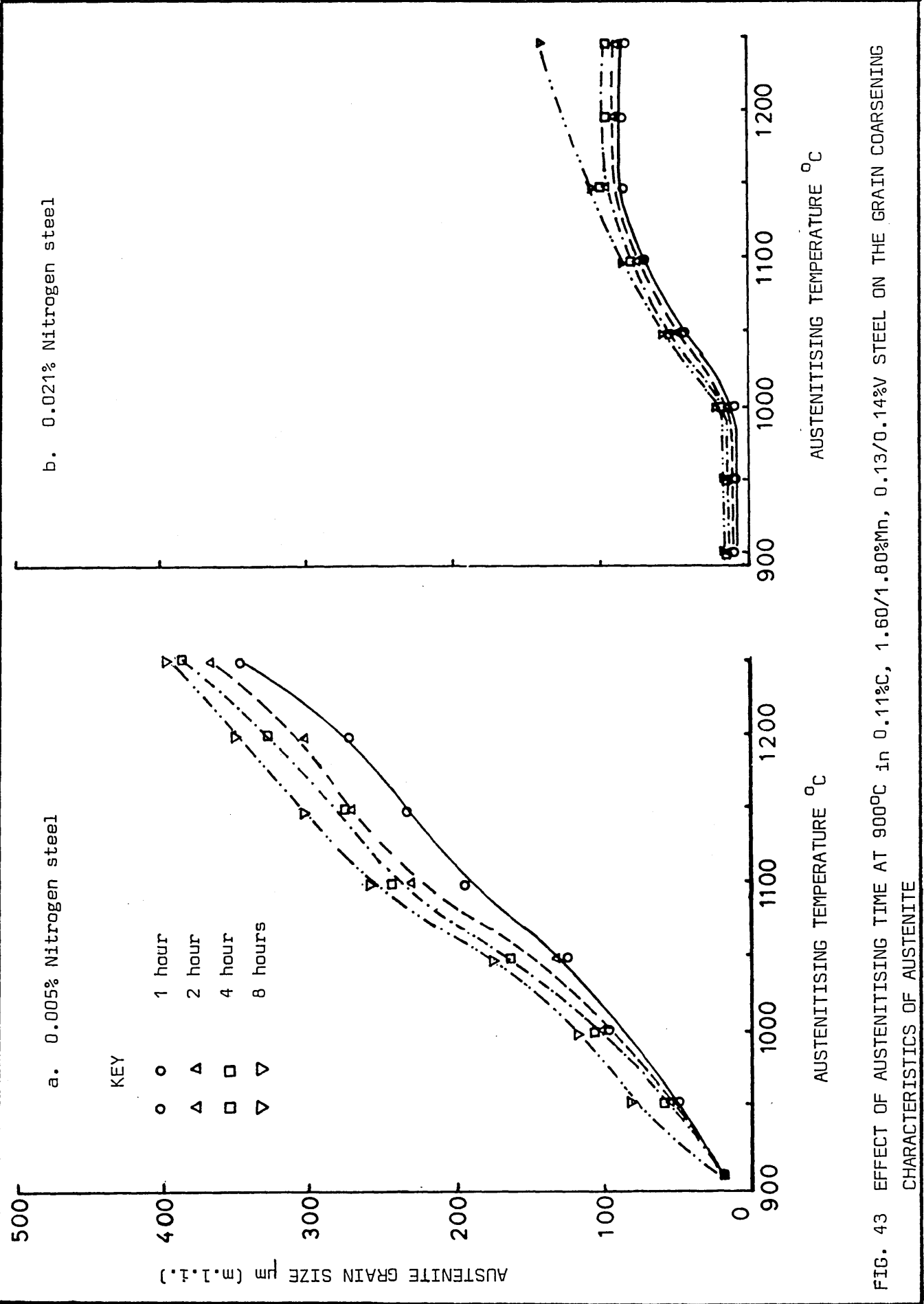
FIG. 43 EFFECT OF AUSTENITISING TIME AT 900°C in 0.11%C, 1.60/1.80%Mn, 0.13/0.14%V STEEL ON THE GRAIN COARSENING CHARACTERISTICS OF AUSTENITE
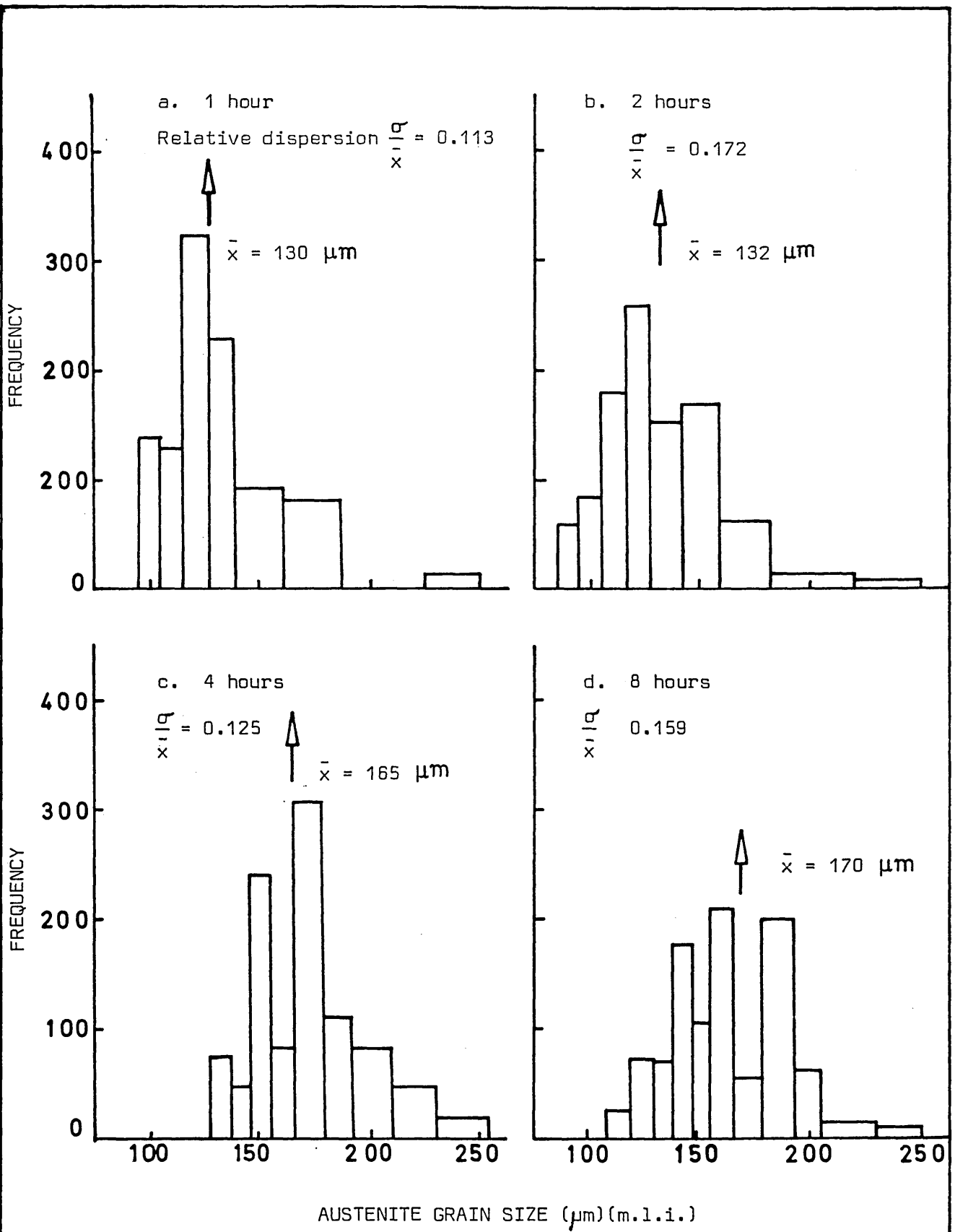
FIG. 44   AUSTENITE GRAIN GROWTH AFTER AUSTENISITISING AT 1050°C UP TO

8 HOURS IN 0.113%C, 0.14%V, 0.005%N STEEL

a. 0.005% Nitrogen steel

	V-free steel
O	0.13/0.19%V steel
▽	
□	0.35/0.41%V steel

b. 0.010% Nitrogen steel

c. 0.020% Nitrogen steel

AUSTENITISING TEMP °C

AUSTENITE GRAIN SIZE μm (m.l.i.)
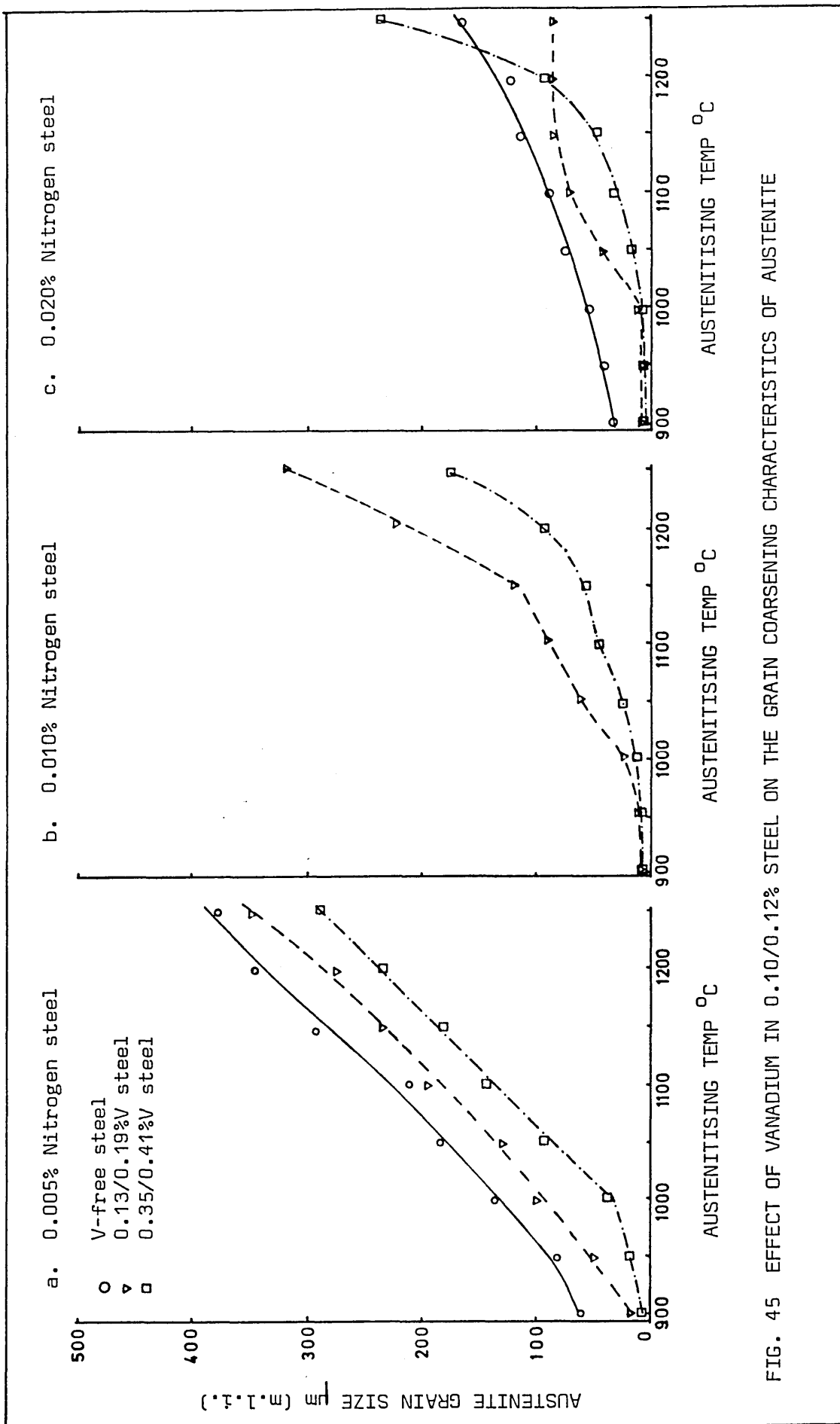
FIG. 45   EFFECT OF VANADIUM IN 0.10/0.12% STEEL ON THE GRAIN COARSENING CHARACTERISTICS OF AUSTENITE

241
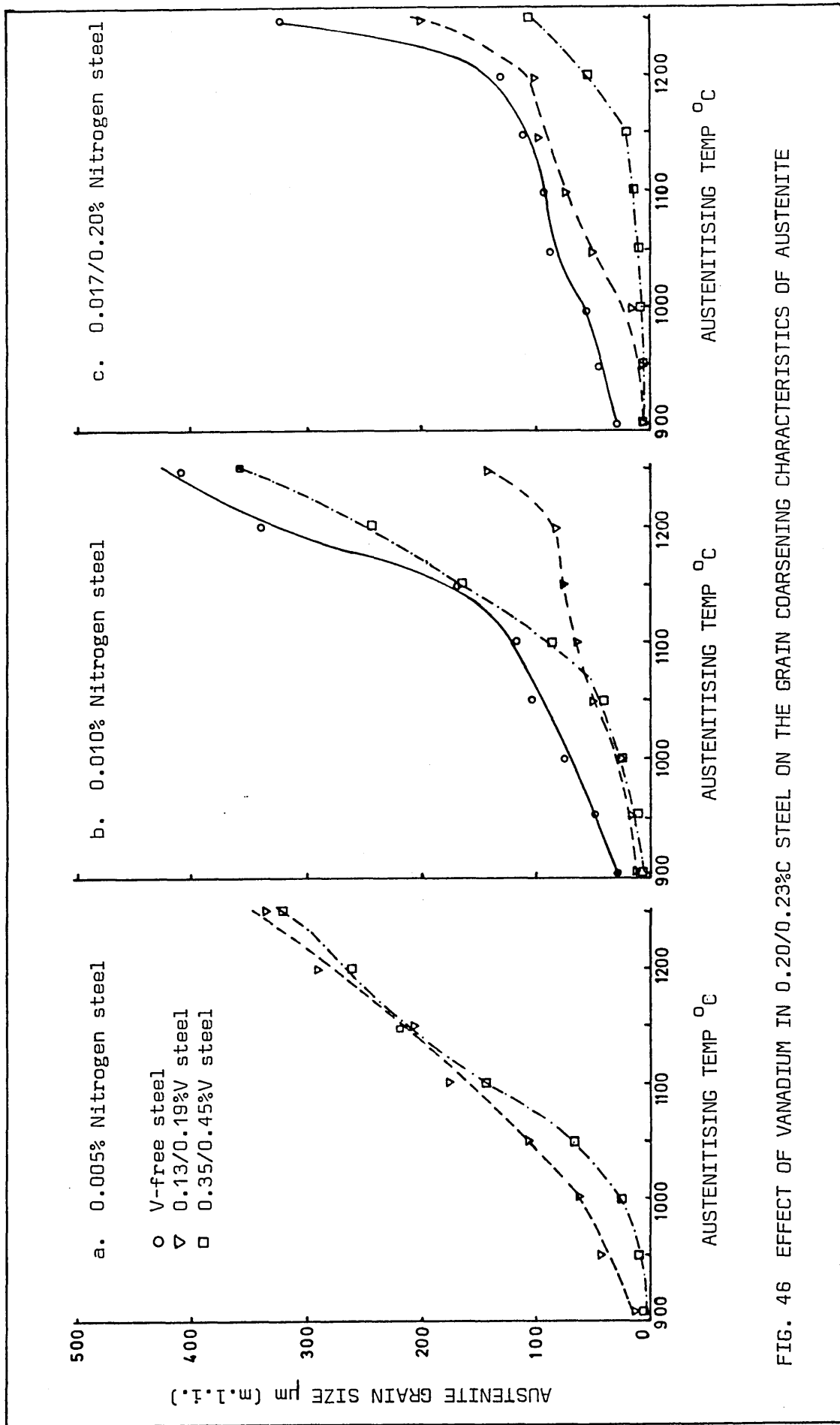
FIG. 46 EFFECT OF VANADIUM IN 0.20/0.23%C STEEL ON THE GRAIN COARSENING CHARACTERISTICS OF AUSTENITE

242
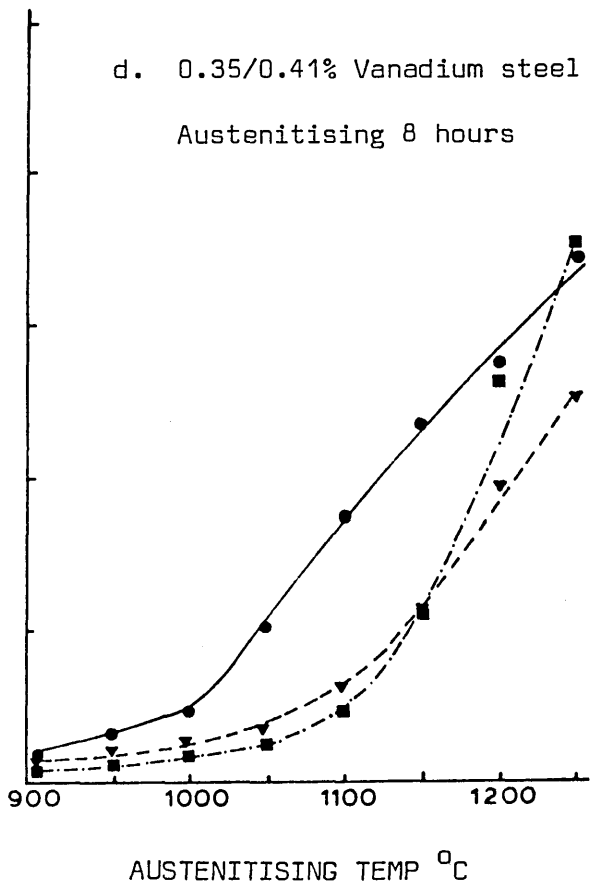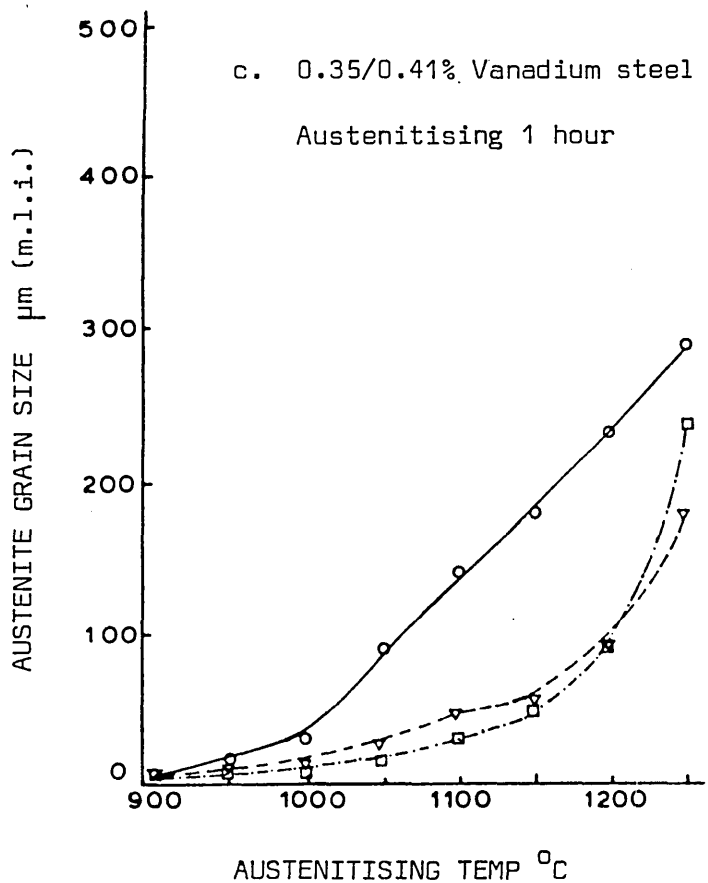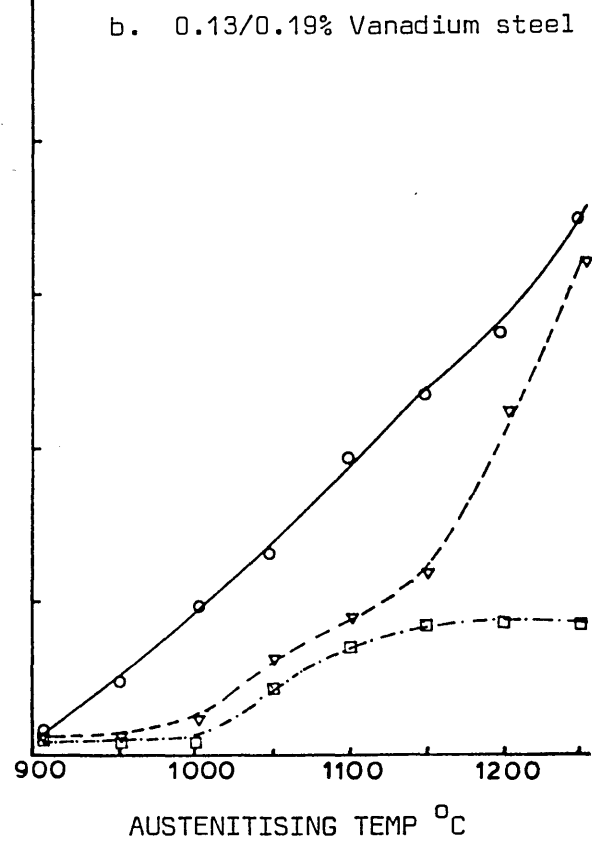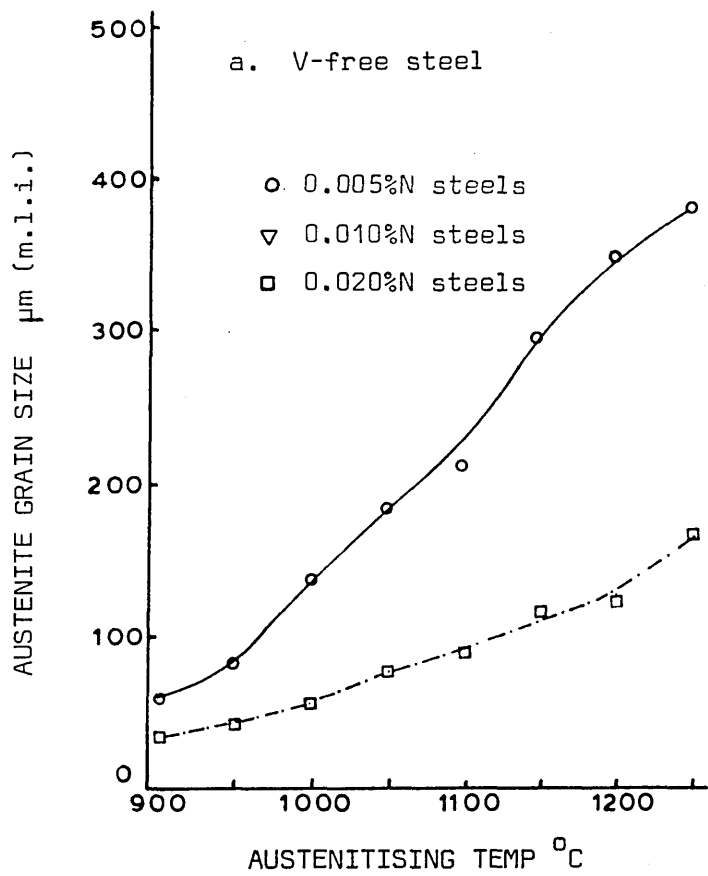
FIG. 47 EFFECT OF NITROGEN IN 0.10/0.126%C, 1.4/1.8%Mn STEEL ON THE GRAIN
COARSENING CHARACTERISTICS OF AUSTENITE
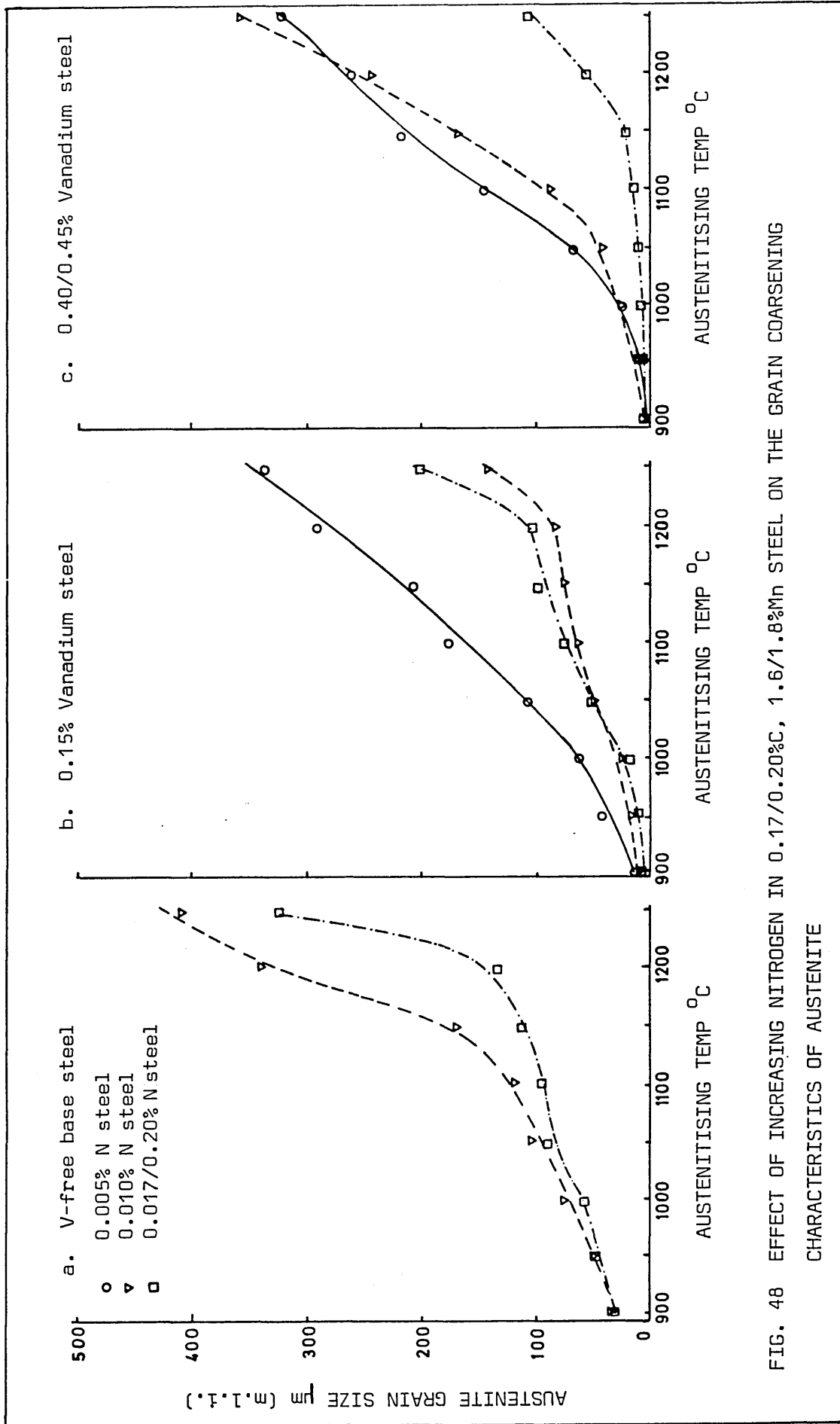
FIG. 48   EFFECT OF INCREASING NITROGEN IN 0.17/0.20%C, 1.6/1.8%Mn STEEL ON THE GRAIN COARSENING CHARACTERISTICS OF AUSTENITE

244
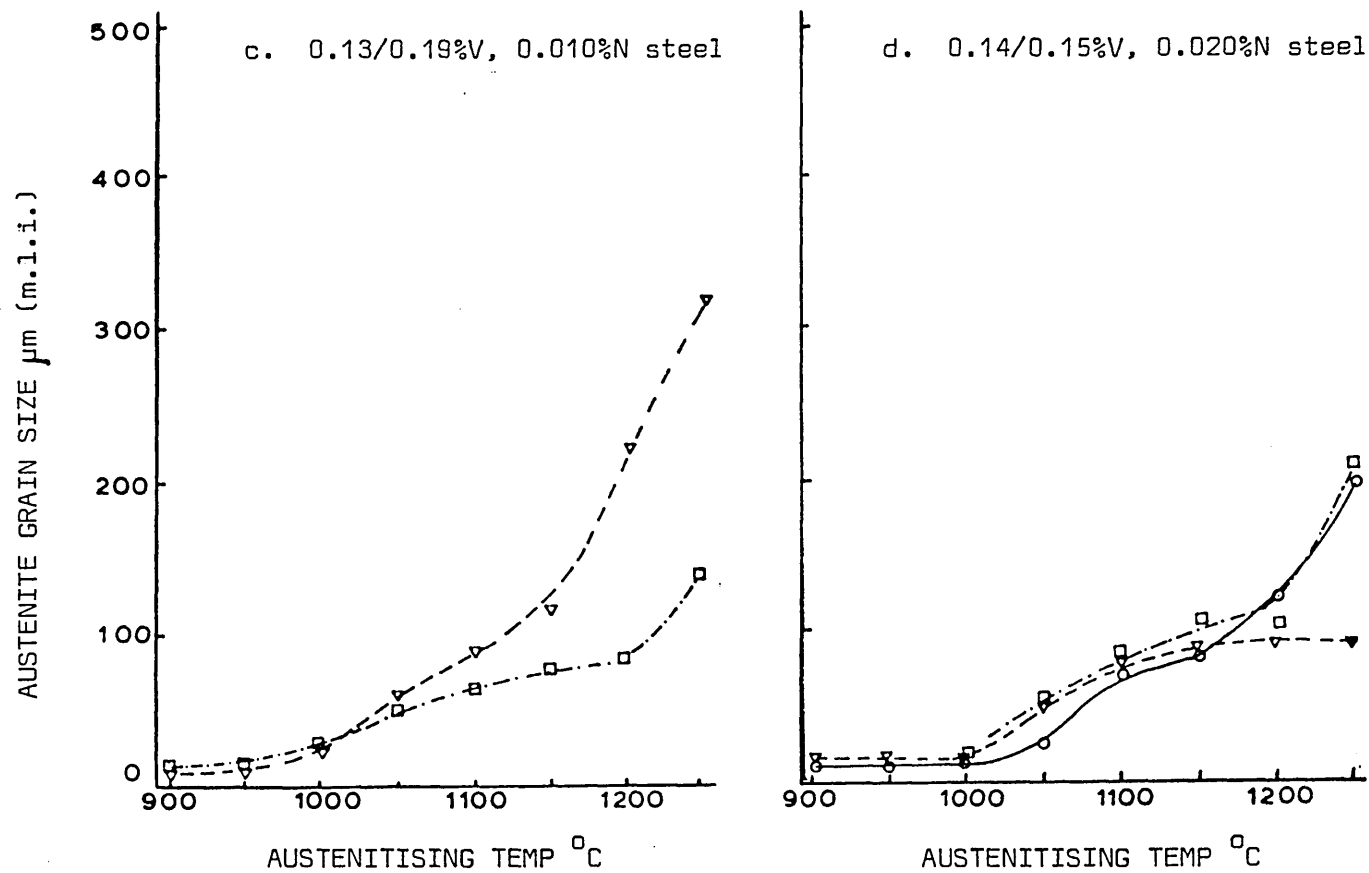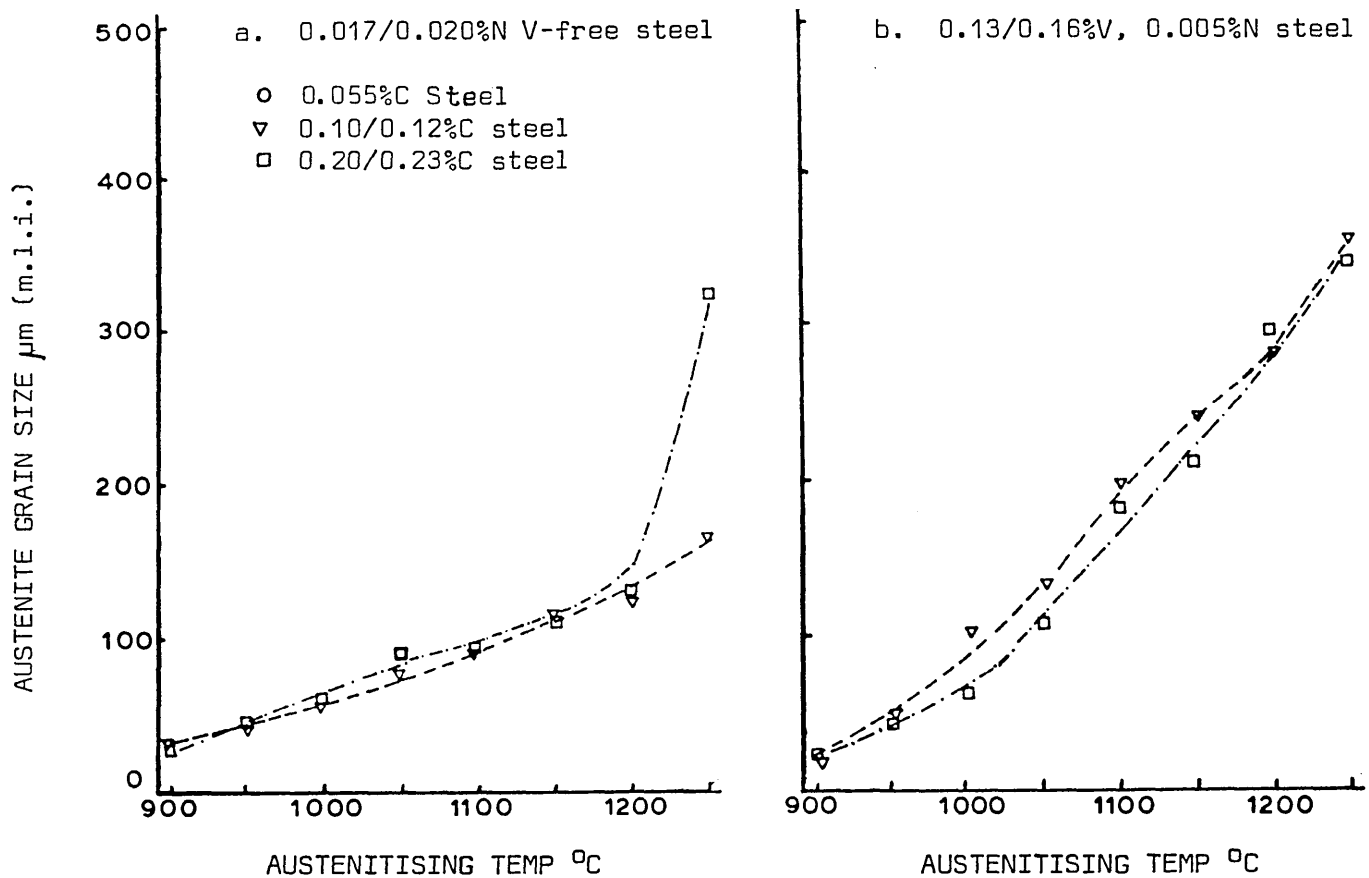
FIG. 49 EFFECT OF CARBON IN 1.6/1.8%Mn STEEL ON THE GRAIN COARSENING CHARACTERISTICS OF AUSTENITE
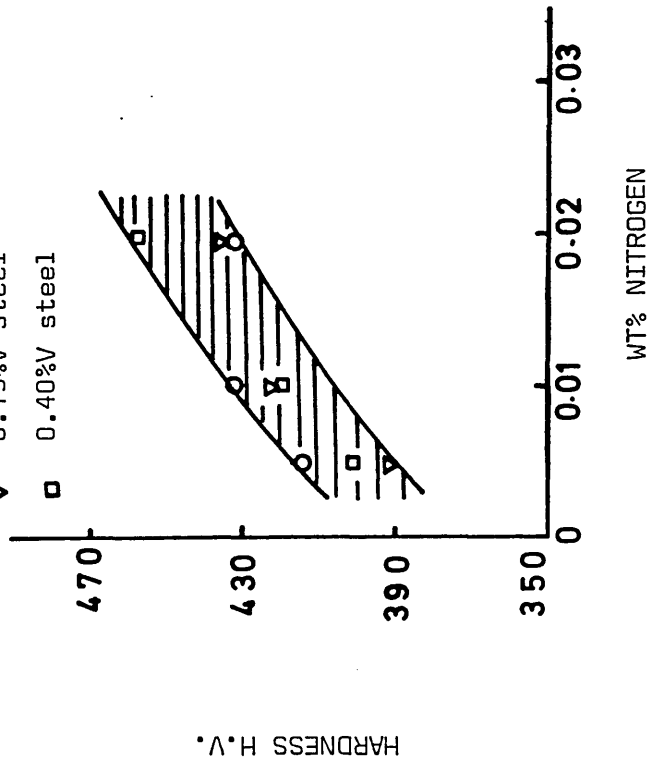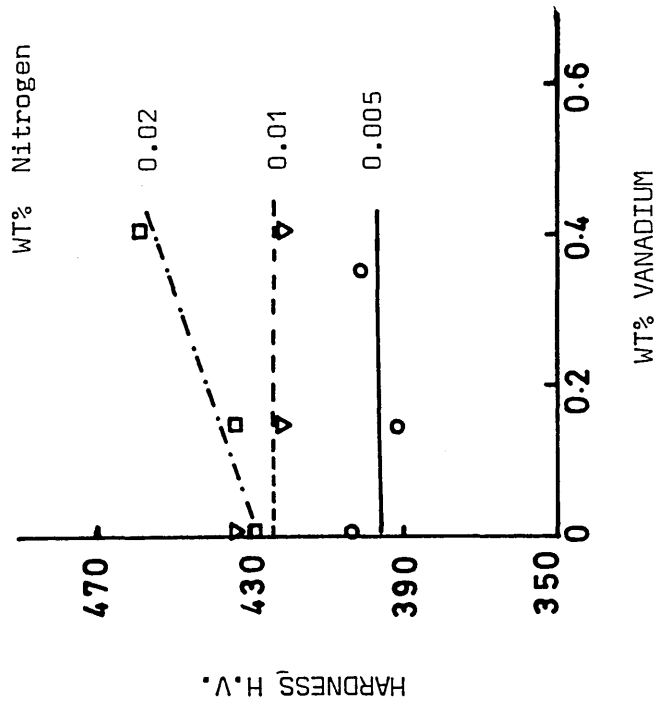
FIG. 50   EFFECT OF VANADIUM AND NITROGEN ON THE HARDNESS OF AS QUENCHED MARTENSITE
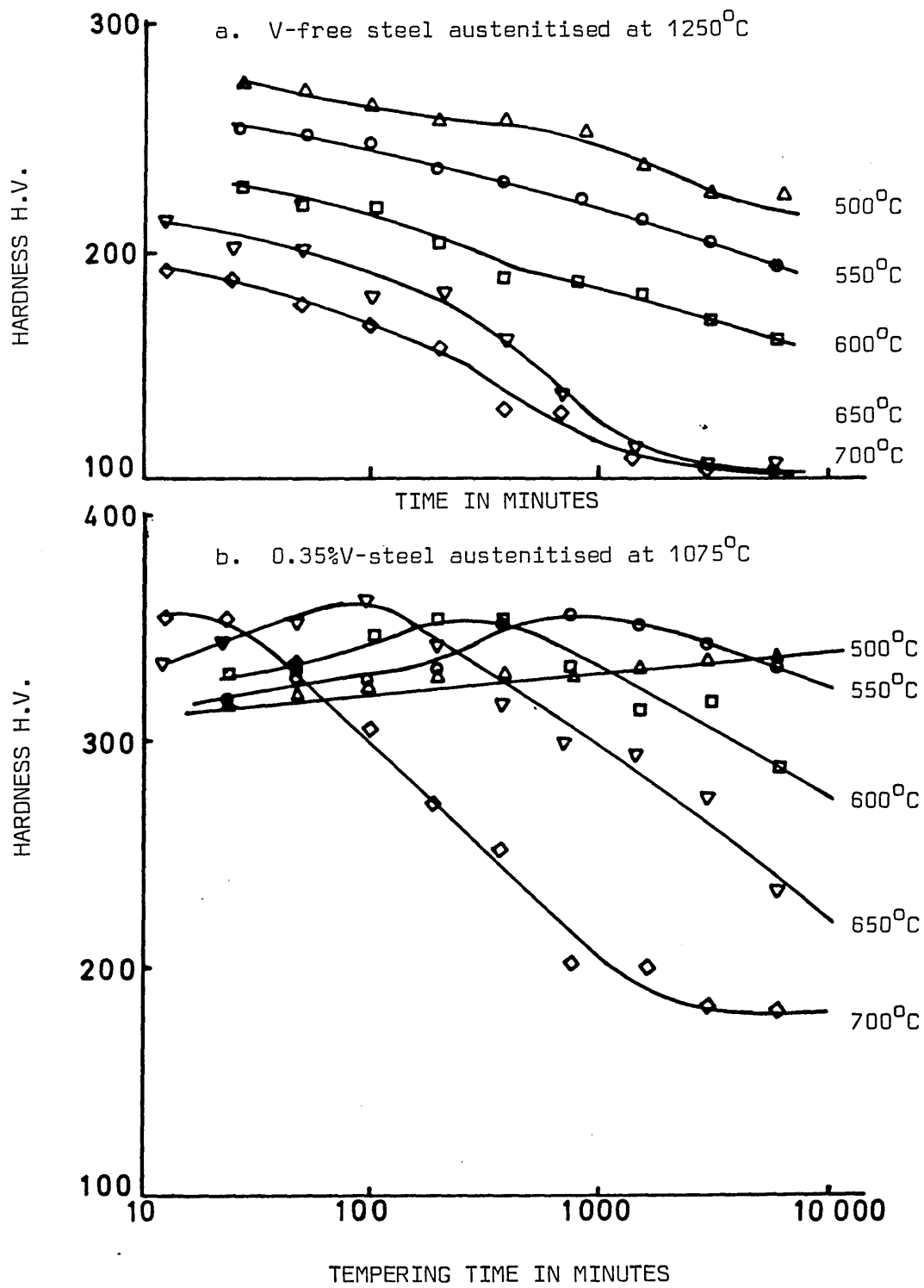
FIG. 51 ISOTHERMAL TEMPERING CURVES FOR 0.10%C, 1.50/1.60%Mn,
0.005/0.006%N STEEL

247
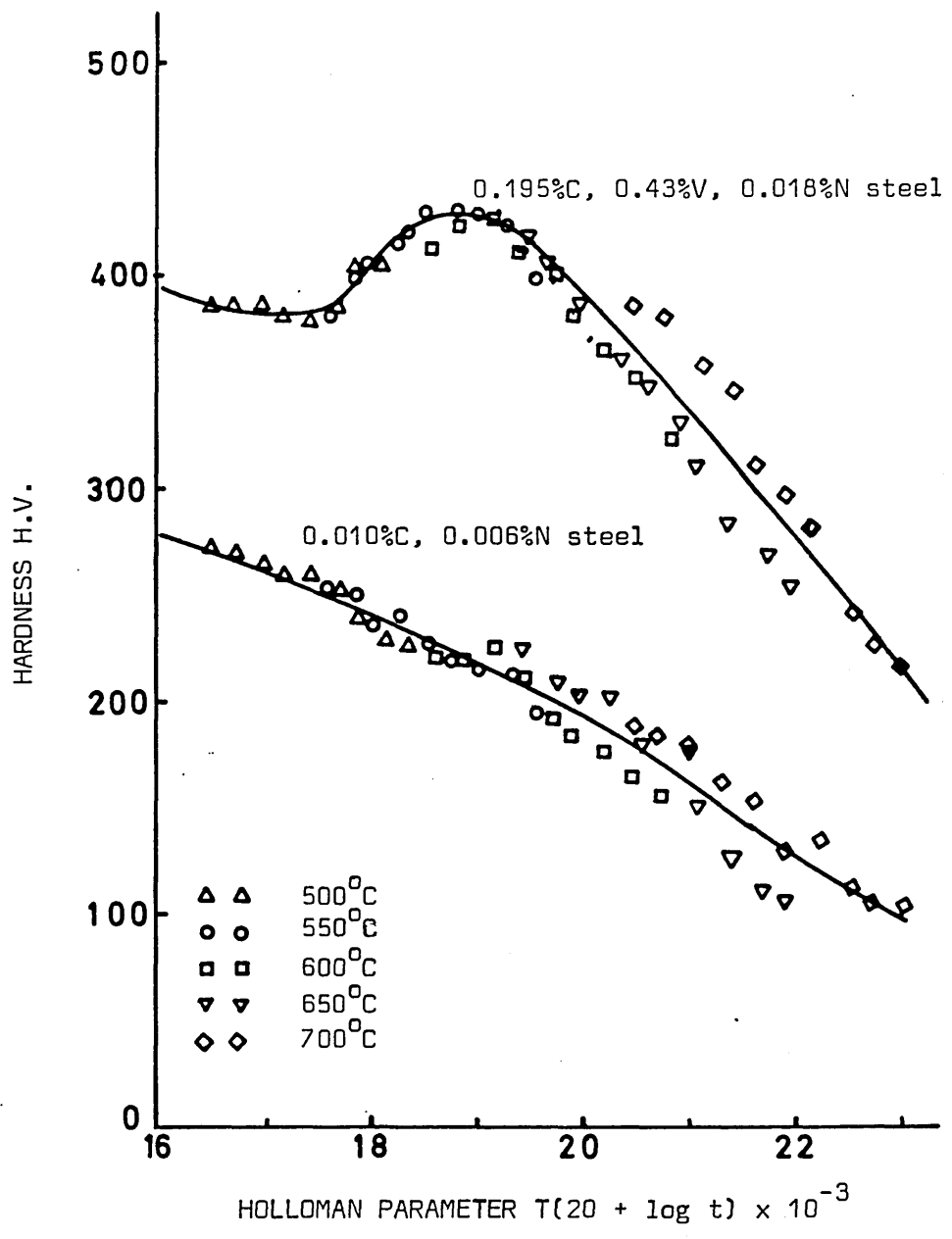
FIG. 52 SCATTER EFFECT OF HARDNESS VERSUS HOLLOMAN PARAMETER

a.

50 HOURS AT 550°C
9000X

b.

100 HOURS AT 550°C
9000X
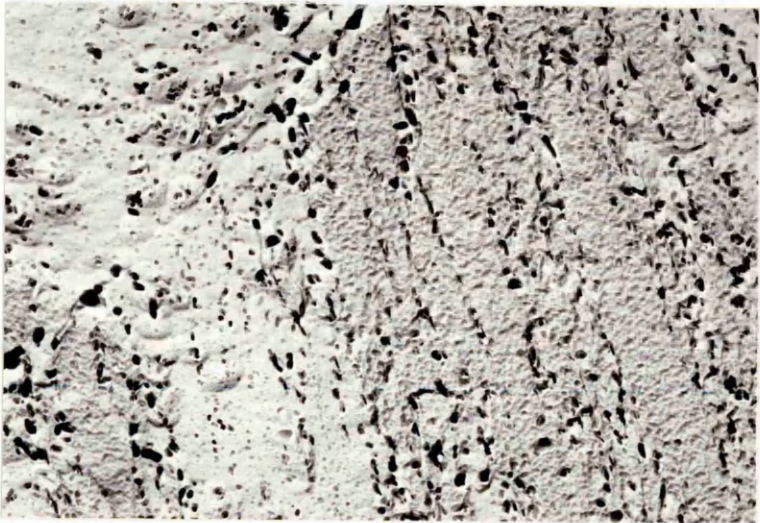
c.

12 HOURS AT 600°C
9000X
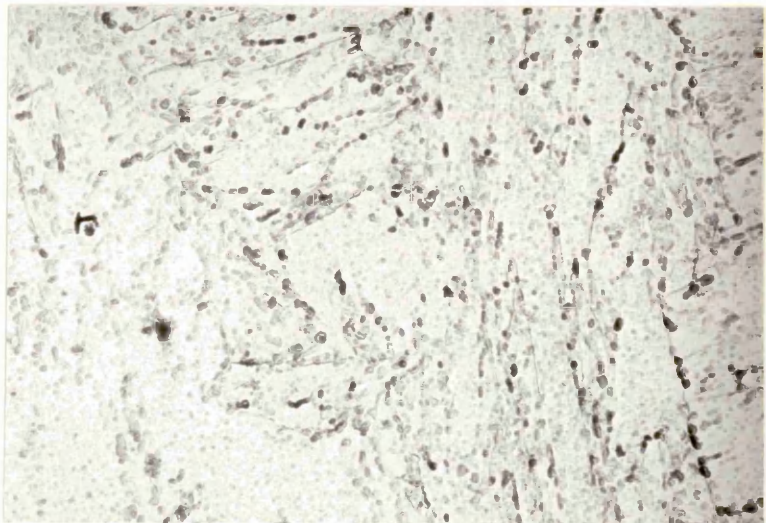
FIG. 53   TEMPERED MICROSTRUCTURES OF 0.12% C, 1.77% Mn, 0.15% V,
0.020% N STEEL
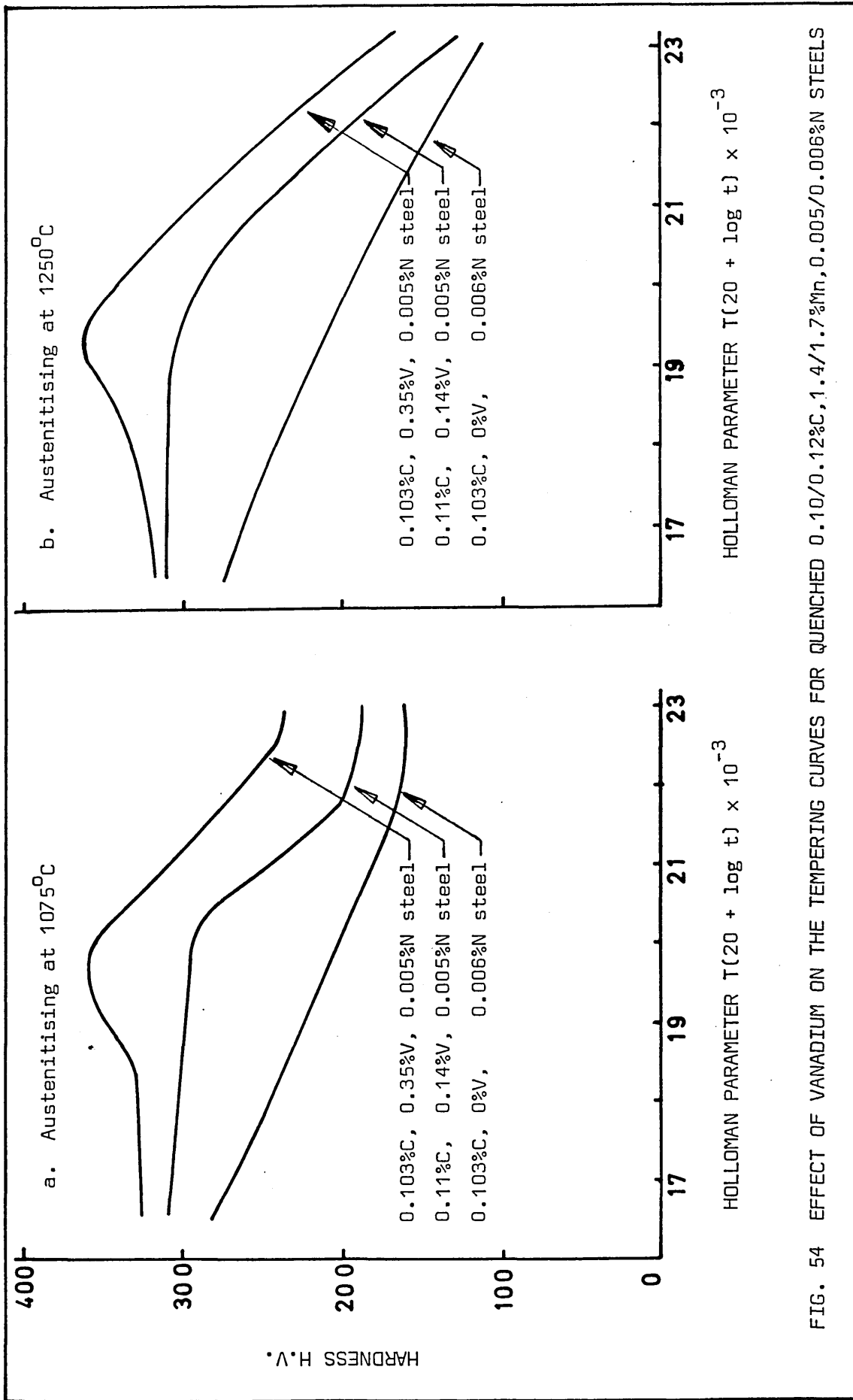
FIG. 54 EFFECT OF VANADIUM ON THE TEMPERING CURVES FOR QUENCHED 0.10/0.12%C,1.4/1.7%Mn,0.005/0.006%N STEELS

a. 0.10/0.123%C, 0.010%N steels

b. 0.12/0.126%C, 0.020%N steels

0.10%C, 0.41%V, 0.01%N steels
0.12%C, 0.13%V, 0.01%N steels
0.123%C, 0%V, 0.01%N steels

0.126%C, 0.415%V, 0.02%N steels
0.12%C, 0.15%V, 0.02%N steels
0.12%C, 0%V, 0.02%N steels

HOLLOMAN PARAMETER T(20 + log t) × 10⁻³

HARDNESS H.V.
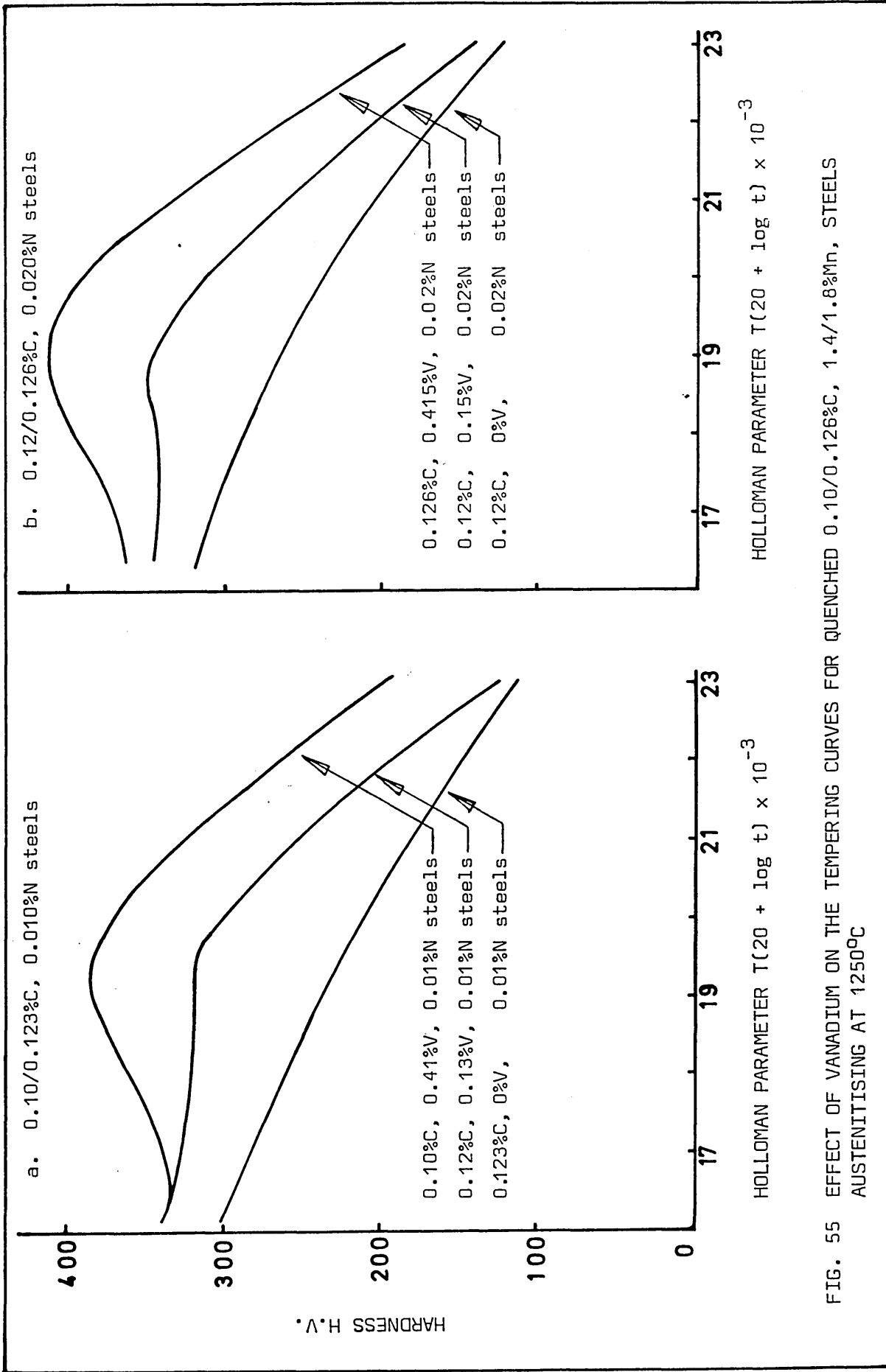
FIG. 55   EFFECT OF VANADIUM ON THE TEMPERING CURVES FOR QUENCHED 0.10/0.126%C, 1.4/1.8%Mn, STEELS
AUSTENITISING AT 1250°C

251
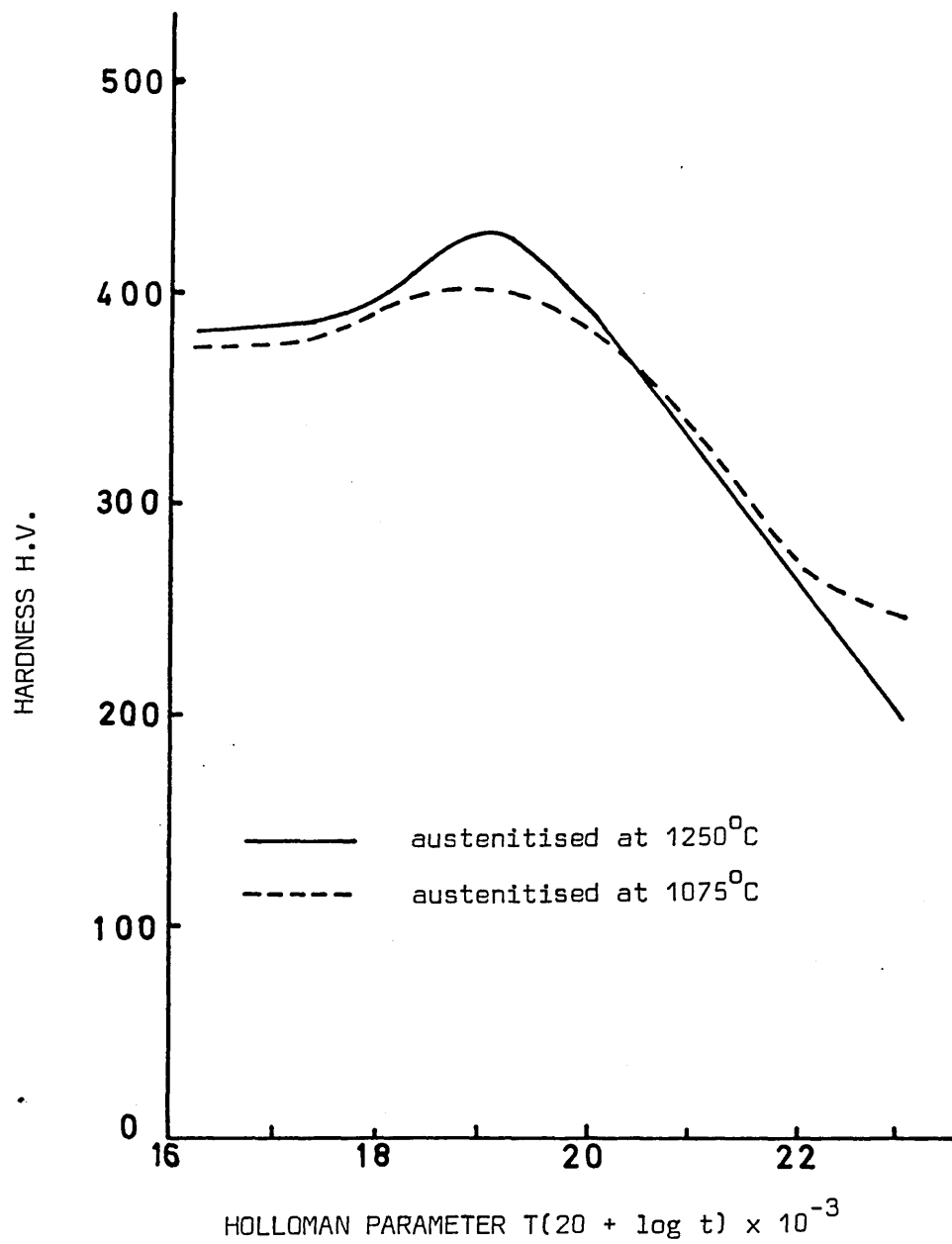
FIG. 56 EFFECT OF AUSTENITISING TEMPERATURE ON TEMPERING
CURVES FOR QUENCHED 0.20%C, 0.45%V, 0.020%N STEEL
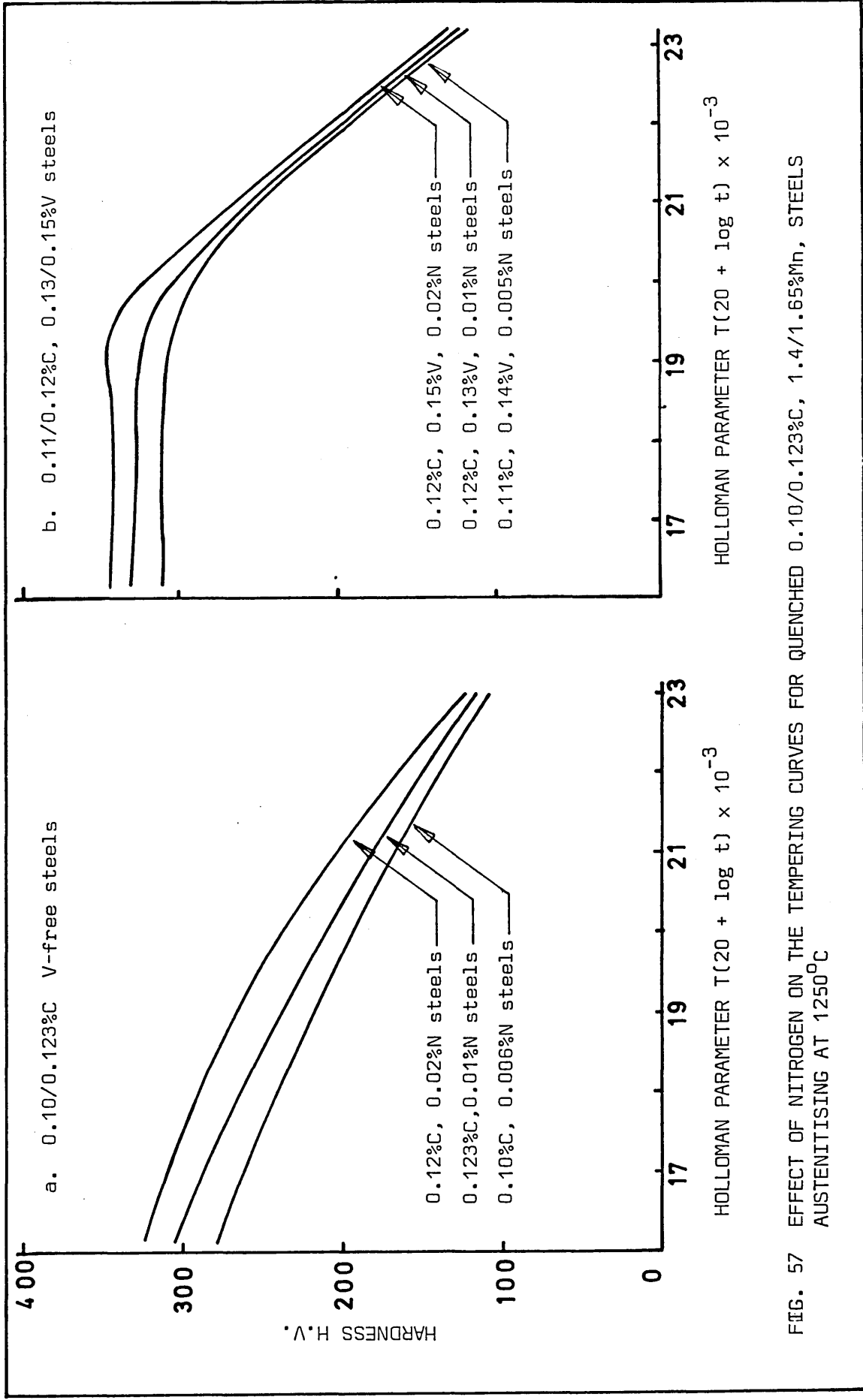
FIG. 57 EFFECT OF NITROGEN ON THE TEMPERING CURVES FOR QUENCHED 0.10/0.123%C, 1.4/1.65%Mn, STEELS
AUSTENITISING AT 1250°C

253

a. Austenitising at 1075°C

0.12%C, 0.41%V, 0.02%N steels
0.11%C, 0.35%V, 0.005%N steels

HOLLOMAN PARAMETER T(20 + log t) × 10^{-3}

b. Austenitising at 1250°C

0.126%C, 0.415%V, 0.02%N steels
0.10%C, 0.41%V, 0.01%N steels
0.103%C, 0.35%V, 0.005%N steels

HOLLOMAN PARAMETER T(20 + log t) × 10^{-3}

HARDNESS H.V.
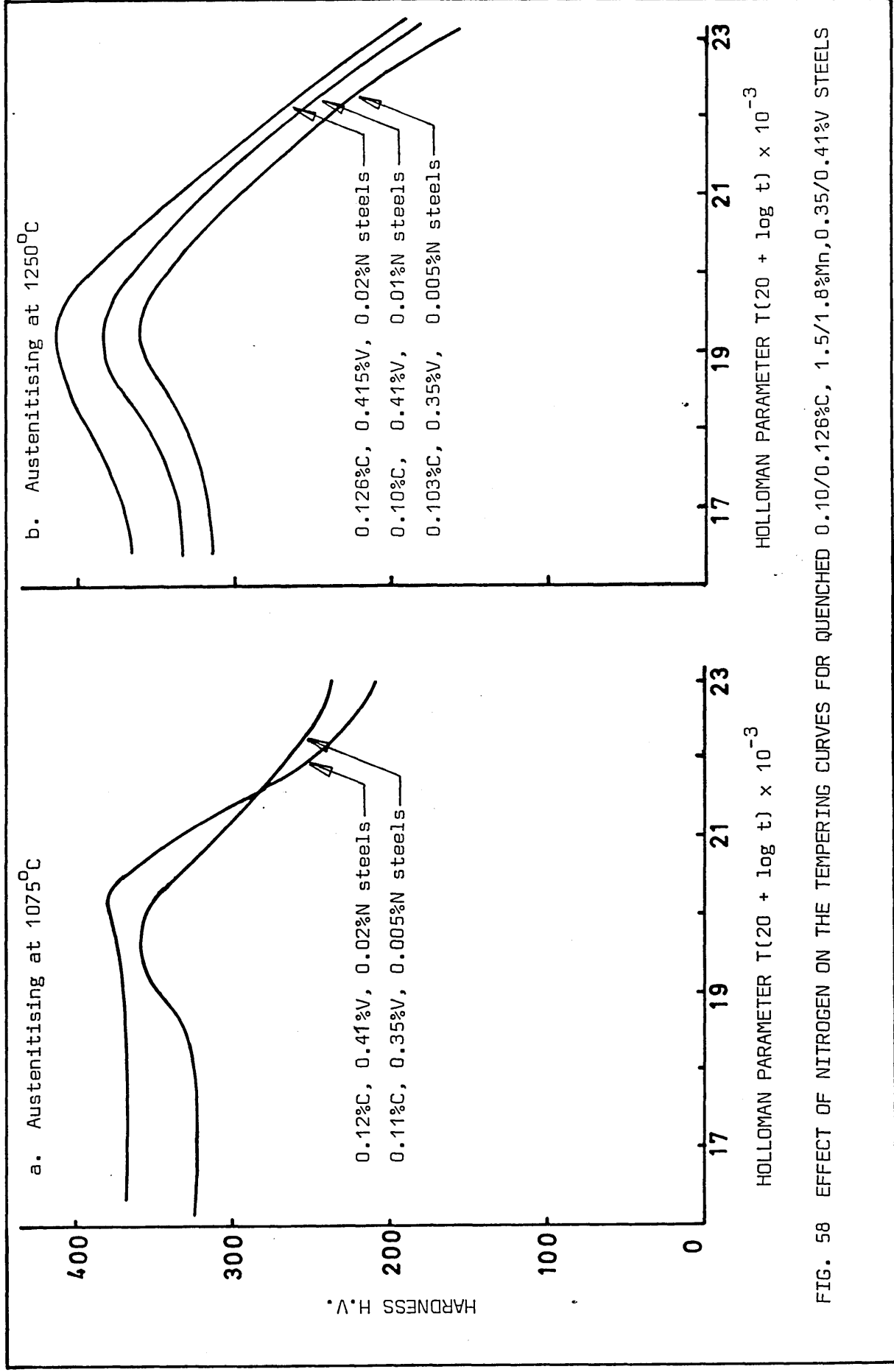
FIG. 58 EFFECT OF NITROGEN ON THE TEMPERING CURVES FOR QUENCHED 0.10/0.126%C, 1.5/1.8%Mn,0.35/0.41%V STEELS

254
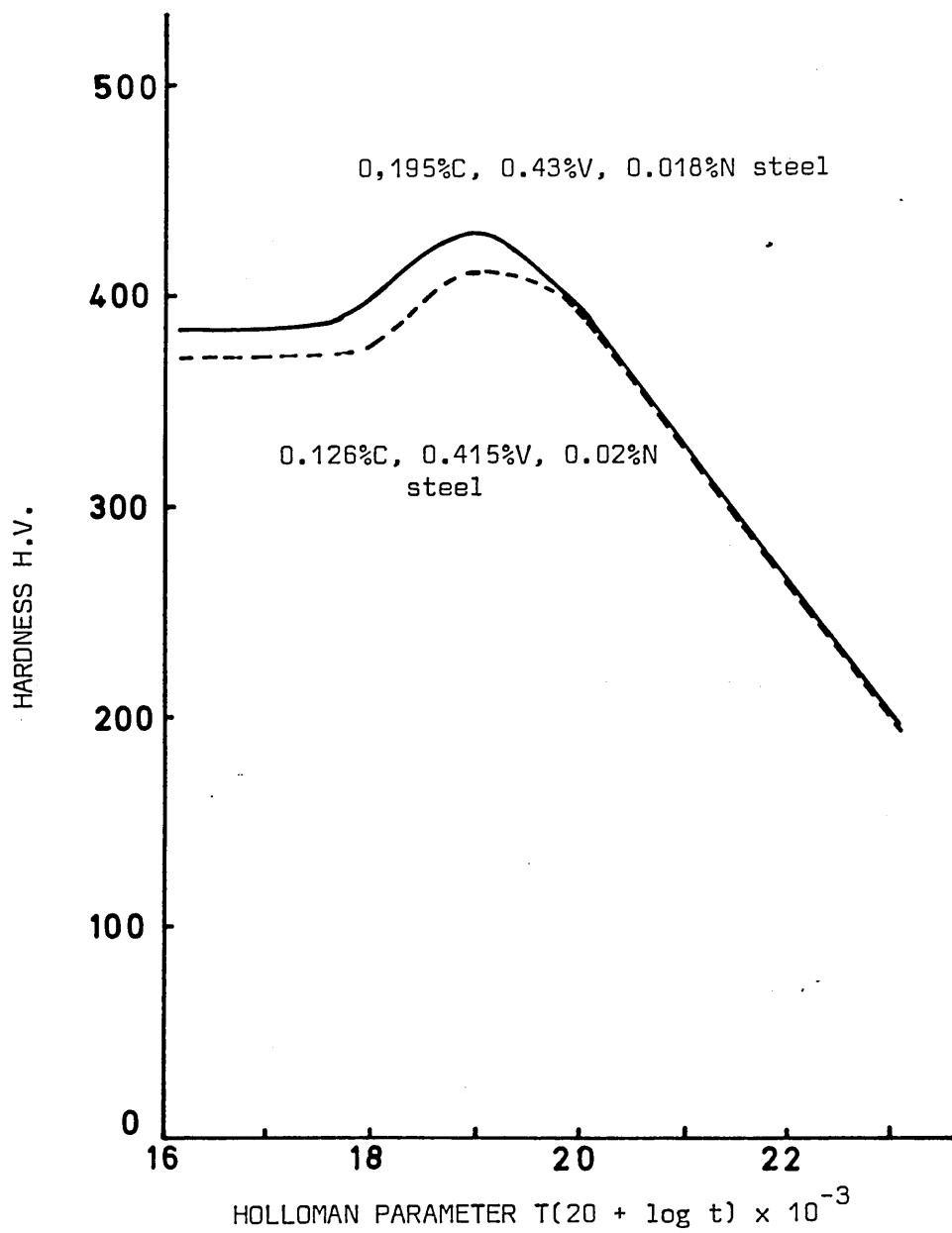
FIG. 59 EFFECT OF CARBON ON TEMPERING CURVE FOR 0.41/0.43%V, 0.018/0.020%N STEEL AUSTENITISING AT 1250°C

FIG. 60   EFFECT OF VANADIUM ON THE FERRITE FORMATION IN
0.12%C, 1.60%Mn, 0.010%N STEELS

256

a. Transformation temperature 750°C

0.005%N steel
0.010%N steel
0.020%N steel

b. Transformation temperature 700°C

c. Transformation temperature 650°C

LOG TRANSFORMATION TIME (SECONDS)
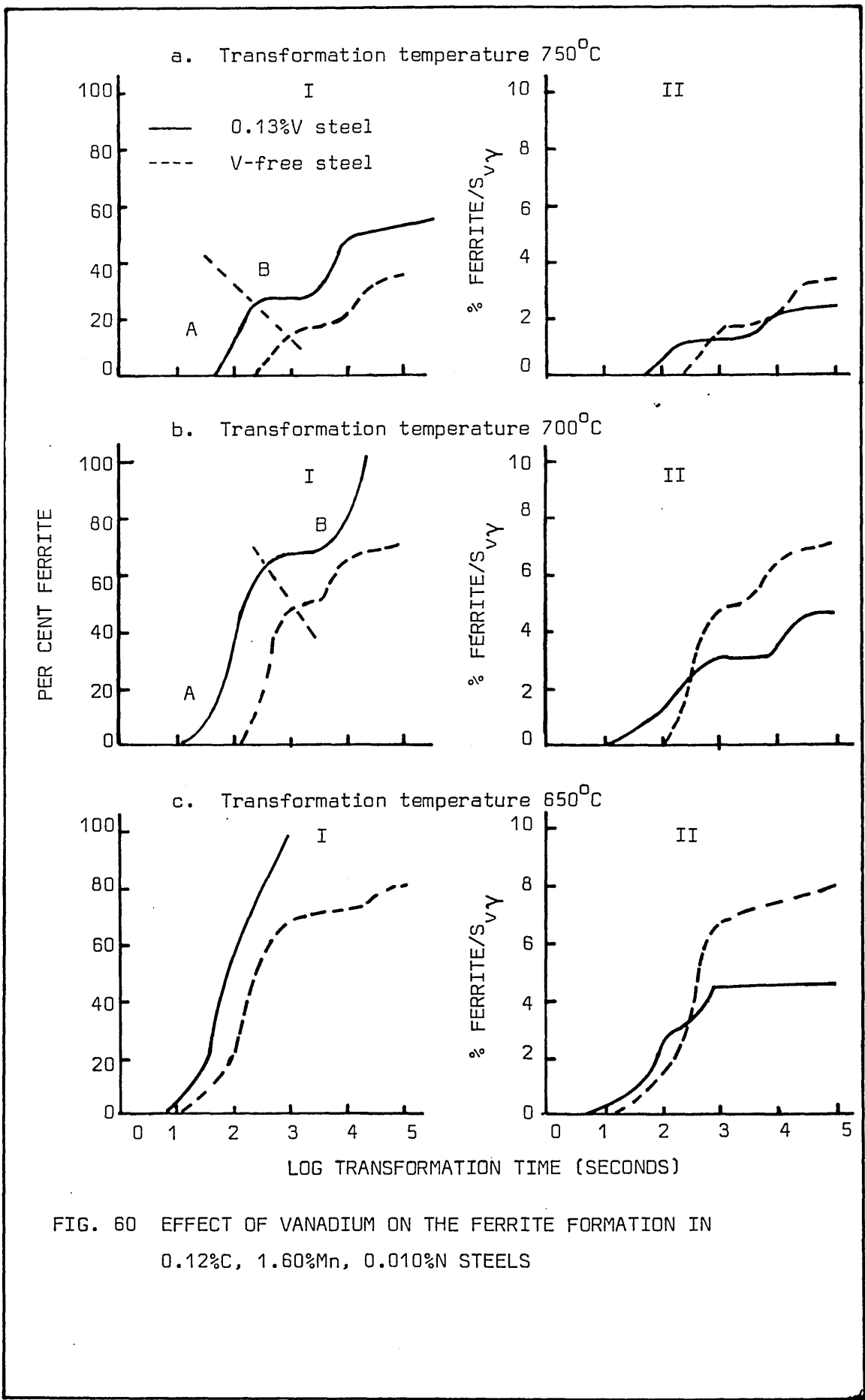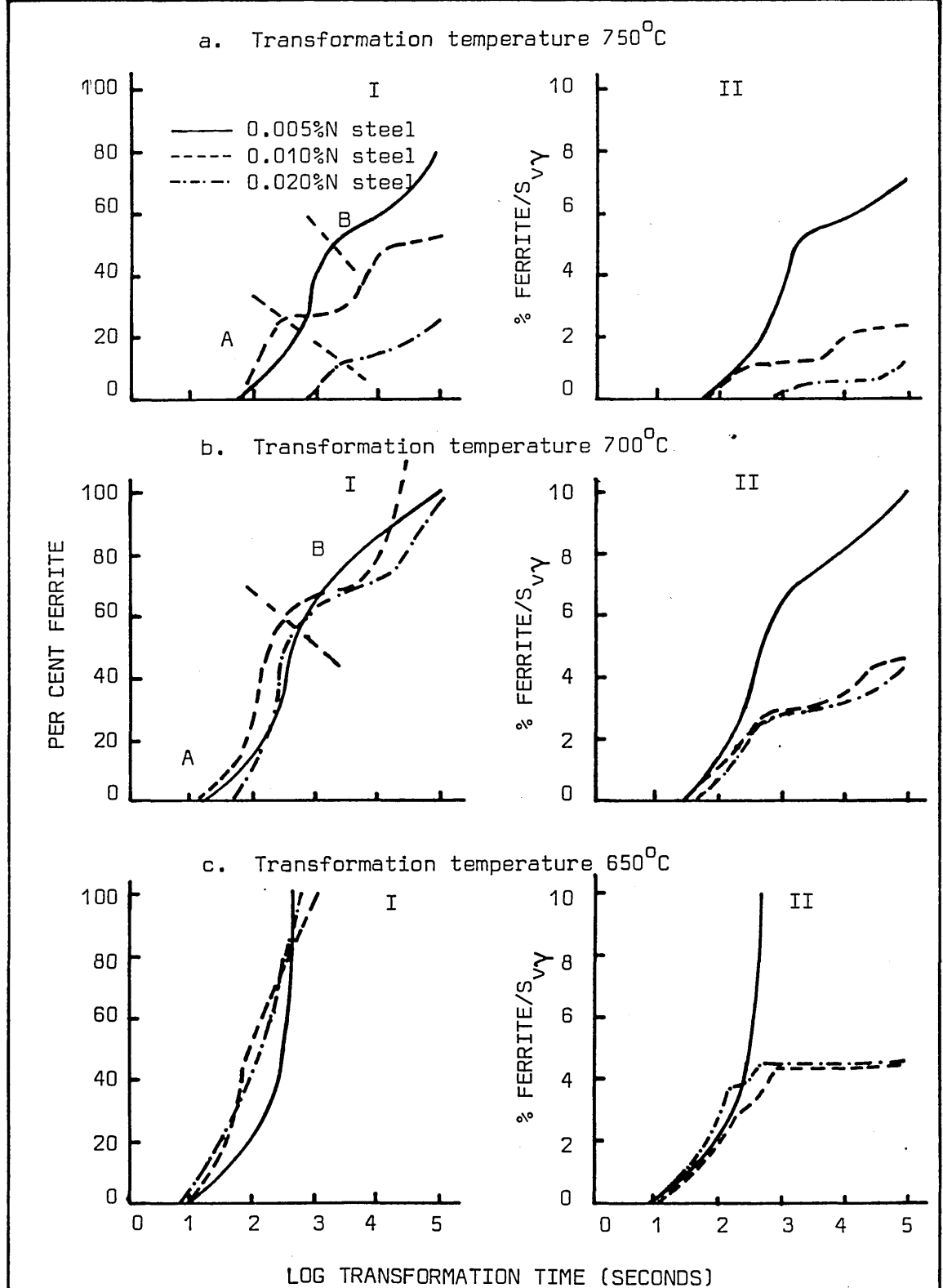
FIG. 61   EFFECT OF INCREASING NITROGEN ON THE FERRITE
FORMATION IN 0.11/0.12%C, 1.6/1.8%Mn, 0.13/0.15%V
STEELS

257
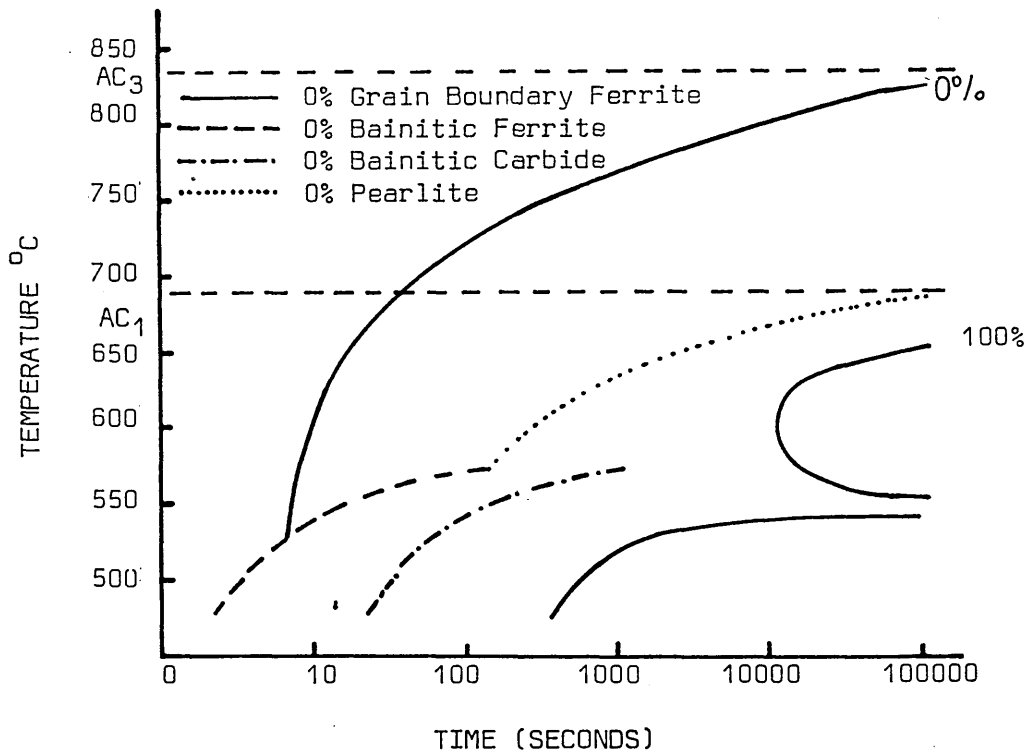
FIG. 62   ISOTHERMAL TRANSFORMATION DIAGRAM FOR 0.123%C,
1.6%Mn, 0.01%N STEEL AUSTENITISED 1250°C, AUSTENITE
GRAIN SIZE 175 μm
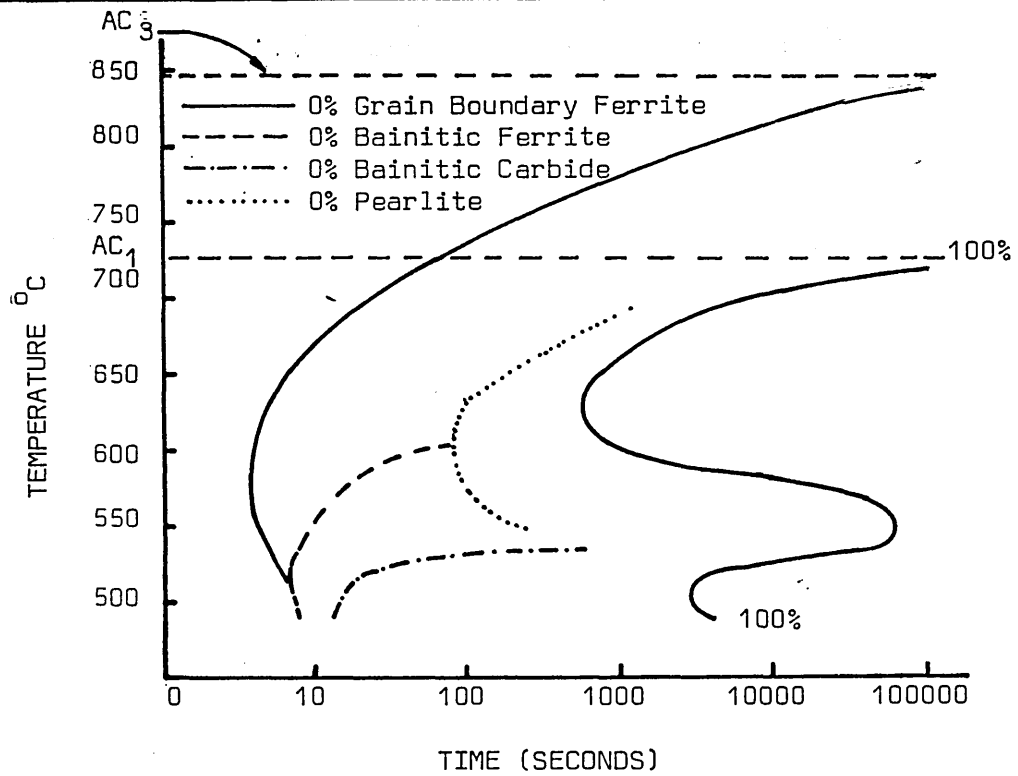
FIG. 63   ISOTHERMAL TRANSFORMATION DIAGRAM FOR 0.12%C,
1.58%Mn, 0.13%V, 0.01%N STEEL AUSTENITISED AT
1250 °C, AUSTENITE GRAIN SIZE 90 μm

258

a.

750°C FOR 2 MINUTES W. Q.
X200

b.

750°C FOR 10 MINUTES W. Q.
X100

c.

700°C FOR 4 MINUTES W. Q.
X500

d.

700°C FOR 10 MINUTES W. Q.
X50

e.

650°C FOR 10 MINUTES W. Q.
X100

f.

600°C FOR 1 MINUTE W. Q.
X100

g.

600°C FOR 7 HOURS W. Q.
X100

h.

550°C FOR 60 SECONDS W. Q.
X200

FIG. 64   TYPICAL MICROSTRUCTURES FROM TIME TEMPERATURE
          TRANSFORMATION DIAGRAMS OF 0.123%C, 1.6%Mn,
          0.010%N STEEL

a.

b.

c.

d.

e.

f.

g.

h.

259 β

a.

750ºC FOR 2 MINUTES W. Q.
X100

b.

750ºC FOR 24 HOURS W. Q.
X200

c.

700ºC FOR 4 MINUTES W. Q.
X200

d.
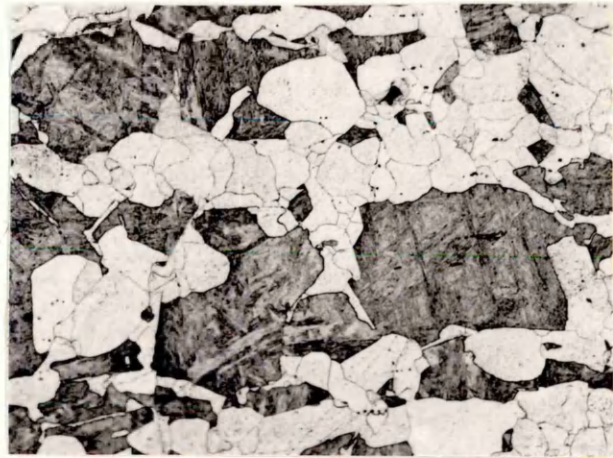
700ºC FOR 7 MINUTES W. Q.
X200

FIG. 65   TYPICAL MICROSTRUCTURES FROM TIME TEMPERATURE TRANSFORMATION
DIAGRAMS OF 0.12%C, 1.58%Mn, 0.13%V, 0.010%N STEEL

260
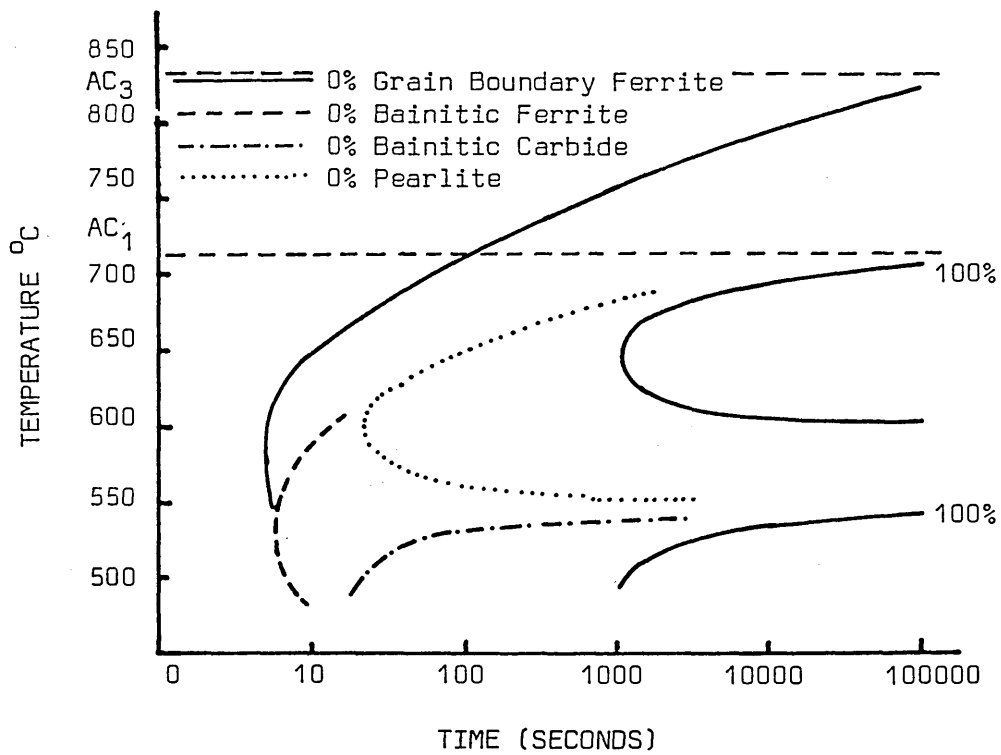
FIG. 66   ISOTHERMAL TRANSFORMATION DIAGRAM FOR 0.11%C, 1.66%Mn, 0.14%V, 0.005%N, AUSTENITISED AT 1250°C, AUSTENITE GRAIN SIZE 198 μm
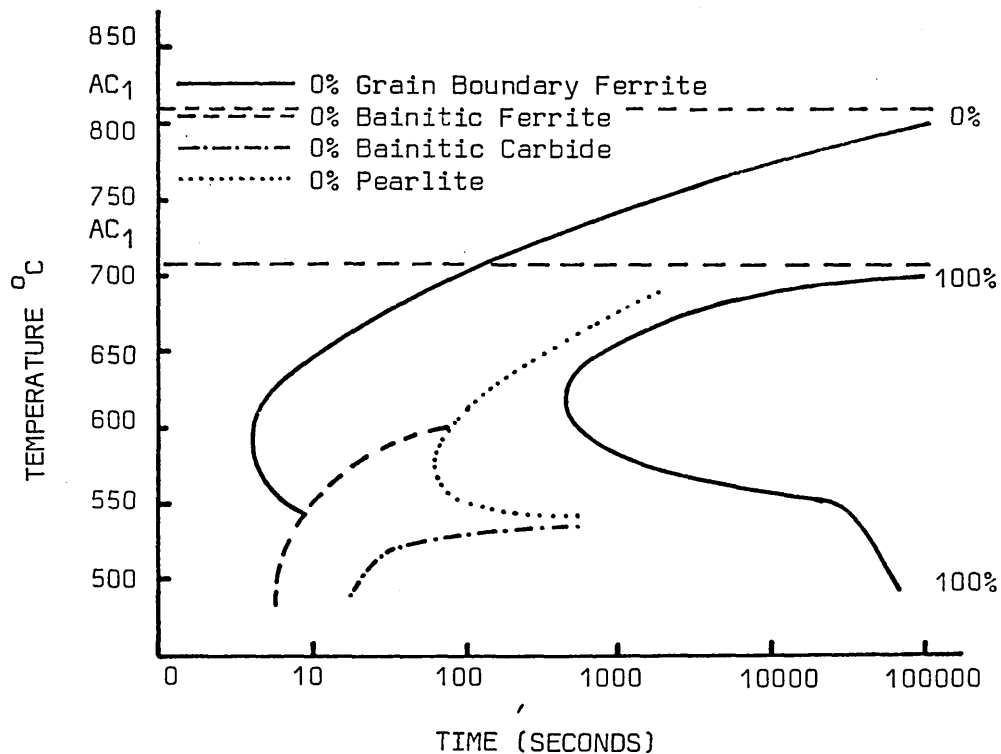
FIG. 67   ISOTHERMAL TRANSFORMATION DIAGRAM FOR 0.12%C, 1.77%Mn, 0.15%V, 0.020%N, STEEL AUSTENITISED AT 1250°C, AUSTENITE GRAIN SIZE 89 μm
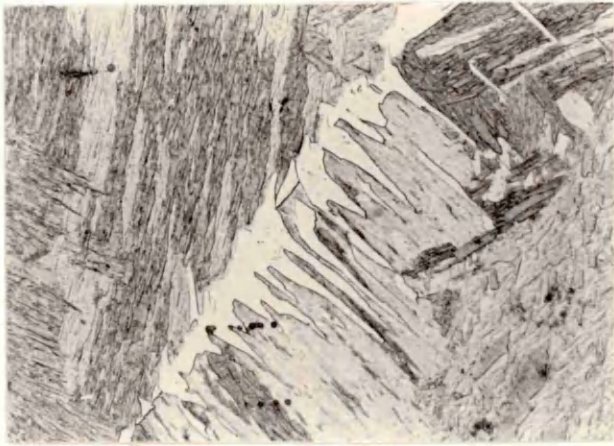
a.

700°C FOR 7 MINUTES W. Q.
X70

b.

650°C FOR 20 SECONDS W. Q.
X500
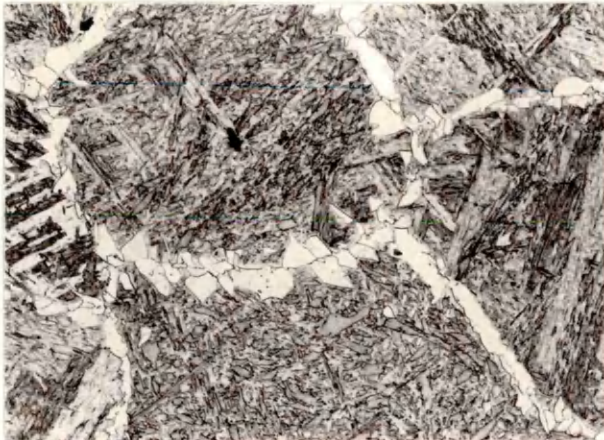
c.

650°C FOR 40 SECONDS W. Q.
X200
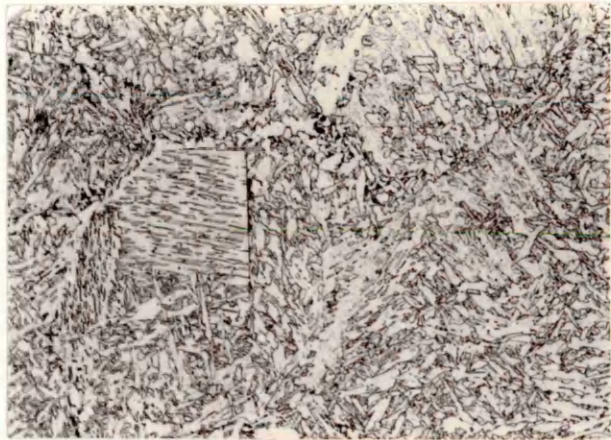
d.

550°C FOR 7 MINUTES W. Q.
X200

FIG. 68   TYPICAL MICROSTRUCTURES FROM TIME TEMPERATURE TRANSFORMATION
DIAGRAMS OF 0.11%C, 1.50%Mn, 0.14%V, 0.005%N STEEL

a.

750°C FOR 1 HOUR W. Q.
X200
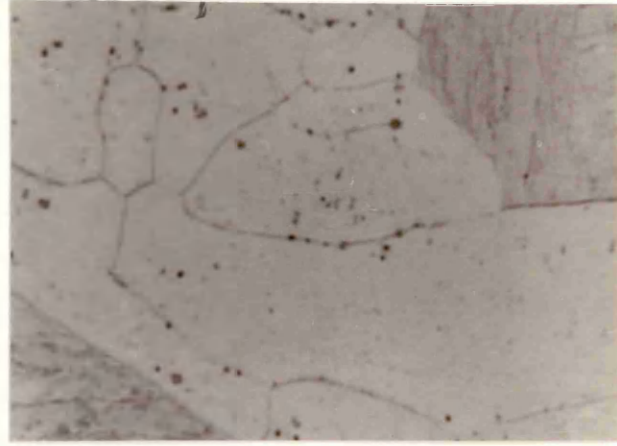
b.

750°C FOR 24 HOURS W. Q.
X2000
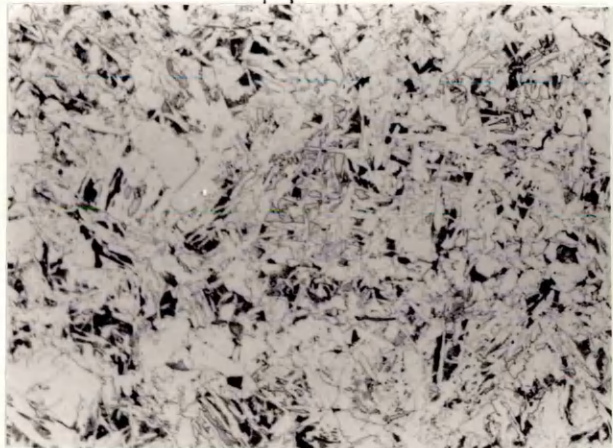
c.

600°C FOR 1 MINUTE W. Q.
X200

d.

600°C FOR 10 MINUTES W. Q.
X200

FIG. 69   TYPICAL MICROSTRUCTURES FROM TIME TEMPERATURE TRANSFORMATION
DIAGRAMS OF 0.12%C, 1.77%Mn, 0.15%V, 0.020%N STEEL
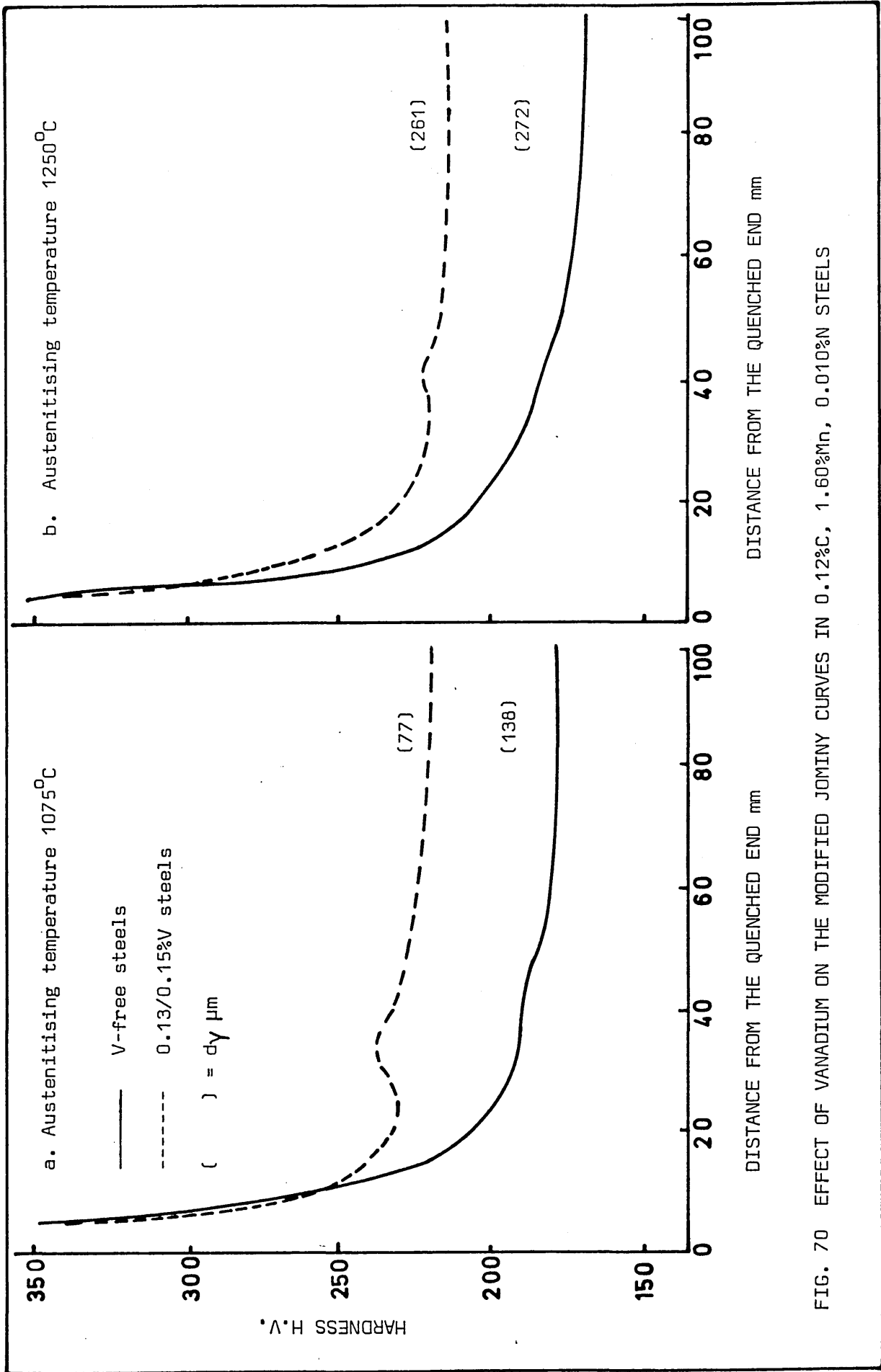
FIG. 70 EFFECT OF VANADIUM ON THE MODIFIED JOMINY CURVES IN 0.12%C, 1.60%Mn, 0.010%N STEELS

264
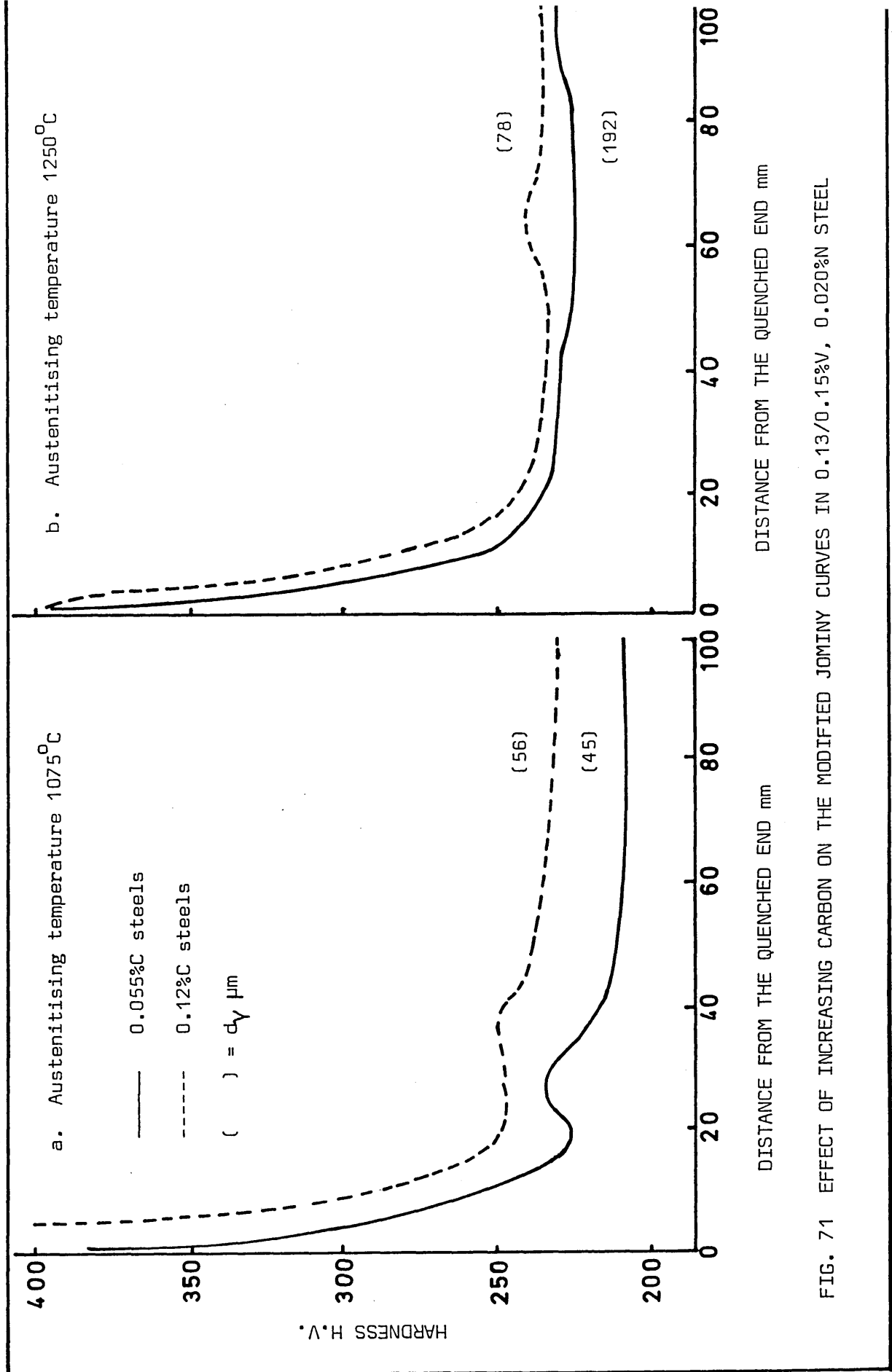
FIG. 71 EFFECT OF INCREASING CARBON ON THE MODIFIED JOMINY CURVES IN 0.13/0.15%V, 0.020%N STEEL

265
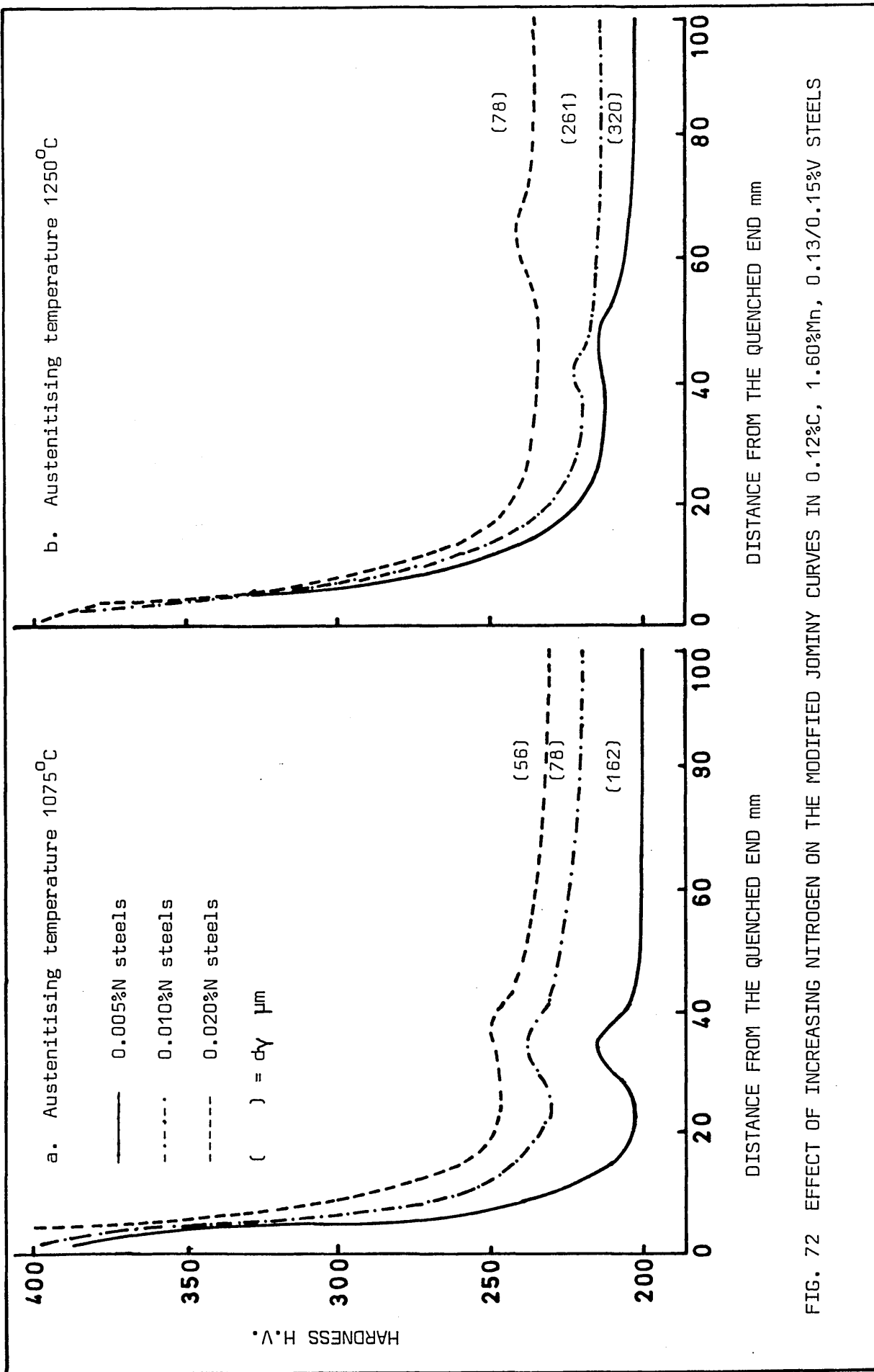
FIG. 72 EFFECT OF INCREASING NITROGEN ON THE MODIFIED JOMINY CURVES IN 0.12%C, 1.60%Mn, 0.13/0.15%V STEELS

266
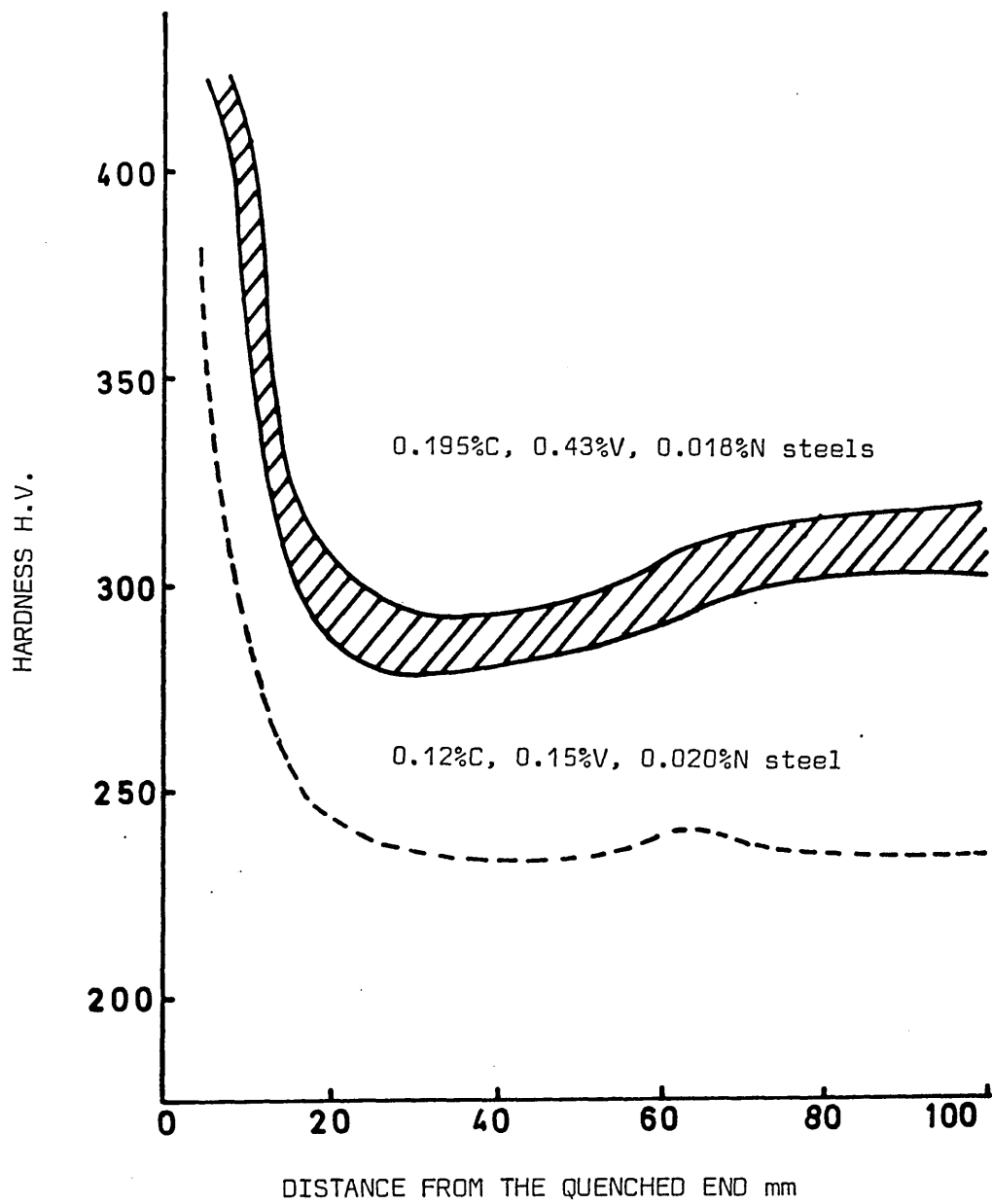
FIG. 73 EFFECT OF SIMULTANEOUSLY INCREASING CARBON AND VANADIUM
CONTENT ON THE MODIFIED JOMINY HARDNESS CURVES
AUSTENITISED AT 1250°C
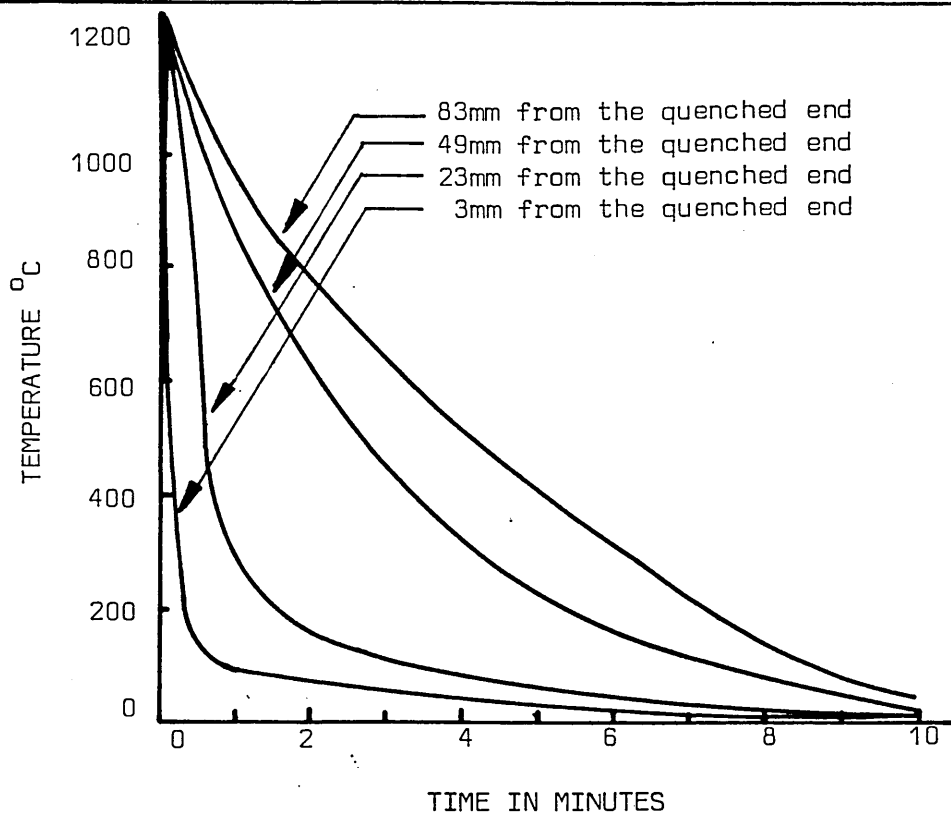
FIG. 74 TYPICAL COOLING CURVES FOR VARYING DISTANCE FROM
FROM THE QUENCHED END OF MODIFIED JOMINY SPECIMEN
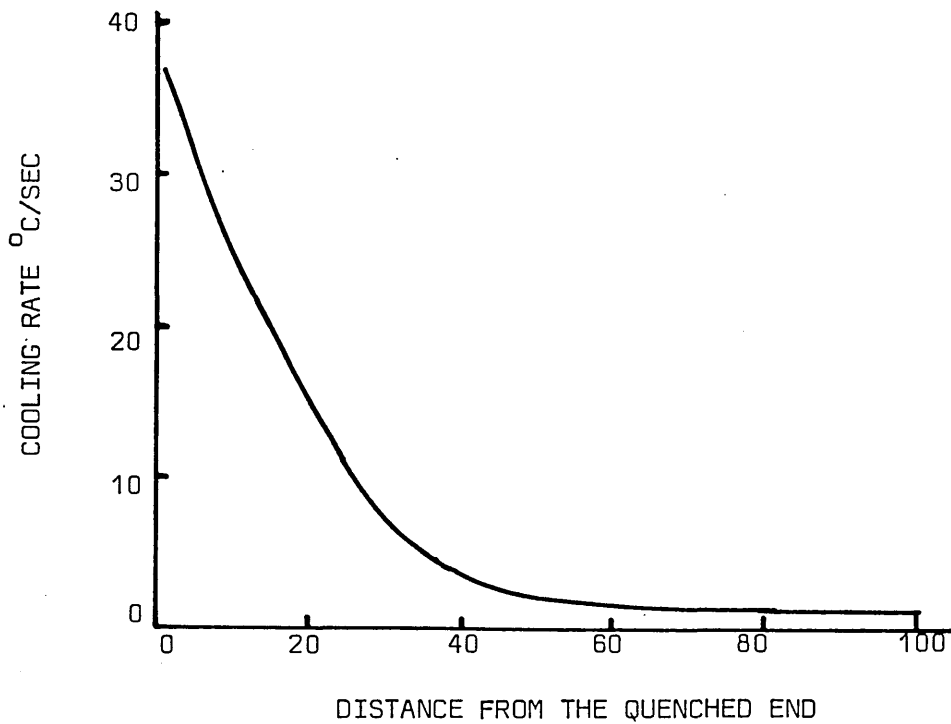
FIG. 75 RATE OF COOLING AS A FUNCTION OF DISTANCE FROM THE
QUENCHED END OF MODIFIED JOMINY SPECIMEN
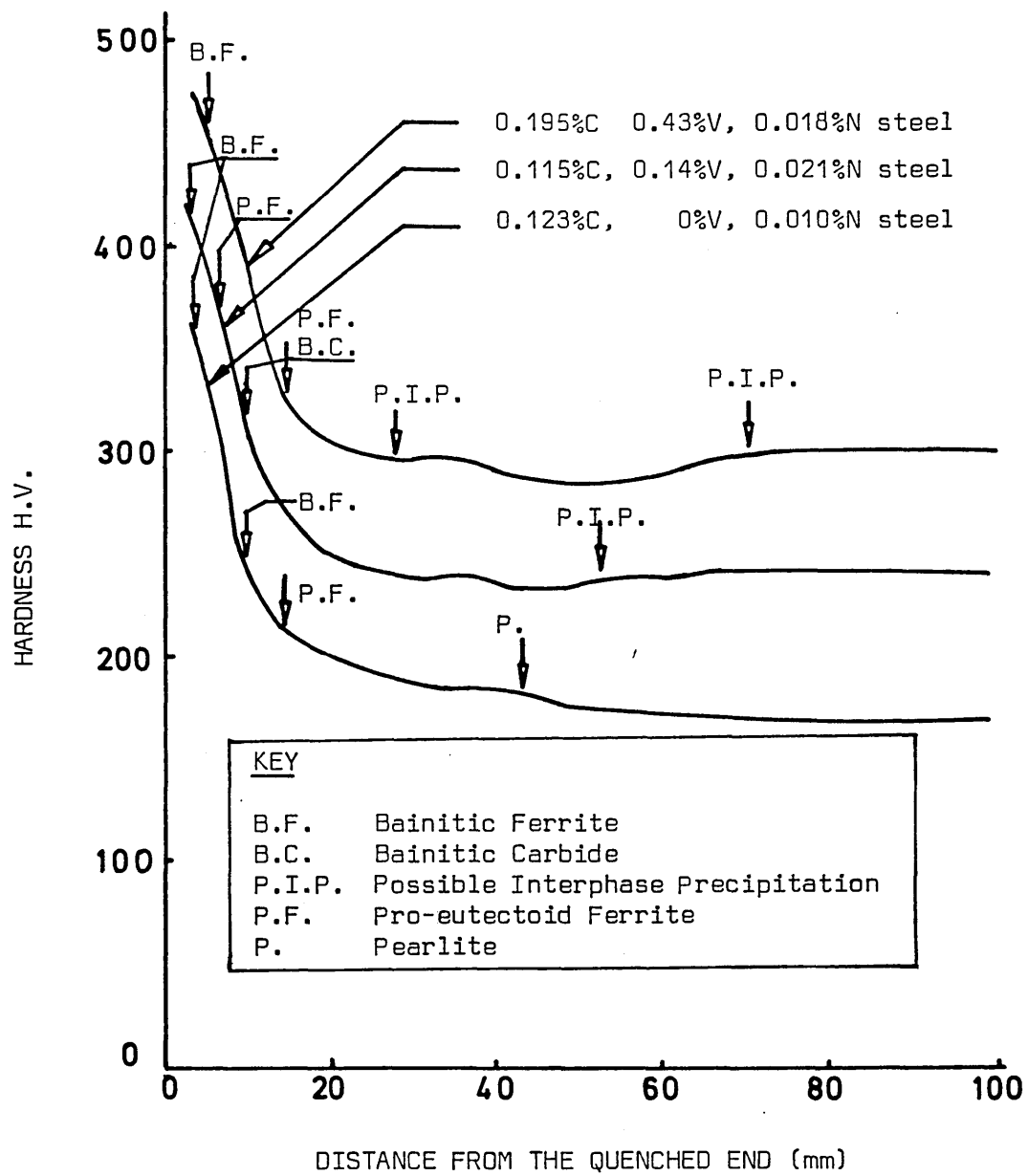
FIG. 76 EFFECT OF CARBON VANADIUM AND NITROGEN ON THE
HARDENABILITY CURVES 1.6%Mn STEEL

a.

1.6 mm FROM THE QUENCHED END
X100

0.123%C, 0.010%N V-FREE
STEEL

b.

24 mm FROM THE QUENCHED END
X100

0.123%C, 0.010%N V-FREE
STEEL

c.

75.5 mm FROM THE QUENCHED END
X100

0.123%, 0.010%N V-FREE
STEEL

d.

1.2 mm FROM THE QUENCHED END
X100

0.115%C, 0.14%V, 0.021%N
STEEL

e.

12.5 mm FROM THE QUENCHED END
X500

0.115%C, 0.14%V, 0.021%N
STEEL

f.

57.2 mm FROM THE QUENCHED END
X100

0.115%C, 0.14%V, 0.021%N
STEEL

g.

7.2 mm FROM THE QUENCHED END
X100

0.195%C, 0.43%V, 0.018%N
STEEL

h.

76 mm FROM THE QUENCHED END
X200

0.195%C, 0.43%V, 0.018%N
STEEL

FIG. 77   TYPICAL MICROSTRUCTURES FROM MODIFIED JOMINY TEST PIECES
AFTER AUSTENITISING AT 1250°C AND END QUENCHED COOLED

a.

b.

c.

d.

e.

f.

g.

270β

h.
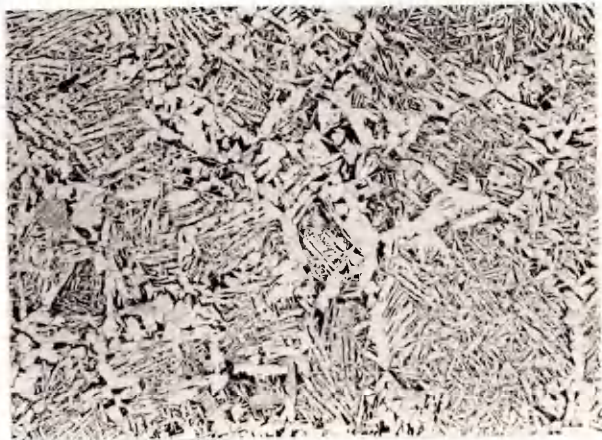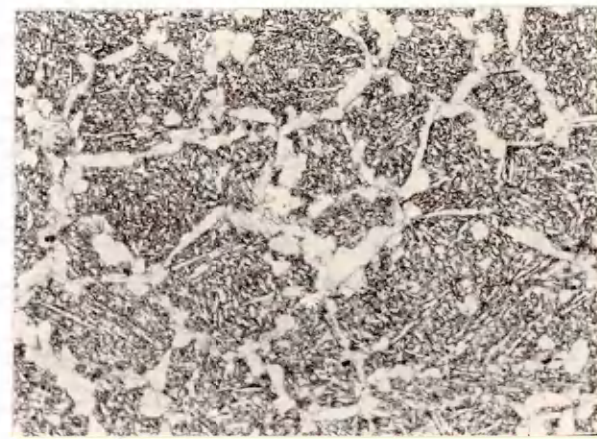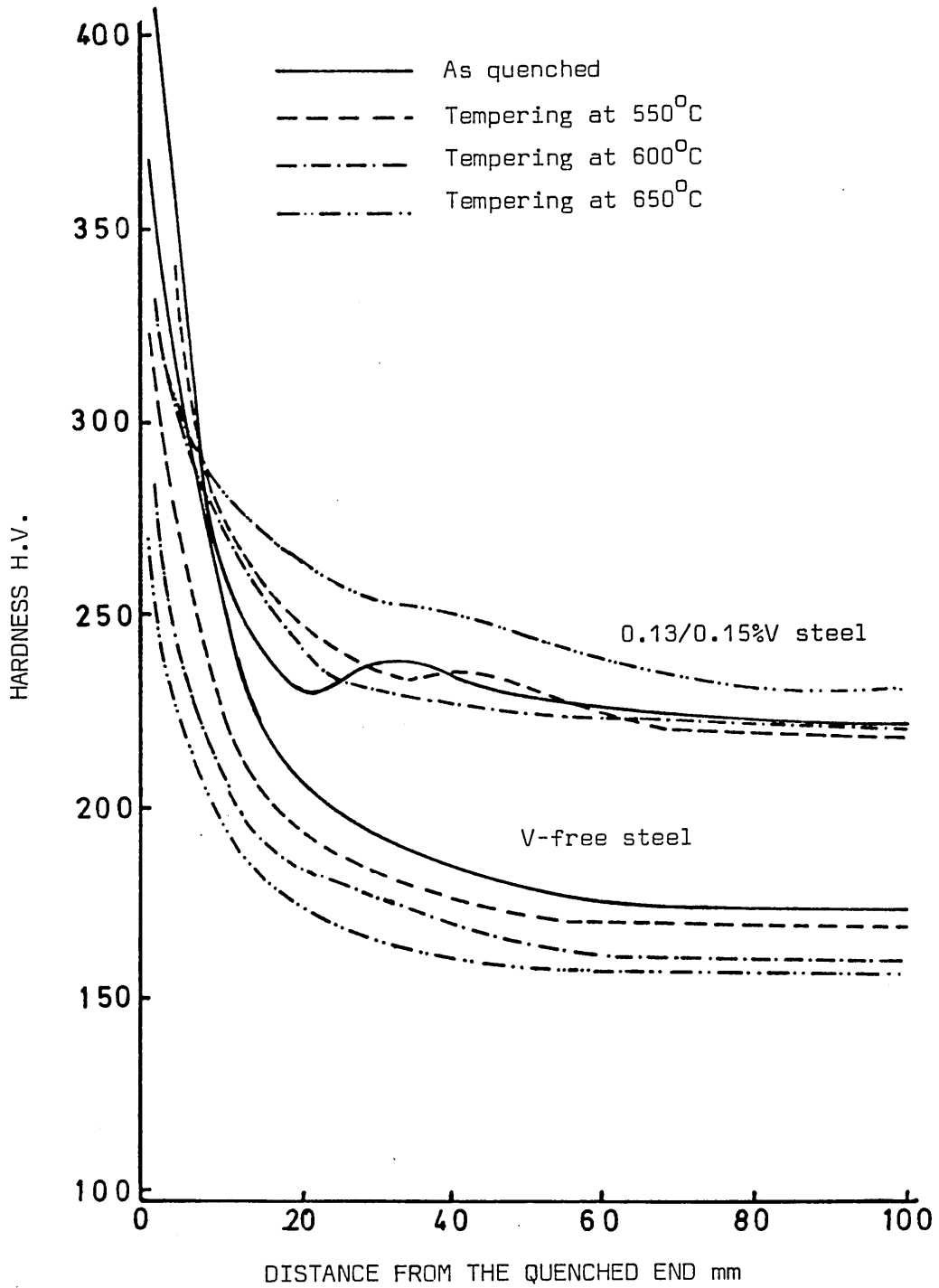
FIG. 78   TEMPERING OF JOMINY BARS IN V-FREE 0.128%C, 1.70%Mn,
          0.0075%N STEEL AND 0.12%C, 0.13/0.15%V, 1.60%Mn,
          0.010%N STEEL AFTER AUSTENITISING AT 1075°C

271
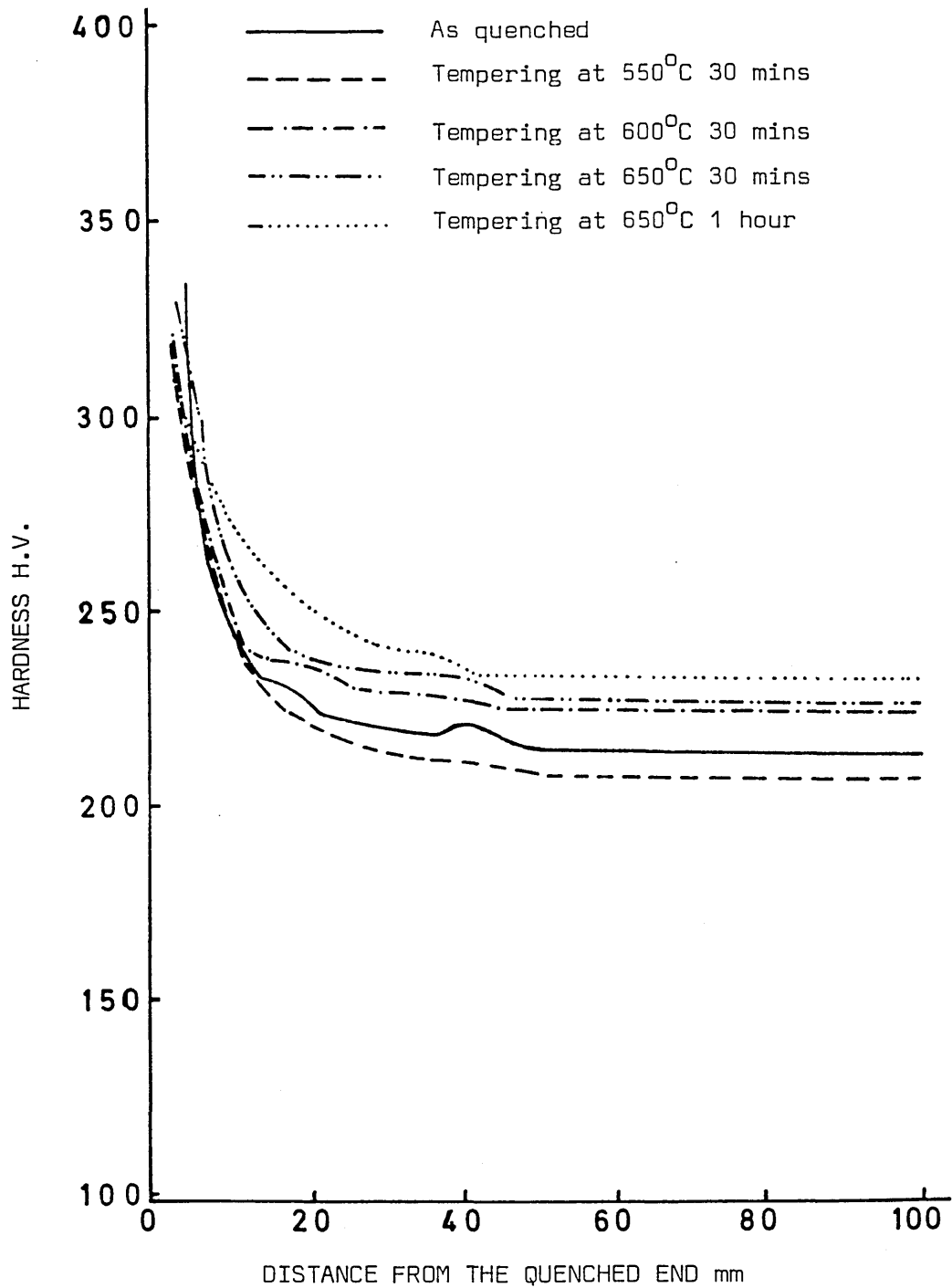
FIG. 79   EFFECT OF TEMPERING OF JOMINY BARS FOR 0.12%C,
0.13/0.15%V, 0.010%N STEEL AFTER AUSTENITISING AT
1250°C

Tempering for 30 minutes at 650°C
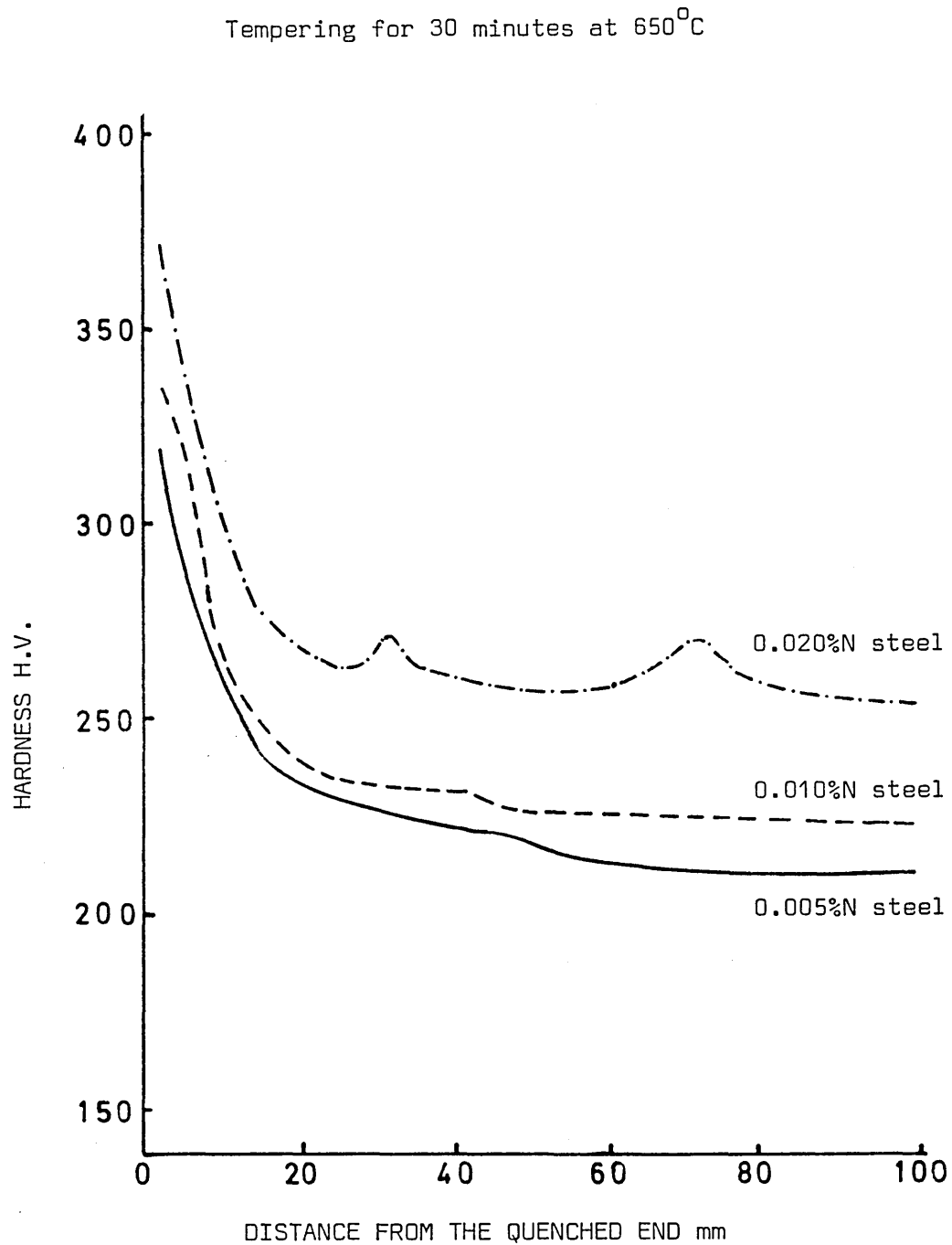
FIG. 80   EFFECT OF INCREASING NITROGEN ON THE TEMPERING OF
JOMINY BARS AFTER AUSTENITISING AT 1250°C

273
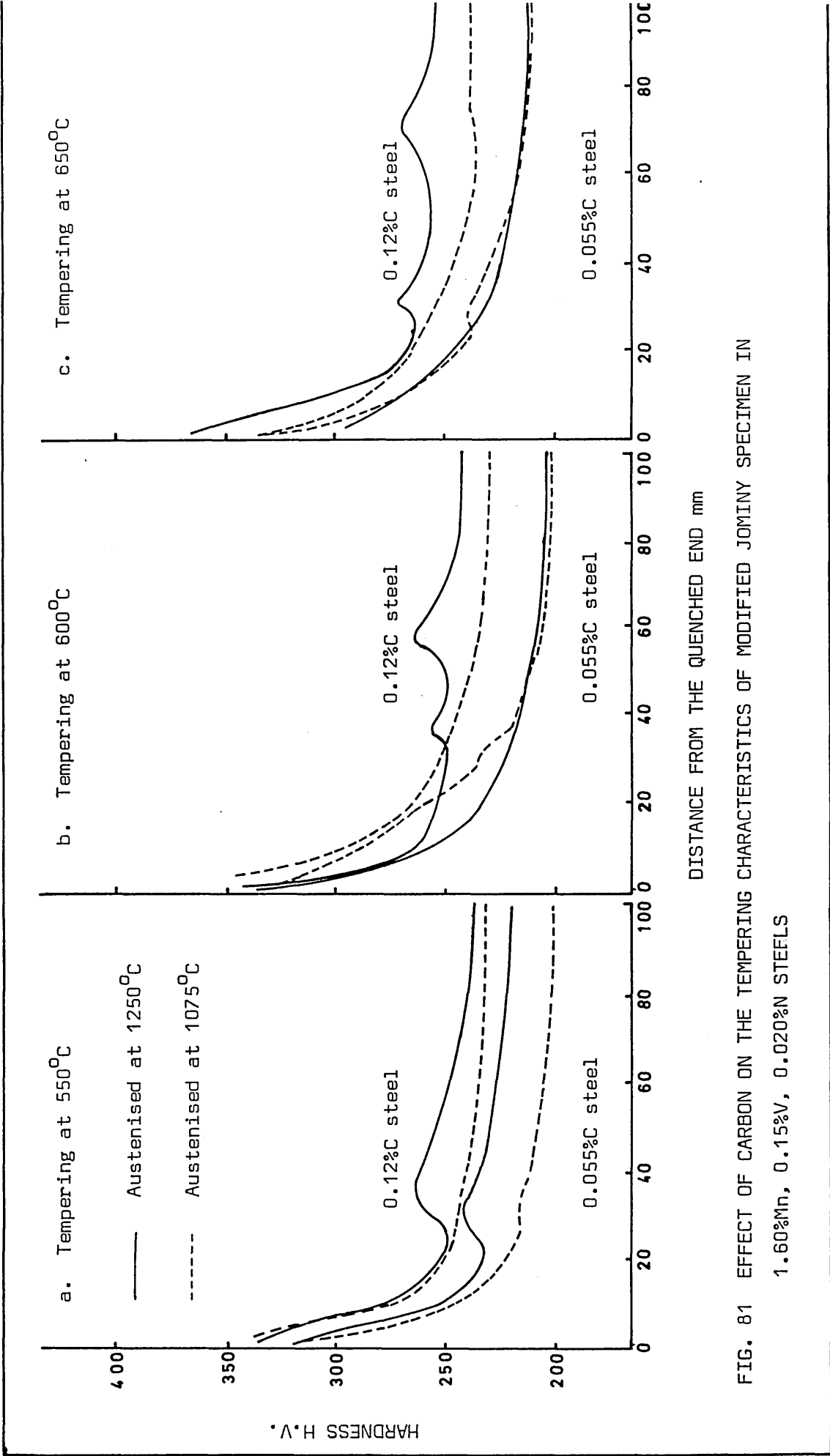
FIG. 81 EFFECT OF CARBON ON THE TEMPERING CHARACTERISTICS OF MODIFIED JOMINY SPECIMEN IN

1.60%Mn, 0.15%V, 0.020%N STEELS

274

a. Tempered for half hour
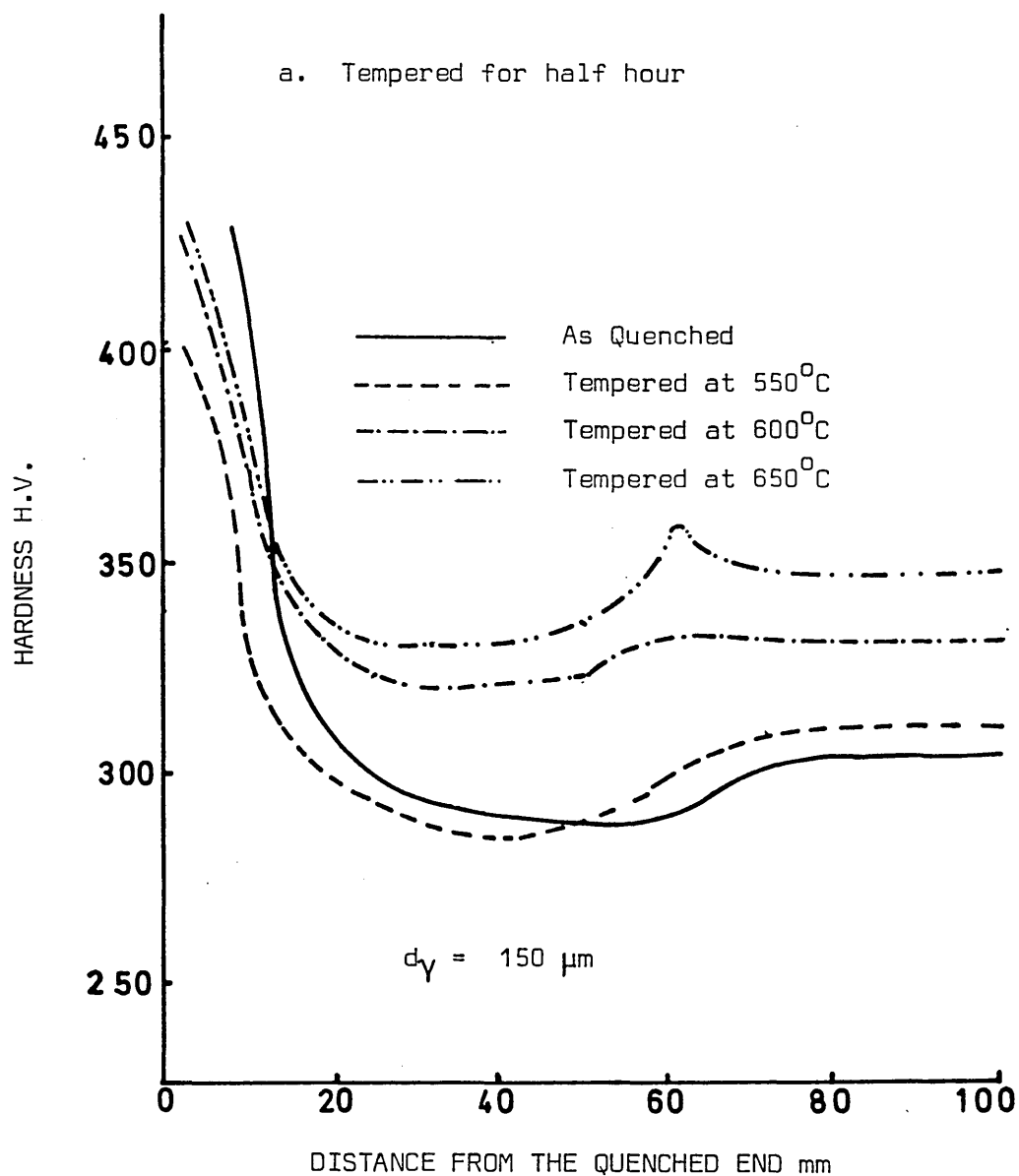
FIG. 82 MODIFIED JOMINY HARDNESS CURVES FOR 0.195%C, 0.43%V, 0.018%N STEEL AUSTENISED AT 1250°C AND THEN TEMPERED

a. 0.12%C, 1.60%Mn, 0.010%N, V-free steel

30% reduction

50% reduction

70% reduction

RECRYSTALLISED AUSTENITE GRAIN SIZE μm (m.l.i.)

DEFORMATION TEMPERATURE °C

b. Effect of Vanadium in 0.010%N steel

30% reduction at 1200°C

30% reduction at 1050°C
50% reduction at 1200°C
50% reduction at 1050°C
70% reduction at 1200°C
70% reduction at 1050°C

MASS % VANADIUM
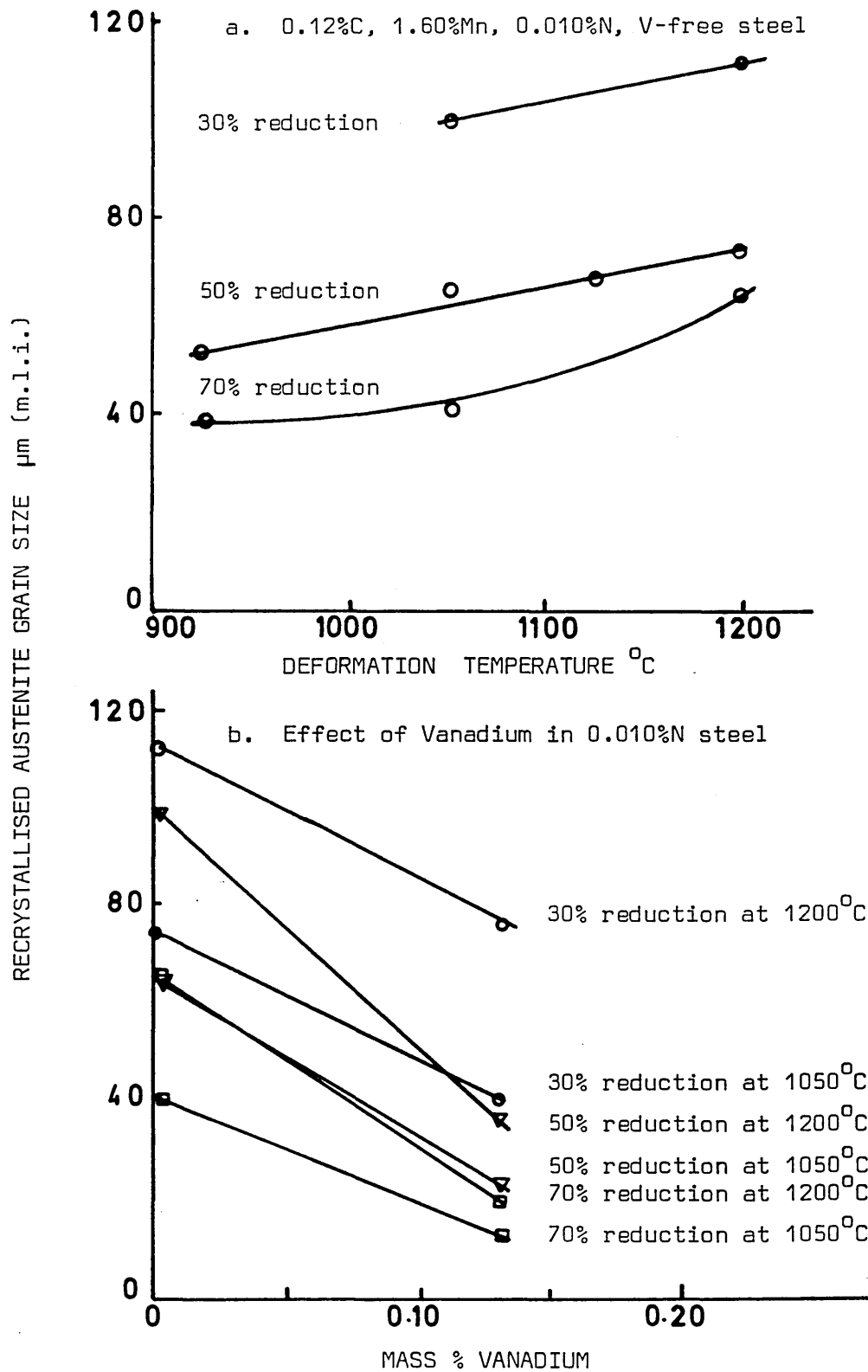
FIG. 83 EFFECT OF VANADIUM ON THE RELATIONSHIP BETWEEN
DEFORMATION TEMPERATURE, AMOUNT OF DEFORMATION AND
RECRYSTALLISED AUSTENITE GRAIN SIZE.

276

a.

50% REDUCTION AT 1200°C
X200

b.
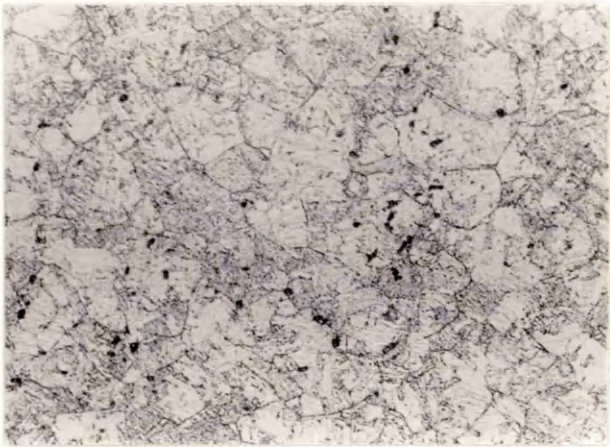
50% REDUCTION AT 1050°C
X100

c.

50% REDUCTION AT 925°C
X200

d.
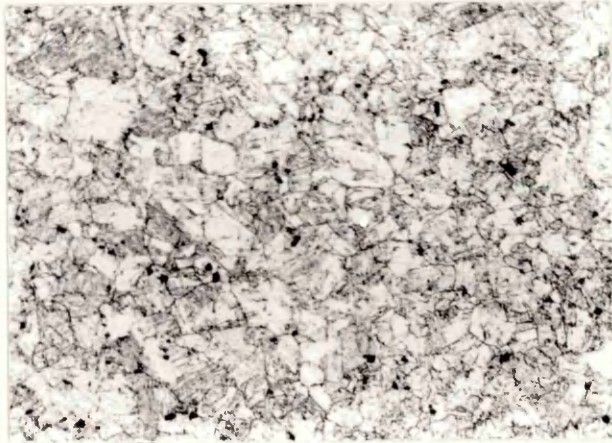
50% REDUCTION AT 825°C
X200

FIG. 84 TYPICAL MICROSTRUCTURES OF THERMO-MECHANICALLY PROCESSED
0.12%C, 1.60%Mn, 0.0%V, 0.010%N STEEL

277

a.

50% REDUCTION AT 1200°C
X200

b.

50% REDUCTION AT 1050°C
X200

c.

50% REDUCTION AT 925°C
X200

d.
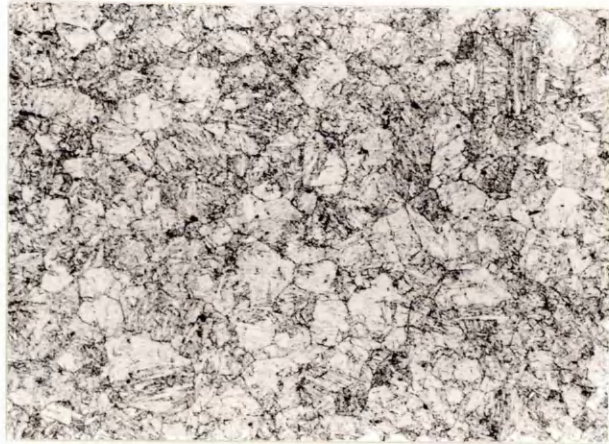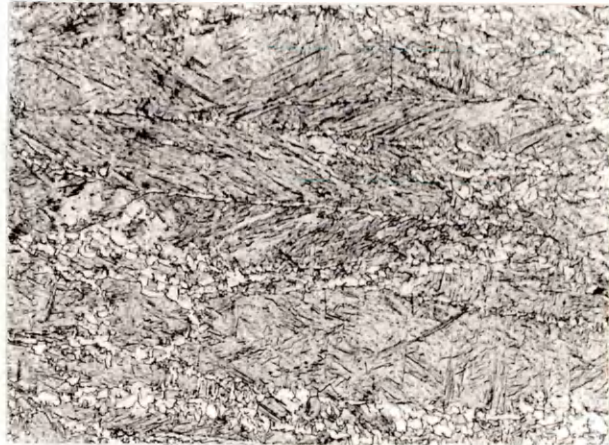
50% REDUCTION AT 825°C
10 SECONDS AT 750° W. Q.
X500

FIG. 85   TYPICAL MICROSTRUCTURES OF THERMO-MECHANICALLY PROCESSED
0.12%C, 1.58%Mn, 0.13/0.19%V, 0.010%N STEEL

278
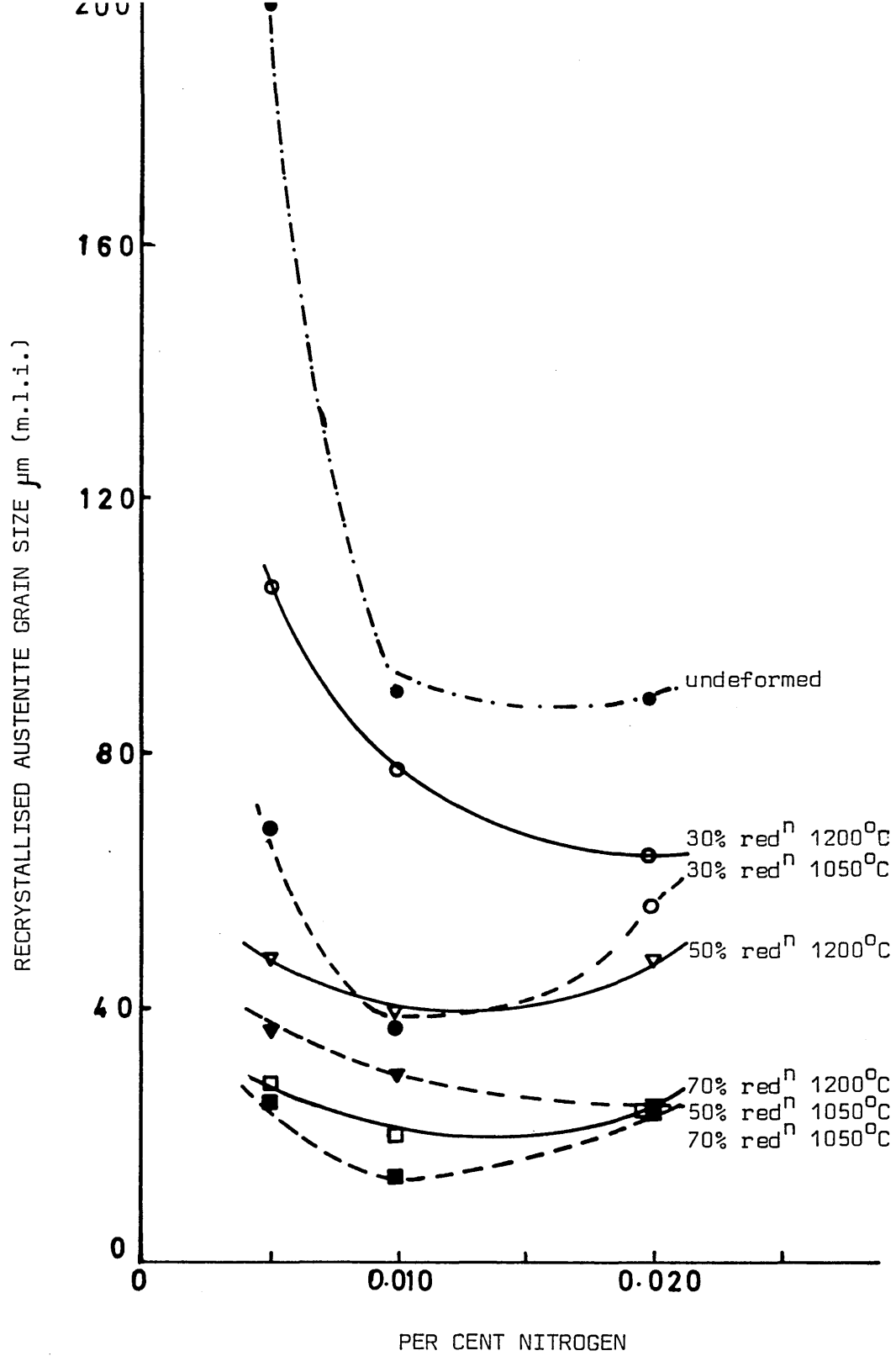
FIG. 86 EFFECT OF NITROGEN ON THE RECRYSTALLISED AUSTENITE
GRAIN SIZE IN 0.12%C STEELS, FOR DIFFERENT THERMO-
MECHANICAL PROCESSING CONDITIONS

279

a.

70% REDUCTION AT 1200°C
X200

b.

50% REDUCTION AT 925°C
X100

c.

70% REDUCTION AT 925°C
X200

d.
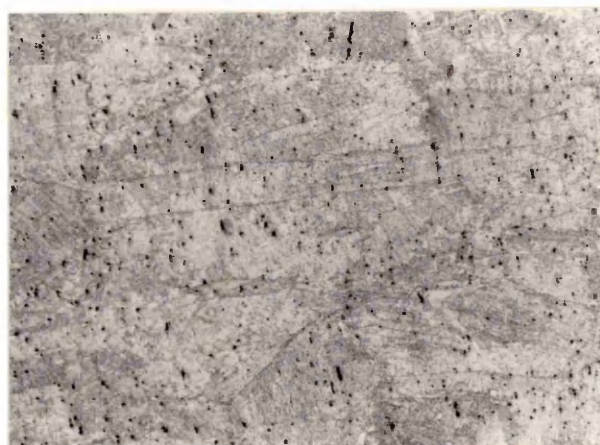
30% REDUCTION AT 875°C
X100

FIG. 87   TYPICAL MICROSTRUCTURES OF THERMO-MECHANICALLY PROCESSED
0.11%C, 1.50%Mn, 0.14%V, 0.005%N STEEL

a.

70% REDUCTION AT 1200°C
X200

b.

50% REDUCTION AT 1050°C
X200

c.
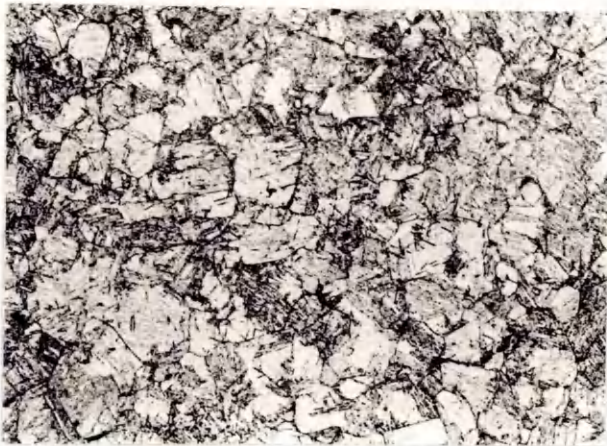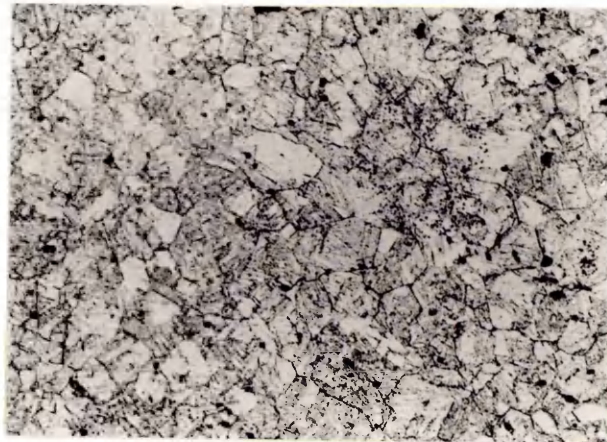
50% REDUCTION AT 925°C
X80

d.

50% REDUCTION AT 875°C
X200

FIG. 88 TYPICAL MICROSTRUCTURES OF THERMO-MECHANICALLY PROCESSED
0.12%C, 1.77%Mn, 0.15%V, 0.020%N STEEL
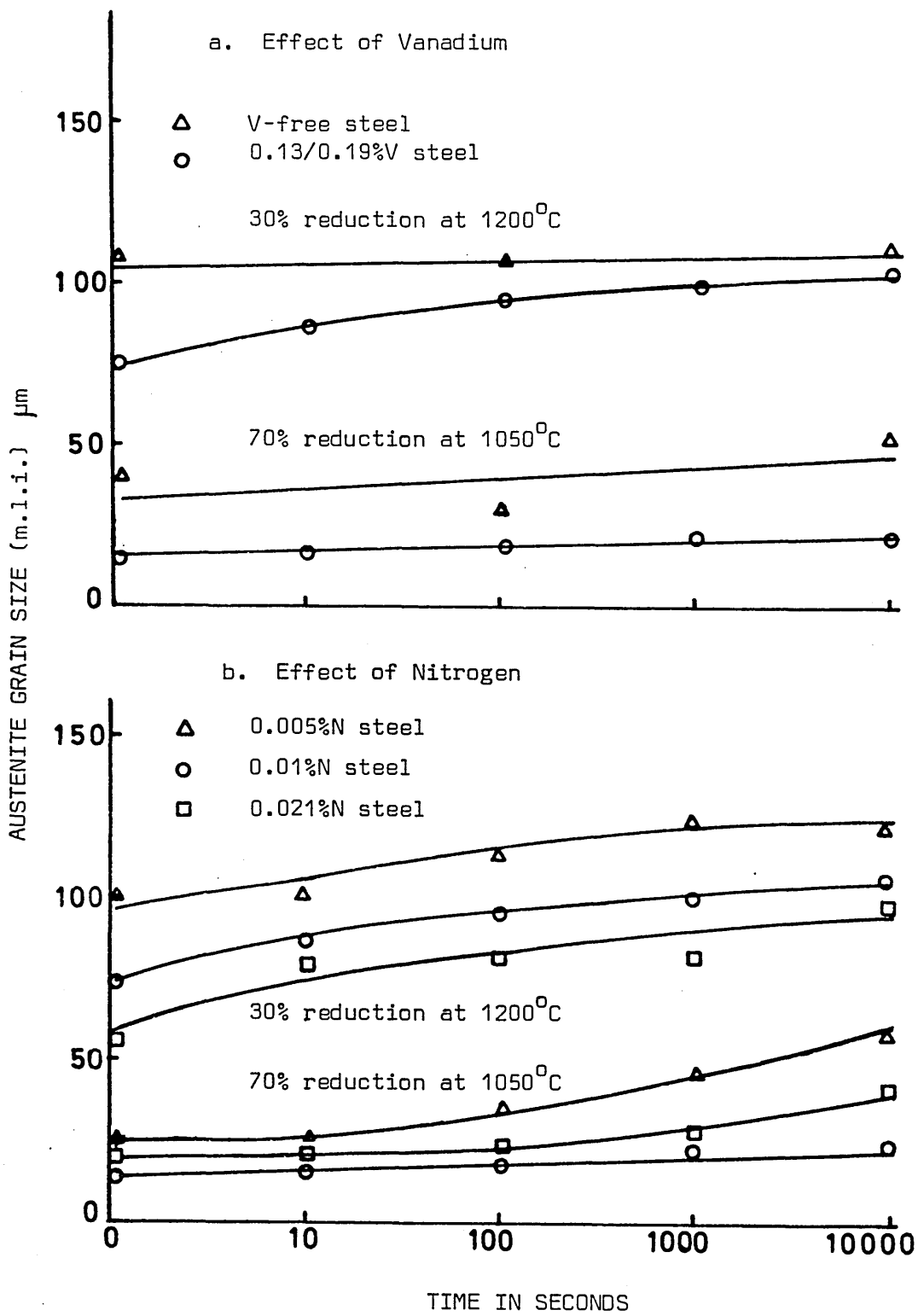
FIG. 89 EFFECT OF VANADIUM AND NITROGEN ON THE GRAIN
COARSENING CHARACTERISTICS AT 925°C
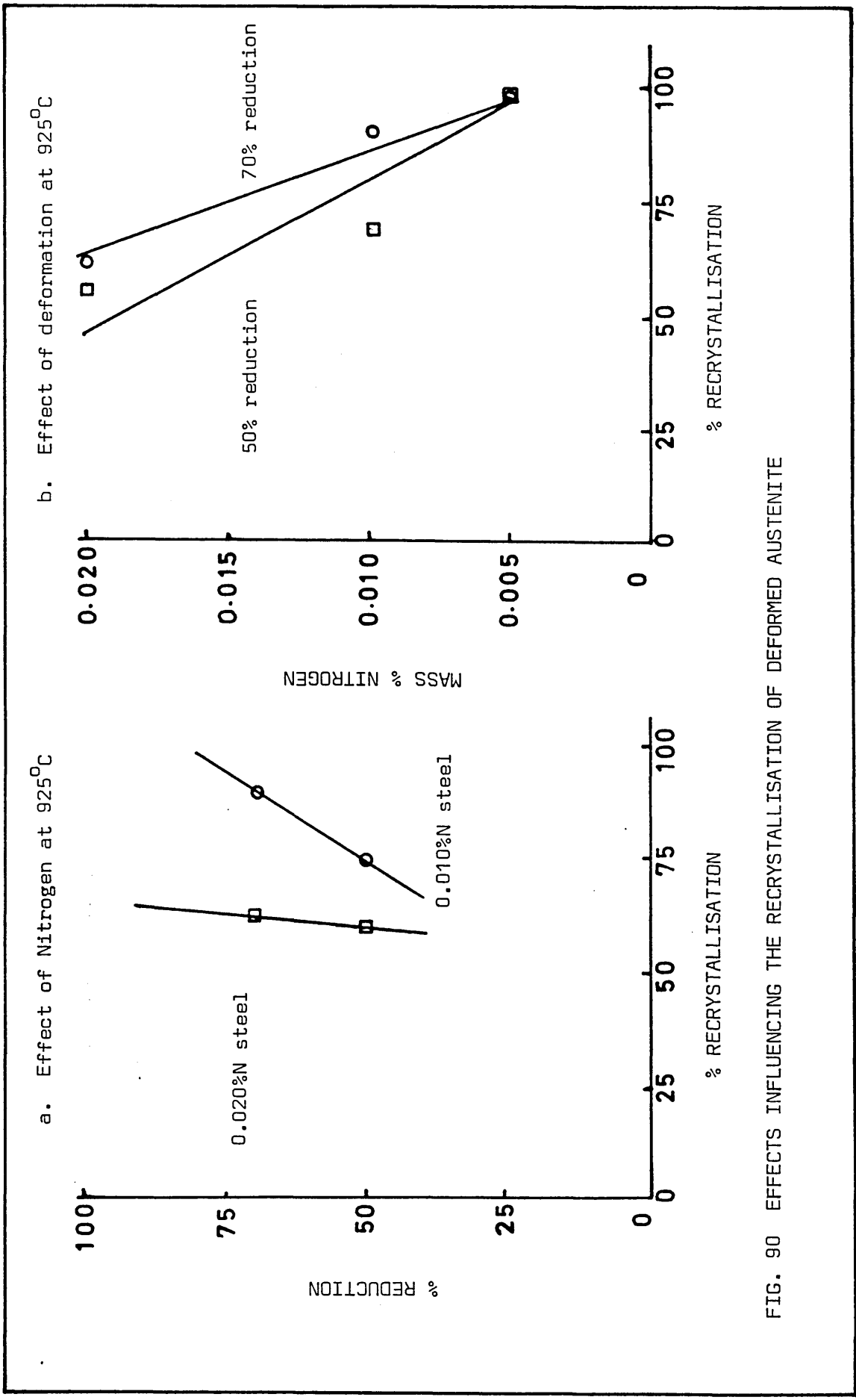
FIG. 90 EFFECTS INFLUENCING THE RECRYSTALLISATION OF DEFORMED AUSTENITE

283

a. 0.123%C, 1.6%Mn, 0.010%N steel

○   30% reduction
△   50% reduction
□   70% reduction

DEFORMATION TEMPERATURE °C

b. 0.12%C, 1.4/1.6%Mn, 0.13/0.19%V,
    0.010%N steel

70% redn

50% redn

30% redn

DEFORMATION TEMPERATURE °C

$S_{v\gamma}$ mm⁻¹
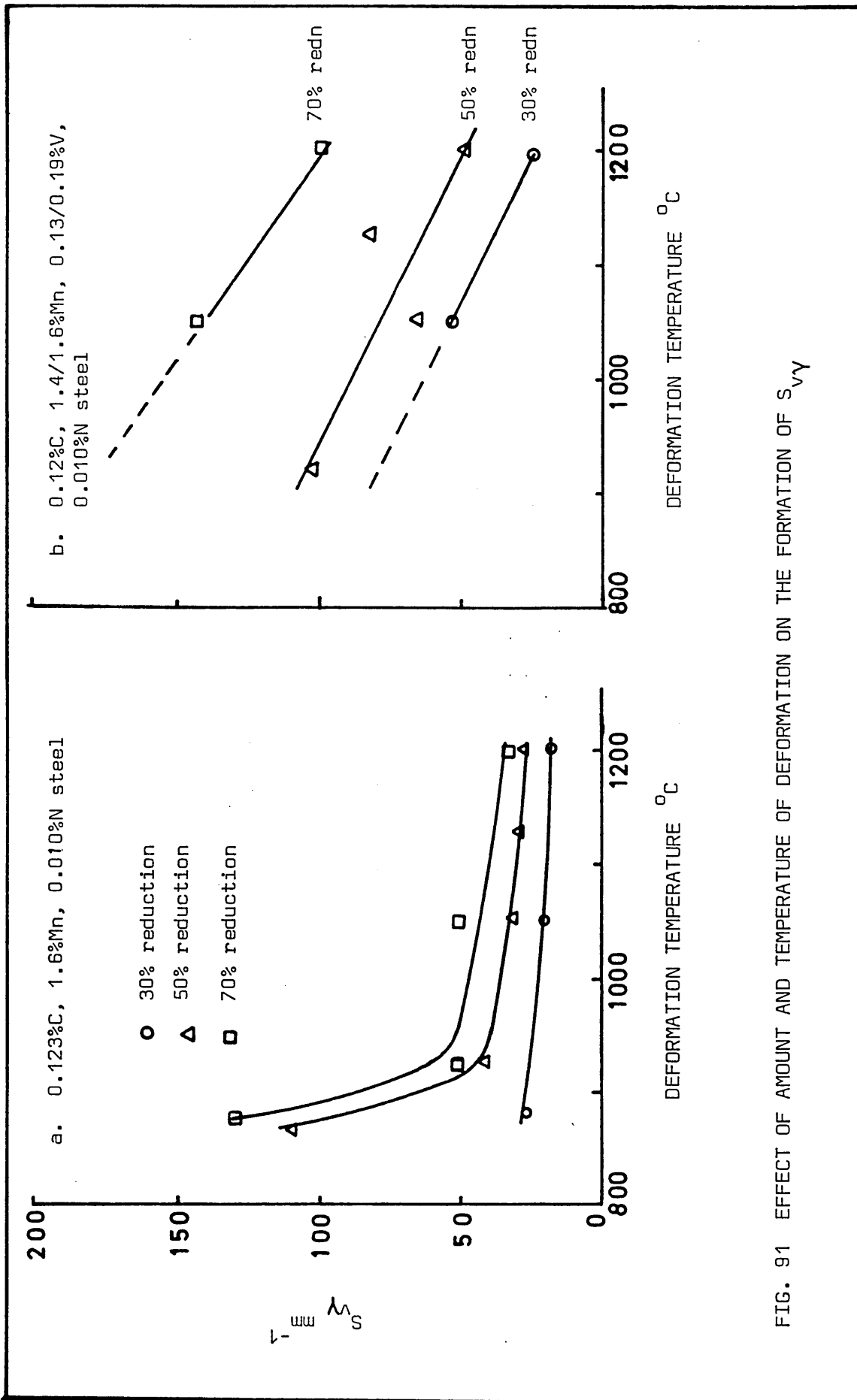
FIG. 91 EFFECT OF AMOUNT AND TEMPERATURE OF DEFORMATION ON THE FORMATION OF $S_{v\gamma}$
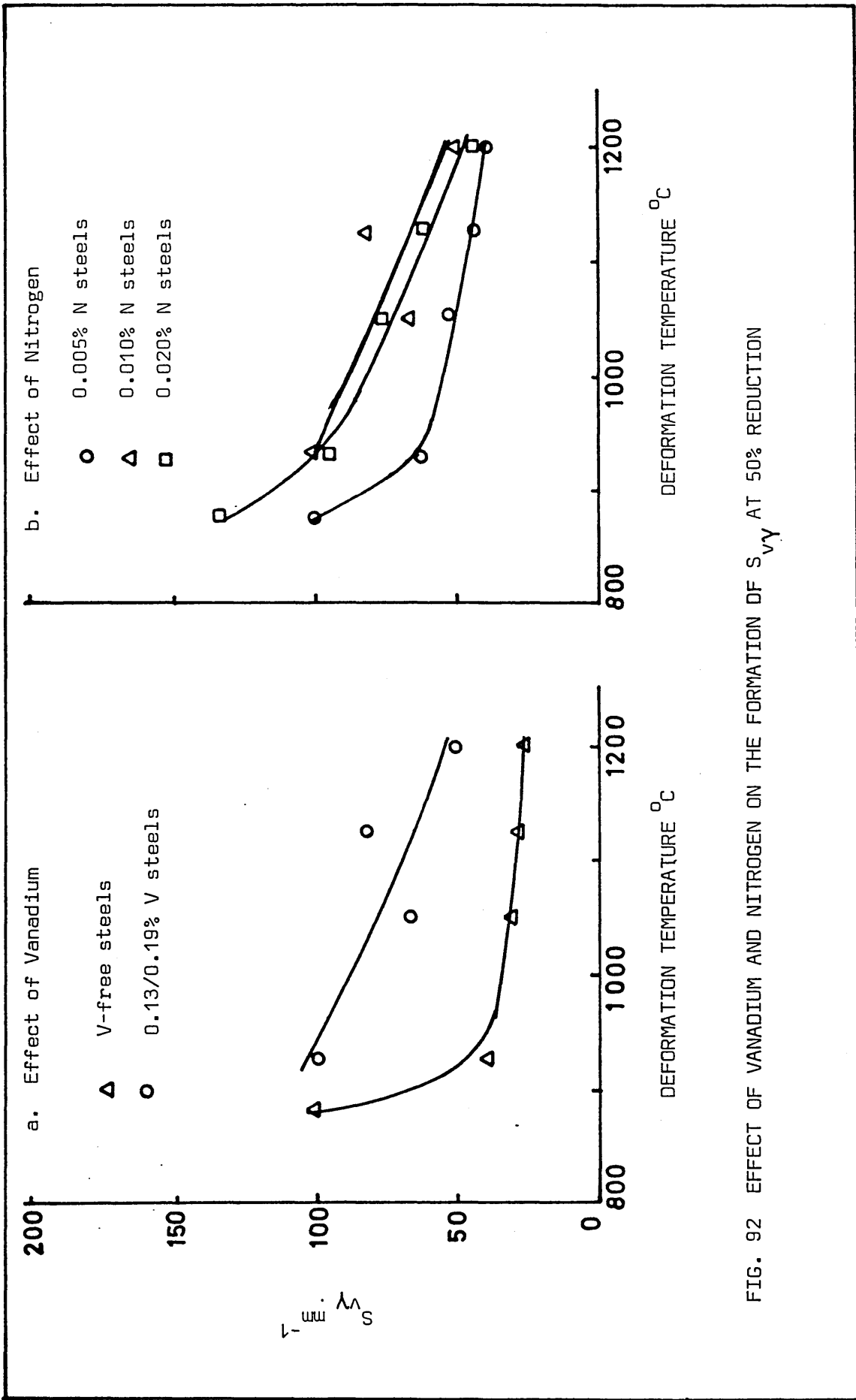
FIG. 92   EFFECT OF VANADIUM AND NITROGEN ON THE FORMATION OF $S_{v\gamma}$ AT 50% REDUCTION
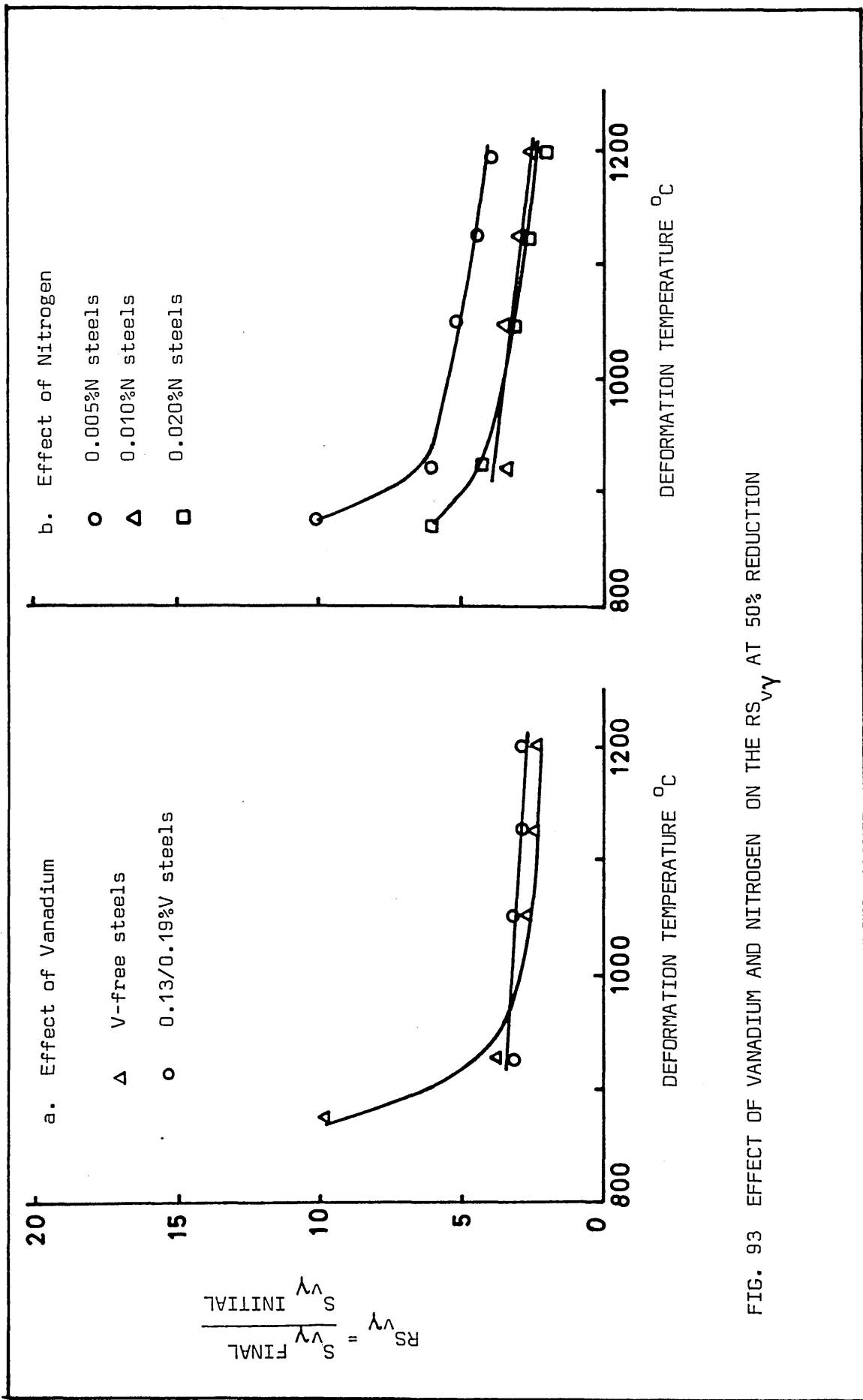
FIG. 93 EFFECT OF VANADIUM AND NITROGEN ON THE $RS_{v\gamma}$ AT 50% REDUCTION

$$RS_{v\gamma} = \frac{S_{v\gamma} \text{ FINAL}}{S_{v\gamma} \text{ INITIAL}}$$

286
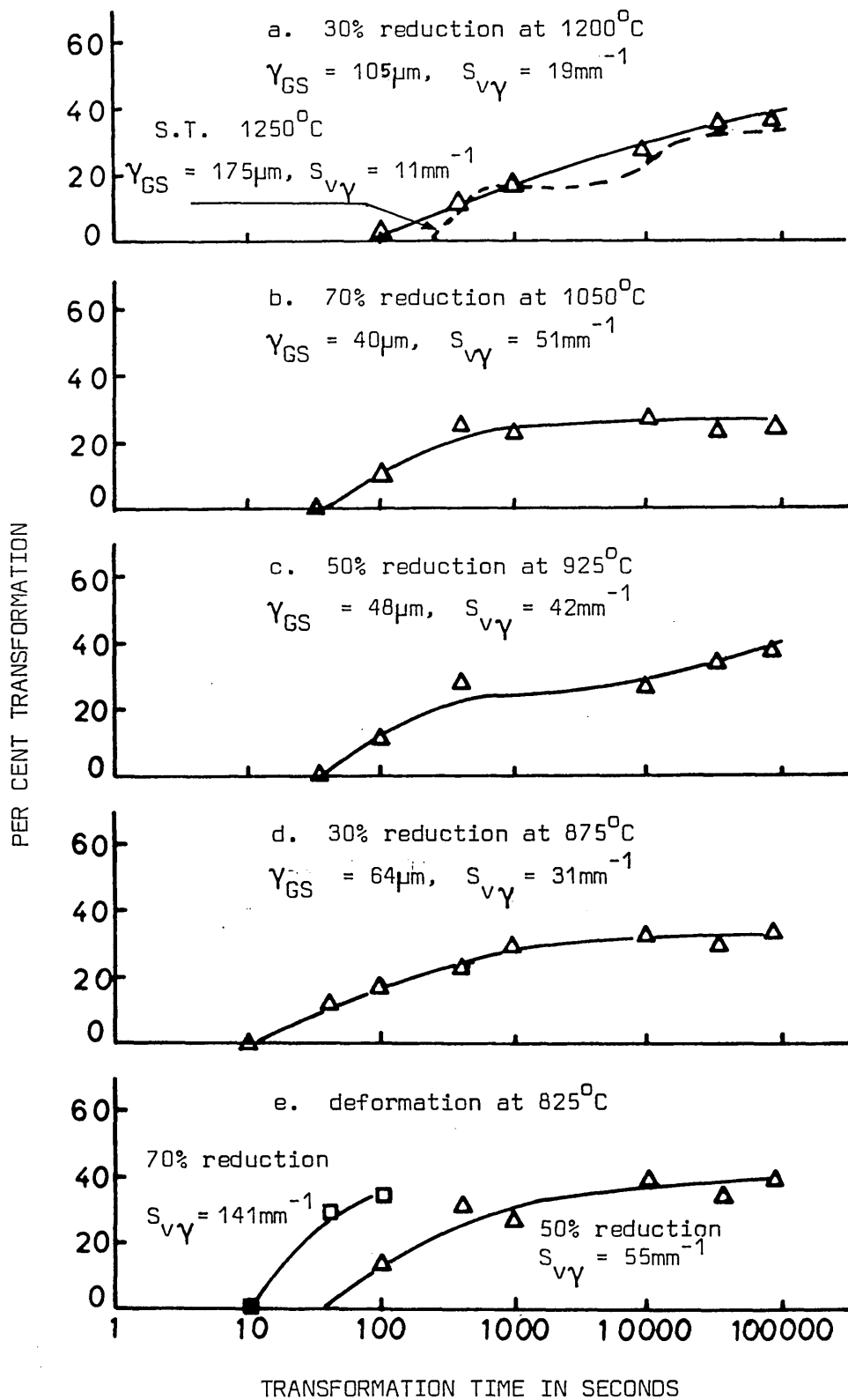
FIG. 94 EFFECT OF DEFORMATION PRIOR TO ISOTHERMAL TRANSFORMATION
AT 750°C IN 0.12%C, 1.60/1.70%Mn, AND 0.0075/0.01%N
STEELS

287

a. 30% REDUCTION AT 1200°C
ISOTHERMALLY TRANSFORMED AT
750°C FOR 24 HOURS W. Q. X200
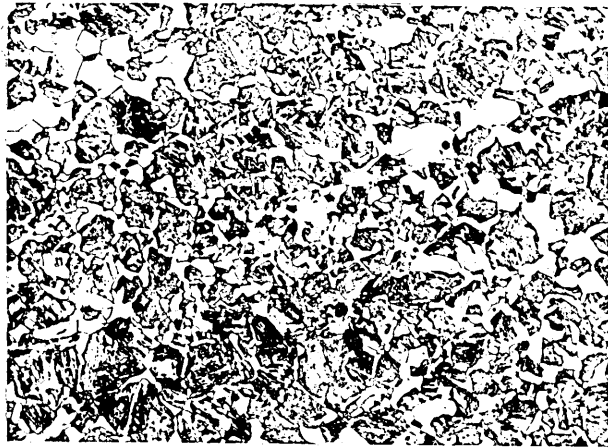
b. 70% REDUCTION AT 1050°C
ISOTHERMALLY TRANSFORMED AT
750°C FOR 1000 SECONDS W. Q. X200
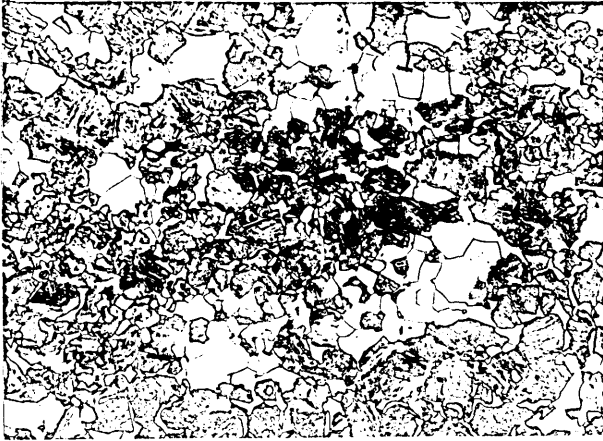
c. 50% REDUCTION AT 925°C
ISOTHERMALLY TRANSFORMED AT
750°C FOR 3 HOURS W. Q. X200
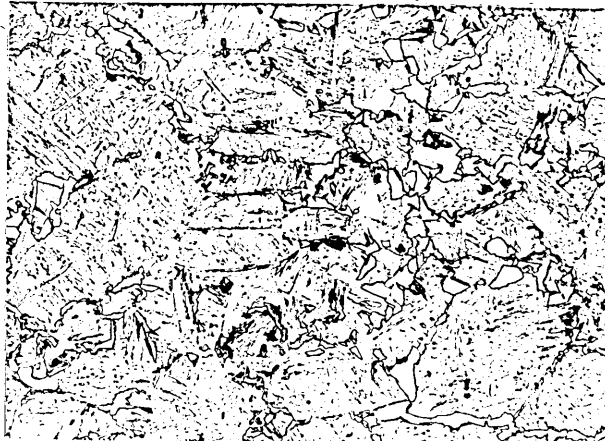
d. 30% REDUCTION AT 875°C
ISOTHERMALLY TRANSFORMED AT
750°C FOR 100 SECS W. Q. X200

e. 50% REDUCTION AT 825°C
ISOTHERMALLY TRANSFORMED AT
750°C FOR 100 SECONDS W. Q. X200

f. 50% REDUCTION AT 825°C
ISOTHERMALLY TRANSFORMED AT
750°C FOR 12 HOURS W. Q. X200

FIG. 95 PARTIALLY TRANSFORMED MICROSTRUCTURES AFTER THERMO-MECHANICAL
PROCESSING OF 0.12%C, 1.6/1.7%Mn, 0.005/0.0075%N VANADIUM-
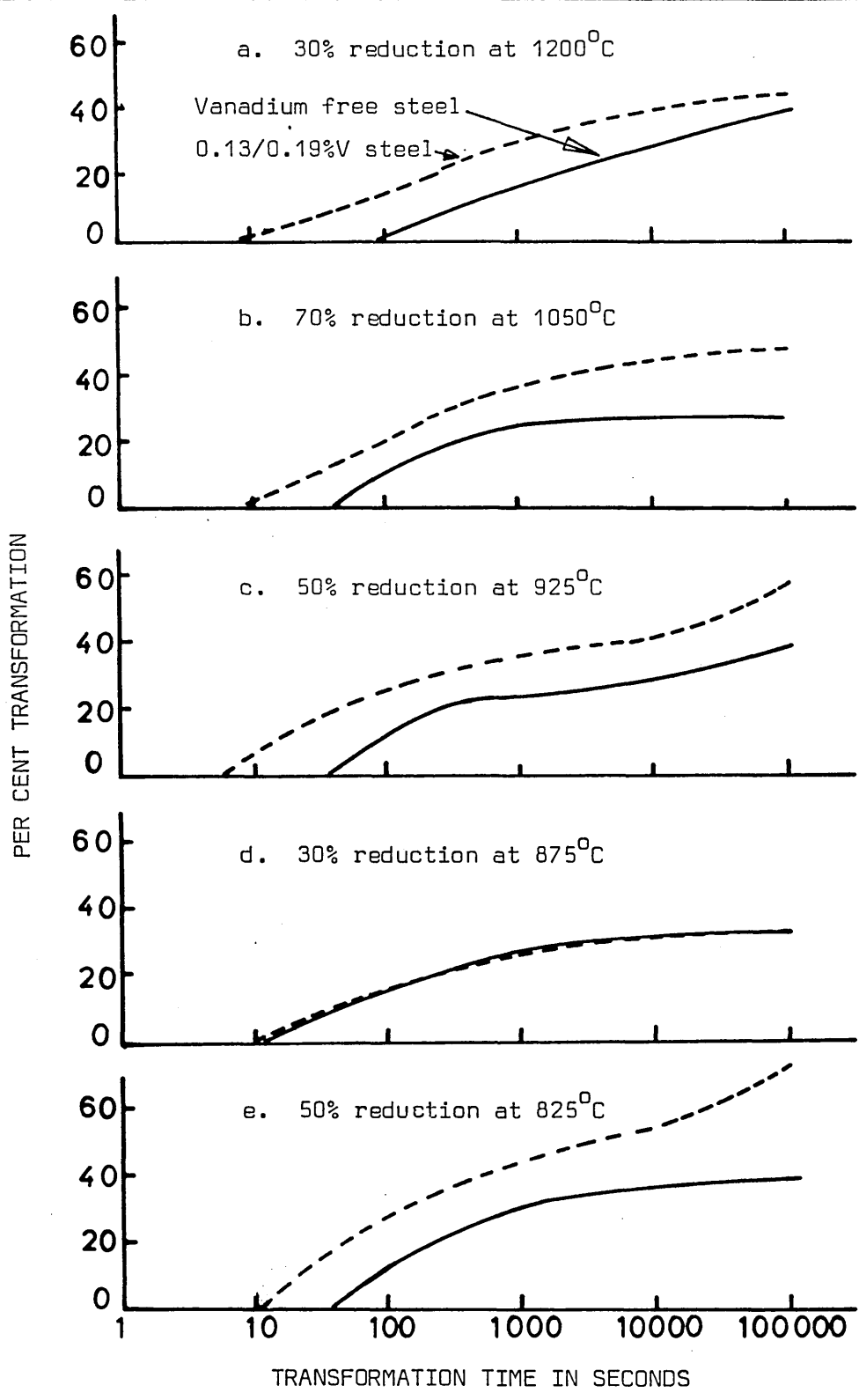FREE STEEL
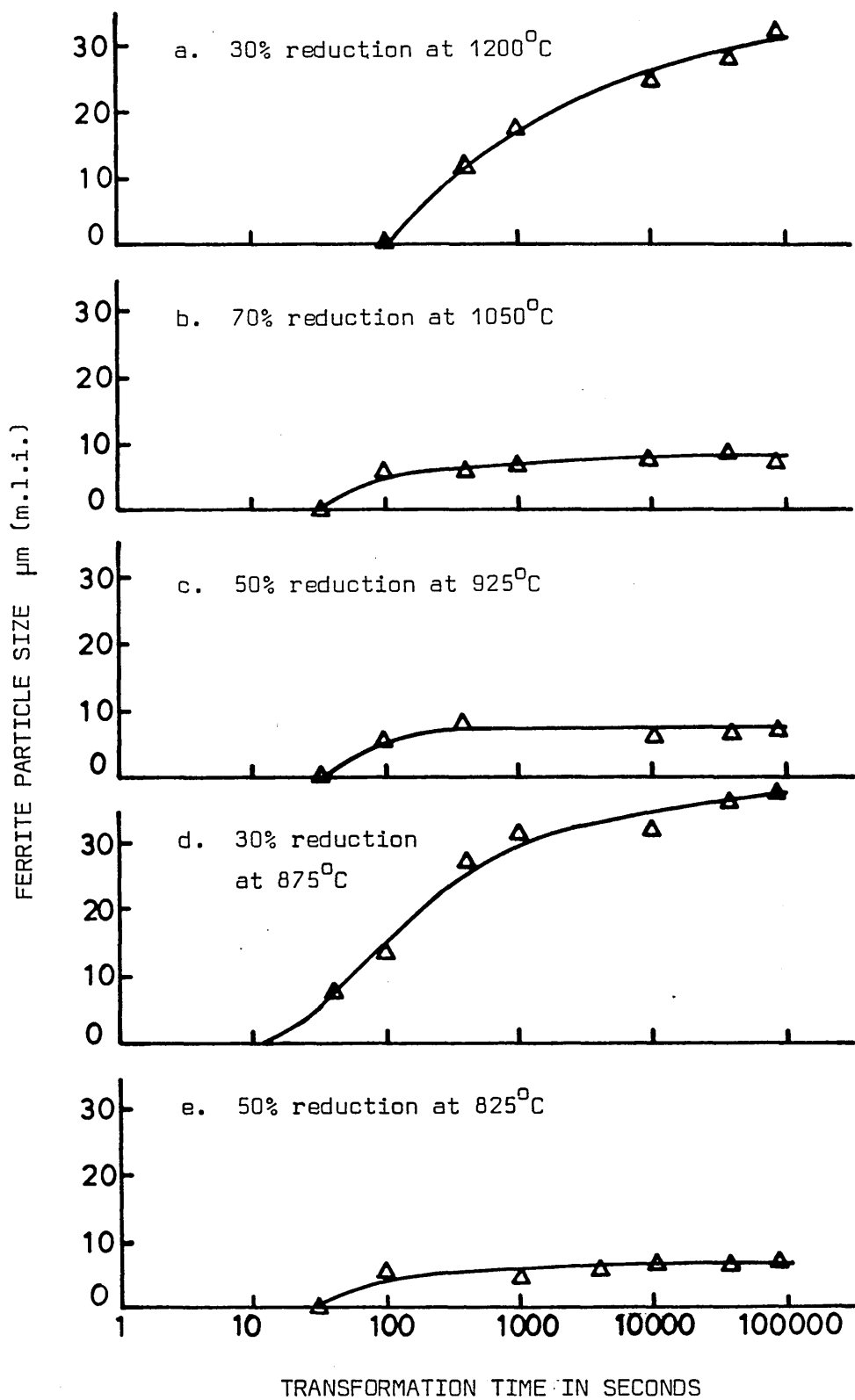
FIG. 96   EFFECT OF DEFORMATION PRIOR TO ISOTHERMAL TRANSFORMATION
AT 750°C ON THE FERRITE PARTICLE SIZE IN 0.12%C,
1.60/1.70%Mn   AND   0.0075/0.010%N   STEELS

289
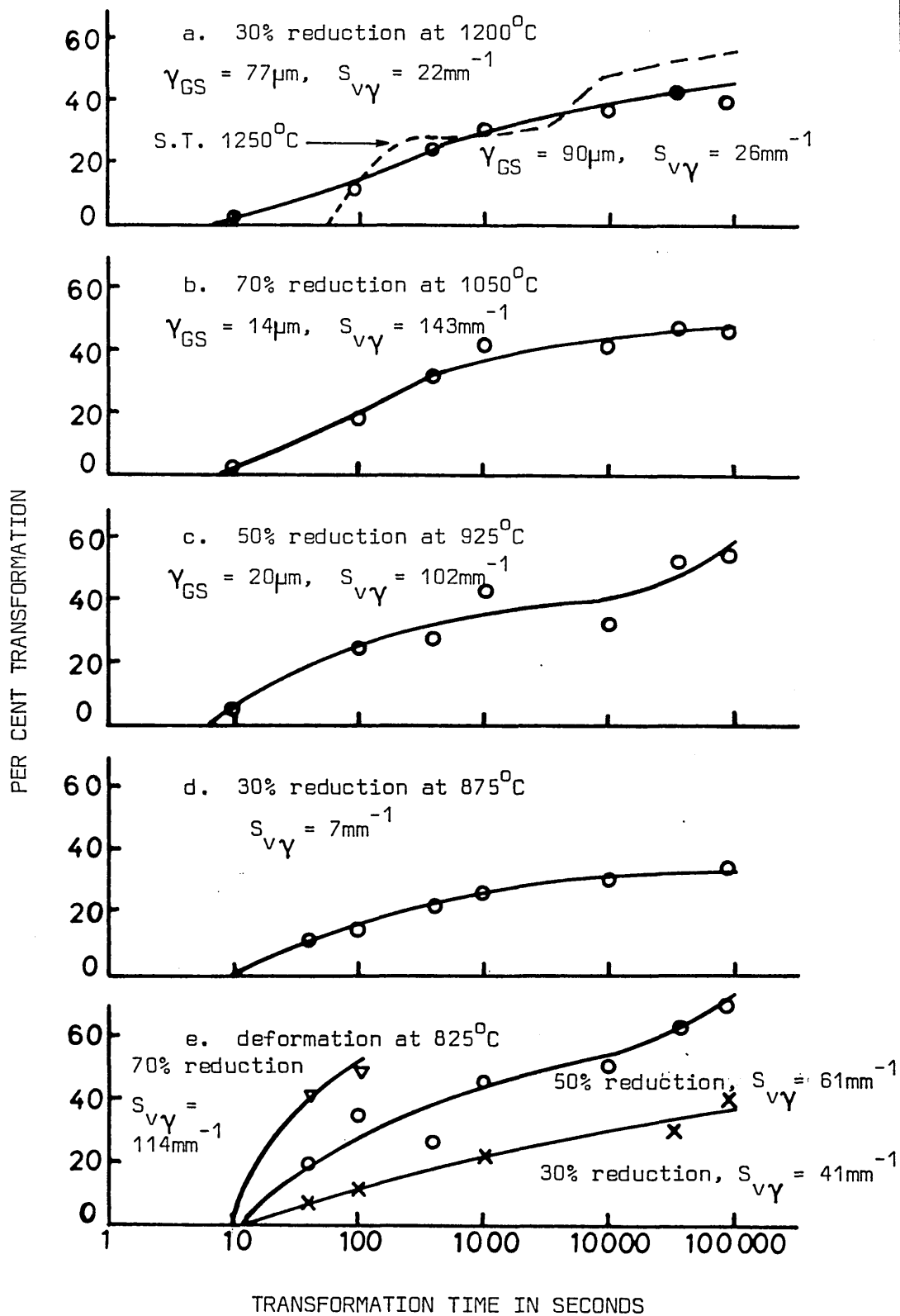
FIG. 97   EFFECT OF DEFORMATION PRIOR TO ISOTHERMAL TRANSFORMATION
AT 750°C IN 0.12%C, 1.4/1.6%Mn, 0.13/0.19%V AND 0.010%N
STEELS
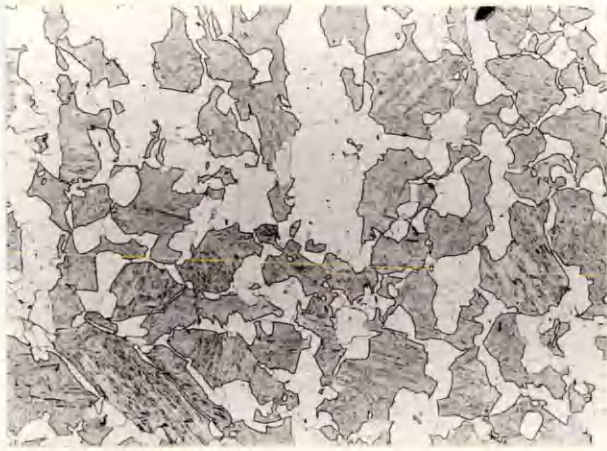
a. 30% REDUCTION AT 1200°C
ISOTHERMALLY TRANSFORMED AT
750°C FOR 24 HOURS W. Q. X200
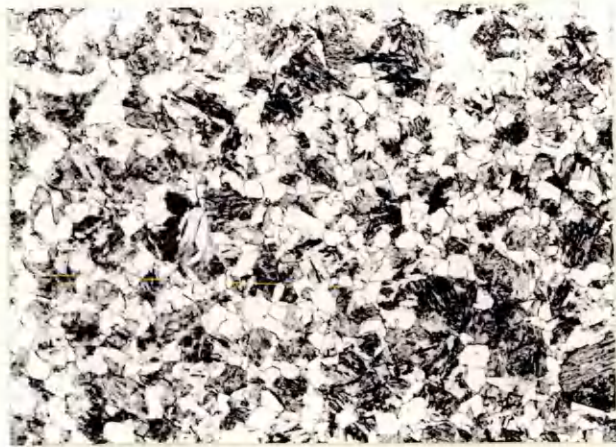
b. 70% REDUCTION AT 1050°C
ISOTHERMALLY TRANSFORMED AT
750°C FOR 100 SECONDS W. Q. X200
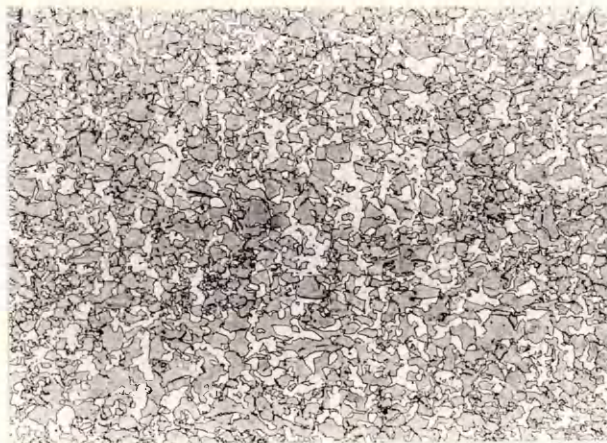
c. 50% REDUCTION AT 925°C
ISOTHERMALLY TRANSFORMED AT
750°C FOR 100 SECONDS W. Q. X50

d. 30% REDUCTION AT 875°C
ISOTHERMALLY TRANSFORMED AT
750°C FOR 1000 SECONDS W. Q. X200

e. 50% REDUCTION AT 825°C
ISOTHERMALLY TRANSFORMED AT
750°C FOR 100 SECONDS W. Q. X200

f. 50% REDUCTION AT 825°C
ISOTHERMALLY TRANSFORMED AT
750°C FOR 24 HOURS W. Q. X200

FIG. 98   PARTIALLY TRANSFORMED MICROSTRUCTURES AFTER THERMO-MECHANICAL
PROCESSING OF 0.12%C, 1.40/1.60%Mn, 0.13/0.19%V, 0.010%N STEEL

291

FIG. 99 EFFECT OF 0.13/0.19%V ADDITION ON THE ISOTHERMAL
TRANSFORMATION AT 750°C IN 0.12/0.13%C, 1.4/1.7%Mn
AND 0.010%N STEELS
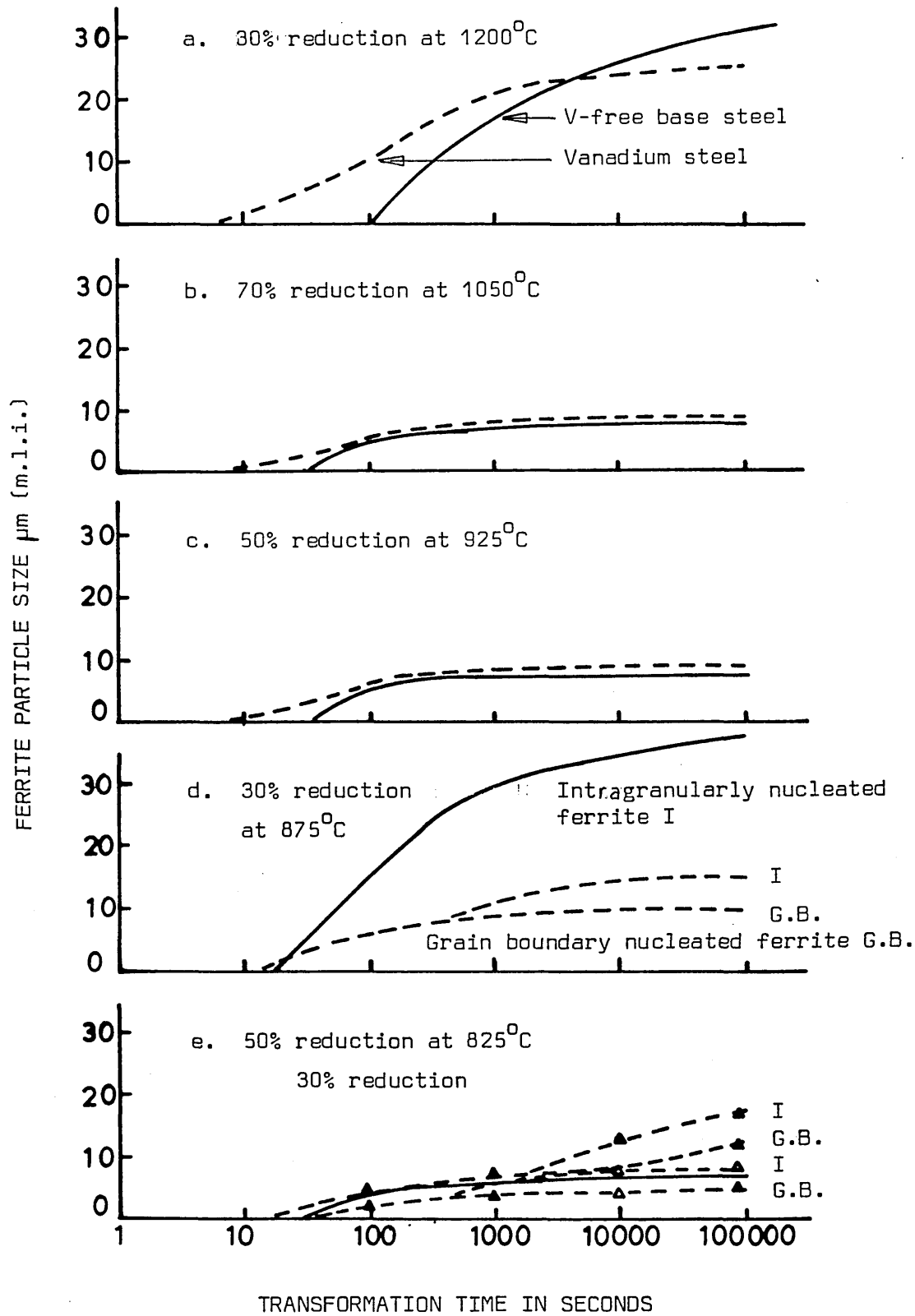
FIG. 100 EFFECT OF 0.13/0.19%V ADDITION ON THE FERRITE
PARTICLE SIZE DURING ISOTHERMAL TRANSFORMATION
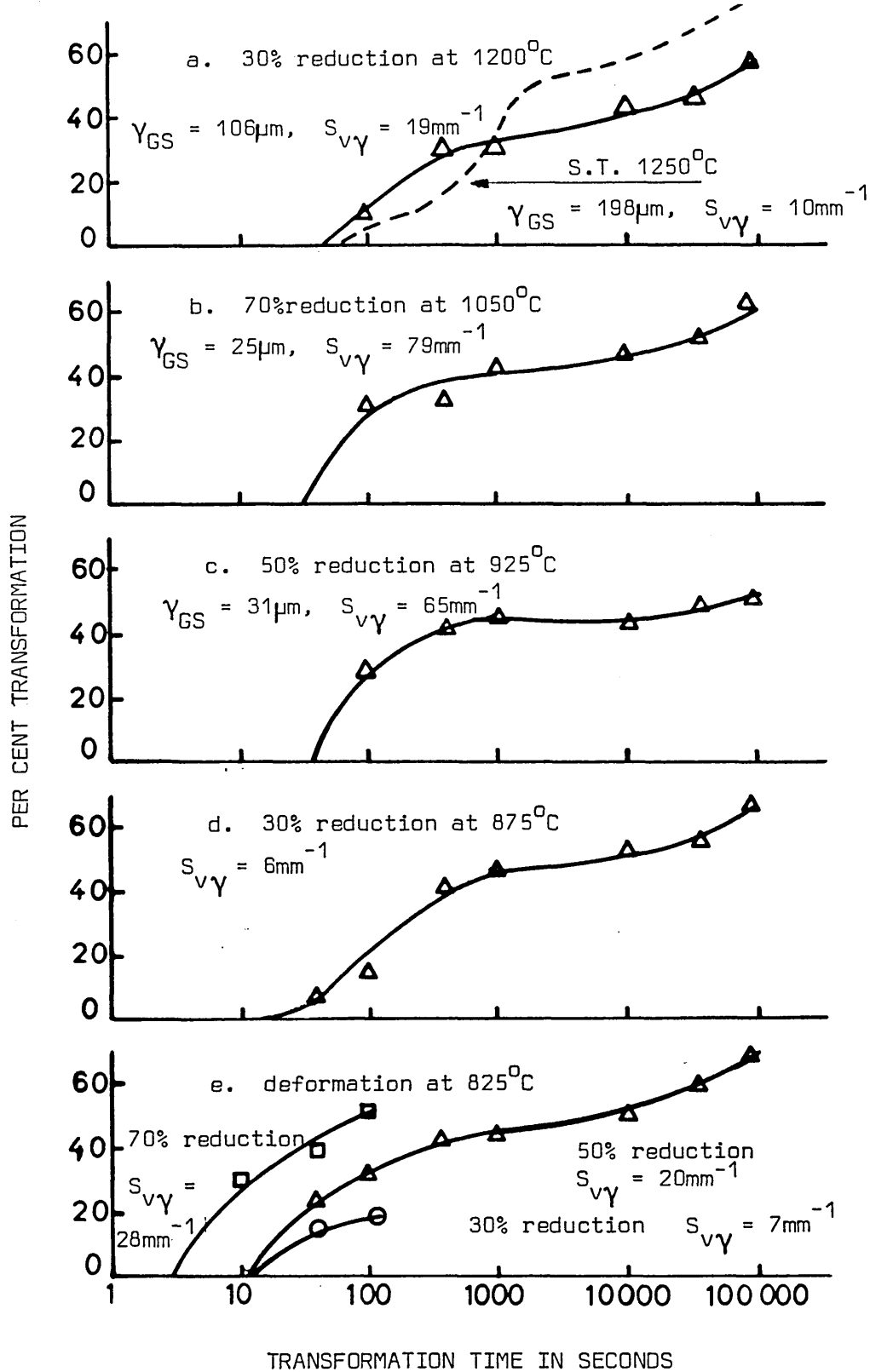AT 750°C IN 0.12%C, 1.4/1.7%Mn AND 0.010%N STEELS

293

FIG. 101 EFFECT OF DEFORMATION PRIOR TO ISOTHERMAL
TRANSFORMATION AT 750°C IN 0.11%C, 1.4/1.5%Mn,
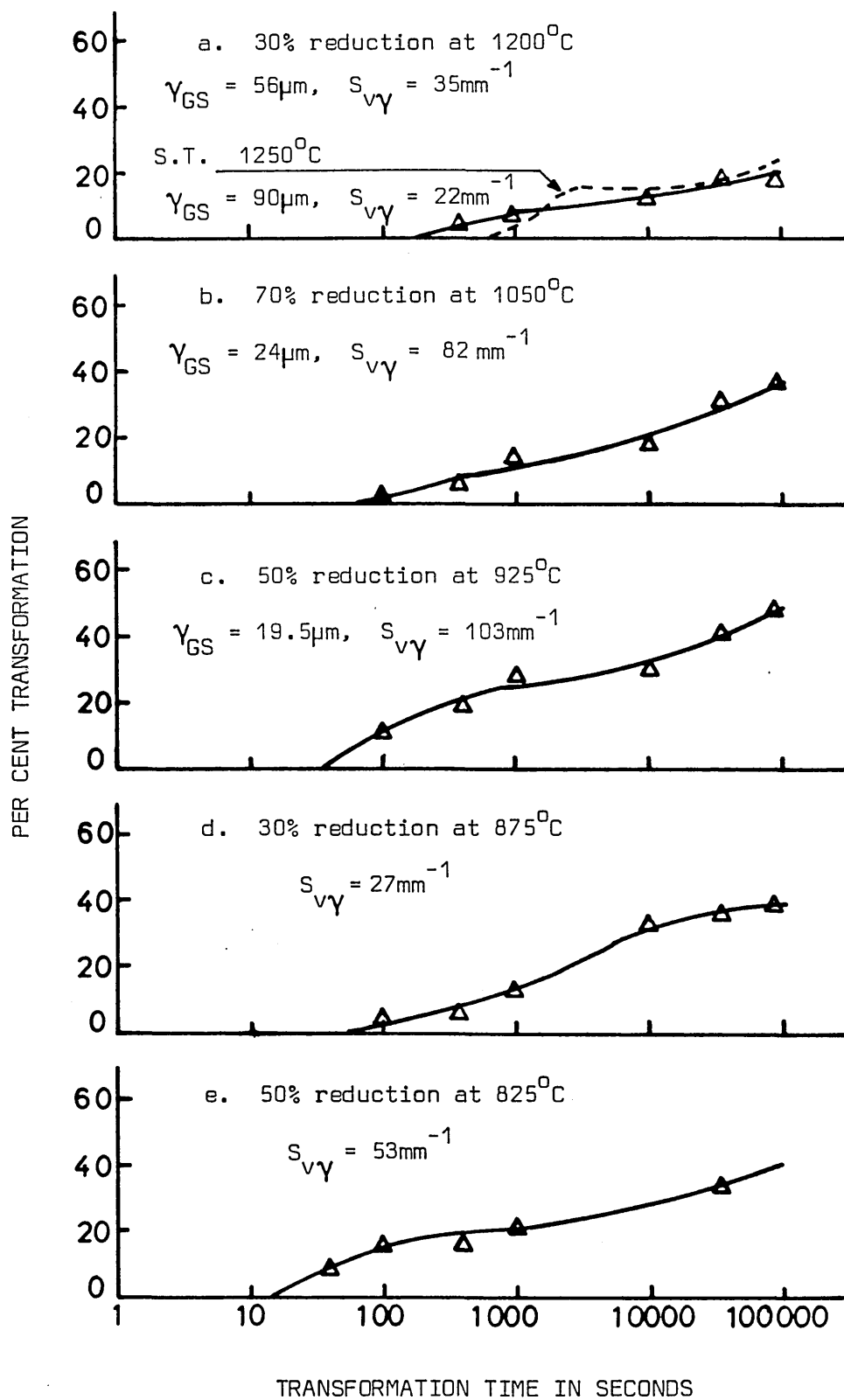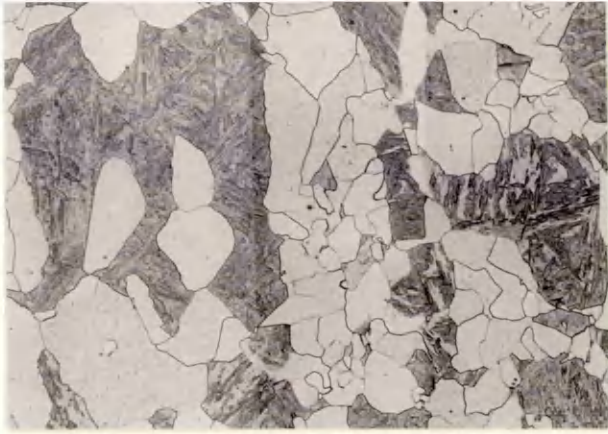0.13/0.15%V AND 0.004/0.005%N STEEL

FIG. 102 EFFECT OF DEFORMATION PRIOR TO ISOTHERMAL
TRANSFORMATION AT 750°C IN 0.11/0.12%C, 1.6/1.8%Mn,
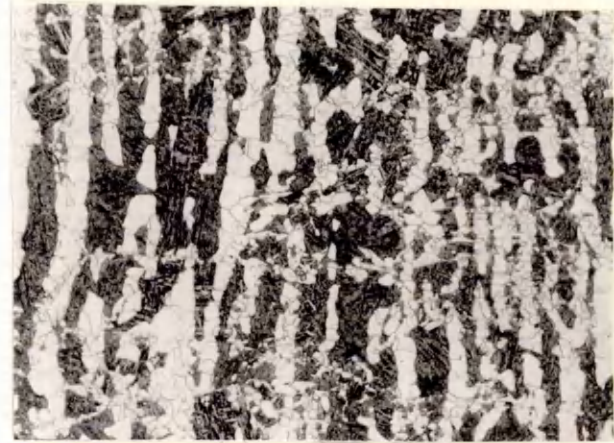1.6/1.8%Mn, 0.14/0.15%V AND 0.020/0.021%N STEELS

a. 30% REDUCTION AT 1200°C
ISOTHERMALLY TRANSFORMED AT
750°C FOR 12 HOURS W. Q. X200

b. 70% REDUCTION AT 1050°C
ISOTHERMALLY TRANSFORMED AT
750°C FOR 1000 SECONDS W. Q. X200

c. 50% REDUCTION AT 925°C
ISOTHERMALLY TRANSFORMED AT
750°C FOR 100 SECONDS W. Q. X100

d. 30% REDUCTION AT 875°C
ISOTHERMALLY TRANSFORMED AT
750°C FOR 24 HOURS W. Q. X50

e. 50% REDUCTION AT 825°C
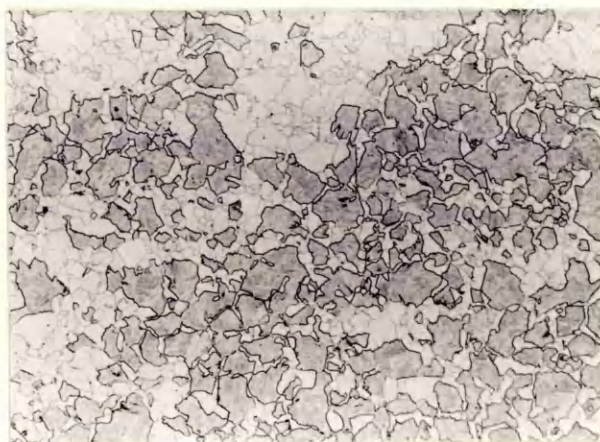ISOTHERMALLY TRANSFORMED AT
750°C FOR 100 SECONDS W. Q. X100

f. 50% REDUCTION AT 825°C
ISOTHERMALLY TRANSFORMED AT
750°C FOR 24 HOURS W. Q. X200

FIG. 103 PARTIALLY TRANSFORMED MICROSTRUCTURES AFTER THERMO-MECHANICAL
PROCESSING OF 0.11%C, 1.45/1.55%Mn, 0.13/0.155%V,
0.004/0.005%N STEEL

a. 30% REDUCTION AT 1200°C
ISOTHERMALLY TRANSFORMED AT
750°C FOR 12 HOURS W. Q. X500

b. 70% REDUCTION AT 1050°C
ISOTHERMALLY TRANSFORMED AT
750°C FOR 12 HOURS W. Q. X200

c. 50% REDUCTION AT 925°C
ISOTHERMALLY TRANSFORMED AT
750°C FOR 10000 SECONDS W. Q. X200

d. 30% REDUCTION AT 875°C
ISOTHERMALLY TRANSFORMED AT
750°C FOR 1000 SECONDS W. Q. X200

e. 30% REDUCTION AT 875°C
ISOTHERMALLY TRANSFORMED AT
750°C FOR 10000 SECONDS W. Q. X200

f. 50% REDUCTION AT 825°C
ISOTHERMALLY TRANSFORMED AT
750°C FOR 12 HOURS W. Q. X200

FIG. 104 PARTIALLY TRANSFORMED MICROSTRUCTURES AFTER THERMO-MECHANICAL
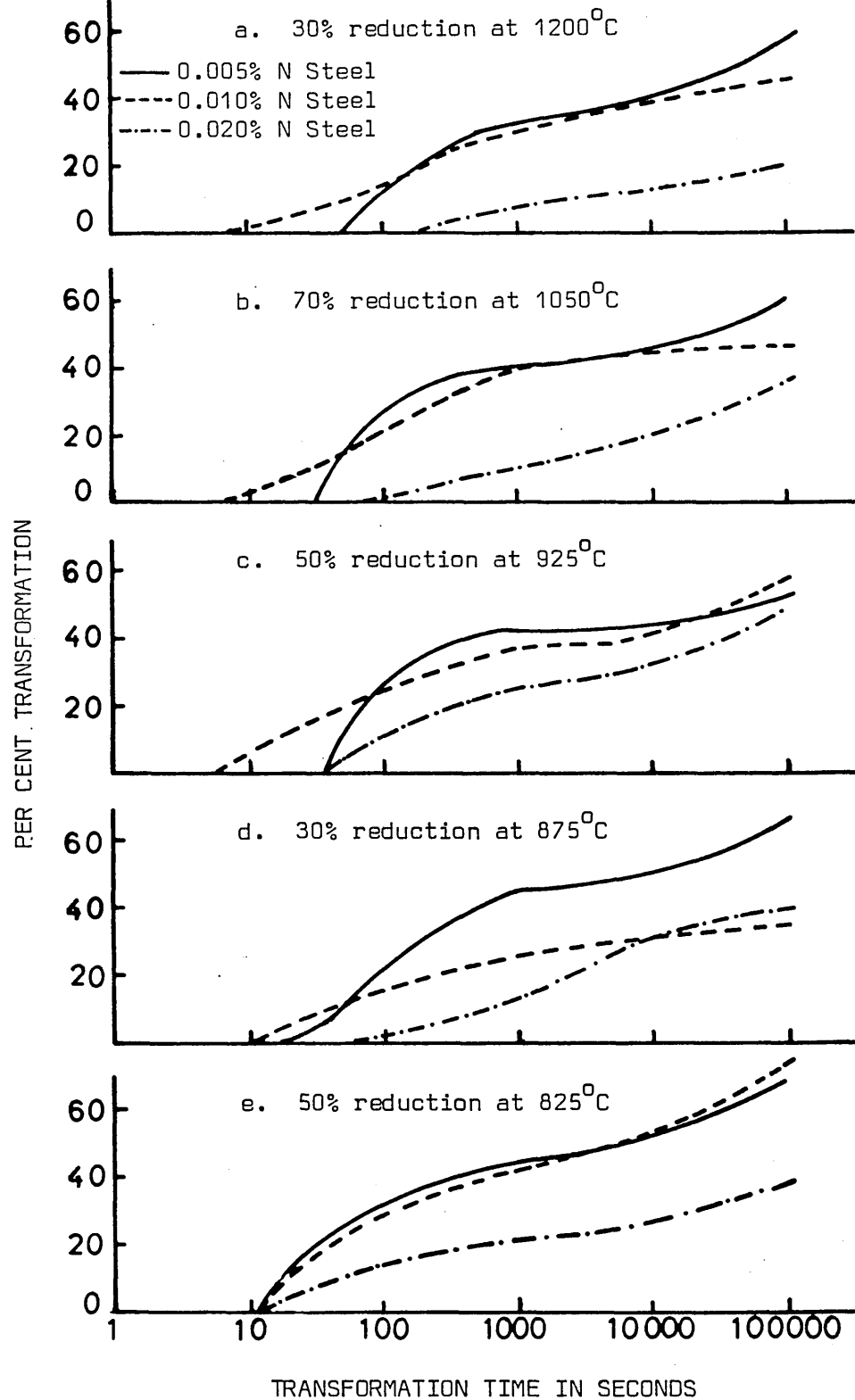PROCESSING OF 0.115/0.122%C, 1.62/1.85%Mn, 0.14/0.15%V,
0.020/0.021%N STEEL

297

FOG. 105 EFFECT OF NITROGEN ON THE ISOTHERMAL TRANSFORMATION
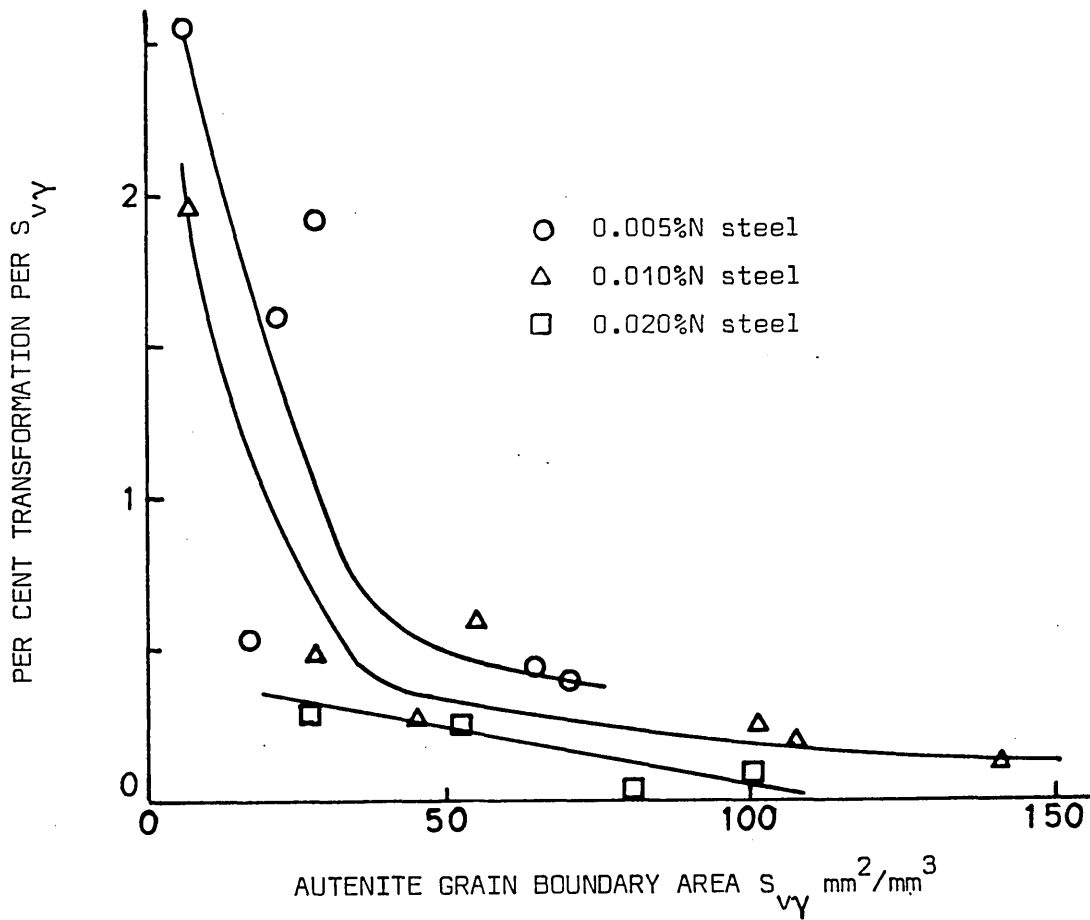AT 750°C IN 0.12/0.128%C, 1.4/1.8%Mn AND
0.13/0.19%V STEELS

298

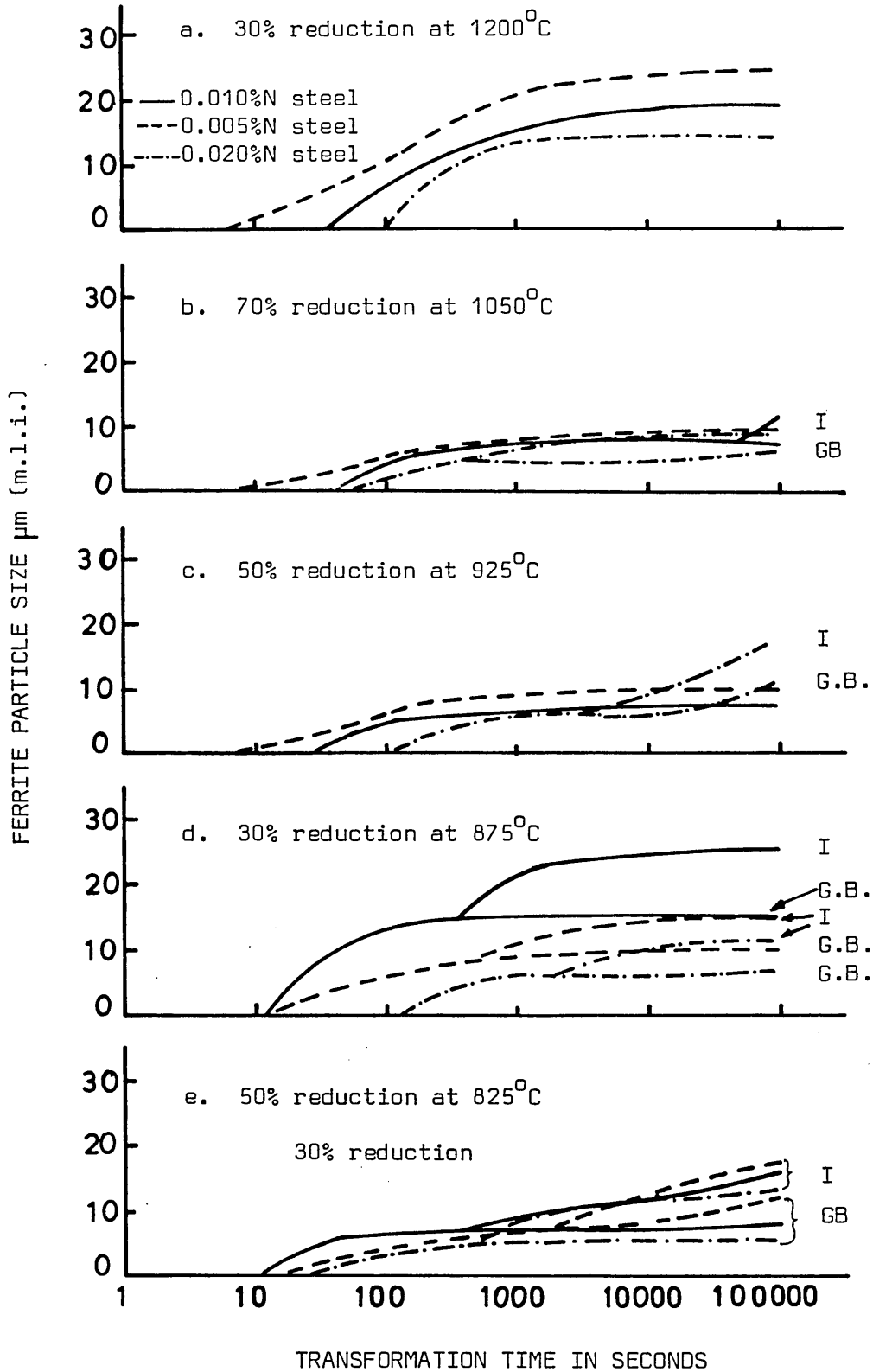FIG. 106 EFFECT OF NITROGEN ON THE $S_{v\gamma}$ ON TRANSFORMATION AT $750^{\circ}C$ FOR 100 SECONDS

FIG. 107 EFFECT OF INCREASING NITROGEN ON THE FERRITE PARTICLE SIZE
SIZE DURING ISOTHERMAL TRANSFORMATION AT 750°C IN 0.11/0.
0.11/0.128%C, 1.4/1.8%Mn AND 0.13/0.19%V STEELS

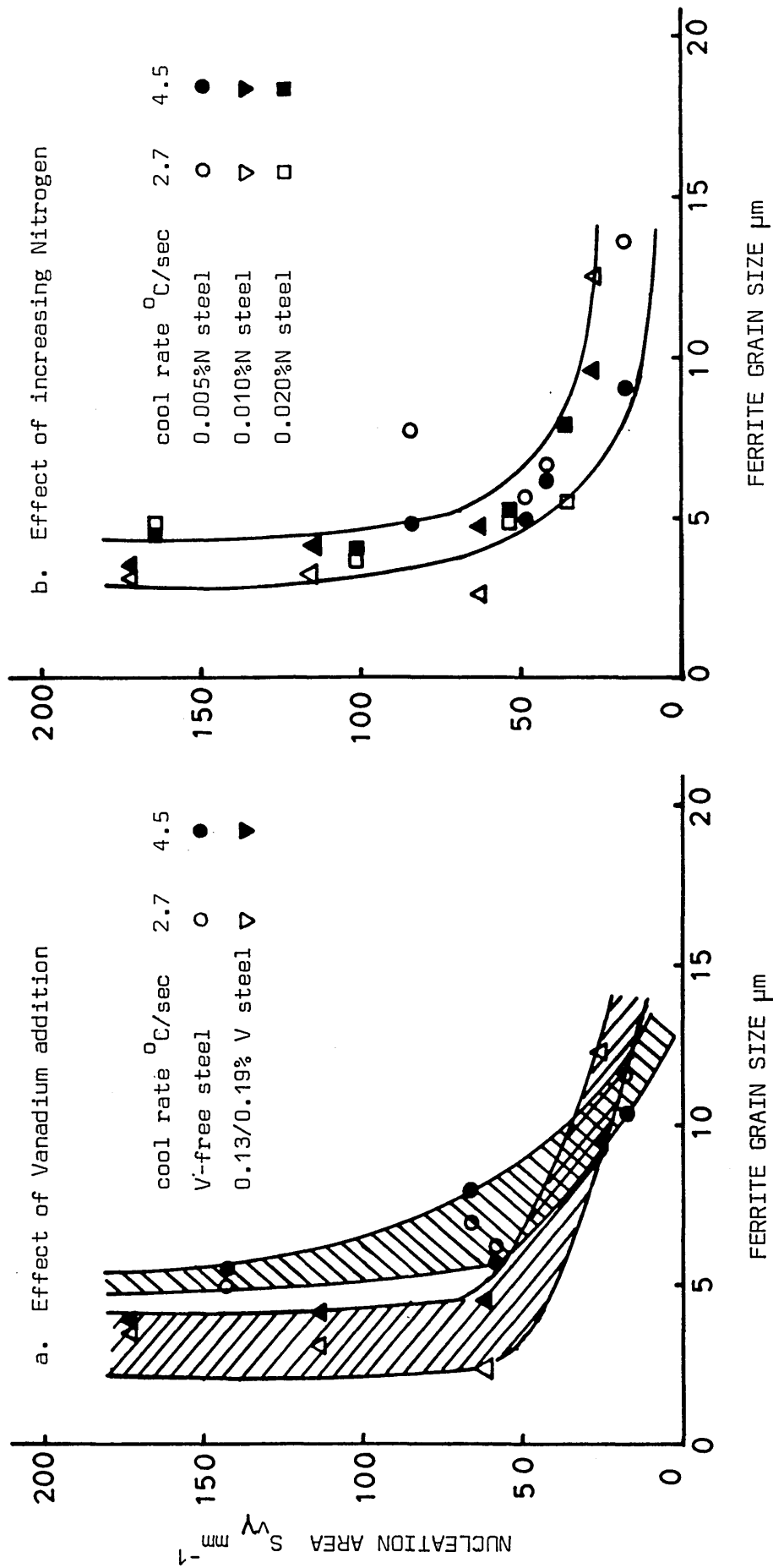300

FIG. 108 EFFECT OF $S_{v\gamma}$ ON THE FERRITE GRAIN SIZE ON CONTINUOUS COOLED STEELS FROM THERMO-MECHANICAL PROCESSING TEMPERATURES.
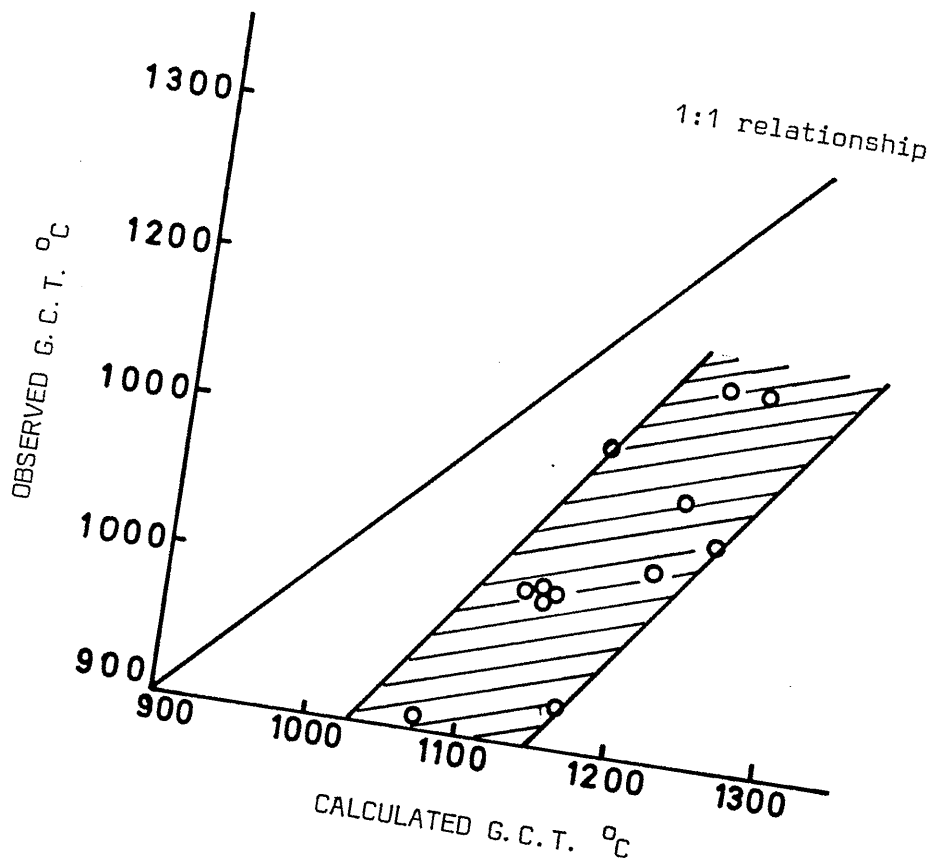
FIG. 109 RELATIONSHIP BETWEEN OBSERVED AND CALCULATED
GRAIN COARSENING TEMPERATURE

MEASUREMENT OF AUSTENITE GRAIN SIZES AND FERRITE PARTICLE SIZES

The method used to determine the austenite grain size was the mean linear intersept (m.l.i.). The m.l.i. for grain size $\bar{d}$ is given by :-

$$\bar{d} = \frac{L}{N} = \frac{1}{N_L}$$

Where N is the number of grains or grain boundaries intersecting a linear traverse of length L.

N_L is the number of grain or grain boundaries per unit length of traverse.

It must be appreciated that the m.l.i. $\bar{d}$, is less than the average diameter of the grains[1] but is used throughout this work. The accuracy of the determination of the m.l.i. has been examined[2] as follows. It was assumed that the distribution of grain size   is normal with a standard deviation $\sigma_{\bar{d}}$. Then 95% of the sample means lies within the range $\mu_x \pm 2$ S.D. where μ_x is the sample mean and S.D. the standard deviation. In the present case the mean value of a random sample of size n clustered about the mean μ_x, has a relative error of the m.l.i.

$$\sigma_{\bar{d}} = \bar{d} \frac{0.7}{\sqrt{n}}$$

where the 95% Confidence limit is $\bar{d} \pm 2\sigma_{\bar{d}}$.

In a ferrite-martensite structure the mean linear intercept was used to estimate the average ferrite particle size,

$$d_f = d_x (1 - V_m)$$

where $\bar{d}_f$ = the true ferrite particle size,
  d_x = the intercepts of ferrite particles,
  V_m = volume fraction of martensite,

The error is thought to come from the measurement of d_x. Hence the 95% Confidence limits.

$$= \bar{d}_f \pm 2 \text{ S.E.}$$

$$= \bar{d}_f \pm 2 (\text{S.D.} / \sqrt{n})$$

Where S.E. is the standard error, S.D. the standard deviation
and n is the number of intercepts counted.

References:

1. DEHOFF, R.T., and RHINE, F.N., Quantitative Microscopy,
   McGraw-Hill, N.Y. 1968.
2. PICKERING, F.B., 'The basis of Quantitative Metallography',
   Monograph No 1, Institution of Metallurgist, 1976. (contains
   relevant references)

PRECIPITATION EXTRACTION USING THE ELECTROLYTIC METHOD

The electolytic method for the extraction of precipitates was used where the material was too hard to be machined to millings, without overheating and possible altering the nature of the precipitates.

A potentiostatic method was used for the construction of polarisation curves, which are a pre-requisited for precipitation extraction, together with a modification of Klinger koch electrolytic cell. An electrolyte of 7% Fe_3Cl, 3% HCl and 3% Ethylene glycol solution[1] was used to dissolve the steel and leave the precipitates intact.

For the construction of standard polarisation curves, electrodes were made up of C-Mn-V steel, without any precipitation by heat treating above the solvus temperature of VC and VN. VC and VN powders were compacted into solid samples and then mounted in cold mounting resin so the same are of 0.78 mm^2 was exposed during the determination of polarisation curves.

The construction of polarisation curves was made by using a potentiostat, in conjuction with the electrolytic cell. The potentiostat mainly comprised of a direct current power supply unit, a reference potential potentiometer, a high gain voltage pre-amplifier and a power amplifier, whereas the electrolytic cell consisted of three electrodes; the working electrodes which was the specimen to be dissolved, the reference electrode and the auxiliary electrode. The working electrode was made positive with respect to the reference electrode. The difference between the potentials developed across the working electrode and reference electrode was amplified by the high gain voltage pre-amplifier and the output signal was fed into the power amplifier such that any increase in the potential difference between the working electrode and the reference electrode resulted in a reduced flow of current from the power amplifier. Consequently if the potential of the working electrode moved in a positive direction with respect to the reference electrode, the output current from the power amplifier was reduced thereby minimising the potential differece between the working and reference electrodes.

The electrochemical cell was that of Klinger Koch[2, 3] with slight modifications. The conical bottom was removed and replaced with a flat one. A circular perforated pipe was introduced just above the bottom for the gas which was oxygen free nitrogen, to be introduced into the solution, thus removing all the oxygen present in the electrolyte.

The C-Mn-V steel was placed in position in the electrolytic cell and oxygen free nitrogen was passed continuously through the solution before and during the time measurements were taken. Once the current had started to flow a 5 minute equilibrium time was allowed before each reading followed by changing the voltage setting. Results obtained are given in Table A.II.1 and presented graphically in Fig. A.II.1. The absolute value of the logarith of the current density was plotted against the voltage setting, using saturated calomel electrode (SCE).

The polarisation curve of the C-Mn-V steel was displaced to a more positive potential than that of VN and VC. It can be seen that there is a separation potential of about 0.7 volts (SCE). Under the established conditions, a specimen was placed in solution with the potential set at +0.2 volts (SCE). The steel dissolved, leaving the precipitates adhered to the surface of the specimen. Frequently removal of the precipitates from the surface was carried out using a nylon brush. When all the specimen was dissolved the precipitates were separated from the mother liquor by centrifuging followed by washing with dilute hydrochloric acid. Distilled water then replaced the hydrochloric acid as a wash which in turn was replaced by alcohol. The alcohol was driven off by a contiuous flow of argon at a temperature of 50°C, in which the precipitates were dried. The precipitate container was then sealed to prevent oxidation. The vanadium, carbon and nitrogen concentrations were measured by chemical analysis.

REFERENCES

1   WATANABE, H., Precipitation Kinetics of Columbium Carbonitride in Austenite of High Strength Low Alloy Steel, Climax Mol. Co., Ann Arbor, Michigan, 1975.
2   KOCH, W., Zeitschrift Fuer Analytische Chemie, Vol. 192, 1963, p.202.
3   KOCH, W., and SUNDERMAN, H., J.I.S.I. Dec. 1958, p.373.

Polarisation data for 0.10% C, 1.6% Mn, 0.415 V and
0.010% N steel, Vanadium Carbide and Vanadium Nitride.

| C-Mn steel		V C		V N	
input + mV	output mA/mm^2	input + mV	output mA/mm^2	input + mV	output mA/mm^2
00	−1.130	00	−0.120	00	−0.308
−	−	40	−0.103	40	−0.266
80	−0.850	80	−0.096	80	−0.266
−	−	120	−0.090	120	−0.256
160	−0.550	160	−0.100	160	−0.266
200	−0.410	200	−0.113	200	−0.241
240	−0.280	240	−0.113	240	−0.226
260	−0.210	−	−	−	−
280	−0.140	280	−0.106	280	−0.183
300	−0.082	−	−	−	−
320	−0.017	320	−0.086	320	−0.156
340	+0.042	−	−	−	−
360	+0.088	360	−0.070	360	−0.101
400	+0.125	400	−0.033	400	−0.083
440	+0.139	440	+0.008	440	−0.050
−	−	−	−	460	−0.033
−	−	480	+0.050	480	−0.019
−	−	−	−	500	−0.008
520	+0.144	520	+0.076	520	−0.000
−	−	560	+0.095	560	+0.009
600	+0.164	600	+0.116	600	+0.012
−	−	640	+0.136	−	−
680	+0.202	680	+0.166	680	+0.014
720	+0.260	720	+0.199	720	+0.022
−	−	760	+0.233	760	+0.023
800	+0.346	800	+0.283	800	+0.027
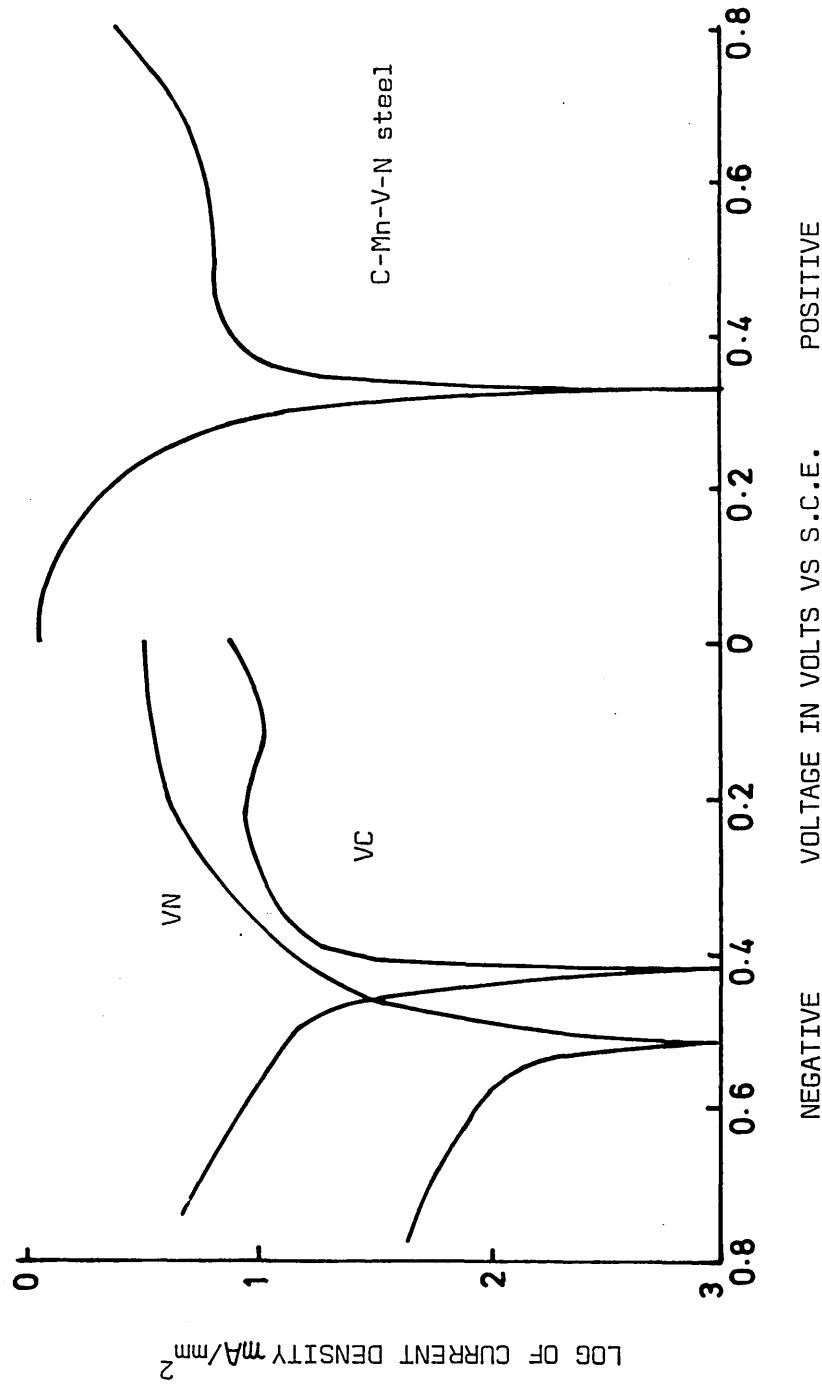
FIG. AII.1 POLARIZATION CURVES FOR 0.10%C, 1.60%Mn, 0.41%V, 0.010%N STEEL, VANADIUM CARBIDE
AND VANADIUM NITRIDE IN ELECTROLYTE OF FERRIC CHLORIDE SOLUTION.

QUANTITATIVE ANALYSIS OF TRANSFORMED STRUCTURES

In order to study the effect of various conditions of austenite in relation to the subsequent transformed ferrite, the volume fraction of transformed ferrite needed to be measured. It has been shown[1] that the volume fraction of a particular phase is equal to the point fraction of the phase using a two dimensional systematic point count. The volume fraction of alpha phase within the sample is given by :-

$$V_f = \frac{P}{P_t}$$

where P are points count in the alpha phase,
and P_t are the total number of points counted.

The accuracy of such determinations was dependent on the total number of points counted and the actual volume fraction of the phase in quenstion. A standard method was adopted, namely that a constant number of points was counted and the relative error determined once the volume fraction has been determined. Hilliard and Cahn[2] proposed a relationship for calculating the relative error in a two dimensional point count which was later modified by Gladman and Woodhead[3], which showed that the relative error :-

$$\frac{\sigma_{Vf}}{V_f} = \sqrt{\frac{(1 - V_f)}{P}}$$

The 95% confidence limits for the volume fraction of alpha are given by :-

Volume fraction of α at 95% C.L. = $V_f \pm 2\sigma_{Vf}$

REFERENCES

1. DEHOFF, R.T., and RHINE, F.N., Quantitative Microscopy, McGraw-Hill, N.Y. 1968.
2. HILLIARD, J. E., and CAHN, J.W., Trans. A.I.M.E., 221, 1961, p.344.
3 GLADMAN, T. and WOODHEAD, J., J.I.S.I., 201, 1963, p.1044.

CALCULATION OF EFFECTIVE INTERFACIAL AREA

The effective interfacial area in the sum of the recrystallised or elongated austenite grain boundary areas and the interfacial area of the deformation bands. These can be evaluated using the following equation[1]

i. For elongated grains

$$Sv \text{ g.b.} = 0.429 \ (N_L)_{||} + 1.571 \ (N_L)_{\perp}$$

ii. For equiaxed grains

$$Sv \text{ g.b.} = 2N_L = 2/D$$

iii. For deformation bands

$$Sv \text{ d.b.} = \varrho/\sin\theta$$

and $Sv = Sv \text{ g.b.} + Sv \text{ d.b.}$

The symbols are as follows.

Sv,   effective interfacial area mm^2/mm^3.

Sv g.b, Sv d.b.,   interfacial area of grain boundaries or deformation bands respectively.

$(N_L)_{||}$, $(N_L)_{\perp}$ intercept numbers per unit length along rolling and thickness direction respectively.

ϱ density of deformation bands mm/mm^{-2}.

θ angle between the deformation band and the thickness of the plate.

D   austenite grain diameter in mm

REFERENCE:

1. KOZASU, et al. Mcro-Alloying 75, Session 1, October 1975, Union Carbide Corporation, p. 100.